



I. R. IRAN

ISSN: 2423-7167

e-ISSN: 1735-9244



International Journal of Engineering

Journal Homepage: www.ije.ir



TRANSACTIONS C: Aspects

Volume 34, Number 12, December 2022

Materials and Energy Research Center

INTERNATIONAL JOURNAL OF ENGINEERING

Transactions A: Basics

DIRECTOR-IN-CHARGE

A. R. Khavandi

EDITOR-IN-CHIEF

G. D. Najafpour

ASSOCIATE EDITOR

A. Haerian

EDITORIAL BOARD

- | | | | |
|------|--|-------|---|
| S.B. | Adelaju, Charles Sturt University, Wagga, Australia | A. | Mahmoudi, Bu-Ali Sina University, Hamedan, Iran |
| K. | Badie, Iran Telecomm. Research Center, Tehran, Iran | O.P. | Malik, University of Calgary, Alberta, Canada |
| M. | Balaban, Massachusetts Ins. of Technology (MIT), USA | G.D. | Najafpour, Babol Noshirvani Univ. of Tech., Babol, Iran |
| M. | Bodaghi, Nottingham Trent University, Nottingham, UK | F. | Nateghi-A, Int. Ins. Earthquake Eng. Seis., Tehran, Iran |
| E. | Clausen, Univ. of Arkansas, North Carolina, USA | S. E. | Oh, Kangwon National University, Korea |
| W.R. | Daud, University Kebangsaan Malaysia, Selangor, Malaysia | M. | Osanloo, Amirkabir Univ. of Tech., Tehran, Iran |
| M. | Ehsan, Sharif University of Technology, Tehran, Iran | M. | Pazouki, Material and Energy Research Center, Meshkindasht, Karaj, Iran |
| J. | Faiz, Univ. of Tehran, Tehran, Iran | J. | Rashed-Mohassel, Univ. of Tehran, Tehran, Iran |
| H. | Farrahi, Sharif University of Technology, Tehran, Iran | S. K. | Sadrnezhaad, Sharif Univ. of Tech, Tehran, Iran |
| K. | Firoozbakhsh, Sharif Univ. of Technology, Tehran, Iran | R. | Sahraeian, Shahed University, Tehran, Iran |
| A. | Haerian, Sajad Univ., Mashhad, Iran | A. | Shokuhfar, K. N. Toosi Univ. of Tech., Tehran, Iran |
| H. | Hassanpour, Shahrood Univ. of Tech., Shahrood, Iran | R. | Tavakkoli-Moghaddam, Univ. of Tehran, Tehran, Iran |
| W. | Hogland, Linnaeus Univ, Kalmar Sweden | T. | Teng, Univ. Sains Malaysia, Gelugor, Malaysia |
| A.F. | Ismail, Univ. Tech. Malaysia, Skudai, Malaysia | L. J. | Thibodeaux, Louisiana State Univ, Baton Rouge, U.S.A |
| M. | Jain, University of Nebraska Medical Center, Omaha, USA | P. | Tiong, Nanyang Technological University, Singapore |
| M. | Keyanpour rad, Materials and Energy Research Center, Meshkindasht, Karaj, Iran | X. | Wang, Deakin University, Geelong VIC 3217, Australia |
| A. | Khavandi, Iran Univ. of Science and Tech., Tehran, Iran | | |

EDITORIAL ADVISORY BOARD

- | | | | |
|-------|--|-------|--|
| S. T. | Akhavan-Niaki, Sharif Univ. of Tech., Tehran, Iran | A. | Kheyroddin, Semnan Univ., Semnan, Iran |
| M. | Amidpour, K. N. Toosi Univ of Tech., Tehran, Iran | N. | Latifi, Mississippi State Univ., Mississippi State, USA |
| M. | Azadi, Semnan university, Semnan, Iran | H. | Oraee, Sharif Univ. of Tech., Tehran, Iran |
| M. | Azadi, Semnan University, Semnan, Iran | S. M. | Seyed-Hosseini, Iran Univ. of Sc. & Tech., Tehran, Iran |
| F. | Behnamfar, Isfahan University of Technology, Isfahan | M. T. | Shervani-Tabar, Tabriz Univ., Tabriz, Iran |
| R. | Dutta, Sharda University, India | E. | Shirani, Isfahan Univ. of Tech., Isfahan, Iran |
| M. | Eslami, Amirkabir Univ. of Technology, Tehran, Iran | A. | Siadat, Arts et Métiers, France |
| H. | Hamidi, K.N.Toosi Univ. of Technology, Tehran, Iran | C. | Triki, Hamad Bin Khalifa Univ., Doha, Qatar |
| S. | Jafarmadar, Urmia Univ., Urmia, Iran | S. | Hajati, Material and Energy Research Center, Meshkindasht, Karaj, Iran |
| S. | Hesaraki, Material and Energy Research Center, Meshkindasht, Karaj, Iran | | |

TECHNICAL STAFF

M. Khavarpour; M. Mohammadi; V. H. Bazzaz, R. Esfandiar; T. Ebadi

DISCLAIMER

The publication of papers in International Journal of Engineering does not imply that the editorial board, reviewers or publisher accept, approve or endorse the data and conclusions of authors.

CONTENTS:

| | | |
|---|--|-----------|
| S. Shafaghizadeh; S. Ebrahimnejad; M. Navabakhsh; S. M. Sajadi | Proposing a model for a resilient supply chain: A meta-heuristic algorithm | 2566-2577 |
| Z. A. Zainal; N. S. N. Rusli; N. A. Shuaib | Effect of Cutting Environment and Swept Angle Selection in Milling Operation | 2578-2584 |
| S. M. S. Moosavi; M. Seifbarghy | A Robust Multi-objective Fuzzy Model for a Green Closed-loop Supply Chain Network under Uncertain Demand and Reliability (A Case Study in Engine Oil Industry) | 2585-2603 |
| D. Siddharth; D. K. J. Saini; P. Singh | An Efficient Approach for Edge Detection Technique Using Kalman Filter with Artificial Neural Network | 2604-2610 |
| V Veda Spandana; G Jamuna Rani; K Venkateswarlu; V. V. Venu Madhav | Experimental Study on Yttria Stabilized and Titanium Oxide Thermal Barrier Coated Piston Effect on Engine Performance and Emission Characteristics | 2611-2616 |
| P. Phani Prasanthi; K. Sivaji Babu; A. Eswar Kumar | Waviness Effect of Fiber on Buckling Behavior of Sisal/Carbon Nanotube Reinforced Composites Using Experimental Finite Element Method | 2617-2623 |
| L. Bahrami; N. Safaie; H. Hamidi | Effect of Motivation, Opportunity and Ability on Human Resources Information Security Management Considering the Roles of Attitudinal, Behavioral and Organizational Factors | 2624-2635 |
| M. S. Mahmood; M. J. Abraham | Effect of Matric Suction on Deformation of Gypseous Sand Using Modified Oedometer | 2636-2641 |
| S. Dhoub | Optimization of Travelling Salesman Problem on Single Valued Triangular Neutrosophic Number using Dhoub-Matrix-TSP1 Heuristic | 2642-2647 |
| S. M. Sadjadi; H. Mashayekhi; H. Hassanpour | A Two-Level Semi-supervised Clustering Technique for News Articles | 2648-2657 |
| Z. Wei | Effects of Deceleration on Secondary Collisions between Adult Occupants and the Vehicle in Frontal Crash Accidents | 2658-2664 |
| D. T. Nguyen; V. T. A. Phan | Engineering Properties of Soil Stabilized with Cement and Fly Ash for Sustainable Road Construction | 2665-2671 |

| | | |
|---|--|-----------|
| R. Chakrabarty; S. Roy; T. Pathak; N. Kumar Mandal | Design of Area Efficient Single Bit Comparator Circuit using Quantum dot Cellular Automata and its Digital Logic Gates Realization | 2672-2678 |
| A. Yadav; N. Kohli; A. Yadav | Prolong Stability Period in Node Pairing Protocol for Wireless Sensor Networks | 2679-2687 |



Proposing a Model For a Resilient Supply Chain: A Meta-heuristic Algorithm

S. Shafaghizadeh^a, S. Ebrahimnejad^b, M. Navabakhsh^{*a}, S. M. Sajadi^c

^a Department of Industrial Engineering, South Tehran Branch, Islamic Azad University, Tehran, Iran

^b Department of Industrial Engineering, Karaj Branch, Islamic Azad University, Karaj, Iran

^c School of Strategy and Leadership, Faculty of Business and Law, Coventry University, Coventry, UK

PAPER INFO

Paper history:

Received 19 May 2021

Received in revised form 08 August 2021

Accepted 19 August 2021

Keywords:

Resilient Supply Chain

Meta-heuristic

NP-hard Problem

Mixed Integer Programming

ABSTRACT

The resilient supply chain considers many capabilities for companies to overcome financial crises and to supply and distribute products. In this study, we addressed the allocation of inventory distribution for a distribution network, including a factory, a number of potential locations for distribution centers and a number of retailers. Customers demand is assumed to be certain and deterministic for all periods but time varying in the limited planning horizon. The proposed model in this research is a linear complex integer programming model with two-objective functions. The first objective function minimizes the total costs of the entire distribution system in the planning horizon, and the second objective function seeks to minimize the difference between the maximum and minimum distances traveled by vehicles over the planning horizon. Therefore, the model tries to satisfy the demand and at the same time reduce costs using the best route transportation option configuration and transportation option. The routing problem is developed, and as the problem is a NP-hard problem, a meta-heuristic method is used to solve it. In this model, the demand volume for each customer in a period of the network, vehicle capacity, factory capacity, constant transportation cost, variable transportation cost, etc., are considered as factors affecting the model. The results show that the model proposed in the network can be used as a lever to improve the performance of the financial economic supply network through saving in routes.

doi: 10.5829/ije.2021.34.12c.01

1. INTRODUCTION

The socio-political, economic and cultural parameters affecting the business environment in today's world face many turmoils and developments [1]. These turmoils increase the likelihood of the occurrence of effective events on supply chain performance. Therefore, if supply chain managers are incapable of well managing unforeseen disruptions, they will face dangerous negative consequences, and this will increase the risk of business continuity and result in financial losses [2]. Supply chain is a consecutive network of business partners involved in manufacturing processes and converting primary raw materials into final products or services to meet customer demand on due time with high quality and the least cost [3]. The occurrence of the events that interrupt the flow of materials, even if these events occur in a remote

location, may lead to large-scale disturbances [4]. Disruptions are sudden and unexpected deteriorations caused by a variety of factors such as natural disasters, arson, loss of vital supplier, war, cyber attacks, economic recession, sanctions and economic shocks, terrorism, etc. [5]. Although the occurrence of these events is unlikely, they will have a lot of consequences for business if they occur [6]. Under such conditions, the need to design a resilient supply chain model becomes more evident because such a chain is ready to face any event; and in addition to providing an efficient and effective response, it is capable of returning to its original or more desirable state after disruption i.e., supply chain resilience. Melnyk et al. [7] believed that now, resilience is at the heart of current supply chain management thinking. Today, any one organization is incapable of establishing its existence without a resilient supply chain and effective

*Corresponding Author Institutional Email:

M_Navabakhsh@azad.ac.ir (M. Navabakhsh)

Please cite this article as: S. Shafaghizadeh, S. Ebrahimnejad, M. Navabakhsh, S. M. Sajadi, Proposing a Model For a Resilient Supply Chain: A Meta-heuristic Algorithm, International Journal of Engineering, Transactions B: Applications, Vol. 34, No. 11, (2021) 2566-2577

communication because managing a company always requires having a dynamic supply and communication sector. Currently, goods supply from a secure supplier at the minimum cost and highest quality is the most important bridge between manufacturers and goods owners, exporters, importers, and consumers. This is while there are still challenges despite the importance of this issue. Offering a fair and affordable price and continuous follow-up of operations from loading to delivery are among these challenges in the network. In Inventory Routing Problem (IRP), the goal of optimization is to find the best strategy for product inventory management and determine the best vehicle configuration, routes, product types and their quantities to deliver to each customer, while minimizing the total cost of inventory and transportation [8]. As the problem of allocating and routing using a network is a hard problem, meta-heuristics are used to solve it. By proposing a mathematical model of inventory routing via a hypothetical network for the meat products industry in this study, we want to reduce the costs associated with the distribution, transportation, and storage of protein products. We use a small example to solve the problem using MATLAB software, and then develop the problem. As the routing problem is a hard-problem, meta-heuristics are used to solve it. The research structure is shown in Figure 1.

2. LITERATURE REVIEW

In this research, Internet network and scientific databases are the most important sources and data are obtained by searching among articles published in scientific journals because the present study is based on the scientific articles and previous works.

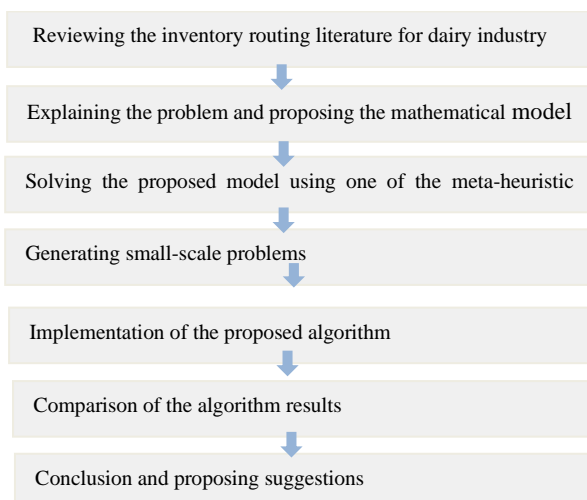


Figure 1. Research structure

2. 1. Transportation Definition

Any problem that seeks to generate a tour or a set of tours on a network or sub-network aiming to optimize one or multiple objectives is called a routing problem.

A routing problem includes the following components:

- Network

The network can be symmetric, asymmetric or hybrid. It can be displayed by a graph. The nodes in this graph represent cities, customers, or terminals, and the edges represent real connectors, such as roads, pipelines, etc.

- Demand

Demand can be constant or variable. It can be related to nodes and edges. The debate of demand is proposed in distribution problems in which a certain amount of goods must be transported and delivered to that node given the demand of the related node or edge. Moreover, these problems are observed in harvest and delivery problems.

- Fleet

Fleet creates constraints in the problem. Fleet can be homogeneous or heterogeneous. It can be generated by one or more vehicles, and can be affected by the vehicles capacity (limited or unlimited), time, or distance.

- Cost

Cost is often constant for vehicle and varies for the way of using it based on the passed distances and/or the travel time. It means that if a customer receives late or incomplete service, this type of service will result in a penalty. Moreover, here, it can propose the profit from the harvest when meeting the customer (node) or choosing the best edge for navigation.

- Objectives

Objectives can be multiple and different. The objective function can be calculated for one time interval or several time intervals. In this case, vehicles and appointments should be allocated to different intervals. Therefore, better results can be considered using multiobjective optimization [9].

2. 2. Resilience

Resilience defined as an organization's ability and capacity to face and overcome crises and challenges and to return to normal business conditions is a very important feature that organizations must be equipped with for the survival and continuity of their business [10]. However, the concern is not only restricted to disasters, but small deviations and uncertainties challenging the organizations are also considered [11]. In this regard, there are various businesses that are incapable of managing vulnerabilities such that they may be eliminated or taken in ownership by powerful organizations against business turmoils [12]. Therefore, all businesses' flexibility and adaptability have become an important necessity in today's rapidly changing environment, and the need to develop a strong attitude towards them is severely felt in all businesses [11]. Resilience literally means to spring back, being

reversible, and resilient [13]. The term "resilience" has been defined in different forms: Masten [14] defined resilience as "a process, ability, or the outcome of successful adaptation in the face of threatening conditions". In fact, resilience is the positive adaptation in response to the adverse conditions [15]. Resilience is not the mere passive resistance against damages or threatening conditions, but the resilient person, is a participant who constructs his surrounding environment. Resilience is a person's ability to establish biological-psychological-spiritual balance when confronted with risky circumstances [11]. It is a kind of self-healing that is accompanied by positive emotional and cognitive consequences [16]. Thus, resilience cannot be regarded equivalent to recovery because in recovery, the person experiences negative consequences and emotional problems [10]. Resilience is a person's ability of successful adaptation in the face of a changing environment, stubbornness, invulnerability, and successful adaptation in the face of high levels of stress and adverse conditions [17]. Overall, resilience is a psychological concept explaining how individuals deal with unexpected situations. Resilience is defined as the resistance against stress, the ability to return to normal state and survive, and to make attempts in adverse circumstances [18].

The supply chain resilience is the adaptability of a supply chain for being ready for disruptions and responding to them, timely and cost-effective recursive recovery, and thus making progress toward post-

disruptions situation, which in the ideal state is better than before the occurrence of disruption. It means that the supply chain resilience can be assessed based on four aspects: 1. The supply chain readiness to face a disruptive event; 2. Responding to that event; 3. Improvement and return; and 4. Growing and achieving a competitive advantage after the occurrence of the event. However, strategies and supply chain resilience capabilities should be directed toward ensuring that these aspects achieve their maxim possibility on due time by spending the least cost. In addition, adaptability is the basis of these four aspects. By adaptation we mean that the supply chain has a latent capability to develop different responses that are consistent with the nature of the threats that are faced by it. It means that the supply chain components are capable of changing themselves in such a way that at any time and on due time they can appropriately respond to disturbing events, rather than referring to an existing certain set of responses and selecting their responses among them whenever a disturbance occurs [19]. Tavakoli et al. developed a model for closed-loop supply chain network design with disruption risk by two factors including extra inventory and lateral transshipment are used as resilience strategies [20]. Table 1 summarized literature review for the comparative studies.

The transshipment option not only can be used to increase the economic supply network performance but also it can help the system to avoid risky routing when the cargos are categorized in decaying hazardous materials.

TABLE 1. Comparison of the recent articles

| Solution | Limitations | Objective | Topic | Year | Authors |
|-------------------------------|--|---|---|------|----------------------------|
| Meta-heuristic method | CO ₂ emission, transportation costs, driving duration, rate of accidents, etc. | Reducing transportation costs and decreasing CO ₂ emission | Carbon emission reduction in road freight transportation sector based on route optimization model | 2020 | Wei and Liu [21] |
| Serial and parallel structure | Traffic flow, balance of entry and exit and, etc. | The proper well-being and price of traffic flows and operating costs | Serial and parallel duopoly competition in multi-segment transportation routes | 2020 | Kuang et al. [22] |
| branch-and-cut algorithm | Availability, balanced flow, vehicle capacity, maintenance cost, clean vehicle, etc., | Reducing logistics costs | Two-echelon inventory-routing problem with fleet management | 2020 | Scheneke mberg et al. [23] |
| Heuristic mixed solution | Customer storage capacity, vehicle capacity, inventory maintenance, cost of customer loss, etc. | Integrated Optimization of decisions in a Supply Chain | Inventory routing under stochastic supply and demand | 2020 | Alvarez et al. [24] |
| Genetic algorithm | The amount of product shipped, the inventory of goods is equal to the demand for goods, the maximum number of selected routes is not more than the number of vehicles, etc. | Maximization of the total profit of the supply chain | Demand management to cope with routes disruptions in location-inventory-routing problem for perishable products | 2020 | Yavari et al. [25] |
| Gurobi programming algorithm | Satisfying the demand, the distribution capacity of the cold storage warehouse is less than its maximum inventory capacity; the time spent by the delivery routes is less than the time, maximum durability of their products etc. | Costs minimization | A mixed integer programming for two-echelon inventory routing problem of perishable products | 2020 | Wang et al. [26] |

| | | | | | |
|---|--|---|--|------|--------------------------|
| CPLEX | Place of loading and unloading, the amount of loading / unloading cannot be greater than the floating capacity and the capacity of the port, the amount of loading and unloading must be equal, etc. | Reducing sailing costs | Load-dependent speed optimization in marine inventory routing | 2020 | Eide et al. [27] |
| CPLEX | Service provision time, vehicle capacity, inventory capacity, etc. | Reducing routing problems | Mata-heuristic search techniques for the consistent inventory routing problem with time windows and split deliveries | 2020 | Ortega et al. [28] |
| Genetic algorithm | Perfect inventory flow balance, inventory flow balance of defective products, production launching, vehicle capacity, etc. | Reducing the inventory and transportation costs | A robust optimization approach for the production-inventory routing problem with simultaneous pickup and deliver | 2020 | Golsefidi and Jokar [29] |
| VaNSAS algorithm | The shopping center capacity, factory capacity, the rubber collection route from a farm, etc. | Minimizing the fuel consumption depending on the road distance and conditions | Variable neighborhood strategy adaptive search for solving green 2-echelon location routing problem | 2020 | Pitakaso et al.[30] |
| Firefly algorithm | Each node is visited at most once, vehicle capacity, integrity of variables, covering demand | Maximizing the prize and minimizing CO2 emission | The firefly algorithm for the environmental prize-collecting vehicle routing problem | 2020 | Trachanatzis et al. [31] |
| The ant colony optimization algorithm (ACO) | All equipment sent to a warehouse does not exceed their storage capacity, each route must start and end in the same warehouse, the working time of each vehicle cannot exceed the defined limit | Reducing the time it takes the relief aids to reach the damaged area and reducing the costs | A location-routing problem with post-disaster relief distribution | 2020 | Wang et al.[32] |
| hybrid genetic algorithm | Carrier expenses, vehicles capacity limitations, and/or long lead time. | Inventory routing problem for hazardous items with transshipment option | Proposing a model for a resilient supply chain: A meta-heuristic algorithm | - | Shafaghizadeh et al. |

Despite the existence of a rather wide variety of studies on IRP problem for deteriorating items the transshipment option has been studied for hazardous items a little. The challenging research question in this context, therefore, is to identify the linkage between the deteriorating rate and the benefit brought by the transshipment policy in terms of economic gain.

3. MATHEMATICAL MODEL

Suppose a supply chain composed of a set of retailers ($\{1, 2, \dots, N\}$) that provides the factory products to the public as a supplier of this type of product. For products such as protein products, the passage of time may lead to the loss of product health benefits and the irreversible health effects on consumers. Transportation vehicles must have particular equipment. There are predetermined routes between suppliers and retailers. To control and get access to the product more easily, a retransmission option has been embedded in the model to meet the demand directly from major suppliers or other retailers. The optimization problem is the ideal configuration of routes, pickups, deliveries, and transportation in each period in order to minimize the total cost of the supply chain (including ordering cost,

inventory maintenance cost, constant and variable transportation costs, shortage cost, and pickup cost) and to minimize the perished products cost in distribution, while all retailers' demand is satisfied as much as possible. It should be noted that spoilage is allowed, but the demands must also be met in each period. In the proposed model, the "partial reorder shortage" is included in the model by introducing a parameter (β), which can be estimated on the basis of the customer time data in retail stores. When a retailer faces shortage, two possible states are identified in real situations. β % of individuals can wait until the next period(s) to receive the product. A period can be defined as the day, week, etc. Therefore the individuals' demand on the balance sheet is considered as saving. $1-\beta$ % of customers, who can not wait, either used the alternative products or left the retail store and referred to other centers.

3. 1. Problem Formulation The two-objective mixed integer programming for the IRP re-shipment problem given the spoilage is formulated as follows: Constraint (3) Models the equation of the retailer inventory and determines that the product inventory status in retail store i in the current period (t) equals $1 - \theta$ % of previous inventory level (I_{t-1}) plus the amount delivered in period t (transportation by vehicles) minus

the amount collected by the vehicle in period t minus the current period demand and β % of the previous period shortage. It is supposed that only β % of the buyers, who face the product shortage, wait for the next period and the demand for the remaining $(1 - \beta)$ % is definitely removed. Moreover, it is supposed that the inventory reduces at a rate of θ and only $(1 - \theta)$ % of the previous inventory remains for future use. Constraint (4) dictates that no supplier gets input. Constraints (5) and (6) ensure that each retailer must not be visited by a particular vehicle more than once per period. In these conditions, split distribution means that the retailer can be visited by different vehicles more than once in a period. If the split distribution is banned, then the constraint can be changed to $\sum_k Y_{ikt} \leq 1$. Constraint (7) is the inventory equation of the vehicle that visits the edge i, j in period t and ensures that the amount of the product transported by the vehicle from node i to node j in period t is equal to the amount of product sent to node i. In addition, the amount picked up by the vehicle from node i minus the amount delivered to this retailer in the current period. Constraint (8) guarantees that the vehicle capacity should not be exceeded and it means that only when x_{ijkt} variable gets a value the vehicle can visit the edge(i,j). Constraint (9) ensures that the vehicles cannot take the delivery of products from the retailer more than the amount of their inventory in the previous period. This constraint also guarantees that the inventory capacity of the retailer cannot be exceeded. Constraint (10) ensures that a journey must start at the center node (node 0) and end at the same point. Constraint (11) is the classic constraint of sub-tour removal. Constraint (12) prohibits product return and determines impossible edges, and finally, constraint (13) defines different types of variables. It should be noted that in constraints (3) and (9), the variable $I_{i(t-1)}$ is replaced with the initial inventory (I_0) in a particular case.

4. THE PROPOSED MODEL TO SOLVE THE PROBLEM

To solve this problem, we use the genetic algorithm-based method. In the following, this method is briefly explained. The reason why we use the genetic algorithm is that the decision variables include two binary matrices (X and Y) and three matrices consisting of integers (Q, Qd, and Qp); which are very consistent with the discrete nature of the genetic algorithm and do not lead to unacceptable solutions, and there is no need to add a stage to test the accuracy of the algorithm solutions.

$$\begin{aligned} \min Z_1 = & \sum_{i \in \omega, k, t} fc_k \cdot X_{0ikt} + \\ & \sum_{(i,j) \in \Omega} \sum_{k,t} vc_k \cdot d_{ij} \cdot Q_{ijkt} + \sum_{i \in \omega, t} h_i \cdot I_{it} + \\ & \sum_{i \in \omega, t} \pi_i \cdot \beta_i \cdot S_{it} + \sum_{i \in \omega, t} \pi'_i \cdot (1 - \beta_i) \cdot S_{it} + \\ & \sum_{i \in \omega, k, t} pc_i \cdot Qp_{ikt} \end{aligned} \quad (1)$$

$$\min Z_2 = \max_t \sum_{i,j \in \Omega, k} (c \cdot Q_{ijkt} + f_k) \times X_{ijkt} \quad (2)$$

$$I_{it} - S_{it} = (1 - \theta) \times I_{i(t-1)} - \beta \times S_{i(t-1)} + \sum_k Qd_{ikt} - \sum_k Qp_{ikt} - D_{it} \quad \forall i \in \omega, t \quad (3)$$

$$Qd_{ikt} = 0 \quad \forall i \in O \quad (4)$$

$$\sum_{j \in \Omega} X_{jikt} = \sum_{j \in \Omega} X_{ijkt} = Y_{ikt} \quad \forall i \in \Omega, k, t \quad (5)$$

$$Y_{ikt} \leq 1 \quad \forall i \in \omega, t, k \quad (6)$$

$$\sum_{j \in \Omega} Q_{jikt} - Qd_{ikt} + Qp_{ikt} = \sum_{j \in \Omega} Q_{ijkt} \quad \forall i \in \omega, k, t \quad (7)$$

$$Q_{ijkt} \leq cv_k \cdot x_{ijkt} \quad \forall i \in \Omega, k, t \quad (8)$$

$$\sum_k Qp_{ikt} \leq (1 - \theta)I_{i(t-1)} \leq (1 - \theta)Ic_i \quad \forall i \in \omega, t \quad (9)$$

4. 1. Genetic Algorithm Genetic algorithm (GA) is a meta-heuristic method in computer science to find approximate solutions for optimization and search problems. GA is a special type of evolutionary algorithms that use biological concepts such as inheritance and mutation. This algorithm was introduced by John Holland for the first time. In GAs, first, multiple solutions are generated for problem randomly or intelligently. This set of solutions is called the first population and each solution is called a chromosome. Then using the GA operators, we combine chromosomes after selecting the best chromosomes and create a mutation in them. Finally, we combine the current population with the new population obtained from the combination and mutation of chromosomes. Figure 2 displays the GA flowchart.

4. 1. 1. Generating The Problem Solutions As Chromosomes To solve this problem, all the

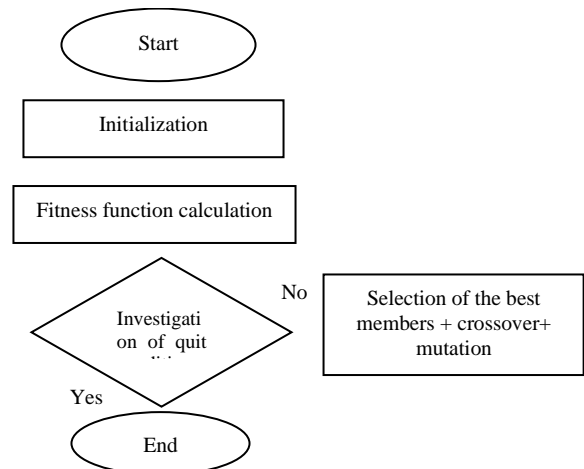


Figure 2. GA flowchart

problem decision variables need to be turned into chromosomes and move towards the optimal answer during the algorithm run. Two variable I_{it} and S_{it} are calculated using other variables. $X_{ijkt}, Y_{ikt}, Q_{ijkt}, Qd_{ikt}, Qp_{ikt}$, and XQ_{ijkt} are variables to be determined and are considered components within the chromosome. X is a binary four-dimensional matrix, Y is a binary three-dimensional matrix, Q is a four-dimensional matrix of positive integers, Qd is a three-dimensional matrix of positive integers, and Qp is a three-dimensional matrix of positive integers. At each stage of the GA, these variables are updated by operators and the result of changing them is reflected in the objective function.

An example of the first dimension of X variable in the GA chromosome of the proposed method is shown in Figure 3.

4. 1. 2. Introduction of Fitness Function

Equation (3) is the first fitness function of the proposed model whose aim is to minimize the total cost of the supply chain, including the constant and variable transportation cost, inventory maintenance cost, shortage cost, and transportation costs. The second objective function is the Equation (2)-(3) that seeks to minimize the maximum path traveled by each product during distribution among all periods. The final fitness function is considered to be a combination of two objective functions to solve this problem: The final fitness function to solve this problem is considered to be combined of two objective functions:

$$F = \alpha Z_1 + \beta Z_2 \tag{14}$$

where the two sub-functions existing in this function are obtained from relations (1) and (2) and α and β are two parameters in this relation showing the importance of each objective function. The nature of the problem requires the minimization of this function value.

4. 1. 3. Initialization To start the algorithm, we randomly initialize these chromosomes' genes and generate a population with n chromosomes. Each chromosome is regarded as a solution to the problem. We can calculate the value of the objective function using chromosomes. Here, the important issue is to preserve the constraints of the problem by chromosomes. In the following, we will discuss this issue.

4. 1. 4. Using Selection Operators In the next step, the chromosome selection is discussed. Considering the theories in the genetic area, to create the next

generation from the current population, we should select some chromosomes from this population for integration and replication that have higher optimality (each chromosome optimality is calculated using the fitness function). The better the chromosome, the greater its chance of being selected. The important point is that we should select a number of chromosomes from the current population and create the next generation accordingly. The most important point in this process is the way in which the chromosome is selected. There are different methods to select chromosomes, and each of which has its own advantages and disadvantages. These methods are as follows:

1. Elitist selection
2. Roulette selection
3. Scaling selection
4. Tournament selection

4. 1. 5. Using Reproduction Operators

combine the genetic information of two parents and generate their offspring. Crossover can be used to stochastically generate offspring from an existing population by combining the information of parents like what happens in sexual reproduction. The resulting offspring usually undergoes a mutation (stochastic change in the genes of offspring's chromosome) after the crossover operator to achieve the final result. Different genetic-based algorithms use various data structures to store genetic information, and using different types of crossover operators, new combinations can be created in each of these genetic representations.

Usually the crossover operator is used on bit array data structures, vectors of real numbers, and trees. There are different types of crossover as follows:

1. Single point crossover
2. K points cross over
3. Flat crossover
4. Crossover for ordered lists

4. 1. 6. Observing the Problem's Constraints

Two techniques are used to observe the problem's constraints. The first technique is observing the constraints implicitly using the algorithm design method. Calculation of I_{it} and S_{it} after initialization or updating chromosomes leads to the implicit observation of the constraint (3). After each genetic operator is executed, the dimension of X matrix becomes symmetric in terms of the two first dimensions, and Y also becomes updated accordingly to observe the constraint (5). Y is binary and this leads to the observation of constraint (6). By calculating the amount of matrix Qp from relation (7),

| | | | | | | | | | | | | | |
|---|-----|-----|-------|----|---|---|---|---|---|---|---|---|---|
| N | N-1 | N-2 | | 10 | 9 | 8 | 7 | 6 | 5 | 4 | 3 | 2 | 1 |
| 0 | 1 | 1 | | 0 | 1 | 1 | 0 | 1 | 0 | 0 | 0 | 1 | 0 |

Figure 3. An example of the first dimension of X variable in the GA chromosome of the proposed method

this constraint can also be observed. In the first dimension of Y , if the first gene is zero, the other genes are also considered to be zero to meet the constraint (10). We substitute the main diagonal of the first and second dimensions of X and the first gene of the second dimension of Q with zero. Therefore, the constraint (12) is also true. Due to the way in which the chromosomes are defined, constraint (13) is also always true. If constraints (8), (9), and (11) are not observed by a chromosome, then we consider the fitness value to be infinite to gradually get distance from solutions and create solutions by observing all constraints. The proposed model flowchart is illustrated in Figure 4.

5. NUMERICAL REPRESENTATION

In this part, we present a small example for optimal solution. Suppose that a supply chain is composed of 5

retailers. The travel distances are given in Table 2. The routes' matrix is an asymmetric directed graph. It means that the roads can be one-way. The deterioration and reorder ratios are supposed to be 0.05 and 0.2, respectively. Table 3 shows the unit maintenance cost, unit repayment and *lost sales cost* (LSC) (in terms of the monetary unit per period per product), initial inventory (product unit) and predicted demand (product unit) for each retailer within five periods. The constant and variable costs (in terms of the monetary unit per product per Km), capacity (product unit), and the value of each vehicle (monetary unit) are shown in Table 4. Due to practical reasons, the delivery lots (Q_d) and vehicle (Q_p) are assumed to be multipliers of 50 and 5, respectively. The unit pickup cost for all vehicles is set at 0.1 (monetary unit). The price of each unit of product is equal to 1000 (monetary unit). Additionally, it is assumed that the orders can be ordered at most until the last period. The proposed model and formulation should be applied based on these data.

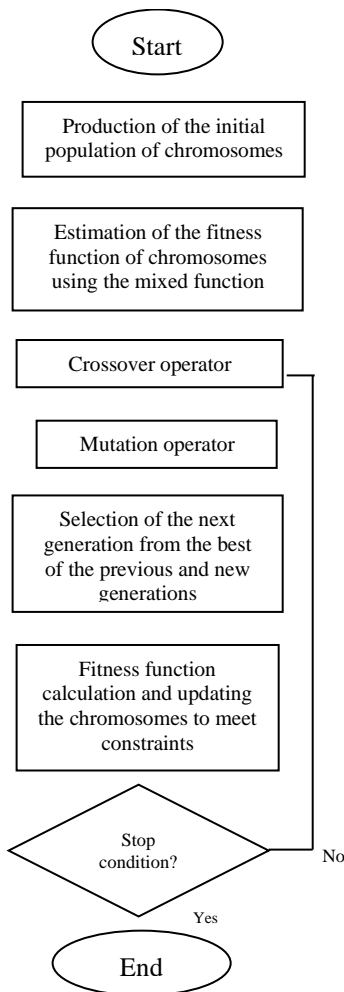


Figure 4. The proposed model flowchart

TABLE 2. Distances between nodes d_{ij} (Km)

| node | 0 | S1 | S1 | S1 | S1 | S1 |
|------|----|----|----|----|----|----|
| 0 | - | 31 | - | 73 | 21 | 31 |
| S1 | 31 | - | - | - | 13 | 62 |
| S2 | 78 | - | - | - | 90 | - |
| S3 | 73 | - | - | - | 62 | 96 |
| S4 | 21 | 13 | 90 | 62 | - | - |
| S5 | 31 | 62 | - | 96 | - | - |

TABLE 3. Retailers' data

| # | IC_i | I_0 | Demand in time period t | | | | | π'_i | π_i | h_i |
|---|--------|-------|-------------------------|-----|-----|-----|-----|----------|---------|-------|
| | | | 1 | 2 | 3 | 4 | 5 | | | |
| 1 | 300 | 0 | 0 | 470 | 310 | 100 | 0 | 200 | 20 | 22 |
| 2 | 500 | 0 | 500 | 0 | 120 | 480 | 120 | 100 | 10 | 12 |
| 3 | 300 | 0 | 0 | 150 | 320 | 0 | 390 | 400 | 40 | 25 |
| 4 | 500 | 0 | 210 | 0 | 230 | 0 | 115 | 200 | 20 | 30 |
| 5 | 300 | 0 | 330 | 120 | 0 | 180 | 0 | 100 | 10 | 15 |

TABLE 4. Retailers' data

| Vehicle | f_k | fc_k | vc_k | cv_k |
|---------|--------|--------|--------|--------|
| 1 | 50000 | 400 | 0.1 | 120 |
| 2 | 70000 | 600 | 0.08 | 210 |
| 3 | 90000 | 700 | 0.06 | 270 |
| 4 | 100000 | 800 | 0.04 | 380 |
| 5 | 150000 | 900 | 0.02 | 530 |

As the proposed model is a multi-objective IRP and the calculation time to determine the solution severely depends on the dimensions of the problem, we develop the proposed algorithm using a compromise programming (lp-metrics) algorithm that enables the proposed GA to generate Pareto solutions. In GA, the fitness function is a criterion to assess the quality of solutions (chromosomes). As the proposed model is a two-objective programming, we have two unaligned fitness functions. As explained before, we merge both objectives to create a single fitness function called lp-metrics. This fitness function is the weighted sum of the normalized deviation of each objective function from its optimum value. The optimum values are separately obtained by running GA and the fitness function is set on its corresponding objective function.

The proposed model and formulation are solved under the MATLAB programming language using CPLEX and the proposed algorithm. By considering only three periods and solving the provided example twice for objective functions, the optimum values are obtained for each of them and allow you to build the lp-metric model:

$$l_p - metrics = w \times \left| \frac{z_1 - 14509}{326070 - 14509} \right| + (1 - w) \times \left| \frac{z_2 - 6696}{28551 - 6696} \right| \quad (15)$$

Here (1-w) means that how much the decision maker is concerned over the second objective function in comparison to total costs. After that, we solve the lp-metric problem under w=0.8 (as a clear example) and show the results in Tables 5, 6 and 7 report the details of the optimal solution of the problem for w=1 and w=0.8.

For w=0.8, the economic performance of the system forms 80% of the priority of the decision makers and the route reduction accounts for 20%. Under this value of w, according to Table 5, the values for Z1 and Z2 are equal to 29612 and 8406, respectively. By changing the relative weight (w), different solutions can be obtained.

TABLE 5. Result of the example problem

| Min lp-metric (w= 0.8) | Min Z ₂ (w= 0) | Min Z ₁ (w= 1) | |
|------------------------|---------------------------|---------------------------|----------------------|
| 29612 | 325690 | 14509 | Z₁ |
| 84.6 | 6451 | 2891 | Z₂ |

TABLE 6. The best solution for w=1

| Period 1 | | Period 2 | | Period 3 | |
|------------------------|-------|------------------------|-------|------------------------|-------|
| X _(i,j,k,t) | Value | X _(i,j,k,t) | Value | X _(i,j,k,t) | Value |
| X(0, 4, 2, 1) | 1 | X(0, 4, 2, 2) | 1 | X(0, 4, 2, 3) | 1 |
| X(4, 2, 2, 1) | 1 | X(4, 2, 2, 2) | 1 | X(4, 2, 2, 3) | 1 |
| X(2, 0, 2, 1) | 1 | X(2, 0, 2, 2) | 1 | X(2, 0, 2, 3) | 1 |
| X(0, 4, 4, 1) | 1 | X(0, 4, 3, 2) | 1 | X(0, 1, 4, 3) | 1 |

| | | | | | |
|--------------------------------|--------------|--------------------------------|--------------|--------------------------------|--------------|
| X(4, 0, 4, 1) | 1 | X(4, 3, 3, 2) | 1 | X(1, 4, 4, 3) | 1 |
| X(0, 1, 5, 1) | 1 | X(3, 5, 3, 2) | 1 | X(4, 0, 4, 3) | 1 |
| X(1, 5, 5, 1) | 1 | X(5, 0, 3, 2) | 1 | X(0, 1, 5, 3) | 1 |
| X(5, 0, 5, 1) | 1 | X(0, 1, 5, 2) | 1 | X(1, 4, 5, 3) | 1 |
| - | - | X(1, 0, 5, 2) | 1 | X(4, 3, 5, 3) | 1 |
| - | - | - | - | X(3, 5, 5, 3) | 1 |
| - | - | - | - | X(5, 0, 5, 3) | 1 |
| - | - | - | - | - | - |
| <i>Qd</i> _(i,j,k,t) | Value | <i>Qd</i> _(i,j,k,t) | Value | <i>Qd</i> _(i,j,k,t) | Value |
| Qd(2, 2, 1) | 200 | Qd(2, 2, 2) | 200 | Qd(4, 2, 3) | 50 |
| Qd(4, 4, 1) | 350 | Qd(3, 3, 2) | 150 | Qd(2, 2, 3) | 150 |
| Qd(5, 5, 1) | 400 | Qd(5, 3, 2) | 50 | Qd(1, 4, 3) | 300 |
| - | - | Qd(1, 5, 2) | 500 | Qd(4, 4, 3) | 50 |
| - | - | - | - | Qd(4, 5, 3) | 150 |
| - | - | - | - | Qd(3, 5, 3) | 350 |
| <i>Qp</i> _(i,j,k,t) | | <i>Qp</i> _(i,j,k,t) | | <i>Qp</i> _(i,j,k,t) | |
| Qp(4, 5, 1) | 140 | - | - | Qp(1, 5, 1) | 15 |

TABLE 7. The best solution for w=0.8

| Period 1 | | Period 2 | | Period 3 | |
|--------------------------------|--------------|--------------------------------|--------------|--------------------------------|--------------|
| X _(i,j,k,t) | Value | X _(i,j,k,t) | Value | X _(i,j,k,t) | Value |
| X(0, 4, 3, 1) | 1 | X(0, 1, 4, 2) | 1 | X(0, 4, 3, 3) | 1 |
| X(4, 1, 3, 1) | 1 | X(1, 5, 4, 2) | 1 | X(4, 0, 3, 3) | 1 |
| X(0, 5, 4, 1) | 1 | X(5, 0, 4, 2) | 1 | X(0, 1, 4, 3) | 1 |
| X(5, 0, 4, 1) | 1 | X(0, 1, 5, 2) | 1 | X(1, 4, 4, 3) | 1 |
| X(0, 4, 5, 1) | 1 | X(1, 4, 5, 2) | 1 | X(4, 2, 4, 3) | 1 |
| X(4, 2, 5, 1) | 1 | X(4, 3, 5, 2) | 1 | X(2, 0, 4, 3) | 1 |
| X(2, 0, 5, 1) | 1 | X(3, 0, 5, 2) | 1 | X(0, 3, 5, 3) | 1 |
| - | - | - | - | X(3, 5, 5, 3) | 1 |
| - | - | - | - | X(5, 1, 5, 3) | 1 |
| - | - | - | - | X(1, 4, 5, 3) | 1 |
| - | - | - | - | X(4, 2, 5, 3) | 1 |
| - | - | - | - | X(2, 0, 5, 3) | 1 |
| <i>Qd</i> _(i,j,k,t) | Value | <i>Qd</i> _(i,j,k,t) | Value | <i>Qd</i> _(i,j,k,t) | Value |
| Qd(4, 3, 1) | 250 | Qd(1, 4, 2) | 150 | Qd(4, 3, 3) | 250 |
| Qd(5, 4, 1) | 350 | Qd(5, 4, 2) | 100 | Qd(1, 4, 3) | 300 |
| Qd(2, 5, 1) | 500 | Qd(1, 5, 2) | 350 | Qd(2, 4, 3) | 50 |
| - | - | Qd(3, 5, 2) | 150 | Qd(3, 5, 3) | 350 |
| - | - | - | - | Qd(2, 5, 3) | 100 |
| <i>Qp</i> _(i,j,k,t) | | <i>Qp</i> _(i,j,k,t) | | <i>Qp</i> _(i,j,k,t) | |
| Qp(4, 5, 1) | 40 | - | - | Qp(1, 5, 1) | 15 |

5. 1. Evaluation of the Performance of the Proposed Method

As we observed in the fitness relation, there are two objective functions that must be minimized. At first, the proposed algorithm calculates the fitness function of the initial population. In each iteration, the best chromosomes are selected for the next generation and if in up to 10 consecutive chromosome replications no chromosome with better performance than the best chromosome in the previous step was generated, the optimization algorithm is stopped. Another stopping condition is to pass a certain amount of iterations. We considered the number of iterations to be 1000. Obviously, the minimum amount of fitness is zero, and if a chromosome can be found with this fitness, the algorithm must be terminated as its continuation is meaningless.

5. 2. Performance Evaluation

By changing the GA parameters, the obtained amount for fitness also changes. We seek the most optimum possible case i.e., the minimum value. In Table 8, we examined the amount of the system fitness for the possibility of different crossovers and obtained the best value.

Another important parameter of GA is the possibility of mutation. As the mutation increases, scanning increases in algorithm such that, as compared to before, the algorithm generates different solutions and may reach the better or even worse solutions than parents. Therefore, the following change is observed.

Figure 5 shows the process of achieving the best filter using the proposed algorithm. It is necessary to mention that in running the GA, the probability of crossover and mutation was 0.8 and 0.3, respectively (Tables 8 and 9). We used a single-point crossover such that 80% of the best chromosomes are combined. In this combination, two chromosomes are broken from a random point and linked together, and two new chromosomes are produced. To select chromosomes, the tournament selection operator was used for performing crossover in which a sub-set of the people in a population is selected and the members compete with each other. Finally, only one person from each sub-group is selected for production. In the proposed method, the number of the members within each set was considered 3.

TABLE 8. Fitness per the possibility of different crossovers

| Crossover possibility | Fitness value |
|-----------------------|---------------|
| 0.5 | 27869 |
| 0.6 | 26412 |
| 0.7 | 25893 |
| 0.8 | 25370 |
| 0.9 | 2601 |

TABLE 9. Fitness for the possibility of different mutations

| Mutation possibility | Fitness value |
|----------------------|---------------|
| 0.05 | 26231 |
| 0.1 | 2610 |
| 0.15 | 25760 |
| 0.2 | 25632 |
| 0.25 | 25399 |
| 0.3 | 25370 |
| 0.35 | 25422 |

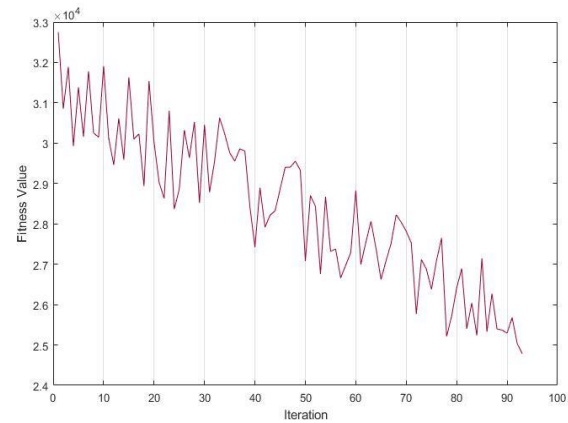


Figure 5. The process of getting access to the near optimal solution using the proposed algorithm

As shown in Figure 5, the proposed algorithm goes through a very good process to acquire a more appropriate solution, and finally in the iterations above 90, it reaches the value of the fitness function for the best member.

5. 3. Comparison

To show the efficiency of the proposed meta-heuristic method, 15 testing problems with different dimensions were generated and solved using the proposed algorithm in the previous chapter, and compared with the lower bound of CPLEX. The proposed method was coded in MATLAB R2018a and all computations were run under Microsoft Windows 10. The number of retailers and periods range from 5, 2 (in problems with small sizes) to 50, 12 (in large problems), respectively. At first, each problem was solved using the lp-metrics method via CPLEX, and then was solved using the proposed GA. The variable cost and demand were respectively generated between (0-130) and (0-500). Table 10 displays the best values of the first objective function of the two algorithms (AOV^1_{LP}, AOV^1_{GA}) and the second objective function of the two algorithms (AOV^2_{LP}, AOV^2_{GA}).

TABLE 10. Fitness of methods

| # | Retailers | Period | GA | | CPLEX | |
|----|-----------|--------|------------------|------------------|------------------|------------------|
| | | | AOV ¹ | AOV ² | AOV ¹ | AOV ² |
| 1 | 5 | 2 | 67752 | 1235 | 84976 | 1821 |
| 2 | 5 | 3 | 68012 | 1935 | 92577 | 3171 |
| 3 | 6 | 3 | 74213 | 2781 | 76852 | 4144 |
| 4 | 10 | 5 | 78201 | 4331 | 80434 | 5323 |
| 5 | 12 | 6 | 84102 | 5651 | 85957 | 7377 |
| 6 | 15 | 6 | 91110 | 6381 | 93207 | 10354 |
| 7 | 18 | 9 | 96555 | 9152 | 996312 | 10731 |
| 8 | 20 | 9 | 111445 | 10242 | 121605 | 10921 |
| 9 | 22 | 9 | 112606 | 11245 | 123763 | 11638 |
| 10 | 24 | 10 | 119024 | 14524 | 145867 | 15531 |
| 11 | 26 | 10 | 130417 | 15241 | 153808 | 15431 |
| 12 | 28 | 10 | 139907 | 16324 | 163475 | 16645 |
| 13 | 30 | 11 | 203447 | 17542 | 211913 | 18445 |
| 14 | 30 | 12 | 294103 | 21321 | 351621 | 22172 |
| 15 | 30 | 12 | 366211 | 22457 | 386841 | 24132 |

In the experimental results, we saw that the proposed method excels over CPLEX in all cases.

5. 4. Concluding Remarks

It is seen that the obtained fitness value also changes by changing the GA parameters. We seek the most optimum state i.e., the minimum value. The value of fitness for the crossover probability of 0.8 was obtained to be the best fitness. The other important parameter of GA is the probability of mutation. The algorithm with mutation probability of 0.3 generated the best solution using a single-point crossover and the tournament selection operator for performing crossover.

The number of retailers and periods range from 5 to 50, in 15 test beds. At first, each problem was solved using the lp-metrics method via CPLEX, and then was solved using the proposed GA. In this comparison, the proposed method showed a better performance in both objective functions.

6. CONCLUSION

There are still major challenges in resilient supply chain. Following up transportation operations from beginning to end is one of the challenges in this area. Products inventory management, routes determination, vehicle selection, etc., are among the problems to be considered in network design. In its traditional state, IRP minimizes the total inventory costs, but it does not take many items into account. The routing problem is a NP-hard problem, thus meta-heuristics should be used to solve it.

Distribution systems include all transportation stages. Research studies indicate that using up-to-date methods in distribution process planning leads to a significant amount of saving in all transportation costs. Making progress in technology whether in terms of hardware or software, and enhancing correlation in information systems in production and trade lead to success in the operation of the distribution network. The development of modeling instruments over recent years has also acted as a factor leading to further development. A proper model must take all the characteristics of the network in the real world into account and develop algorithms that find proper solutions for real instances within logical time. Meta-heuristics such as GA are a very suitable option for this issue.

The mathematical model of this research is of integer type that solves the perishable inventory routing problem. The proper route selection and the reduction of the improper transportation options are among the features of this model that reduce the total costs of the supply chain. The efficiency of the GA was assessed in the results. In fact, the time of finding the solution depends on the problem's dimensions because the proposed model is considered a multi-objective IRP. The GA-based method proposed here should preserve the constraints. The comparison in 15 problems showed a better performance by the proposed method compared to Cplex. It is suggested that researchers propose and compare other bi-objective algorithms and meta-heuristics to solve the problem using the formulation.

7. REFERENCES

1. Mills J., Schmitz J., Frizelle G., "A strategic review of supply networks", *International Journal of Operations and Production Management*, Vol. 24, (2004), 1012-1036.
2. Pfohl H. C., Köhler. H., Thomas D., "State of the art in supply chain risk management research: empirical and conceptual findings and a roadmap for the implementation in practice", *Logistics Research*, Vol. 2, (2010), 33-44, doi: 10.1590/0104-530X3800-20.
3. Mensah P., Merkurjev Y., "Developing a resilient supply Chain", *Procedia-Social and Behavioral Sciences*, Vol. 110, (2014), 309-319, doi: 10.1108/09600030410545436.
4. Christopher M., "Creating resilient supply chains", *Logistics Europe*, Vol.12, (2014), 14-21.
5. Rajesh R., "Supplier selection in resilient supply chains: a grey relational analysis approach", *Journal of Cleaner Production*, Vol. 86, (2015), 343-359, doi:10.1016/j.jclepro.2014.08.054.
6. Sawik T., "Selection of resilient supply portfolio under disruption risk", *Omega*, Vol. 41, (2013), 259-269, doi: 10.1016.
7. Melnyk. S, Closs. D. J, Griffis.S. E, Zobel. C. W, Macdonald. J. R, "Understanding supply chain resilience. *Supply Chain Management Review*, Vol. 18, (2014), 34-41.
8. Delfani F., Kazemi A., Seyedhosseini S. M., Niaki S. T. A., "A Green Hazardous Waste Location-routing Problem Considering the Risks Associated with Transportation and Population", *International Journal of Engineering, Transactions B:*

- Applications*, Vol. 33, No. 11, (2020), 2272-2284, doi: 10.5829/IJE.2020.33.11B.18.
9. Akbarzadeh Z., Safaei Ghadikolaie. A.H, Madhoushi. M, Aghajani. H, "A Hybrid Fuzzy Multi-criteria Decision Making Model Based on Fuzzy DEMATEL with Fuzzy Analytical Network Process and Interpretative Structural Model for Prioritizing LARG Supply Chain Practices", *International Journal of Engineering, Transactions C: Aspects*, Vol. 32, No. 3, (2019), 413-423. doi: 10.5829/ije.2019.32.03c.09
 10. Hillmann J., Guenther E., "Organizational resilience: a valuable construct for management research?", *International Journal of Management Reviews*, Vol. 23, (2020), 7-44, doi:10.1111/ijmr.12239.
 11. Fasey K. J., Sarkar M., Wagstaff C. R., Johnston J., "Defining and Characterizing organizational resilience in elite sport", *Psychology of Sport and Exercise*, Vol. 52, (2021), 101834, doi: 10.1016.
 12. Douglas S., "Building organizational resilience through human capital management strategy", *Development and Learning in Organizations: An International Journal*, (2021), doi: 10.1108.
 13. Ungar M., "Multisystemic resilience: Adaptation and transformation in contexts of change", Oxford University Press: USA, 2021.
 14. Masten A. S., "Resilience in developing systems: The promise of integrated approaches", *European Journal of Developmental Psychology*, Vol. 13, (2016), 297-312, doi: 10.1080/17405629.
 15. Orth D., Schuldis. P. M., "Organizational learning. and unlearning capabilities for resilience during COVID-19", *The Learning Organization*, (2021), doi: 10.1108.
 16. Ngoc Su. D., Luc Tra. D., Thi Huynh H. M., Nguyen H. H. T., O'Mahony. B, "Enhancing resilience in the Covid-19 crisis: lessons from human resource management practices in Vietnam", *Current Issue in Tourism*, (2021), 1-17, doi: 10.1080/13683500.
 17. Khan I. U., Hameed Z., Hamayun M., "Investigating the acceptance of electronic banking in the rural areas of Pakistan: An application of the unified model", *Business and Economic Review*, Vol. 11, (2019), 57-87, doi: 0.22547/BER/11.3.3.
 18. Tallaki M., Bracci E., "Risk Perception, Accounting, and Resilience in Public Sector Organizations: A Case Study Analysis", *Journal of Risk and Financial Management*, Vol. 14, (2021), doi: 10.3390/jrfm14010004.
 19. Soni U., Jain V., Kumar S., "Measuring supply chain resilience using a deterministic modeling approach", *Computers & Industrial Engineering*, Vol. 74, (2014), 11-25, doi: 10.1016/.
 20. Jalali G., Tavakoli-Moghaddam R., Ghomi-Avill. M, Jabbarzadeh. A., "A Network Design Model for a Resilient Closed- Loop Supply Chain with Lateral Transshipment", *International Journal of Engineering*, Vol. 30, (2017), 374-383.
 21. Wei R., Liu C., "Research on carbon emission reduction in road freight transportation sector based on regulation-compliant route optimization model and case study", *Sustainable Computing: Informatics and Systems*, Vol. 28, (2022), doi: 10.1016.100408.
 22. Kuang Z., Lian Z., Lien J. W., Zheng J., "Serial and parallel duopoly competition in multi-segment transportation routes", *Transportation Research Part E: Logistics and Transportation Review*, Vol. 133, (2020), doi: 10.1016.101821.
 23. Schenekemberg C. M., Scarpin C.T., Pécora Jr. J.E., Guimarães T. A., Coelho L. C., "The two-echelon inventory-routing problem with fleet management", *Computers and Operations Research*, Vol. 121, (2020), doi: 10.1016.104944.
 24. Alvarez A., Cordeau J. F., Jans R., Munari P., Morabito R., "Inventory routing under stochastic supply and Demand", *Omega*, Vol. 102, (2020), doi:10.1016.102304.
 25. Yavari M., Enjavi H., Geraeli M., "Demand management to cope with routes disruptions in location-inventory-routing problem for perishable products", *Research in Transportation Business & Management*, Vol. 37, (2020), doi: 10.1016.100552.
 26. Ji Y., Du J., Han X., Wu X., Huang R., Wang S., Liu Z., "A mixed integer robust programming model for two-echelon inventory routing problem of perishable products", *Physica A: Statistical Mechanics and its Applications*, Vol. 548, (2020), doi: 10.1016.124481.
 27. Eide L., Årdal G. C. H., Evsikova N., Hvattum L. M., Urrutia S., "Load-dependent speed optimization in maritime inventoryRouting", *Computers and Operations Research*, Vol. 123, (2020), doi:10.1016.105051.
 28. Ortega E. J. A., Schilde M., Doerner K. F., "Matheuristic search techniques for the consistent inventory routing problem with time windows and split deliveries", *Operations Research Perspectives*, Vol. 7, (2020), doi:10.1016.100152.
 29. Golshefidi A. H., Jokar M. R. A., "A robust optimization approach for the production-inventory-routing problem with simultaneous pickup and delivery", *Computers & Industrial Engineering*, Vol. 143, (2020), doi: 10.1016.106388.
 30. Pitakaso R., Sethanan K., Theeraviriya C., "Variable Neighborhoodstrategy adaptive search for solving green 2-echelon location routing problem", *Computers and Electronics in Agriculture*, Vol. 173, (2020), doi:10.1016.105406.
 31. Trachanatzis D., Rigakis M., Marinaki M., Marinakis Y., "A firefly algorithm for the environmental prize-collecting vehicle routing problem", *Swarm and Evolutionary Computation*, Vol. 57, (2020), doi:10.1016.100712.
 32. Wei X., Qiu H., Wang D., Duan J., Wang Y., Cheng. T. C. E., "An integrated location-routing problem with post-disaster relief Distribution", *Computers and Industrial Engineering*, (2020), 147, doi:10.1016.106632.

Persian Abstract

چکیده

زنجیره تامین تاب‌آور، قابلیت‌های فراوانی برای عبور از بحران‌های مالی و تامین و توزیع محصولات برای شرکت‌ها قائل می‌شود. در این مطالعه، ما به یک مسئله تخصیص توزیع موجودی برای سیستم شبکه توزیع که شامل یک کارخانه، تعدادی محل بالقوه برای مراکز توزیع و تعدادی خرده فروش است می‌پردازیم. فرض بر این می‌باشد تقاضای مشتریان برای تمام دوره‌ها به صورت قطعی و مشخص است. اما مدت زمان آن در افق برنامه‌ریزی محدود متفاوت است. مدل پیشنهادی این تحقیق به صورت یک مدل برنامه‌ریزی عدد صحیح مختلط خطی و با دو تابع هدف مدلسازی می‌شود. که در تابع هدف اول مجموع هزینه‌های کل سیستم توزیع را در افق برنامه‌ریزی حداقل می‌کند و تابع هدف دوم به دنبال حداقل کردن اختلاف حداکثر و حداقل مسافت طی شده توسط وسایل نقلیه در طول افق برنامه‌ریزی است بنابراین مدل سعی دارد با استفاده از بهترین پیکربندی مسیرها و گزینه حمل و نقل، تقاضا را برآورده کند و هزینه‌ها را به طور همزمان کاهش دهد. برای حل مسئله از یک مثال کوچک استفاده کرده و آن را با نرم افزار MATLAB حل و سپس مسئله را توسعه داده و از آنجائیکه مسأله مسیریابی یک مسأله سخت یا NP HARD می‌باشد، برای حل آن از روش‌های حل فراابتکاری استفاده می‌شود. در این مدل عواملی چون: حجم تقاضا برای هر مشتری در یک دوره در شبکه، ظرفیت وسیله نقلیه، ظرفیت کارخانه، هزینه ثابت حمل و نقل، هزینه متغیر حمل و نقل و غیره به عنوان عوامل مؤثر بر مدل مد نظر قرار گرفته است. نتایج نشان می‌دهد که مدل ارائه شده در شبکه می‌تواند به عنوان اهرمی برای افزایش عملکرد شبکه تامین اقتصادی از طریق صرفه‌جویی در مسیرها استفاده شود.



Effect of Cutting Environment and Swept Angle Selection in Milling Operation

Z. A. Zailani^{a,b}, N. S. N. Rusli^a, N. A. Shuaib^{a,c}

^a Faculty of Mechanical Engineering and Technology, Universiti Malaysia Perlis, 02600, Arau, Perlis, Malaysia

^b Sustainable Manufacturing Technology Research Group, Faculty of Mechanical Engineering Technology, Universiti Malaysia Perlis, Arau, Perlis, Malaysia

^c Green Design and Manufacture Research Group, Center of Excellence Geopolymer & Green Technology (CEGeoGTech), Universiti Malaysia Perlis, Kangar, Perlis, Malaysia

PAPER INFO

Paper history:

Received 23 February 2021

Received in revised form 19 August 2021

Accepted 25 August 2021

Keywords:

Milling

Minimum Quantity Lubrication

Dry Cutting

Swept Angle

Tool Wear

ABSTRACT

Cutting fluids are frequently aimed to enhance machinability through cooling, lubricating and flushing actions. However, their use in machining creates major concerns in terms of health footprint and environmental effects throughout their lifecycle. Alternative methods, such as dry cutting and minimum quantity lubrication, were used to mitigate these issues. This research also will investigate the effect of swept angle selection, 30% and 60% of tool diameter step over under different cutting conditions during milling of aluminium alloy material. Their impact on tool wear, surface roughness, burr and chip formation were compared. Results pointed that the application of lower swept angle in conjunction with minimum quantity lubricant system has significantly reduced tool wear, decreased burr and chip formation, as well as improved surface quality as compared to dry machining. The work clearly shows how the importance of swept angle selection and cutting condition in refining machining performance could improve the machinability of the material.

doi: 10.5829/ije.2021.34.12c.02

NOMENCLATURE

| | | | |
|-------|---------------------|-------|-------------------------------------|
| L_c | length of chip | R_a | surface roughness arithmetical mean |
| V_B | flank wear | W_b | burr width |
| r_e | cutting edge radius | | |

1. INTRODUCTION

In machining processes, cutting fluids are commonly used for cooling, removing metal particles, reducing friction, and protecting the tool, workpiece and machine tool [1]. In addition, it is also responsible for a variety of secondary functions, such as transporting chips, cleaning of tools, workpieces, and fixtures. However, some drawbacks have also been correlated with the use of cutting fluids because of their cost, environmental impact, and hazards to workers [2]. Additionally, this cutting fluid also has a harmful impact on health such as leukemia, skin cancer, lung cancer, asthma etc. [3]. Therefore, numerous substitutions to the conventional cutting fluids are currently being explored in the industry.

New methods have been developed over the past decades to address the major difficulties of cutting fluids. The key alternatives such as dry machining and minimum quantity lubrication (MQL) were commonly evaluated from a technical point of view and have been found as viable substitutes in optimizing machining performance as well as diminishing hazards [4]. To avoid risky cutting fluids during the machining process, dry machining is appointed. This owing to its benefit that translated into zero pollution when no need a cost for coolant, its maintenance, and disposal [5]. Nevertheless, dry machining causes excessive temperature increases which leads to poor tool life and damage to the machined surface [6]. Wherever it is not possible to completely remove cutting fluids, a very small amount of lubrication,

*Corresponding Author Institutional Email: zailani@unimap.edu.my
(Z. A. Zailani)

pulverized only at a required point, which is known as Minimum Quantity Lubrication Machining (MQL), is used [7]. This method helps to improve surface finish quality and tool life, minimize lubrication costs, and decrease tool wear and cutting temperature.

Aluminium makes up about 70% of the whole Boeing 777 [8]. The main factor for its use is its high strength-to-weight ratio. However, the use of aluminum, whose high thermal conductivity combined with extreme adherent tendency causes excessive heat generation at the cutting zone, and difficulties in heat dissipation [9]. Common issues in the machining of aluminum alloys are built-up edge and adhesion of the material to cutting tool due to high ductility and thermal conductivity of the work material [10].

Milling is one of the most popular common manufacturing processes to remove material from a workpiece with a rotary cutter by moving towards an angle with the machine axis [11]. Due to the various degree-of-freedom in the milling process, complex structures could be produced. In milling, cutting speed, spindle speed, depth of cut, and feed rate are the main governing parameters [12]. The relationship between the cutting tool and surface quality is also closely related. In addition, cutting parameters, tool life, machine tool characteristics, process variables, and workpiece materials all played a role in mechanical machining. It is a key performance metric that monitors surface integrity and ready-to-use consumer aesthetics [13]. Although the swept angle is one of the main parameters that determine the tool wear, surface roughness, burr and chip formation characteristics, its importance has not been well investigated and documented in the literature.

Swept angle or tool engagements are identified as part of the tool involved in the workpiece during the process of machining which the swept angle is an important factor that affects the tool wear, surface roughness, chip formation, and burr formation during slot milling. Hence, when the cutting tool and workpiece are fully engaged, the resulting effect would be greater [14]. Therefore, the purpose of this research is to perform an experimental study on the effect of the swept angle selection under the different cutting conditions in the milling process. The following sections will provide a detailed explanation for the study.

2. EXPERIMENTAL DETAILS

2. 1. Experimental Setup and Machining Conditions

The workpiece material selected to be machined was a rectangular aluminium alloy 7075 with dimensions of 150 mm width, 150 mm length, and 4 mm height. 4-flutes end mill high speed steels (HSS) cutting tool with 4.0 mm diameter was used. This experiment

was conducted using Tongtai EZ-5A CNC Milling Machine. A constant cutting velocity of 63 m/min, table feed rate of 440 mm/min, and depth of cut of 1 mm were used as established from pilot tests.

Two different cutting conditions were studied, namely dry and minimum quantity lubricant (MQL) with base lubricant (Solcut oil). For MQL, the nozzle was placed at the tool entry point to enhance oil entrapment [15]. The flow rate was 40 ml/h with a compressed air pressure of six bar. In this experiment, two values of swept angle were used for each condition; 30% and 60% of tool diameter stepover. Each condition was repeated three times using new cutting tools.

2. 2. Swept Angle Selection A swept angle refers to the percentage of the tool that engages in the machining process with the workpiece. The values will be chosen using Equation (1):

$$\text{Swept angle} = \frac{\text{tool step over (\%)}}{100} \times \text{tool diameter} \quad (1)$$

Figure 1 shows the swept angle of the cutting tool on the workpiece which consists of 66.4° (30% tool diameter stepover) and 101.5° (60% tool diameter stepover). Both stepovers were selected to signify high and low angle of engagement.

2. 3. Tool Wear, Cutting-edge Radius, Surface Roughness, Burr Formation and Chip Length

Every tool and workpiece for each cutting condition was then examined using Xoptron XST60 Stereo Microscopy System to capture tool wear, burr and chip formation. Flank wear (V_B) were measured on the side flank face, and cutting-edge radius (r_c) was determined by placing the best-fitting circle at the tool flank face intersection. While a width of burr formation (W_b) was measured for top burr. Then, the length of chip formation (L_c) was also quantified. For all measurements, a Java-based image processing, Image J software was used concurrently. A Mitutoyo F-3000 surface roughness tester was used to measure surface roughness using arithmetical mean (R_a) value. Systematic uncertainties were minimized by first calibrating the equipment to be used. In addition, random vagueness was addressed by performing each measurement at least five times.

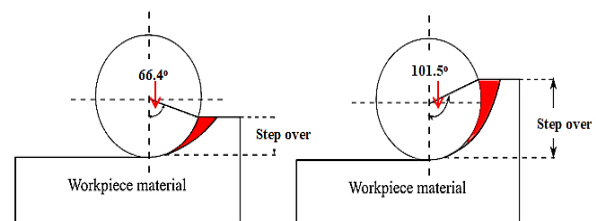


Figure 1. Swept angles of the cutting tool on the workpiece

3. RESULT AND DISCUSSION

3. 1. Tool Wear Modes Optical images were used to identify the wear modes after milling ten consecutive slots. In this experiment, several types of wear were found i.e. outer corner wear, crater wear, chipping, and flank wear. Among all wear modes, the most dominant was flank wear. Figure 2 shows examples of wear modes that could be witnessed on the cutting tools. The main reason for these occurrences is due to high force and continuous contact between the tool and the workpiece during penetration that lead to heat generation through frictional action. It is pertinent to note that the thermal property (i.e. conductivity) of the HSS cutting tool is significantly lower than aluminum workpiece, therefore, most of the heat that generated in all shear zones are likely to circulated in the workpiece. This situation would soften the workpiece material thus resulting in welded chips or material adhesion that cause build-up in the flute area specifically under dry cutting. This phenomenon could drive to premature process disturbances.

3. 2. Tool Flank Wear For the flank wear measurements, the tools were imaged from the bottom face. The results have shown that the flank wear (VB) was significantly affected by the swept angles and cutting conditions. Figure 3 shows the average flank wear growth for different swept angles and cutting conditions.

It can be seen clearly that machining under dry cutting condition shows a substantial amount of wear on the flank surface, as shown in Figure 4. Meanwhile, machining under MQL confronts lesser values under similar parametric settings condition. This is due to the fact that the oil which acts as a cooling and lubricating agent could significantly reduce the temperature and frictional forces between the cutting tool and workpiece.

It can be observed that under MQL condition the cutting-edge shape was relatively sharper compared to dry cutting which was rounded in shape.

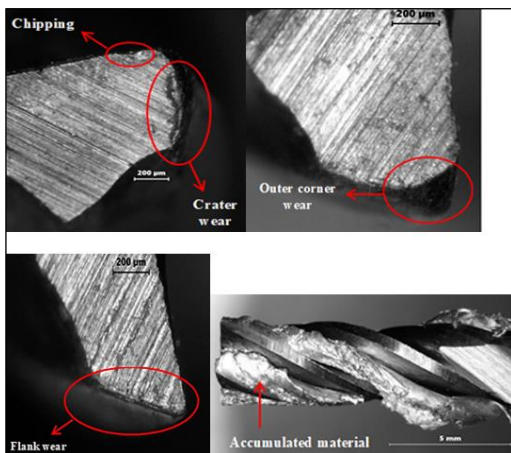


Figure 2. Tool wear modes

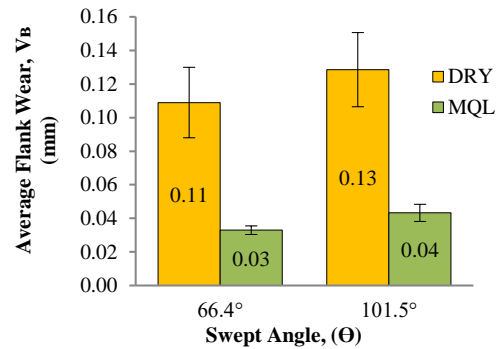


Figure 3. Average flank wear under different swept angles and cutting conditions

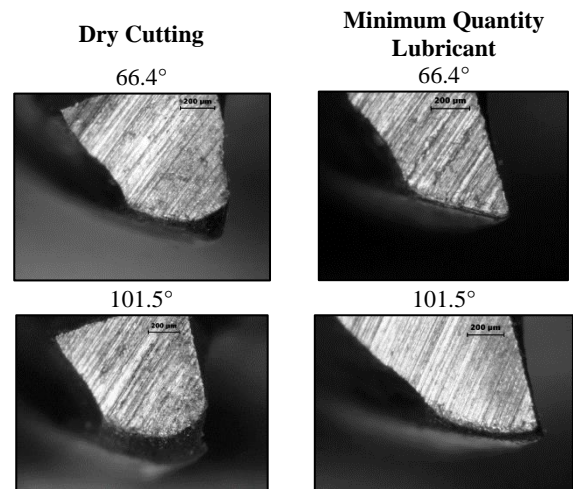


Figure 4. Tool wear growth for both different swept angles and cutting conditions

The highest flank wear was attained under swept angle 101.5° for both cutting conditions. This has happened for the reason that an increase in swept angle leads to excessive tool loading and deflection, thus resulting in an increase in tool wear. As a result, the both cutting condition (dry and MQL) display a slight increment. With 66.4° swept angle, the average flank wear was lowered by 15% and 25% respectively under dry and MQL condition. Despite a significant difference in flank wear values, both conditions are acceptable according to ISO 8688-2 [16], which is below 0.3 mm. It is also noted that the flank wear in the cutting process with both swept angles 66.4° and 101.5° under MQL condition is significantly lower compared to dry condition. In addition, the use of the smaller value of swept angle also contributes to lesser flank wear.

3. 3. Cutting Edge Radius Cutting edge radius was also used to monitor the tool condition since it is an appropriate indicator of the amount of tool wear. The edge corner radius of the tool was measured by fitting a

circle tangent line to straight lines. In this experiment, edge radius (r_e) deterioration was found on the tool cutting edge. Figure 5 shows the changes of cutting-edge deterioration for both conditions after machining processes.

Figure 6 shows the changes of cutting-edge radius for both swept angles and cutting condition. In this figure, more effective cutting-edge radius occurred when using the swept angle of 66.4° compared to the swept angle of 101.5° . But, the values for dry and MQL (after machining) shows prominent changes, especially under dry condition. Furthermore, as expected, the higher swept angle implied a higher value of r_e , which increased by 90% and 68% under dry and MQL conditions, respectively, when compared to the lower swept angle. Dry cutting contributed to higher r_e due to lack of lubricating and cooling action that led to higher specific cutting energy. In general, the result showed that the use of a lower swept angle has resulted in lowering tool wear by retaining the sharp edges for both conditions.

3. 4. Surface Roughness Surface roughness (R_a) is a measured parameter that can be used to analyze the

quality of the machining process. It should be noted that roughness quality sturdily depends on feed per tooth and tool edge radius. In this experiment, average surface roughness was measured at three main points, i.e. entry, middle, and exit. Figure 7 shows the variations of average surface roughness under different swept angles and cutting conditions.

The roughness has been evaluated using the arithmetic average deviation of profile, R_a . These bar graphs give an insight into how the surface responds to change in swept angle for both dry and MQL environments. From these results, it can be seen that the 101.5° of swept angle produces the higher R_a as compared to the 66.4° of swept angle. Besides, under dry condition, machined surfaces appear rougher, especially with adhered or sticky material. It is obviously seen in Figure 8. In contrast, it was found that the adhered material was completely removed when MQL was applied. This could be due to the application of MQL reduces the temperature effect and hence; the adherence propensity.

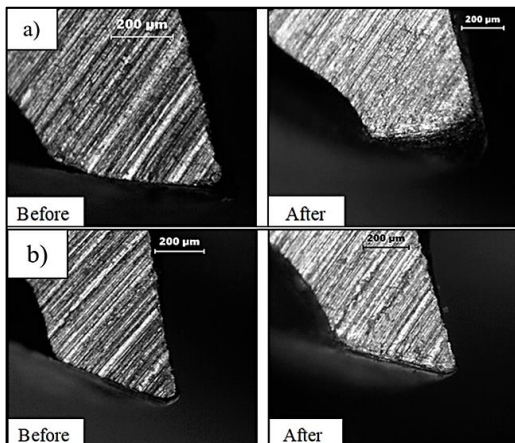


Figure 5. Cutting-edge deterioration under (a) Dry cutting and (b) MQL condition

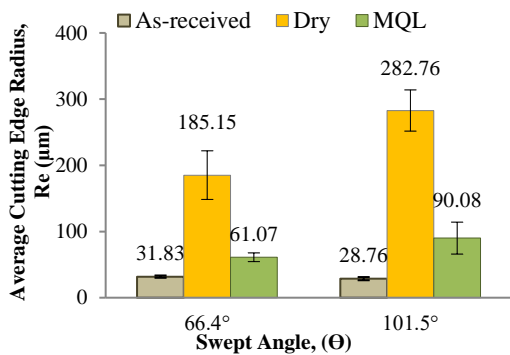


Figure 6. Changes of cutting-edge radius for both swept angles and cutting conditions

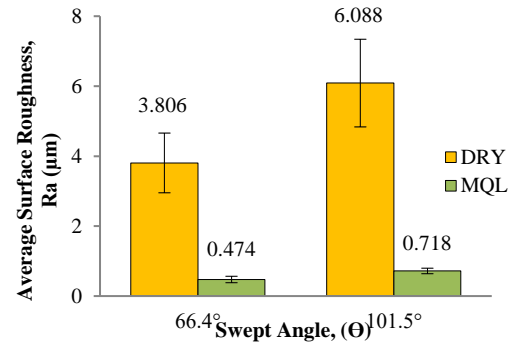


Figure 7. Average comparisons for surface roughness, R_a .

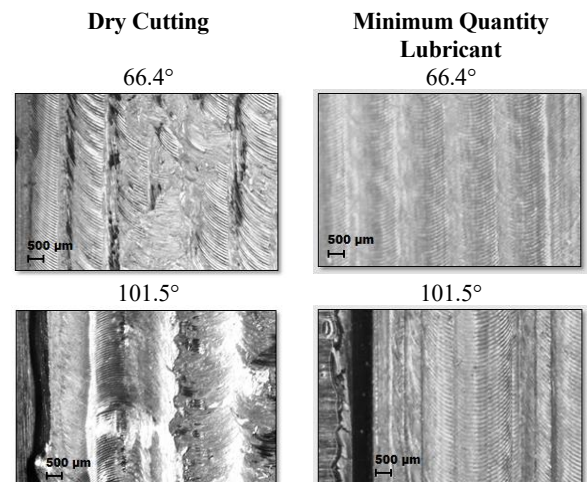


Figure 8. Surface pattern for both swept angles and cutting conditions

The results also appear that R_a grows rapidly under dry condition when compared to MQL method. This is due to more intensive stress and temperature at the workpiece and tool interface that lead to quick tool wear. Under MQL method, the pressurized air with oil to the cutting zone promotes rapid removal of the chips whilst retaining the tool shape. Higher tool wear and chipping could create valleys and marks on the machined surface. Also, it is important to note that due to the high ductility of aluminium, it could promote roughness on the surface.

Overall, it is concluded that the lower swept angle by varying machining under MQL condition provide superior surface finish than dry condition as step-over reduced the interruption in cutting process. In addition, lubricant used in MQL would lessen adhesion and interaction of tool and workpiece thus reducing friction as well as tool wear.

3. 5. Burr Formation

There were four types of burr created which were top burr, exit burr, entrance burr, side burr, and bottom burr. They were designated through their cross-sectional area. It was found that the most dominant burr was the top burr which formed on top of the workpiece surface. Figure 9 shows the top burr formation under different swept angles and cutting conditions where different features could be identified. Wider top burrs with large curvature were created under dry cutting, in comparison with those obtained in MQL which was thinner. Under MQL, the use of oil makes the shearing process became smoother and easier, and hence resulting in reduced burr size.

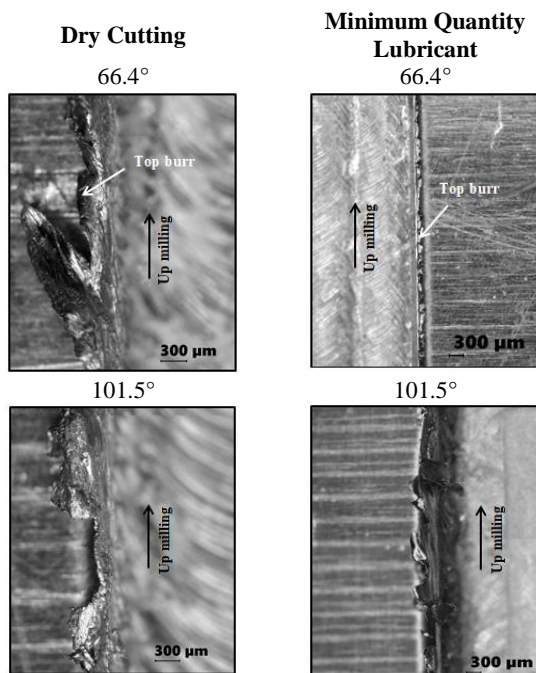


Figure 9. Burr formation under different swept angles and cutting conditions

Figure 10 shows the average burr width under different cutting conditions. It can be seen that a significant reduction in burr width values was obtained with MQL system. This improved performance was possibly due to the enhanced lubrication that retained the sharpness of the tools. The reason why the tool wear rate under dry cutting is high is due to the ploughing effect, which happens when the cutters are not removing the material but pushing it off to the slot side instead to create burr. In addition, a larger swept angle also plays a significant role by increasing the width of burrs.

Based on Figure 10, it shows that burr width (W_b) for after 10th slots produce bigger and wavier burrs compared to burr width for first slot. For a swept angle of 101.5°, the result shows an increasing pattern for both cutting conditions compared to the swept angle of 66.4°. It can be seen that the W_b was lessened under MQL method compared dry method for both swept angles. This is because the effect of the cutting fluid on tool wear and due to the amount of sweep subtended by cutting edge which makes them engages and leaves the workpiece during the slot milling process. Overall, the observed phenomenon is directly related to each other, where the swept angle will cause the tool wear and increase in the cutting-edge radius that would significantly increase the ploughing effect that would finally result in the formation of the top burr.

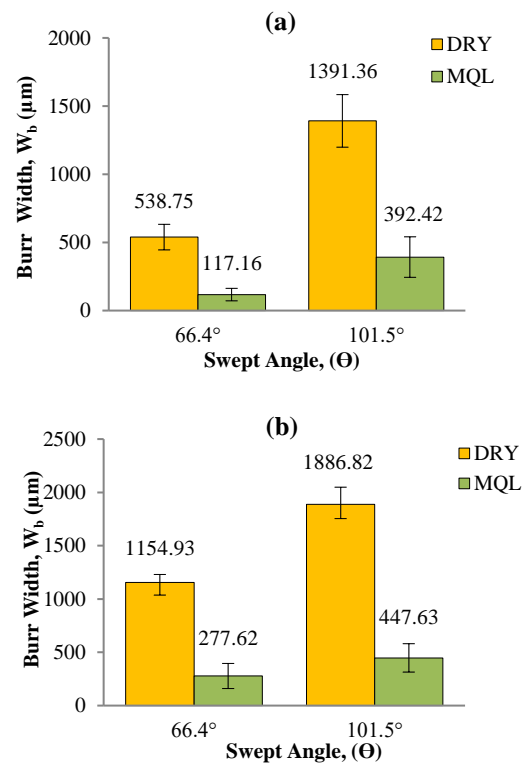


Figure 10. Average burr width under different cutting condition after (a) 1st slot; and (b) 10th slot

3. 6. Chip Formation The mechanism of chip formation is a major strain deformation method, with partial fracturing is caused by internal cracking or voiding in or near the primary shear zone and likely crack formation around the cutting edge. So, it is important to measure the length of chip formation for each chip collected from these experiments. Figure 11 displays the average comparisons between swept angles for the length of chip formation under different machining conditions.

The result shows that machining in dry condition formed longer chips than in MQL condition. This is particularly evident when a higher swept angle was used. In principle, the higher value of swept angle applied during operation, the longer the chips.

Microscopy images of chip formation in different swept angle and cutting conditions is shown in Figure 12. It shows a typical chip pattern when machining aluminum alloy under various cutting conditions. It is important to note that small well-broken chips are desirable in machining. A shorter chip was observed

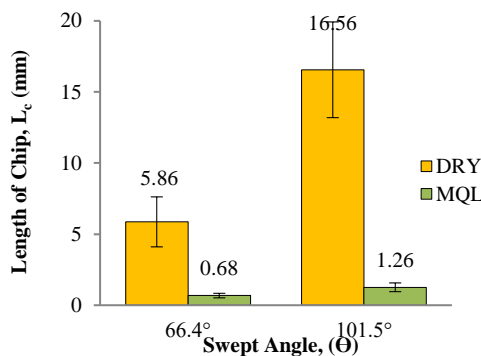


Figure 11. Average comparisons in length of chip formation

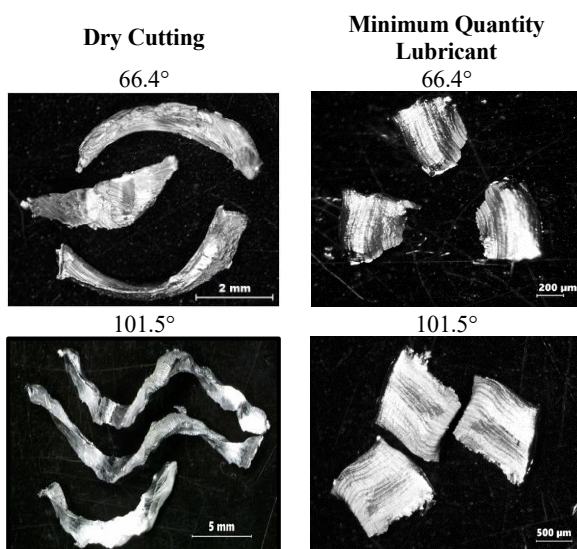


Figure 12. Chip pattern under different swept angles and cutting conditions

under MQL condition for both swept angles. While, continuous non-uniform with severe curled chips were found under dry cutting. This had happened due to the fact that the chips were exposed to intense heat and hence leading to huge plastic deformation. Under MQL condition, flat morphology of chips was formed owing to the reduction in cutting temperature. All the findings confirmed that lubrication action through MQL system is desirable in terms of chip formation as it produces shorter chip as compared to dry machining.

4. CONCLUSION

From this study, it was obvious that the significant used of minimum quantity lubrication (MQL) as an alternative method to substitute the used of conventional metal working fluid in machining operations was proven. Besides, the impact of swept angle selection and their influence under the different cutting conditions was also demonstrated. The result showed that the lower swept angle applied, the better result in the form of reduced tool wear and burr formation, improved surface roughness and chip formation. This is confirmed in both dry and MQL condition. Swept angle and cutting condition plays an important role in determining tool wear (flank wear and edge radius), surface roughness, burr, and chip formation. For that reason, the results established that a parametric combination between lower swept angle of 66.4° under MQL condition have demonstrated minimal tool wear and better surface quality.

5. ACKNOWLEDGEMENT

The first author gratefully acknowledges the financial funding of the government of Malaysia and University Malaysia Perlis. This research was supported by Fundamental Research Grant Scheme (FRGS 9003-00741), Ministry of Higher Education, Malaysia.

6. REFERENCES

1. Benedicto, E., Carou, D. and Rubio, E. M., "Technical, economic and environmental review of the lubrication/cooling systems used in machining processes," *Procedia Engineering*, Vol. 184, (2017) 99-116. DOI: 10.1016/j.proeng.2017.04.075.
2. Madanchi, N., Thiede, S., Gutowski, T. and Herrmann C., "Modeling the impact of cutting fluid strategies on environmentally conscious machining systems" *Procedia CIRP*, Vol. 80, (2019), 150-155. DOI: 10.1016/j.procir.2019.01.068.
3. Li, K., Aghazadeh, F., Hatipkarasulu, S. and Ray T. G., "Health risks from exposure to metal-working fluids in machining and grinding operations," *International Journal of Occupational Safety and Ergonomics*, Vol. 9, (2003), 75-95. DOI: 10.1080/10803548.2003.11076555.

4. Mahboob Ali, M. A., Azmi, A. I. and Khalil A. N. M., "Specific cutting energy of Inconel 718 under dry, chilled-air and minimal quantity nanolubricants," *Procedia CIRP*, Vol. 77, (2018), 429-432. DOI: 10.1016/j.procir.2018.08.290.
5. Sharma, V. S., Dogra, M. and Suri, N. M., "Cooling techniques for improved productivity in turning," *International Journal Machine Tools and Manufacture*, Vol. 49, (2009), 435-453. DOI: 10.1016/j.ijmachtools.2008.12.010.
6. Khan, W. A., Hoang, N. M., Tai, B. and Hung W. N. P., "Through-tool minimum quantity lubrication and effect on machinability," *Journal of Manufacturing Process*, Vol. 34, (2018), 750-757. DOI: 10.1016/j.jmapro.2018.03.047.
7. Banerjee N. and Sharma A., "A comprehensive assessment of minimum quantity lubrication machining from quality, production, and sustainability perspectives," *Sustainable Materials and Technologies*, Vol. 17, (2018), e00070. <https://doi.org/10.1016/j.susmat.2018.e00070>.
8. Smith, B., "The Boeing 777". *Advanced Materials and Processes*, Vol. 161, (2003), 41-44.
9. Shokrani, A., Dhokia, V. and Newman, S. T., "Environmentally Conscious Machining of Difficult-to-Machine Materials with regards to Cutting Fluids". *International Journal of Machine Tools and Manufacture*, Vol. 57, (2012), 83-101. DOI: 10.1016/j.ijmachtools.2012.02.002.
10. Astakhov, V. P. (2014). *Drills: Science and Technology of Advanced Operations*. Taylor and Francis Group (LLC).
11. Iqbal A., Al-Ghamdi K. A. and Hussain G., "Effects of tool life criterion on sustainability of milling," *Journal of Cleaner Production*, Vol. 139, (2016), 1105-1117. DOI: 10.1016/j.jclepro.2016.08.162.
12. Venkata Vishnu A., and Sudhakar Babu S., "Mathematical Modeling and Multi Response Optimization for Improving Machinability of Alloy Steel Using RSM, Grey Relational Analysis and Jaya Algorithm," *International Journal of Engineering, Transactions C: Aspects*, Vol. 34, No. 9 (2021), 2157-2166. DOI: 10.5829/IJE.2021.34.09C.13.
13. Azuddin M. and Abdullah W., "A study on surface roughness and burr formation of Al6061 with different spindle speed and federate for small end milling cutter," *International Journal of Integrated Engineering*, Vol. 1, (2009), 7-14.
14. Caldeirani Filho J. and Diniz A. E., "Influence of cutting conditions on tool life, tool wear and surface finish in the face milling process," *Journal of the Brazilian Society of Mechanical Sciences*, Vol. 24, (2002), 10-14. DOI: 10.1590/S0100-73862002000100002.
15. Abidin Z.Z., Mativenga P.T. and Harrison G., "Chilled air system and size effect in micro-milling of nickel-titanium shape memory alloys". *International Journal Precision Engineering and Manufacturing-Green Technology*, Vol. 7, (2020), 283-297. DOI: 10.1007/s40684-019-00040-5.
16. ISO 8688-2, Tool life testing in milling, Part 2: End milling, 1989.

Persian Abstract

چکیده

مابعات برش اغلب به منظور افزایش قابلیت ماشینکاری از طریق خنک کننده، روان کننده و شستشو انجام می شود. با این حال، استفاده از آنها در ماشینکاری نگرانی های عمده ای را از نظر ردپای سلامتی و اثرات محیطی در طول چرخه زندگی آنها ایجاد می کند. روشهای جایگزین، مانند برش خشک و حداقل مقدار روغن کاری، برای کاهش این مسائل استفاده شد. این تحقیق همچنین تأثیر انتخاب زاویه جارو شده، ۳۰ و ۶۰ درصد قطر ابزار را تحت شرایط برش مختلف در طول آسیاب مواد آلیاژ آلومینیوم بررسی می کند. تأثیر آنها بر سایش ابزار، زبری سطح، شکل و شکل تراشه مقایسه شد. نتایج نشان داد که استفاده از زاویه جاروب پایین در ارتباط با حداقل مقدار سیستم روان کننده باعث کاهش قابل توجه سایش ابزار، کاهش ساییدگی و تشکیل تراشه و همچنین بهبود کیفیت سطح در مقایسه با ماشینکاری خشک می شود. این کار به وضوح نشان می دهد که چگونه اهمیت انتخاب زاویه جارو و شرایط برش در پالایش عملکرد ماشینکاری می تواند قابلیت ماشینکاری مواد را بهبود بخشد.



A Robust Multi-objective Fuzzy Model for a Green Closed-loop Supply Chain Network under Uncertain Demand and Reliability (A Case Study in Engine Oil Industry)

S. M. S. Moosavi^a, M. Seifbarghy^{*b}

^a Department of Industrial Engineering, Science and Research Branch, Islamic Azad University, Tehran, Iran

^b Department of Industrial Engineering, Faculty of Engineering, Alzahra University, Tehran, Iran

PAPER INFO

Paper history:

Received 28 April 2021

Received in revised form 28 July 2021

Accepted 22 August 2021

Keywords:

Green Closed Loop Supply Chain

Robust Fuzzy Programming

Multi-objective

Reliability

Engine Oil Industry

ABSTRACT

Given the importance of supply chain and environmental issues, this paper presents a new mathematical model for a green closed-loop supply chain (GCLSC) network with the objectives of maximizing profits, maximizing the number of jobs created, and maximizing reliability. Due to the uncertainty on some parameters such as demand and transportation costs, the new method of robust fuzzy programming model was utilized. Multi-objective Grey Wolf Optimizer (MOGWO) and Non-dominated Sorting Genetic Algorithm II (NSGA II) were used to tackle the problems for larger sizes. A number of instances of the problem in larger sizes were solved. The results from comparing the algorithms considering some criteria including means of objective functions, spacing index, distance index from ideal point, maximum amplitude index, Pareto response number index and computational time showed the fast convergence and high efficiency of MOGWO algorithm for this problem. Finally, the implementation of the model for a real case study in Iranian engine oil industry, showed the efficiency of the obtained solutions for this network.

doi: 10.5829/ije.2021.34.12c.03

1. INTRODUCTION

In today's world, economic and industrial change is happening faster than ever before. The goal of organizations and companies is to maintain and increase profits as well as greater survival and durability in the market. The globalization of economic activities, along with the rapid growth of technology as well as limited resources, has put companies in an intense competition. One of the competitive advantages for companies is to make activities such as supply chain more efficient and effective. The term supply chain management (SCM) was coined in the late 1980s and became more widely used in 1990s. In this view, in order to survive in competitive markets, organizations must not only manage and optimize their organizational units, but must integrate all the organizational units in the network, including the suppliers and the customers. However, in

recent years, increasing competition in the global market to quickly meet customer needs and provide quality products has led to negative environmental effects, including an increase in greenhouse gas emission. Government laws, environmental pressures, and growing public awareness have forced companies to collect discarded products and goods and to consider more environmental factors in future products. This has led to the creation of a new management concept called green supply chain, which is actually a new paradigm for environmental protection along with SCM [1].

Supply chain is an attitude that has been considered by organizations and companies in recent years. In this approach, all components and circles that are together to provide a product or service to the customer, are considered and try to make strategic, tactical, and operational decisions in such a way that the entire supply chain is more efficient and effective against competing

*Corresponding Author Institutional Email:
m.seifbarghy@alzahra.ac.ir (M.seifbarghy)

chains. A supply chain is not limited to components and places of production, but includes all components of production and services from the initial suppliers to the final customers [2]. Lack of coordination and integration between different parts of the supply chain result in to an increase in the cost of goods and consequently an increase in price, failure to deliver products on time, etc., which ultimately cause to an increase in consumer dissatisfaction. A supply chain is a flow of materials and information between different levels of a manufacturing or service network that includes suppliers, manufacturers, distributors, wholesalers, retailers, and end customers. In recent years, organizations and companies have taken responsibility for waste products based on the nature of the products, legal and environmental requirements, as well as the re-acquisition of value. In view of the above, the supply chain network is broader and includes product collection, inspection, repair, recycling and destruction centers [3].

Since the introduction of the first supply chain design ideas in the late 1970s, nothing has attracted the attention of governments, corporate executives and the public as much as green supply chain design, which is the most important tool for organizations to adapt their activities to the environment. It should be noted that the concept of green supply chain is not just a general slogan for idealistic people, but in many countries, organizations have made every effort to implement it. Today, some of the leading companies are already actively implementing green projects, for example IKEA, the world's largest furniture maker, has set up a train network emphasizing green train operations. In addition, General Electric, IBM, and HP have all considered green products with the adoption of new energy-saving technologies, and in addition to product design, they have considered SCM to relieve environmental concerns [4].

On the other hand, government regulations and increasing customer awareness of the environment have made environmental aspects important in the work of researchers, building models and working frameworks for the effectiveness of the ecosystem in the supply chain networks. China, for example, has set a target of reducing carbon emissions by 10% in the Ninth Eleventh Development Plan, and the central government is studying and preparing for environmental protection oversight policies which are expected to play a positive role in solving the environmental problems. To implement a green supply chain network, it is not just enough to pay attention to being green; on the other hand, it is important to implement the green factors when designing the physical facilities and operating the supply chain. Furthermore, a good design can reduce CO₂ emissions all over the supply chain network.

Due to the importance of the GCLSC (which is a combination of forward and reverse supply chain), this paper presents a new model of multi-objective GCLSC

which incorporates some real-world features. The importance of implementing new models to reduce operational costs as well as pollution has been emphasized in this article by addressing a three-objective model including maximizing network profits, recruitment rates and reliability. Considering the governmental restrictions and laws on the amount of greenhouse gas emissions, the addressed restrictions have implemented in the given mathematical model. Uncertainty on demand and some other cost parameters has also led to the use of the new fuzzy robust method. Finally, for the assessment of the model performance in the real world, a real case study in the Iranian engine oil industry has been studied.

The structure of the paper is as follows: In section 2, the literature review is given and the research gap is presented. In section 3, the initial version of the uncertain multi-objective GCLSC model is proposed and then its converted version is given. In this section, a solid fuzzy optimization method is used to control the uncertainty of the model. In section 4, the solution algorithms, the design of the primary chromosome, as well as the comparison indicators of the algorithms are presented. In section 5, the results from model implementation in an Iranian engine oil industry are discussed. Finally, in section 6, the conclusions from this research together with further research ideas are presented.

2. LITERATURE REVIEW

In this section, some of the most important researches in the field of closed-loop supply chain (CLSC) network design are reviewed. Kim et al. [5] established a multi-cycle CLSC with the objective of maximizing factory profit. The network was designed to start with the return of used products and return by the customer and then accumulated and dismantled in the collection center. Some of the returned products were sent to the reproduction department and the usable parts were transferred to the renovation department and repaired. Finally, the parts were assembled, reproduced and classified for sale to foreign suppliers as new products [5]. Ahmadi-javid and Hoseinpour [6] modeled a distribution network considering location-inventory decisions and pricing with limited inventory capacity. They used Lagrange release algorithm to solve their problem [6]. Kaya and Urek [2] developed a definitive CLSC network model with simultaneous location-inventory and pricing decisions. They used the refrigeration and forbidden search simulation algorithm to tackle the problem [2]. Ahmadzadeh and Vahdani [7] presented a model for integrated location-inventory and pricing decisions in the CLSC network. Their main purpose was to decide on the optimal locations of facilities, taking into account inventory costs and product

pricing. They used genetic algorithms, firewalls and colonial competition algorithms to solve their problem [7]. Amin et al. [4] in their research, designed and optimized a CLSC network with tire remanufacturing based on tire retrieval options, with the objective of maximization of the total profit. The application of this model based on a realistic network in Toronto, Canada has been discussed using a geographical map. In this model, he uses a new decision tree-based method to calculate the net present value of the income over several periods under various sources of uncertainty, such as demand and return. In addition, discount cash flow in this method was considered as a new innovative approach. This method can be used to compare the profitability of different design options for a CLSC [4]. In a study, Hajiaghahi-Keshteli and Fard [8] developed a new mixed-integer programming model to create a multi-purpose stable CLSC network scheme for the first time, assuming a reduction in transportation costs. To address the problem, not only traditional and recent metaphors are used, but also algorithms are combined according to their strengths, especially in intensification and diversification. To evaluate the efficiency and effectiveness of these algorithms, they are compared with four evaluation criteria for optimal Pareto analysis [8]. Mardan et al. [9] provided a comprehensive mathematical model for the multi-cycle, multi-product, multi-model, and two-objective GCLSC. The purpose of this model was to minimize the total cost and emission of ambient gases by deciding on the locations of the facilities, the amount of transportation and the inventory balance. The results showed that the proposed solution approach reduced the total cost by more than 13 percent and can even be used for larger and more complex industrial applications in the real world [9]. Yadegari et al. [10] developed a memetic algorithm (MA) with priority-based coding/decoding method based on a flexible neighborhood search (NS) strategy to improve strategies for simultaneous configuration of the chains. In addition, to avoid the time-consuming repair process in the discrete solution dealership, it provided a way to convert the discrete dealership to a continuous method, and finally, to accelerate the proposed algorithm, the multi-stage simulation (MSA) re-embedding was embedded into the MA [10]. In a study, Yavari and Zaker [11] examined the design of a GCLSC network for biodegradable products under uncertain conditions. Demand, rate of return and quality of returned products were considered as uncertain parameters of the model [11]. Saedinia et al. [12] proposed a nonlinear mixed-integer programming model to consider the price and position of facilities in a CLSC in the information and communication technology (ICT) industry to obtain the total profit generated by the sale of new ICT products. The structure of this network included suppliers, collection and distribution centers (C-D centers),

disassembly centers and customer areas. In C-D centers, an inventory policy of continuous review was applied and it was assumed that the ordering time is random. Numerical results showed how to allocate facilities to each other, inventory management and pricing of ICT products; therefore, the proposed models and methods could help ICT companies in determining their policies for maximum profit [12]. In a research, Nayeri et al. [13] presented a robust multi-objective fuzzy optimization model in the design of a stable CLSC network. In this study, they considered parameters such as demand and transportation costs to be uncertain [13]. Prakash et al. [14] presented a model of a CLSC network in which parameters such as risk and demand were considered. They optimized the developed model using the combined robust method [14]. Fatollahi fard et al. [15] presented a model for CLSC network system in case of uncertainty for water reverse purification and developed a multi-objective stochastic optimization model with triple bottom line optimization. Fazli-Khalaf and Hamidieh [16] designed a reliable multi-echelon CLSC network model which maximized the social responsibility while minimized the fixed establishing and variable processing costs of the network. To cope with the uncertainty of parameters, stochastic programming was applied and an effective reliable modelling method was employed to appropriately control unpleasant economic impacts of disruptions. On the uncertainty in supply chain, Hamidieh et al. [17] proposed a robust reliable bi-objective supply chain network design model which was capable of controlling different kinds of uncertainties, concurrently. Stochastic bi-level scenario based programming approach was used to model various scenarios related to strike of disruptions. Tables 1 and 2 give some abbreviated forms of employed terms and comparison of the GCLSC researches.

TABLE 1. Abbreviated forms of employed terms

| Abbreviation | Term |
|--------------|--------------------------|
| SPR | Single Product |
| MPR | Multi Product |
| SPE | Single Period |
| MPE | Multi Period |
| QN | Quantitative |
| QA | Qualitative |
| FS | Forward Supply Chain |
| RS | Reverse Supply Chain |
| CS | Closed-Loop Supply Chain |
| L | Location |
| A | Allocation |
| R | Routing |
| SH | Shortage |

| | | | |
|------|-------------------------------------|-----|---------------------------------|
| SS | Supplier Selection | MRE | Max Reliability |
| D | Discount | MQL | Min Queue Length |
| Q | Queueing System | MSC | Max Supply Chain Responsiveness |
| FP | Fuzzy Programming | MNV | Max Net Value |
| SP | Stochastic Programming | MPR | Max Profit |
| RP | Robust Programming | MSL | Max Service Level |
| RFP | Robust-Fuzzy Programming | MDL | Min Number of Days Lost |
| RSP | Robust-Stochastic Programming | MDT | Min Delivery Time |
| FSP | Fuzzy-Stochastic Programming | MCO | Min Cost |
| RFSP | Robust-Fuzzy-Stochastic Programming | MLR | Min Loss of Raw Materials |
| DE | Deterministic | MNV | Min Number of vehicles |
| CS | GAMS-Lingo | MCE | Min Co2 Emission |
| MO | Multi Objective Decision Method | MSH | Min Shortage |
| MH | Meta-Heuristics Algorithm | MNJ | Max Number of Jobs |
| FO | Fuzzy Optimization Method | MRI | Min Risk |

TABLE 2. Comparison of the GCLSC researches

| Research | Year | Model | Objective | Variable | Uncertainty | Solution | Case Study |
|------------------------------|-------|--------------|--------------------|-----------------------|-------------|----------|------------|
| Alshamsi and Diabat [18] | 2018 | SPR, SPE, QN | MPR | L, A, | DE | CS | |
| Rad and Nahavandi [19] | 2018 | MPR, MPE, QN | MCO, MCE | L, A, SH, D | DE | MO | * |
| Fakhrzad et al. [20] | 2018 | MPR, MPE, QN | MCO, MDT, MCE, MRE | L, A, R, SS | DE | MH | |
| Pourjavad and Mayorga [21] | 2019a | MPR, MPE, QN | MCO | L, A, SH | DE | CS | * |
| Yadegari et al. [10] | 2019 | SPR, MPE, QN | MCO | L, A | DE | CS | * |
| Polo et al. [22] | 2019 | SPR, MPE, QN | MPR | L, A, SH | RP | CS | |
| Ghahremani Nahr et al. [23] | 2019 | MPR, MPE, QN | MCO | L, A, SH, SS, D | RFP | MH | |
| Pourjavad and Mayorga [24] | 2019b | MPR, MPE, QN | MCO, MCE, MNJ | L, A, SS | FP | MO | |
| Darestani and Hemmati [25] | 2019 | MPR, MPE, QN | MCO, MCE | L, A, SH, SS, D, Q | RP | MO | |
| Zhang et al. [26] | 2019 | SPR, SPE, QN | MDT, MDL | L, A | RFP | MO | |
| Fazli khalaf et al. [27] | 2019 | MPR, MPE, QN | MCO, MDT, MRE | L, A, SH, R | RFP | FO | * |
| Alkhayyal [28] | 2019 | MPR, SPE, QN | MCO, MCE | L, A | DE | MO | * |
| Mardan et al. [9] | 2019 | MPR, MPE, QN | MCO, MCE | L, A, R, SS | DE | CS | |
| Ghahremani- Nahr et al. [29] | 2020b | MPR, MPE, QN | MCO, MCE | L, A, SH, D | RP | MO | |
| Jiang et al. [30] | 2020 | SPR, SPE, QN | MPR, MSL | L, A | DE | MO | |
| Gholizadeh et al. [31] | 2020 | MPR, MPE, QN | MPR | A, R | RP | MH | |
| Prakhash et al. [14] | 2020 | SPR, SPE, QN | MCO | L, A | RP | CS | * |
| Pourmehdi et al. [32] | 2020 | SPR, SPE, QN | MCE, MPR, MSL | L, A | SP | FO | * |
| Mohtashemi et al. [33] | 2020 | SPR, SPE, QN | MCO, MCE | L, A, SS, Q | DE | MH | |
| Liu et al. [34] | 2021 | MPR, MPE, QN | MCO, MCE | L, A | RFP | CS | * |
| Zahedi et al. [35] | 2021 | MPR, MPE, QN | MNV, MSL | L, A, R | DE | MH | * |
| Boronoos et al. [36] | 2021 | MPR, MPE, QN | MCO, MCE | L, A | RFP | MO | * |
| Habib et al. [37] | 2021 | SPR, MPE, QN | MCO | L, A | RFP | CS | * |
| This paper | | MPR, MPE, QN | MPR, MRE, MNJ | L, A, R, SH, SS, D, Q | RFP | MO | * |

As a research gap, according to the given literature, a comprehensive uncertain model which includes three aspects of economic, social and environmental with uncertainty on some key parameters of the model has not been studied. Furthermore, the application of the model in engine oil industry has not been studied. The major novelties and features of this paper are:

- Developing a three-objective model for CLSC design of engine oil industry
- Using robust fuzzy programming to tackle with the uncertainties in demand, transportation costs and capacity levels of facilities
- Development of two meta-heuristic algorithms in order to solve the problem for large sizes
- Solving the model for small and large sizes of the problem
- Solving the model utilizing the real data of engine oil industry

3. PROBLEM DESCRIPTION AND MODELING

In this paper, a GCLSC network is modeled under the uncertainty of some of the most important parameters of the problem (i.e. demand and transportation costs). Figure 1 shows the under-study GCLSC network in which the main purpose is to supply engine oil products to customers in the primary market and to increase the energy recovery and to meet the secondary market demand of returned products. In this case, the suppliers, who are actually in charge of supplying the raw materials, send the raw materials to the manufacturers who produce the final products. Manufacturers produce the final products using a combination of some predetermined materials and send them to distributors. Distributors distribute the final products according to the uncertain demand of customers for each product, taking into account the shortage. In the given model, the reverse supply chain is also considered. The main purpose of designing such a network is to properly manage and reuse

returned products from customers. In this network, according to various issues, a percentage of products are collected at the collection center and after inspection are sent to one of the specified centers for energy recovery, recycling or disposal in the landfill. Recycled products can be reused in the primary market or sold to the secondary market as lower level quality product by adding some raw materials or changing the structure of the product. In the meantime, some returned products may no longer be reusable, even after recycling because of the poor quality; In this case, they are sent to the landfill for disposal.

There are three types of strategic, tactical and operational decisions in this model. At the strategic level, the problem is to determine the number and capacities of potential network facilities including production, distribution, recycling and collection centers. At the tactical level, the optimal flows of materials, products and returned items are determined between different facilities of the network. At the operational level, the appropriate vehicles between facilities are selected. According to the following assumptions, the model of the problem can be formulated.

1. The objective functions of the problem include maximizing the profit of the entire supply chain network, maximizing the number of created jobs and maximizing the reliability of the CLSC network.
2. Demand, supply capacities, transportation costs and some operating costs are considered to be uncertain.
3. Shortage is permitted.
4. The transport fleet is considered heterogeneous.
5. The cost of greenhouse gas emissions is considered as part of the first objective function.
6. Establishment of facility capacity at different levels has different costs.

According to the mentioned assumptions, the set, parameters and decision variables of the model are as follows:

3. 1. Sets

- A Set of customers fixed points $a = \{1,2, \dots, A\}$
- K set of potential distribution centers $k = \{1,2, \dots, K\}$
- J set of potential manufacturing centers $j = \{1,2, \dots, J\}$
- I set of raw material supply centers $i = \{1,2, \dots, I\}$
- L set of disposal centers $l = \{1,2, \dots, L\}$
- N set of potential recycling centers $n = \{1,2, \dots, N\}$
- M set of potential collection centers $m = \{1,2, \dots, M\}$
- E set of energy recovery centers $e = \{1,2, \dots, E\}$
- B Set of secondary market fixed points $b = \{1,2, \dots, B\}$
- G Set of potential facility capacity levels $g = \{1,2, \dots, G\}$
- P Product range (i.e. engine oil and its products in the case study) $p = \{1,2, \dots, P\}$
- H set of raw materials $h = \{1,2, \dots, H\}$
- V set of vehicles $v = \{1,2, \dots, V\}$

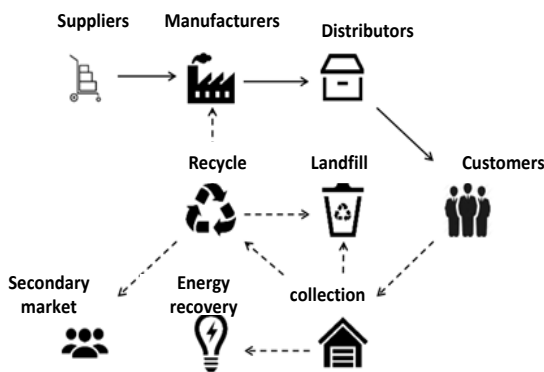


Figure 1. The under-study GCLSC network

3. 2. Parameters

| | | | |
|------------------------|--|-----------------------|--|
| \overline{Dem}_{ap} | Demand of customer a for product p | D_{ml} | Distance of collection center m from disposal center l |
| O_{hp} | The amount of raw material h required to produce one unit of product p | D_{nl} | Distance of recycling center n from disposal center l |
| α_{ap} | Percentage of product p returned by customer a | D_{nb} | Distance of recycling center n from secondary market b |
| β_{mp} | Percentage of product p transferable to energy recovery center by collection center m | π_{ap} | Shortage cost of product p at customer a |
| γ_{mp} | Percentage of product p transferable to recycling center by collection center m , $\beta_{mp} + \gamma_{mp} < 1, \forall m, p$ | \overline{PC}_{jp} | Production cost of product p in manufacturing center j |
| δ_{np} | Percentage of product p transferred to disposal center by recycling center n | \overline{SC}_{ih} | Cost of supplying raw material h by supplier i |
| σ_{np} | Percentage of product p transferred to production center by recycling center n , $\delta_{np} + \sigma_{np} < 1, \forall n, p$ | \overline{DC}_{kp} | Shipping Cost of one unit of product p from distribution center k |
| $CapJ_{jPg}$ | Capacity for producing product p at Manufacturer center j at capacity level g | \overline{CC}_{mp} | Cost of collecting one unit of product p at collection center m |
| $CapK_{kp}$ | Capacity allocated by distributor k to product p at capacity level g | \overline{RC}_{np} | Cost of recycling one unit of product p in recycling center n |
| $CapM_{mi}$ | Capacity allocated by collection center m to product p at capacity level g | \overline{LC}_{lp} | Disposal cost of one unit of product p at disposal center l |
| $CapN_{np}$ | Capacity allocated by recycling center n to product p at capacity level g | \overline{RPC}_{jp} | Cost of remanufacturing product p in remanufacturing center j |
| \overline{CapI}_{ih} | Capacity of supplier i for replenishment of raw material h | $Co2_v$ | Amount of carbon dioxide emission by vehicle v per unit distance |
| $CapL_{lp}$ | Capacity allocated by disposal center l to product p | CO_2^{GOV} | The acceptable amount of carbon dioxide emissions in the supply chain network determined by government |
| $Capw_v$ | Weight capacity of vehicle v | E_{jg} | Amount of carbon dioxide emissions due to construction of manufacturing center j with capacity level g |
| $Capv_v$ | Volume capacity of vehicle v | E_{kg} | Amount of carbon dioxide emission due to construction of distribution center k with capacity level g |
| w_h | Weight of one unit of raw material h | E_{mg} | Amount of carbon dioxide emission due to construction of collection center m with capacity level g |
| w_p | Weight of one unit of product p | E_{ng} | Amount of carbon dioxide emission due to construction of recycling center n with a capacity level g |
| v_h | Volume of one unit of raw material h | Pe_{jp} | Amount of carbon dioxide emission due to producing one unit of product p in the production center j |
| v_p | Volume of one unit of product unit p | Ce_{mp} | Amount of carbon dioxide emission due to collection of one unit of product p in collection center m |
| Pr_{ap} | Selling price of one unit of product p to customer a | Re_{np} | Amount of carbon dioxide emission due to recycling one unit of product p at recycling center n |
| Pr_{ep} | Selling price of one unit of product p to energy recovery center e | Le_{lp} | Amount of carbon dioxide emission due to disposal of one unit of product p at disposal center l |
| Pr_{bp} | Selling price of one unit of product p to secondary market b | RPe_{jp} | Amount of carbon dioxide emission due to remanufacturing product p in manufacturing center j |
| F_{jg} | Fixed cost of constructing manufacturing center j at capacity level g | ϑ | Fixed cost of excess carbon dioxide emission |
| F_{kg} | Fixed cost of constructing distribution center k with capacity level g | JOB_{jg} | Number of job opportunities created by constructing manufacturing center j with capacity level g |
| F_{mg} | Fixed cost of constructing collection center m with capacity level g | JOB_{kg} | Number of job opportunities created by constructing distribution center k with a capacity level g |
| F_{ng} | Fixed cost of constructing recycling center n with capacity level g | JOB_{mg} | Number of job opportunities created by constructing collection center m with capacity level g |
| FC_v | Fixed cost of utilizing vehicle v | | |
| \overline{FV}_v | The variable cost of vehicle v per unit distance between two facilities | | |
| D_{ka} | Distance of distribution center k from customer a | | |
| D_{jk} | Distance of production center j from distribution center k | | |
| D_{ij} | Distance of supplier i from manufacturing center j | | |
| D_{nj} | Distance of recycling center n from manufacturing center j | | |
| D_{am} | Distance of customer a from collection center m | | |
| D_{me} | Distance of the collection center m from energy recovery center e | | |
| D_{mn} | Distance of collection center m from recycling center n | | |

JOB_{ng} Number of job opportunities created by constructing recycling center n with capacity level g
 ALD_{jg} Average number of days lost because of work injuries due to construction of manufacturing center j with capacity level g
 ALD_{kg} Average number of days lost because of work injuries due to construction of distribution center k with capacity level g
 ALD_{mg} Average number of days lost because of work injuries due to construction of collection center m with capacity level g
 ALD_{ng} Average number of days lost because of work injuries due to construction of recycling center n with capacity level g
 φ_{ALD} Significance factor of the total number of lost days due to injuries in the workplace
 θ_{job} Significance factor of the number of job opportunities created
 Re_{ijh} Reliability of shipping raw material h from supplier i to manufacturing center j
 Re_{jkp} Reliability of shipping product p from manufacturing center j to distribution center k
 Re_{kap} Reliability of shipping product p from distribution center k to customer a

Y_{jkv} If vehicle v is assigned to the rout from manufacturing center j to distribution center k , it takes 1, otherwise it takes 0.
 Y_{ijv} If vehicle v is assigned to the rout from supplier i to manufacturing center j , it takes 1 and otherwise 0.
 Y_{nfv} If vehicle v is assigned to the rout from recycling center n to manufacturing center j , it takes 1 and otherwise 0.
 Y_{amv} If vehicle v is assigned to the rout from customer a to collection center m , it takes 1 and otherwise 0.
 Y_{mev} If vehicle v is assigned to the rout from collection center m to energy recovery center e , it takes 1, otherwise it takes 0.
 Y_{mnv} If vehicle v is assigned to the rout from collection center m to recycling center n , it takes 1, otherwise it takes 0.
 Y_{mlv} If vehicle v is assigned to the rout from collection center m to disposal center l , it takes 1, otherwise it takes 0.
 Y_{nlv} If vehicle v is assigned to the rout from recycling center n to disposal center l , it takes 1, otherwise it takes 0.
 Y_{nbv} If vehicle v is assigned to the rout from recycling center n to secondary market b , it takes 1, otherwise it takes 0.

3. 3. Decision Variables

Q_{kap} The amount of product p shipped from distribution center k to customer a
 Q_{jkp} The amount of product p shipped from manufacturing center j to distribution center k
 Q_{ijh} The amount of raw material h shipped from supplier i to manufacturing center j
 Q_{njp} The amount of product p returned from the recycling center n to production center j
 Q_{amp} The amount of product p returned from customer a to collection center m
 Q_{mep} The amount of product p returned from collection center m to energy recovery center e
 Q_{mnp} The amount of product p returned from collection center m to recycling center n
 Q_{mlp} The amount of product p returned from collection center m to disposal center l
 Q_{nlp} The amount of product p returned from recycling center n to disposal center l
 Q_{nbp} The amount of product p returned from recycling center n to secondary market b
 S_{ap} The amount of shortage of product p at customer a
 U_{jg} If manufacturing center j is established with capacity level of g , it takes 1 and otherwise it takes 0.
 U_{kg} If distribution center k is established with capacity level of g , it takes 1, otherwise it takes 0.
 U_{mg} If collection center m is established with capacity level of g , it takes 1, otherwise it takes 0.
 U_{ng} If recycling center n is established with capacity level of g , it takes 1, otherwise it takes 0.
 Y_{kav} If vehicle v is assigned for shipping to customer a from distribution center k , it takes 1, otherwise it takes 0.

3. 4. Proposed Model

$$\begin{aligned}
 \max Z_1 = & \sum_k \sum_a \sum_p Pr_{ap} Q_{kap} + \\
 & \sum_m \sum_e \sum_p Pr_{ep} Q_{mep} + \sum_n \sum_b \sum_p Pr_{bp} Q_{nbp} - \\
 & \sum_j \sum_g F_{jg} U_{jg} - \sum_k \sum_g F_{kg} U_{kg} - \sum_m \sum_g F_{mg} U_{mg} \\
 & - \sum_n \sum_g F_{ng} U_{ng} - \sum_i \sum_j \sum_v FC_v Y_{ijv} - \\
 & \sum_j \sum_k \sum_v FC_v Y_{jkv} - \sum_k \sum_a \sum_v FC_v Y_{kav} - \\
 & \sum_a \sum_m \sum_v FC_v Y_{amv} - \sum_m \sum_l \sum_v FC_v Y_{mlv} - \\
 & \sum_m \sum_e \sum_v FC_v Y_{mev} - \sum_m \sum_n \sum_v FC_v Y_{mnv} - \\
 & \sum_n \sum_l \sum_v FC_v Y_{nlv} - \sum_n \sum_b \sum_v FC_v Y_{nbv} - \\
 & \sum_n \sum_j \sum_v FC_v Y_{njv} - \sum_i \sum_j \sum_v \bar{F}\bar{V}_v D_{ij} Y_{ijv} - \\
 & \sum_j \sum_k \sum_v \bar{F}\bar{V}_v D_{jk} Y_{jkv} - \sum_k \sum_a \sum_v \bar{F}\bar{V}_v D_{ka} Y_{kav} - \\
 & \sum_a \sum_m \sum_v \bar{F}\bar{V}_v D_{am} Y_{amv} - \sum_m \sum_l \sum_v \bar{F}\bar{V}_v D_{ml} Y_{mlv} - \\
 & \sum_m \sum_e \sum_v \bar{F}\bar{V}_v D_{me} Y_{mev} - \sum_m \sum_n \sum_v \bar{F}\bar{V}_v D_{mn} Y_{mnv} \\
 & - \sum_n \sum_l \sum_v \bar{F}\bar{V}_v D_{nl} Y_{nlv} - \sum_n \sum_b \sum_v \bar{F}\bar{V}_v D_{nb} Y_{nbv} \\
 & - \sum_n \sum_j \sum_v \bar{F}\bar{V}_v D_{nj} Y_{njv} - \sum_i \sum_j \sum_h \bar{S}c_{ih} Q_{ijh} - \\
 & \sum_j \sum_k \sum_p \bar{P}c_{jp} Q_{jkp} - \sum_k \sum_a \sum_p \bar{D}c_{kp} Q_{kap} - \\
 & \sum_a \sum_m \sum_p \bar{C}c_{mp} Q_{amp} - \sum_m \sum_n \sum_p \bar{R}c_{np} Q_{mnp} - \\
 & \sum_m \sum_l \sum_p \bar{L}c_{lp} Q_{mlp} - \sum_n \sum_l \sum_p \bar{L}c_{lp} Q_{nlp} - \\
 & \sum_n \sum_j \sum_p \bar{P}Rc_{jp} Q_{njp} - \vartheta \sum_i \sum_j \sum_v Co2_v D_{ij} Y_{ijv} \\
 & - \vartheta \sum_j \sum_k \sum_v Co2_v D_{jk} Y_{jkv} \\
 & - \vartheta \sum_k \sum_a \sum_v Co2_v D_{ka} Y_{kav}
 \end{aligned} \tag{1}$$

$$\begin{aligned}
 & -\vartheta \sum_a \sum_m \sum_v Co2_v D_{am} Y_{amv} \\
 & -\vartheta \sum_m \sum_l \sum_v Co2_v D_{ml} Y_{mlv} \\
 & -\vartheta \sum_m \sum_e \sum_v Co2_v D_{me} Y_{mev} \\
 & -\vartheta \sum_n \sum_b \sum_v Co2_v D_{nb} Y_{nbv} \\
 & -\vartheta \sum_n \sum_l \sum_v Co2_v D_{nl} Y_{nlv} \\
 & -\vartheta \sum_m \sum_n \sum_v Co2_v D_{mn} Y_{mnv} \\
 & -\vartheta \sum_n \sum_j \sum_v Co2_v D_{nj} Y_{njv} - \vartheta \sum_j \sum_g E_{jg} U_{jg} \\
 & -\vartheta \sum_k \sum_g E_{kg} U_{kg} - \vartheta \sum_m \sum_g E_{mg} U_{mg} - \\
 & \vartheta \sum_n \sum_g E_{ng} U_{ng} - \vartheta \sum_j \sum_k \sum_p R_{ejp} Q_{jkp} \\
 & -\vartheta \sum_a \sum_m \sum_p C_{emp} Q_{amp} - \\
 & \vartheta \sum_m \sum_n \sum_p R_{enp} Q_{mnp} \\
 & -\vartheta \sum_m \sum_l \sum_p L_{elp} Q_{mlp} - \vartheta \sum_n \sum_l \sum_p L_{elp} Q_{nlp} - \\
 & \vartheta \sum_n \sum_j \sum_p R_{pej} Q_{njp} + \vartheta CO_2^{GOV} \\
 & - \sum_a \sum_p \pi_{ap} S_{ap}
 \end{aligned}$$

$$\begin{aligned}
 & max Z_2 = \\
 & \theta_{job} \left\{ \sum_j \sum_g JOB_{jg} U_{jg} + \sum_k \sum_g JOB_{kg} U_{kg} + \right. \\
 & \left. \sum_m \sum_g JOB_{mg} U_{mg} + \sum_n \sum_g JOB_{ng} U_{ng} \right\} \\
 & - \varphi_{ALD} \left\{ \sum_j \sum_g ALD_{jg} U_{jg} + \sum_k \sum_g ALD_{kg} U_{kg} + \right. \\
 & \left. \sum_m \sum_g ALD_{mg} U_{mg} + \sum_n \sum_g ALD_{ng} U_{ng} \right\}
 \end{aligned} \tag{2}$$

$$\begin{aligned}
 & max Z_3 = 1 - \prod_i \prod_a \left(1 - \right. \\
 & \left. \left(\prod_j \prod_k \prod_h \prod_p \prod_v \left(1 - \left(\frac{Re_{ijh} Y_{ijv} *}{Re_{jhp} Y_{jpv} *} \right) \right) \right) \right)
 \end{aligned} \tag{3}$$

s. t.:

$$\sum_k Q_{kap} + S_{ap} = \overline{Dem}_{ap}, \quad \forall a, p \tag{4}$$

$$\sum_a Q_{kap} = \sum_j Q_{jkp}, \quad \forall k, p \tag{5}$$

$$\sum_i \sum_h O_{hp} Q_{ijh} + \sum_n Q_{njp} = \sum_k Q_{jkp}, \quad \forall j, p \tag{6}$$

$$\alpha_{ap} \sum_k Q_{kap} = \sum_m Q_{amp}, \quad \forall a, p \tag{7}$$

$$\beta_{mp} \sum_a Q_{amp} = \sum_e Q_{mep}, \quad \forall m, p \tag{8}$$

$$\gamma_{mp} \sum_a Q_{amp} = \sum_n Q_{mnp}, \quad \forall m, p \tag{9}$$

$$\sum_a Q_{amp} = \sum_l Q_{mlp} + \sum_n Q_{mnp} + \sum_e Q_{mep}, \quad \forall m, p \tag{10}$$

$$\delta_{np} \sum_m Q_{mnp} = \sum_l Q_{nlp}, \quad \forall n, p \tag{11}$$

$$\sigma_{np} \sum_m Q_{mnp} = \sum_j Q_{njp}, \quad \forall n, p \tag{12}$$

$$\sum_m Q_{mnp} = \sum_l Q_{nlp} + \sum_j Q_{njp} + \sum_b Q_{nbp}, \quad \forall n, p \tag{13}$$

$$\sum_k Q_{jkp} \leq \sum_g Cap_{jgp} U_{jg}, \quad \forall j, p \tag{14}$$

$$\sum_a Q_{kap} \leq \sum_g Cap_{kgp} U_{kg}, \quad \forall k, p \tag{15}$$

$$\sum_a Q_{amp} \leq \sum_g Cap_{mpg} U_{mg}, \quad \forall m, p \tag{16}$$

$$\sum_m Q_{mnp} \leq \sum_g Cap_{npg} U_{ng}, \quad \forall n, p \tag{17}$$

$$\sum_j Q_{ijh} \leq \overline{Cap}_{ih}, \quad \forall i, h \tag{18}$$

$$\sum_m Q_{mlp} + \sum_n Q_{nlp} \leq Cap_{lp}, \quad \forall l, p \tag{19}$$

$$\sum_g U_{ng} \leq 1, \quad \forall n \tag{20}$$

$$\sum_g U_{mg} \leq 1, \quad \forall m \tag{21}$$

$$\sum_g U_{jg} \leq 1, \quad \forall j \tag{22}$$

$$\sum_g U_{kg} \leq 1, \quad \forall k \tag{23}$$

$$\sum_h Q_{ijh} w_h \leq \sum_v Cap_{wv} Y_{ijv}, \quad \forall i, j, v \tag{24}$$

$$\sum_p Q_{jkp} w_p \leq \sum_v Cap_{wv} Y_{jkv}, \quad \forall j, k, v \tag{25}$$

$$\sum_p Q_{kap} w_p \leq \sum_v Cap_{wv} Y_{kav}, \quad \forall k, a, v \tag{26}$$

$$\sum_p Q_{amp} w_p \leq \sum_v Cap_{wv} Y_{amv}, \quad \forall a, m, v \tag{27}$$

$$\sum_p Q_{mlp} w_p \leq \sum_v Cap_{wv} Y_{mlv}, \quad \forall m, l, v \tag{28}$$

$$\sum_p Q_{mnp} w_p \leq \sum_v Cap_{wv} Y_{mnv}, \quad \forall m, n, v \tag{29}$$

$$\sum_p Q_{mep} w_p \leq \sum_v Cap_{wv} Y_{mev}, \quad \forall m, e, v \tag{30}$$

$$\sum_p Q_{nlp} w_p \leq \sum_v Cap_{wv} Y_{nlv}, \quad \forall n, l, v \tag{31}$$

$$\sum_p Q_{njp} w_p \leq \sum_v Cap_{wv} Y_{njv}, \quad \forall n, j, v \tag{32}$$

$$\sum_p Q_{nbp} w_p \leq \sum_v Cap_{wv} Y_{nbv}, \quad \forall n, b, v \tag{33}$$

$$\sum_h Q_{ijh} v_h \leq \sum_v Cap_{v} Y_{ijv}, \quad \forall i, j, v \tag{34}$$

$$\sum_p Q_{jkp} v_p \leq \sum_v Cap_{v} Y_{jkv}, \quad \forall j, k, v \tag{35}$$

$$\sum_p Q_{kap} v_p \leq \sum_v Cap_{v} Y_{kav}, \quad \forall k, a, v \tag{36}$$

$$\sum_p Q_{amp} v_p \leq \sum_v Cap_{v} Y_{amv}, \quad \forall a, m, v \tag{37}$$

$$\sum_p Q_{mlp} v_p \leq \sum_v Capv_v Y_{mlv}, \quad \forall m, l, v \quad (38)$$

$$\sum_p Q_{mnp} v_p \leq \sum_v Capv_v Y_{mnv}, \quad \forall m, n, v \quad (39)$$

$$\sum_p Q_{mep} v_p \leq \sum_v Capv_v Y_{mev}, \quad \forall m, e, v \quad (40)$$

$$\sum_p Q_{nlp} v_p \leq \sum_v Capv_v Y_{nlv}, \quad \forall n, l, v \quad (41)$$

$$\sum_p Q_{njp} v_p \leq \sum_v Capv_v Y_{njv}, \quad \forall n, j, v \quad (42)$$

$$\sum_p Q_{nbp} v_p \leq \sum_v Capv_v Y_{nbv}, \quad \forall n, b, v \quad (43)$$

$$\begin{aligned} &Q_{kap}, Q_{jkp}, Q_{ijh}, Q_{njp}, Q_{amp}, Q_{mep}, Q_{mnp}, Q_{mlp}, \\ &Q_{nlp}, Q_{nbp}, S_{ap} \geq 0 \end{aligned} \quad (44)$$

$$\begin{aligned} &U_{jg}, U_{kg}, U_{mg}, U_{ng}, Y_{kav}, Y_{jkv}, Y_{ijv}, Y_{njv}, Y_{amv}, Y_{mev}, \\ &Y_{mnv}, Y_{mlv}, Y_{nlv}, Y_{nbv} \in \{0,1\} \end{aligned} \quad (45)$$

Equation (1) gives the first objective function of the model which maximizes the profit of the supply chain. The income part of the addressed profit is composed of the total sale amount of final products to the customers in the primary markets, the total sale amount of lower quality recycled products in the secondary market and the energy from lower quality returned products. The cost part of the addressed profit is composed of fixed construction costs, fixed and variable costs of using the vehicle, costs of producing excess carbon dioxide greater than the accepted amount, and operating costs of producing the final products. Equation (2) gives the second objective function which maximizes the number of jobs created by the establishment of new potential centers. In this regard, the average number of lost days because of work injuries is also included. Equation (3) gives the third objective function which maximizes the reliabilities of the routes of the final products from the supplier to the customers of the primary markets. Equation (4) shows how to meet the customers' demands at the primary markets considering the possible shortages. Equation (5) guarantees the equality of input to and output from each distribution center for each product. Equation (6) shows the equality of input to and output from each manufacturing center. Equation (7) calculates the fraction of products which are discarded by customers due to lower quality. Equation (8) gives the fraction of low quality products which are converted into energy and new products. Equation (9) gives the fraction of low quality products which are remanufacture or sold. Equation (10) gives the equality relation of collecting returned products in the collection center. Equation (11) gives the fraction of low quality returned products which cannot be used in any way and should be disposed. Equation (12) shows the percentage of returned products which can be remanufactured at the manufacturing centers. Equation (13) gives the equality relation at the

recycling center. Inequalities (14) to (19) give the capacity constraints and ensure that if any potential center is opened with a specific capacity level, the corresponding capacity level is observed. Equations (20) to (23) ensure that a maximum capacity level for each potential center can be used. Inequalities (24) to (33) are related to weight capacity constraint of vehicles for shipping raw materials and products. Inequalities (34) to (43) are related to volume capacity constraint of vehicles for shipping raw materials and products. Constraints (44) and (45) give the status of the decision variables of the model.

3. 5. Possibilistic Fuzzy Programming Method for Uncertain Numbers

Suppose that a parameter a_{ij} is an uncertain parameter with mean of μ_{ij} and standard deviation of σ_{ij} . It is also assumed that all considered uncertain parameters are independent from each other; therefore, the mean and standard deviation of the estimated set of possible random numbers can be shown as follows [38]:

$$S_{ij} = \{x_k | x_k \in \text{assumed distribution}; k = 1, \dots, N\} \quad (46)$$

In the above relation x_k is a possible random data value. Value of N is a sufficient number of random sets that state all the conditions necessary to generate a possible random data. Also, for accurate estimation of the probabilistic data, the fuzzy constraint coefficient of the numbers $T = \tilde{A} = (A^-, A^0, A^+)$ is defined. As a result, the function of the triangular fuzzy distribution is as follows:

| | | |
|-------|---|---|
| | Represents the most reliable value of set S_{ij} . When a value of 1 is assigned to it as membership degree of a fuzzy number, then it is equal to mean of S_{ij} random distribution function. | $A^0 = \frac{\sum_{i=1}^N x_i}{N}$ |
| A^- | Represents the minimum value of set S_{ij} | $A^- = \inf(x_i) \quad i = 1, \dots, N$ |
| A^+ | Represents the maximum value of set S_{ij} | $A^+ = \sup(x_i) \quad i = 1, \dots, N$ |

As a result, according to the above-mentioned definitions, the following equation is used to control the possible parameter of a_{ij} with mean μ_{ij} and standard deviation of σ_{ij} .

$$\begin{aligned} &\max C^T X \\ &s. t.: \\ &\frac{A^- + 4A^0 + A^+}{6} X \leq b \\ &X > 0 \end{aligned} \quad (47)$$

3. 6. Probabilistic Planning Method Consider the following linear programming model given in Equation (48):

$$\begin{aligned}
 & \min E = cx + fy \\
 & \text{s. t.:} \\
 & Ax \geq_f d \\
 & Bx = 0 \\
 & Sx \leq_f Ny \\
 & Ty \leq 1 \\
 & y \in \{0,1\}, x \geq 0
 \end{aligned}
 \tag{48}$$

In the above model, the fixed cost of constructing new centers and the variable costs of transportation and operation are represented by f and c . Parameters related to constraint coefficients are represented by h A , B , S and T . N and d represent the capacity of the facility and the customer demand for the products, respectively. Furthermore, x and y represent the continuous and binary variables, respectively. Capacity and demand parameters are assumed to be possibly fuzzy. Therefore, the model can be stated as in Equation (49):

$$\begin{aligned}
 & \min E = cx + fy \\
 & \text{s. t.:} \\
 & Ax \geq d - \tilde{t}(1 - \alpha) \\
 & Bx = 0 \\
 & Sx \leq Ny + [\tilde{r}(1 - \beta)]y \\
 & Ty \leq 1 \\
 & y \in \{0,1\}, x \geq 0
 \end{aligned}
 \tag{49}$$

In which, \tilde{t} and \tilde{r} are two fuzzy numbers representing to deal with the given soft constraints. In the above model, α and β represent the minimum level of satisfaction index of flexible constraints. It is also assumed that \tilde{t} and \tilde{r} are considered as triangular fuzzy numbers shown as $\tilde{t} = (t^p, t^m, t^o)$ and $\tilde{r} = (r^p, r^m, r^o)$. Consider that α and β are parameters between zero and one; i.e. $0 \leq \alpha, \beta \leq 1$. To ensure that the considered constraints with uncertain parameters are feasible, it is necessary to control them using the flexible robust programming method. Thus, we use the penalty technique to prevent from non-feasibility as follows:

$$\begin{aligned}
 & \min E = cx + fy + \theta[t(1 - \alpha)] + \lambda[r(1 - \beta)]y \\
 & \text{s. t.:} \\
 & Ax \geq d - t(1 - \alpha) \\
 & Bx = 0 \\
 & Sx \leq Ny + [r(1 - \beta)]y \\
 & Ty \leq 1 \\
 & y \in \{0,1\}, x \geq 0
 \end{aligned}
 \tag{50}$$

where λ and θ are the penalty coefficients. The final model of the problem is given as in Equations (51)-(95):

$$\begin{aligned}
 \max Z_1 = & \sum_k \sum_a \sum_p Pr_{ap} Q_{kap} + \\
 & \sum_m \sum_e \sum_p Pr_{ep} Q_{mep} + \sum_n \sum_b \sum_p Pr_{bp} Q_{nbp} - \\
 & \sum_j \sum_g F_{jg} U_{jg} - \sum_k \sum_g F_{kg} U_{kg} - \sum_m \sum_g F_{mg} U_{mg} \\
 & - \sum_n \sum_g F_{ng} U_{ng} - \sum_i \sum_j \sum_v FC_v Y_{ijv} - \\
 & \sum_j \sum_k \sum_v FC_v Y_{jkv} - \sum_k \sum_a \sum_v FC_v Y_{kav} - \\
 & \sum_a \sum_m \sum_v FC_v Y_{amv} - \sum_m \sum_l \sum_v FC_v Y_{mlv} - \\
 & \sum_m \sum_e \sum_v FC_v Y_{mev} - \sum_m \sum_n \sum_v FC_v Y_{mnv} - \\
 & \sum_n \sum_l \sum_v FC_v Y_{nlv} - \sum_n \sum_b \sum_v FC_v Y_{nbv} - \\
 & \sum_n \sum_j \sum_v FC_v Y_{njv} - \\
 & \sum_i \sum_j \sum_v \left(\frac{Fv_{ij}^- + 4Fv_{ij}^0 + Fv_{ij}^+}{6} \right) D_{ij} Y_{ijv} - \\
 & \sum_j \sum_k \sum_v \left(\frac{Fv_{jk}^- + 4Fv_{jk}^0 + Fv_{jk}^+}{6} \right) D_{jk} Y_{jkv} - \\
 & \sum_m \sum_e \sum_v \left(\frac{Fv_{me}^- + 4Fv_{me}^0 + Fv_{me}^+}{6} \right) D_{me} Y_{mev} - \\
 & \sum_k \sum_a \sum_v \left(\frac{Fv_{ka}^- + 4Fv_{ka}^0 + Fv_{ka}^+}{6} \right) D_{ka} Y_{kav} - \\
 & \sum_a \sum_m \sum_v \left(\frac{Fv_{am}^- + 4Fv_{am}^0 + Fv_{am}^+}{6} \right) D_{am} Y_{amv} - \\
 & \sum_m \sum_l \sum_v \left(\frac{Fv_{ml}^- + 4Fv_{ml}^0 + Fv_{ml}^+}{6} \right) D_{ml} Y_{mlv} - \\
 & \sum_n \sum_b \sum_v \left(\frac{Fv_{nb}^- + 4Fv_{nb}^0 + Fv_{nb}^+}{6} \right) D_{nb} Y_{nbv} - \\
 & \sum_n \sum_j \sum_v \left(\frac{Fv_{nj}^- + 4Fv_{nj}^0 + Fv_{nj}^+}{6} \right) D_{nj} Y_{njv} - \\
 & \sum_m \sum_n \sum_v \left(\frac{Fv_{mn}^- + 4Fv_{mn}^0 + Fv_{mn}^+}{6} \right) D_{mn} Y_{mnv} - \\
 & \sum_n \sum_l \sum_v \left(\frac{Fv_{nl}^- + 4Fv_{nl}^0 + Fv_{nl}^+}{6} \right) D_{nl} Y_{nlv} - \\
 & \sum_i \sum_j \sum_h \left(\frac{Sc_{ih}^- + 4Sc_{ih}^0 + Sc_{ih}^+}{6} \right) Q_{ijh} - \\
 & \sum_j \sum_k \sum_p \left(\frac{Pc_{jp}^- + 4Pc_{jp}^0 + Pc_{jp}^+}{6} \right) Q_{jkp} - \\
 & \sum_a \sum_m \sum_p \left(\frac{Cc_{mp}^- + 4Cc_{mp}^0 + Cc_{mp}^+}{6} \right) Q_{amp} - \\
 & \sum_m \sum_n \sum_p \left(\frac{Rc_{np}^- + 4Rc_{np}^0 + Rc_{np}^+}{6} \right) Q_{mnp} - \\
 & \sum_m \sum_l \sum_p \left(\frac{Lc_{lp}^- + 4Lc_{lp}^0 + Lc_{lp}^+}{6} \right) Q_{mlp} - \\
 & \sum_k \sum_a \sum_p \left(\frac{Dc_{kp}^- + 4Dc_{kp}^0 + Dc_{kp}^+}{6} \right) Q_{kap} - \\
 & \sum_n \sum_l \sum_p \left(\frac{Lc_{lp}^- + 4Lc_{lp}^0 + Lc_{lp}^+}{6} \right) Q_{nlp} - \\
 & \sum_n \sum_j \sum_p \left(\frac{Prc_{jp}^- + 4Prc_{jp}^0 + Prc_{jp}^+}{6} \right) Q_{njp} - \\
 & -\vartheta \sum_i \sum_j \sum_v Co2_v D_{ij} Y_{ijv} \\
 & -\vartheta \sum_j \sum_k \sum_v Co2_v D_{jk} Y_{jkv} \\
 & -\vartheta \sum_k \sum_a \sum_v Co2_v D_{ka} Y_{kav}
 \end{aligned}
 \tag{51}$$

$$\begin{aligned}
 & -\vartheta \sum_a \sum_m \sum_v Co2_v D_{am} Y_{amv} \\
 & -\vartheta \sum_m \sum_l \sum_v Co2_v D_{ml} Y_{mlv} \\
 & -\vartheta \sum_m \sum_e \sum_v Co2_v D_{me} Y_{mev} \\
 & -\vartheta \sum_n \sum_b \sum_v Co2_v D_{nb} Y_{nbv} \\
 & -\vartheta \sum_n \sum_l \sum_v Co2_v D_{nl} Y_{nlv} \\
 & -\vartheta \sum_m \sum_n \sum_v Co2_v D_{mn} Y_{mnv} \\
 & -\vartheta \sum_n \sum_j \sum_v Co2_v D_{nj} Y_{njv} - \vartheta \sum_j \sum_g E_{jg} U_{jg} \\
 & -\vartheta \sum_k \sum_g E_{kg} U_{kg} - \vartheta \sum_m \sum_g E_{mg} U_{mg} - \\
 & \vartheta \sum_n \sum_g E_{ng} U_{ng} - \vartheta \sum_j \sum_k \sum_p P_{ejp} Q_{jkp} \\
 & -\vartheta \sum_a \sum_m \sum_p C_{emp} Q_{amp} - \\
 & \vartheta \sum_m \sum_n \sum_p R_{enp} Q_{mnp} \\
 & -\vartheta \sum_m \sum_l \sum_p L_{elp} Q_{mlp} - \vartheta \sum_n \sum_l \sum_p L_{elp} Q_{nlp} - \\
 & \vartheta \sum_n \sum_j \sum_p R_{pejp} Q_{njp} + \vartheta CO_2^{GOV} \\
 & - \sum_a \sum_p \pi_{ap} S_{ap} - \sum_a \sum_p \theta [Dem_{ap}^+ (1 - \alpha_1)] - \\
 & \sum_i \sum_h \lambda [CapI_{ih}^- (1 - \beta_1)]
 \end{aligned}$$

$$\begin{aligned}
 & max Z_2 = \\
 & \theta_{job} \left\{ \sum_j \sum_g JOB_{jg} U_{jg} + \sum_k \sum_g JOB_{kg} U_{kg} + \right. \\
 & \left. \sum_m \sum_g JOB_{mg} U_{mg} + \sum_n \sum_g JOB_{ng} U_{ng} \right\} \\
 & - \varphi_{ALD} \left\{ \sum_j \sum_g ALD_{jg} U_{jg} + \sum_k \sum_g ALD_{kg} U_{kg} + \right. \\
 & \left. \sum_m \sum_g ALD_{mg} U_{mg} + \sum_n \sum_g ALD_{ng} U_{ng} \right\}
 \end{aligned} \tag{52}$$

$$\begin{aligned}
 & max Z_3 = 1 - \prod_i \prod_a \left(1 - \right. \\
 & \left. \left(1 - \prod_j \prod_k \prod_h \prod_p \prod_v \left(1 - \left(\begin{matrix} Re_{ijh} Y_{ijv} * \\ Re_{jkp} Y_{jkv} * \\ Re_{kap} Y_{kav} \end{matrix} \right) \right) \right) \right)
 \end{aligned} \tag{53}$$

s. t.:

$$\sum_k Q_{kap} + S_{ap} = (Dem_{ap}^o + [Dem_{ap}^+ (1 - \alpha_1)]), \quad \forall a, p \tag{54}$$

$$\sum_a Q_{kap} = \sum_j Q_{jkp}, \quad \forall k, p \tag{55}$$

$$\sum_i \sum_h O_{hp} Q_{ijh} + \sum_n Q_{njp} = \sum_k Q_{jkp}, \quad \forall j, p \tag{56}$$

$$\alpha_{ap} \sum_k Q_{kap} = \sum_m Q_{amp}, \quad \forall a, p \tag{57}$$

$$\beta_{mp} \sum_a Q_{amp} = \sum_e Q_{mep}, \quad \forall m, p \tag{58}$$

$$\gamma_{mp} \sum_a Q_{amp} = \sum_n Q_{mnp}, \quad \forall m, p \tag{59}$$

$$\sum_a Q_{amp} = \sum_l Q_{mlp} + \sum_n Q_{mnp} + \sum_e Q_{mep}, \quad \forall m, p \tag{60}$$

$$\delta_{np} \sum_m Q_{mnp} = \sum_l Q_{nlp}, \quad \forall n, p \tag{61}$$

$$\sigma_{np} \sum_m Q_{mnp} = \sum_j Q_{njp}, \quad \forall n, p \tag{62}$$

$$\sum_m Q_{mnp} = \sum_l Q_{nlp} + \sum_j Q_{njp} + \sum_b Q_{nbp}, \quad \forall n, p \tag{63}$$

$$\sum_k Q_{jkp} \leq \sum_g CapJ_{jgp} U_{jg}, \quad \forall j, p \tag{64}$$

$$\sum_a Q_{kap} \leq \sum_g CapK_{kpg} U_{kg}, \quad \forall k, p \tag{65}$$

$$\sum_a Q_{amp} \leq \sum_g CapM_{mpg} U_{mg}, \quad \forall m, p \tag{66}$$

$$\sum_m Q_{mnp} \leq \sum_g CapN_{npg} U_{ng}, \quad \forall n, p \tag{67}$$

$$\sum_j Q_{ijh} \leq (CapI_{ih}^o + [CapI_{ih}^- (1 - \beta_1)]), \quad \forall i, h \tag{68}$$

$$\sum_m Q_{mlp} + \sum_n Q_{nlp} \leq CapL_{lp}, \quad \forall l, p \tag{69}$$

$$\sum_g U_{ng} \leq 1, \quad \forall n \tag{70}$$

$$\sum_g U_{mg} \leq 1, \quad \forall m \tag{71}$$

$$\sum_g U_{jg} \leq 1, \quad \forall j \tag{72}$$

$$\sum_g U_{kg} \leq 1, \quad \forall k \tag{73}$$

$$\sum_h Q_{ijh} w_h \leq \sum_v Capw_v Y_{ijv}, \quad \forall i, j, v \tag{74}$$

$$\sum_p Q_{jkp} w_p \leq \sum_v Capw_v Y_{jkv}, \quad \forall j, k, v \tag{75}$$

$$\sum_p Q_{kap} w_p \leq \sum_v Capw_v Y_{kav}, \quad \forall k, a, v \tag{76}$$

$$\sum_p Q_{amp} w_p \leq \sum_v Capw_v Y_{amv}, \quad \forall a, m, v \tag{77}$$

$$\sum_p Q_{mlp} w_p \leq \sum_v Capw_v Y_{mlv}, \quad \forall m, l, v \tag{78}$$

$$\sum_p Q_{mnp} w_p \leq \sum_v Capw_v Y_{mnv}, \quad \forall m, n, v \tag{79}$$

$$\sum_p Q_{mep} w_p \leq \sum_v Capw_v Y_{mev}, \quad \forall m, e, v \tag{80}$$

$$\sum_p Q_{nlp} w_p \leq \sum_v Capw_v Y_{nlv}, \quad \forall n, l, v \tag{81}$$

$$\sum_p Q_{njp} w_p \leq \sum_v Capw_v Y_{njv}, \quad \forall n, j, v \tag{82}$$

$$\sum_p Q_{nbp} w_p \leq \sum_v Capw_v Y_{nbv}, \quad \forall n, b, v \tag{83}$$

$$\sum_h Q_{ijh} v_h \leq \sum_v Capv_v Y_{ijv}, \quad \forall i, j, v \tag{84}$$

$$\sum_p Q_{jkp} v_p \leq \sum_v Capv_v Y_{jkv}, \quad \forall j, k, v \tag{85}$$

$$\sum_p Q_{kap} v_p \leq \sum_v Capv_v Y_{kav}, \quad \forall k, a, v \tag{86}$$

$$\sum_p Q_{amp} v_p \leq \sum_v Capv_v Y_{amv}, \quad \forall a, m, v \tag{87}$$

$$\sum_p Q_{mlp} v_p \leq \sum_v Cap v_v Y_{mlv}, \quad \forall m, l, v \quad (88)$$

$$\sum_p Q_{mnp} v_p \leq \sum_v Cap v_v Y_{mnv}, \quad \forall m, n, v \quad (89)$$

$$\sum_p Q_{mep} v_p \leq \sum_v Cap v_v Y_{mev}, \quad \forall m, e, v \quad (90)$$

$$\sum_p Q_{nlp} v_p \leq \sum_v Cap v_v Y_{nlv}, \quad \forall n, l, v \quad (91)$$

$$\sum_p Q_{njp} v_p \leq \sum_v Cap v_v Y_{njv}, \quad \forall n, j, v \quad (92)$$

$$\sum_p Q_{nbp} v_p \leq \sum_v Cap v_v Y_{nbv}, \quad \forall n, b, v \quad (93)$$

$$Q_{kap}, Q_{jkp}, Q_{ijh}, Q_{njp}, Q_{amp}, Q_{mep}, Q_{mnp}, Q_{mlp}, \quad (94)$$

$$Q_{nlp}, Q_{nbp}, S_{ap} \geq 0$$

$$U_{jg}, U_{kg}, U_{mg}, U_{ng}, Y_{kav}, Y_{jkv}, Y_{ijv}, Y_{njv}, Y_{amv}, \quad (95)$$

$$Y_{mev}, Y_{mnv}, Y_{mlv}, Y_{nlv}, Y_{nbv} \in \{0,1\}$$

4. SOLUTION ALGORITHM

In this section, the solution representation and the major solution algorithm are presented.

4. 1. Designing Solution Representation

The complexity of supply chain network models has been demonstrated in many researches. The CLSC network models are studied to tackle the two problems of facility location and flow optimization [39]. The complexity of these models can be reduced to the complexity of the location problems; on the other hand, Np-Hard nature of these problems has been proven by many researchers [40]. As a result, meta-heuristic algorithms such as NSGA II and MOGWO can be used to tackle them. The first step is to design solution representation, which is the same in both algorithms. This coding is known as priority-based encryption, introduced by Gen et al. [41]. In this encoding, the supply chain network is divided into its constituent levels, and each level is considered in the design of the solution structure according to the capacity, demand, type of vehicle, and etc. Figure 2 shows an example of a two-tier supply chain network with three sources and four depots. In this structure, sources have been selected and replenish the demand of depots

Figure 3 shows a sample of the original solution and its decoding. The priority-based decoding modified in Figure 3 is in accordance with the following four steps:

Step 1. First, the largest priority (number) is selected from the chromosomes related to the sources. If the source is able to supply all the depots, the priority of other sources reduces to zero. In this case, location is done for sources which do not have zero priority.

Step 2. The highest priority (number) from the whole chromosome is selected as the first level of allocation

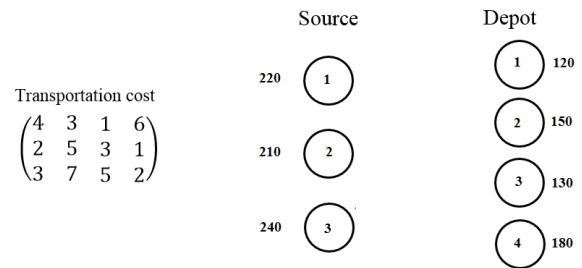


Figure 2. An example of a two-level supply chain network structure

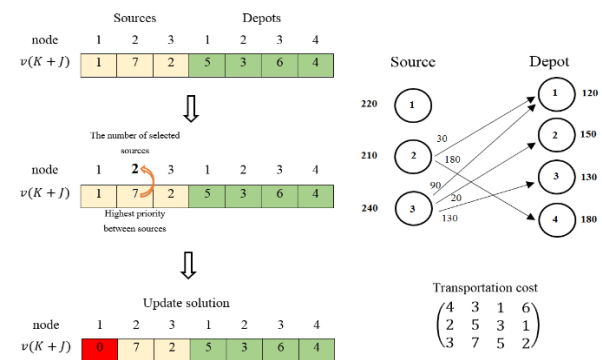


Figure 3. How priority-based encoding and decoding Modified

Step 3. Based on the shipping cost, the lowest shipping cost is obtained from the allocation level selected from step 2 (source/depot), with the new allocable level (depot/source), and the second allocation level is determined.

Step 4. After determining the source and depot, the minimum amount of depot demand and source capacity is considered as the optimal amount of allocation. After the allocation operation, the amount of depot demand as well as the capacity of the source is updated.

4. 2. Performance of Mogwo

Gray wolves are predators at the top of the food pyramid or the food chain. Gray wolves mostly prefer to live in groups. The average group size is 5-12 wolves. Wolves have a very precise and orderly social dominant hierarchy shown in Figure 4 [42].

Leaders consist of a male and a female called Alpha. Alpha is primarily responsible for decisions about hunting, where to sleep, when to wake up, and so on. Alpha decisions are communicated to the group; however, some democratic behaviors have also been observed in which an Alpha follows the other wolves in the group. In communities, the entire herd endorses Alpha. Alpha Wolf is also known as the dominant wolf, because the commands must be executed by the group. Alpha wolves are only allowed to mate in the herd.

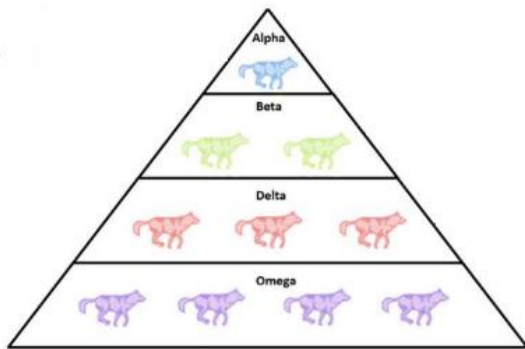


Figure 4. Gray wolf social hierarchy

It is important to note that Alpha is not necessarily the strongest member of the herd, but the best member in terms of management in the herd. The second level in the gray wolf hierarchy is Beta. Beta is the wolf that help Alpha make decisions or other herd decisions. The Beta wolf can be male or female, and he is the best replacement for Alpha in the event of his death or aging. Beta executes Alpha commands across the herd and gives feedback to Alpha. Omega wolf is the foot of the lowest class in the gray wolf hierarchy. Omega wolves usually have to follow all the high-level and dominant wolves. They are the last wolves allowed to eat. If the wolf is not an Alpha or Omega, it is called a Delta. Delta wolves must be subject to Alpha and Beta. However, they dominate Omega. In this paper, the behavior of gray wolf hunting is applied to solve the problem of CLSC. When designing the gray wolf algorithm, in order to mathematically model the social wolf hierarchy, Alpha (α) is considered as the most appropriate solution. Subsequently Beta (β) and Delta (δ) are the second and third most suitable solutions. The rest of the candidate solutions are assumed to be Omega (X). Gray wolves must find and surround their prey in order to hunt. Therefore, the following equations (96)-(97) update the positions of the wolves around the prey.

$$\vec{D} = |\vec{C} \cdot \vec{X}_p(t) - \vec{X}(t)| \tag{96}$$

$$\vec{X}(t + 1) = \vec{X}(t) - \vec{A} \cdot \vec{D} \tag{97}$$

In the above equations, \vec{C} and A are the coefficient vectors. \vec{X}_p represents the hunting position vector and X is the gray wolf position vector. This is an equilibrium equation between siege and hunting. Therefore, the search radius must be optimized during the process; for this purpose, the equations for the two coefficients used in the above equations are as (98)-(99).

$$\vec{A} = 2\vec{a} \cdot \vec{r}_1 - \vec{a} \tag{98}$$

$$\vec{C} = 2\vec{r}_2 \tag{99}$$

As a result, the following equations (100)-(102) are used to perform the hunting.

$$\vec{D}_\alpha = |\vec{C}_1 \cdot \vec{X}_\alpha - \vec{X}|, \vec{D}_\beta = |\vec{C}_2 \cdot \vec{X}_\beta - \vec{X}|, \vec{D}_\delta = |\vec{C}_3 \cdot \vec{X}_\delta - \vec{X}| \tag{100}$$

$$\vec{X}_1 = \vec{X}_\alpha - \vec{A}_1 \cdot \vec{D}_\alpha, \vec{X}_2 = \vec{X}_\beta - \vec{A}_2 \cdot \vec{D}_\beta, \vec{X}_3 = \vec{X}_\delta - \vec{A}_3 \cdot \vec{D}_\delta \tag{101}$$

$$\vec{X}(t + 1) = \frac{\vec{X}_1 + \vec{X}_2 + \vec{X}_3}{3} \tag{102}$$

5. COMPUTATIONAL RESULTS

In this section, initially, some numerical examples in different sizes are designed and solved. Due to the NP-Hard nature of the problem, the two algorithms of MOGWO and NSGA II were used in order to tackle the problem. At the end, we will implement the model for a real case study in Iranian engine oil industry.

5. 1. Solving the Problem for Small Sizes In this section, small sized numerical examples are designed as the given structure in Table 3. Furthermore, the required data are randomly generated as in Table 4.

All parameters generated in Tables 4 are randomly based on uniform distribution.

TABLE 3. The structure of the designed numerical examples for small size

| Set | G | I | N | L | P | V | H | B | E | M | J | K | A |
|--------|---|---|---|---|---|---|---|---|---|---|---|---|---|
| Values | 3 | 3 | 3 | 3 | 2 | 3 | 3 | 3 | 3 | 3 | 3 | 3 | 4 |

TABLE 4. Limits of problem parameter intervals based on uniform distribution

| Approximate range | Parameter |
|-----------------------|--|
| $\sim U(0.03,0.05)$ | w_h |
| $\sim U(0.08,0.1)$ | w_p |
| $\sim U(0.3,0.5)$ | v_h |
| $\sim U(0.5,0.8)$ | v_p |
| $\sim U(10000,12000)$ | $F_{jg}, F_{kg}, F_{mg}, F_{ng}$ |
| $\sim U(1000,1200)$ | FC_v |
| $\sim U(10,100)$ | $D_{ka}, D_{jk}, D_{ij}, D_{nj}, D_{am}$ |
| $\sim U(10,100)$ | $D_{me}, D_{mn}, D_{ml}, D_{nl}, D_{nb}$ |
| $\sim U(5,8)$ | $Co2_v$ |
| $\sim U(50,100)$ | $E_{jg}, E_{kg}, E_{mg}, E_{ng}$ |
| 0.5 | ϑ |
| 1 | $\varphi_{ALD}, \theta_{Job}$ |

| $\sim U(0.1,0.4)$ | $Re_{ijh}, Re_{jkp}, Re_{kap}$ | | |
|---------------------|--|---------------------|--|
| $\sim U(1,2)$ | O_{np} | | |
| $\sim U(0.1,0.2)$ | α_{ap} | | |
| $\sim U(0.3,0.4)$ | β_{mp}, γ_{mp} | | |
| $\sim U(0.2,0.3)$ | δ_{np}, σ_{np} | | |
| $\sim U(1000,1200)$ | $Pr_{ap}, Pr_{ep}, Pr_{bp}, CapL_{1p}$ | | |
| $\sim U(5000,6000)$ | $CapJ_{jpg}, CapK_{kpg}$ | | |
| $\sim U(2000,3000)$ | $CapM_{mpg}, CapN_{npg}$ | | |
| $\sim U(500,700)$ | $Capw_v, Capv_v$ | | |
| $\sim U(50,80)$ | π_{ap} | | |
| 10000 | Co_2^{GOV} | | |
| $\sim U(1,3)$ | $Pe_{jp}, Ce_{mp}, Re_{np}$ | | |
| $\sim U(1,3)$ | Le_{ip}, RPe_{jp} | | |
| $\sim U(500,1000)$ | $JOB_{jg}, JOB_{kg}, JOB_{mg}, JOB_{ng}$ | | |
| $\sim U(10,20)$ | $ALD_{jg}, ALD_{kg}, ALD_{mg}, ALD_{ng}$ | | |
| Level 3 | Level 2 | Level 1 | Parameter |
| $\sim U(2000,3000)$ | $\sim U(1500,2000)$ | $\sim U(1000,1500)$ | \overline{Dem}_{ap} |
| $\sim U(8000,9000)$ | $\sim U(7000,8000)$ | $\sim U(6000,700)$ | \overline{Capl}_{ih} |
| $\sim U(8,10)$ | $\sim U(7,8)$ | $\sim U(5,7)$ | \overline{FV}_v |
| $\sim U(3,4)$ | $\sim U(2,3)$ | $\sim U(1,2)$ | $\overline{Rc}_{np}, \overline{Lc}_{ip}, \overline{R\overline{Pc}}_{jp}$ |
| $\sim U(3,4)$ | $\sim U(2,3)$ | $\sim U(1,2)$ | $\overline{Pc}_{jp}, \overline{Sc}_{ih}, \overline{Dc}_{kp}, \overline{Cc}_{mp}$ |

After generating the values for the small size sample, the three-objective problem is solved utilizing optimization package of GAMS. For this purpose, the comprehensive criterion method has been used. Therefore, the optimal value of the first objective function turns out to be 18838690, the optimal value of the second objective function turns out to be 9683 and the optimal value of the third objective function turns out to be 1. As a result, with the same weight for all three objective functions, the efficient solution obtained from solving the problem includes the value of 18266820.14 for the first objective function, 9683 for the second objective function and 0.998 for the third objective function. Table 5 gives the optimal location of the facilities resulting from the addressed solution.

A set of efficient solutions using the comprehensive criterion method is given as in Table 6.

According to the results from Table 6, by increasing the number of facilities, including suppliers and manufacturing centers, the amount of total costs increases and at the same time the number of jobs created and the reliability rates increases due to increasing the number of facilities.

In the following, the sensitivity analysis of the CLSC network model is given under the parameters of the solid fuzzy optimization method. Figure 5 shows the changes of the values of the objective functions for different parameters $\alpha 1$ and $\beta 1$, assuming that the values of θ and λ are constant and equal to 1.

TABLE 5. Optimal location of selected facilities along with capacity level

| Facilities | Selected location along with capacity level | Facilities | Selected location along with capacity level |
|---------------------|---|-------------------|---|
| Production center | Center 1 with capacity level 2 | Collection center | Center 1 with capacity level 2 |
| | Center 2 with capacity level 1 | | Center 2 with capacity level 3 |
| | Center 3 with capacity level 3 | | Center 3 with capacity level 3 |
| Distribution center | Center 1 with capacity level 3 | Recycling Center | Center 1 with capacity level 3 |
| | Center 2 with capacity level 2 | | Center 2 with capacity level 3 |
| | Center 3 with capacity level 1 | | Center 3 with capacity level 2 |

TABLE 6. A set of efficient solutions obtained from solving the small size instances

| Efficient solution | Objective function 1 | Objective function 2 | Objective function 3 |
|--------------------|----------------------|----------------------|----------------------|
| 1 | 18081104.67 | 9455 | 0.986 |
| 2 | 18135294.68 | 9459 | 0.988 |
| 3 | 18223710.81 | 9501 | 0.990 |
| 4 | 18266820.14 | 9683 | 0.998 |
| 5 | 18329116.28 | 9726 | 0.992 |
| 6 | 18338314.06 | 9737 | 0.994 |
| 7 | 18364072.99 | 9772 | 1.000 |
| 8 | 18369916.05 | 9784 | 1.000 |
| 9 | 18440417.30 | 9847 | 1.000 |

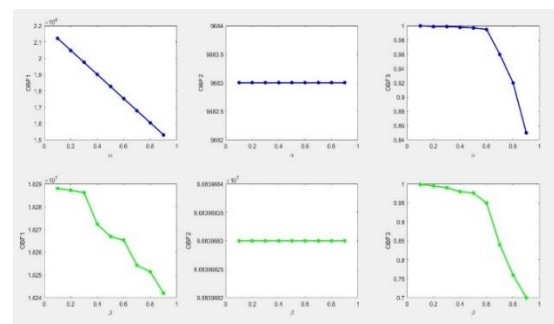


Figure 5. Changes in the values of the first objective function for stable fuzzy optimization parameters

According to the results of sensitivity analysis, by increasing the values of α_1 and β_1 , the first and third objective functions increases. This indicates that the amount of demand increases as the uncertainty increases and as a result, shipping costs increase and reliability to meet customer demand decreases. On the other hand, by increasing the uncertainty rate, the amount of supplier capacity decreases and therefore the amount of transportation costs increases. As transportation costs increase, the profit of the chain decreases.

5. 2. Comparing Solution for Small Size Problem

In order to evaluate the performances of NSGA II and MOGWO algorithms, some indicators are considered for comparing the Pareto front solutions Table 7 shows the indicators obtained from NSGA II and MOGWO algorithms in comparison with the comprehensive criterion as a benchmark method. According to the results obtained from this table, the comprehensive criterion method outperforms other algorithms considering the average values of the objective functions. NSGA II works better considering maximum expansion index and metric distance index and finally MOGWO outperforms other algorithms considering the number of Pareto-optimal front (*NPF*) and computational time (CPU time).

5. 3. Solving The Problem for Larger Sizes

The following 15 sample problems are designed according to the data given in Table 2 for larger sizes. Each instance of the problem is run five times using MOGWO and NSGA II algorithms. The addressed indicators' values are given as in Table 8.

Table 9 shows the output results of the T-Test on the means of the objective functions and comparison results. According to Table 9 and considering the value of P test statistics, there is no significant difference between the means of the obtained objective functions and also the comparison indices of meta-heuristic algorithms.

TABLE 7. Indicators obtained from solving the problem for small size using different methods

| Indicator | LP Metrics | NSGA II | MOGWO |
|---|-------------|-------------|-------------|
| The average of the first objective function | 18283196.33 | 18242715.39 | 18280678.07 |
| OBF1 | 9662.66 | 9598.56 | 9583.89 |
| OBF2 | 0.994 | 0.992 | 0.993 |
| <i>NPF</i> | 9 | 16 | 19 |
| <i>MSI</i> | 359312.84 | 367355.83 | 336298.71 |
| <i>MID</i> | 157221.08 | 204193.5 | 170039.61 |
| <i>SM</i> | 0.6272 | 0.495 | 0.684 |
| <i>CPU time</i> | 14.67 | 8.16 | 5.99 |

TABLE 8. The indicators' values for comparing the algorithms for large size instances

| Problem | OBF1* 100000 | OBF2* 100 | OBF3 | <i>NPF</i> | <i>MSI</i> * 1000 | <i>SM</i> * 1000 | <i>MID</i> | CPU time |
|---------|-----------------|--------------|-------|------------|----------------------|---------------------|------------|-------------|
| NSGA II | | | | | | | | |
| 1 | 292.2 | 17.0 | 0.986 | 15 | 2.5 | 3.0 | 0.63 | 18.2 |
| 2 | 354.9 | 30.5 | 0.994 | 17 | 3.9 | 2.8 | 0.88 | 54.0 |
| 3 | 380.1 | 38.1 | 0.993 | 25 | 3.5 | 4.6 | 0.59 | 85.1 |
| 4 | 415.6 | 63.2 | 0.991 | 12 | 3.0 | 5.3 | 0.64 | 121.2 |
| 5 | 603.2 | 72.9 | 0.994 | 23 | 3.1 | 3.3 | 0.55 | 167.7 |
| 6 | 767.5 | 72.9 | 0.993 | 20 | 3.9 | 5.1 | 0.79 | 217.2 |
| 7 | 821.4 | 81.2 | 0.984 | 16 | 2.8 | 4.7 | 0.84 | 272.8 |
| 8 | 856.4 | 86.5 | 0.983 | 13 | 4.5 | 2.0 | 0.77 | 334.5 |
| 9 | 880.6 | 111.8 | 1.000 | 16 | 4.1 | 4.4 | 0.71 | 409.8 |
| 10 | 1026.6 | 131.8 | 0.983 | 17 | 4.9 | 3.5 | 0.82 | 479.8 |
| 11 | 1173.6 | 152.7 | 0.981 | 11 | 4.9 | 4.6 | 0.82 | 520.0 |
| 12 | 1524.2 | 154.6 | 0.991 | 19 | 4.7 | 2.0 | 0.84 | 662.9 |
| 13 | 1729.0 | 180.6 | 0.998 | 13 | 2.6 | 3.8 | 0.82 | 763.6 |
| 14 | 1800.9 | 202.2 | 0.993 | 16 | 2.7 | 3.6 | 0.97 | 905.1 |
| 15 | 1824.9 | 232.9 | 0.984 | 19 | 3.6 | 3.8 | 0.6 | 1338.1 |
| MOGWO | | | | | | | | |
| 1 | 290.3 | 16.9 | 0.982 | 14 | 4.8 | 4.3 | 0.85 | 11.23 |
| 2 | 353.4 | 31.2 | 0.987 | 14 | 5.1 | 2.9 | 0.62 | 12.99 |
| 3 | 377.0 | 40.6 | 0.984 | 19 | 4.5 | 4.3 | 0.56 | 16.88 |
| 4 | 413.9 | 63.5 | 0.99 | 14 | 5.5 | 3.4 | 0.80 | 31.45 |
| 5 | 609.6 | 73.5 | 0.987 | 23 | 5.2 | 2.1 | 0.73 | 43.46 |
| 6 | 768.8 | 75.2 | 0.999 | 25 | 5.9 | 2.5 | 0.73 | 91.88 |
| 7 | 858.0 | 82.4 | 0.998 | 21 | 4.8 | 4.1 | 0.83 | 118.71 |
| 8 | 865.1 | 87.5 | 0.981 | 15 | 4.3 | 3.4 | 0.89 | 165.12 |
| 9 | 874.4 | 109.3 | 0.995 | 19 | 3.7 | 2.4 | 0.68 | 241.44 |
| 10 | 1071.1 | 133.0 | 0.985 | 11 | 5.0 | 3.0 | 0.83 | 325.88 |
| 11 | 1230.6 | 157.6 | 0.989 | 24 | 5.4 | 3.8 | 0.71 | 442.66 |
| 12 | 1540.5 | 158.5 | 0.991 | 24 | 4.5 | 2.5 | 0.92 | 618.78 |
| 13 | 1707.9 | 176.8 | 0.999 | 23 | 3.7 | 4.2 | 0.92 | 774.56 |
| 14 | 1797.4 | 201.7 | 0.988 | 14 | 4.1 | 2.7 | 0.63 | 993.45 |
| 15 | 1840.7 | 248.8 | 1.000 | 19 | 3.8 | 4.7 | 0.81 | 1334.4 |

Therefore, other multi-criteria decision making methods should be used to select the most efficient algorithm in terms of comparable indicators.

5. 4. Selecting the Most Efficient Algorithm using TOPSIS Method

In the previous section, significant comparisons were made to determine the significant difference between the averages of the

computational index obtained by solving the problems using NSGA II and MOGWO algorithms. The results showed that there was no significant difference between the results. In this section, TOPSIS multi-criteria decision making method has been used in order to select the most efficient algorithm. Table 10 shows the total averages obtained from the solved 75 instances of the problem.

After scaling the results of Table 10, the result shows the efficiency of MOGWO algorithm with an obtained weight of 0.9675.

5. 5. Implementation of the Model for a Real Case Study

MOGWO algorithm is used to solve the

problem for a real case study in Iranian engine oil industry. The system of raw material supply, distribution as well as product recycling and disposal has been studied. 31 provinces of Iran are considered as suppliers, manufacturers, distribution centers and also the final consumers of the products. The main goal in solving such a problem is to select each province of the country as the main center of manufacturing, distribution, collection center, etc. The data used are estimated from the consensus of experts in the engine oil industry. According to the results, the efficient solutions obtained from problem solving are shown as in Table 11. The Pareto front is shown in Figure 6.

TABLE 9. T-Test results on the means of the objective functions

| Indicator | Algorithm | Number of instances | Average | Standard deviation | 95% confidence interval | T test statistics | P test statistics | | | | | | | | | | | | | | | | | | | | | | | | | | | | | | | | | | | | | | | | | | | | | | | | | | | | | | | | | | | | | | | | | | | | | | | | | | | | | | | | |
|-------------------------------|-----------|---------------------|----------|--------------------|-------------------------|-------------------|-------------------|-------------------------------|---------|----|-------|--------|------------------|------|-------|-------|----|-------|--------|-------------------------------|---------|----|-------|--------|------------------|------|-------|-------|----|-------|--------|-------------------------------|---------|----|-------|-------|------------------|------|-------|-------|----|-------|-------|-------------------------------|---------|----|-------|-------|------------------|------|-------|-------|----|-------|-------|-------------------------------|---------|----|-------|-------|------------------|------|-------|-------|----|-------|-------|--------------------|---------|----|-------|-------|------------------|------|-------|-------|----|-------|-------|--------------------|---------|----|-----|----|------------|------|-------|
| Mean of Object Function 1 | NSGA II | 75 | 96345248 | 13904657 | (-41422359 39453573) | 0.05 | 0.961 | | | | | | | | | | | | | | | | | | | | | | | | | | | | | | | | | | | | | | | | | | | | | | | | | | | | | | | | | | | | | | | | | | | | | | | | | | | | | | | | |
| | MOGWO | 75 | 97329641 | 13966932 | | | | Mean of Object Function 2 | NSGA II | 75 | 10864 | 1681 | (-5136 4766) | 0.08 | 0.939 | MOGWO | 75 | 11049 | 1731 | Mean of Object Function 3 | NSGA II | 75 | 0.989 | 0.0015 | (-0.0051 .00417) | 0.21 | 0.838 | MOGWO | 75 | 0.990 | 0.0017 | Number of efficient answers | NSGA II | 75 | 16.80 | 1 | (-5.02 1.42) | 1.15 | 0.261 | MOGWO | 75 | 18.60 | 1.2 | Maximum Expansion | NSGA II | 75 | 37002 | 2202 | (-16087 4529) | 1.24 | 0.197 | MOGWO | 75 | 47310 | 1748 | Distance from the ideal point | NSGA II | 75 | 38805 | 2896 | (-2526 12347) | 1.36 | 0.186 | MOGWO | 75 | 33895 | 2157 | Metric distance | NSGA II | 75 | 0.751 | 0.032 | (-0.1045 0.0725) | 0.37 | 0.714 | MOGWO | 75 | 0.767 | 0.029 | Computational time | NSGA II | 75 | 423 | 95 | (-217 367) | 0.53 | 0.601 |
| Mean of Object Function 2 | NSGA II | 75 | 10864 | 1681 | (-5136 4766) | 0.08 | 0.939 | | | | | | | | | | | | | | | | | | | | | | | | | | | | | | | | | | | | | | | | | | | | | | | | | | | | | | | | | | | | | | | | | | | | | | | | | | | | | | | | |
| | MOGWO | 75 | 11049 | 1731 | | | | Mean of Object Function 3 | NSGA II | 75 | 0.989 | 0.0015 | (-0.0051 .00417) | 0.21 | 0.838 | MOGWO | 75 | 0.990 | 0.0017 | Number of efficient answers | NSGA II | 75 | 16.80 | 1 | (-5.02 1.42) | 1.15 | 0.261 | MOGWO | 75 | 18.60 | 1.2 | Maximum Expansion | NSGA II | 75 | 37002 | 2202 | (-16087 4529) | 1.24 | 0.197 | MOGWO | 75 | 47310 | 1748 | Distance from the ideal point | NSGA II | 75 | 38805 | 2896 | (-2526 12347) | 1.36 | 0.186 | MOGWO | 75 | 33895 | 2157 | Metric distance | NSGA II | 75 | 0.751 | 0.032 | (-0.1045 0.0725) | 0.37 | 0.714 | MOGWO | 75 | 0.767 | 0.029 | Computational time | NSGA II | 75 | 423 | 95 | (-217 367) | 0.53 | 0.601 | MOGWO | 75 | 348 | 106 | | | | | | | | |
| Mean of Object Function 3 | NSGA II | 75 | 0.989 | 0.0015 | (-0.0051 .00417) | 0.21 | 0.838 | | | | | | | | | | | | | | | | | | | | | | | | | | | | | | | | | | | | | | | | | | | | | | | | | | | | | | | | | | | | | | | | | | | | | | | | | | | | | | | | |
| | MOGWO | 75 | 0.990 | 0.0017 | | | | Number of efficient answers | NSGA II | 75 | 16.80 | 1 | (-5.02 1.42) | 1.15 | 0.261 | MOGWO | 75 | 18.60 | 1.2 | Maximum Expansion | NSGA II | 75 | 37002 | 2202 | (-16087 4529) | 1.24 | 0.197 | MOGWO | 75 | 47310 | 1748 | Distance from the ideal point | NSGA II | 75 | 38805 | 2896 | (-2526 12347) | 1.36 | 0.186 | MOGWO | 75 | 33895 | 2157 | Metric distance | NSGA II | 75 | 0.751 | 0.032 | (-0.1045 0.0725) | 0.37 | 0.714 | MOGWO | 75 | 0.767 | 0.029 | Computational time | NSGA II | 75 | 423 | 95 | (-217 367) | 0.53 | 0.601 | MOGWO | 75 | 348 | 106 | | | | | | | | | | | | | | | | | | | | |
| Number of efficient answers | NSGA II | 75 | 16.80 | 1 | (-5.02 1.42) | 1.15 | 0.261 | | | | | | | | | | | | | | | | | | | | | | | | | | | | | | | | | | | | | | | | | | | | | | | | | | | | | | | | | | | | | | | | | | | | | | | | | | | | | | | | |
| | MOGWO | 75 | 18.60 | 1.2 | | | | Maximum Expansion | NSGA II | 75 | 37002 | 2202 | (-16087 4529) | 1.24 | 0.197 | MOGWO | 75 | 47310 | 1748 | Distance from the ideal point | NSGA II | 75 | 38805 | 2896 | (-2526 12347) | 1.36 | 0.186 | MOGWO | 75 | 33895 | 2157 | Metric distance | NSGA II | 75 | 0.751 | 0.032 | (-0.1045 0.0725) | 0.37 | 0.714 | MOGWO | 75 | 0.767 | 0.029 | Computational time | NSGA II | 75 | 423 | 95 | (-217 367) | 0.53 | 0.601 | MOGWO | 75 | 348 | 106 | | | | | | | | | | | | | | | | | | | | | | | | | | | | | | | | |
| Maximum Expansion | NSGA II | 75 | 37002 | 2202 | (-16087 4529) | 1.24 | 0.197 | | | | | | | | | | | | | | | | | | | | | | | | | | | | | | | | | | | | | | | | | | | | | | | | | | | | | | | | | | | | | | | | | | | | | | | | | | | | | | | | |
| | MOGWO | 75 | 47310 | 1748 | | | | Distance from the ideal point | NSGA II | 75 | 38805 | 2896 | (-2526 12347) | 1.36 | 0.186 | MOGWO | 75 | 33895 | 2157 | Metric distance | NSGA II | 75 | 0.751 | 0.032 | (-0.1045 0.0725) | 0.37 | 0.714 | MOGWO | 75 | 0.767 | 0.029 | Computational time | NSGA II | 75 | 423 | 95 | (-217 367) | 0.53 | 0.601 | MOGWO | 75 | 348 | 106 | | | | | | | | | | | | | | | | | | | | | | | | | | | | | | | | | | | | | | | | | | | | |
| Distance from the ideal point | NSGA II | 75 | 38805 | 2896 | (-2526 12347) | 1.36 | 0.186 | | | | | | | | | | | | | | | | | | | | | | | | | | | | | | | | | | | | | | | | | | | | | | | | | | | | | | | | | | | | | | | | | | | | | | | | | | | | | | | | |
| | MOGWO | 75 | 33895 | 2157 | | | | Metric distance | NSGA II | 75 | 0.751 | 0.032 | (-0.1045 0.0725) | 0.37 | 0.714 | MOGWO | 75 | 0.767 | 0.029 | Computational time | NSGA II | 75 | 423 | 95 | (-217 367) | 0.53 | 0.601 | MOGWO | 75 | 348 | 106 | | | | | | | | | | | | | | | | | | | | | | | | | | | | | | | | | | | | | | | | | | | | | | | | | | | | | | | | |
| Metric distance | NSGA II | 75 | 0.751 | 0.032 | (-0.1045 0.0725) | 0.37 | 0.714 | | | | | | | | | | | | | | | | | | | | | | | | | | | | | | | | | | | | | | | | | | | | | | | | | | | | | | | | | | | | | | | | | | | | | | | | | | | | | | | | |
| | MOGWO | 75 | 0.767 | 0.029 | | | | Computational time | NSGA II | 75 | 423 | 95 | (-217 367) | 0.53 | 0.601 | MOGWO | 75 | 348 | 106 | | | | | | | | | | | | | | | | | | | | | | | | | | | | | | | | | | | | | | | | | | | | | | | | | | | | | | | | | | | | | | | | | | | | |
| Computational time | NSGA II | 75 | 423 | 95 | (-217 367) | 0.53 | 0.601 | | | | | | | | | | | | | | | | | | | | | | | | | | | | | | | | | | | | | | | | | | | | | | | | | | | | | | | | | | | | | | | | | | | | | | | | | | | | | | | | |
| | MOGWO | 75 | 348 | 106 | | | | | | | | | | | | | | | | | | | | | | | | | | | | | | | | | | | | | | | | | | | | | | | | | | | | | | | | | | | | | | | | | | | | | | | | | | | | | | | | | | | |

TABLE 10. Average values of the indicators for the two algorithms

| Algorithm | Objective function 1 | Objective function 2 | Objective function 3 | NPF | MSI | MID | SM | CPU-Time |
|-----------|----------------------|----------------------|----------------------|-------|-------|-------|-------|----------|
| NSGA II | 96345248 | 10864 | 0.989 | 16.80 | 37002 | 38805 | 0.751 | 423 |
| MOGWO | 97329641 | 11049 | 0.990 | 18.60 | 47310 | 33895 | 0.767 | 348 |

TABLE 11. Efficient solutions from the case study in Iranian engine oil industry

| Efficient solutions | Objective function 1 | Objective function 2 | Objective function 3 |
|---------------------|----------------------|----------------------|----------------------|
| 1 | 7387708657310.84 | 20873 | 0.81 |
| 2 | 7439665190205.53 | 22619 | 0.83 |

| | | | |
|---|------------------|-------|------|
| 3 | 7857645842071.79 | 22921 | 0.84 |
| 4 | 7881325572261.93 | 28900 | 0.87 |
| 5 | 7999451000125.68 | 29678 | 0.87 |
| 6 | 8256810244200.38 | 30959 | 0.89 |
| 7 | 8351376182362.55 | 31184 | 0.90 |

| | | | |
|----|------------------|-------|------|
| 8 | 8446676226610.35 | 36302 | 0.92 |
| 9 | 8773999647463.98 | 37314 | 0.95 |
| 10 | 8796633076821.11 | 37407 | 0.96 |
| 11 | 8953631688404.11 | 39097 | 0.96 |
| 12 | 9145413649915.65 | 41468 | 0.97 |
| 13 | 9415968260535.70 | 42790 | 0.98 |

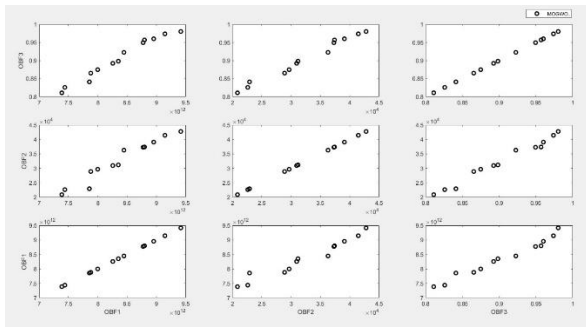
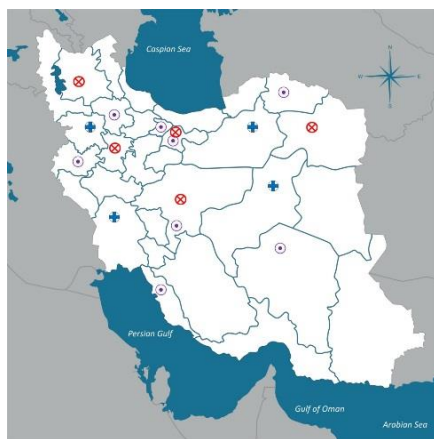


Figure 6. Pareto front solutions from solving the problem in Iranian engine oil industry



⊗ Manufacturing centers
 ⊙ Distribution centers
 ⊕ Collection and destruction centers

Figure 7. Provincial centers selected for the case study of Iranian engine oil industry

Based on the obtained results, the implementation of such a network in Iran has a profit of 8362023479869.43, which can lead to job creation for 32424 people. Furthermore, the reliability of implementing such a system is equal to 90%. Figure 7 shows the provincial centers for selecting the manufacturing, distribution and collection centers.

6. CONCLUSIONS AND FURTHER RESEARCH IDEAS

Global economic conditions and environmental issues importance leads to excessive attention of governments

to the design of CLSC networks. In this paper, by presenting a mathematical model, an attempt was made to design a comprehensive network of supply, manufacturing, refining and supply of products to customers in which social, economic and environmental issues were observed. Due to the uncertainty of some parameters such as demand and cost factors, the robust fuzzy optimization method was used to tackle the existed uncertainty. The results showed an increase in total costs of the chain and decrease in reliability when the uncertainty rate increases. MOGWO and NSGA II algorithms were used to solve the problem. The results of solving the problem for larger sizes showed the performance of the MOGWO algorithm against the NSGA II algorithm. In order to compare the two algorithms, some indicators including means of objective functions, distance index, distance index from ideal point, maximum amplitude index, Pareto solution number index and computational time were applied.

As further research, it is suggested to consider a competitive chain for the problem under study. Other methods of uncertainty can also make the model closer to the real world situations. The results help the managers of the engine oil industry to analyze the results of the designed network for the most pessimistic and optimistic situations in product demand, and to be able to properly manage the construction of different facilities in the supply chain. Managers can also make good decisions about social and environmental issues which have become so much important in industries like engine oil from the viewpoint of international and national norms.

7. REFERENCES

- Sakhaii, M., Tavakkoli-Moghaddam, R., Bagheri, M., Vatani, B. "A robust optimization approach for an integrated dynamic cellular manufacturing system and production planning with unreliable machines", *Applied Mathematical Modelling*, Vol. 40, No. 1, (2016), 169-191. <https://doi.org/10.1016/j.apm.2015.05.005>
- Kaya, O., Urek, B. "A mixed integer nonlinear programming model and heuristic solutions for location, inventory and pricing decisions in a closed loop supply chain", *Computers and Operations Research*, Vol. 65, (2016), 93-103. <https://doi.org/10.1016/j.cor.2015.07.005>
- Ghahremani-Nahr, J., Pasandideh, S. H. R., Niaki, S. T. A. "A robust optimization approach for multi-objective, multi-product, multi-period, closed-loop green supply chain network designs under uncertainty and discount", *Journal of Industrial and Production Engineering*, Vol. 37, No. 1, (2020a), 1-22. <https://doi.org/10.1080/21681015.2017.1421591>
- Amin, S. H., Zhang, G., Akhtar, P. "Effects of uncertainty on a tire closed-loop supply chain network", *Expert Systems with Applications*, Vol. 73, (2017), 82-91. <https://doi.org/10.1016/j.eswa.2016.12.024>
- Kim, D., Cai, J., Ariyur, K. B., Braun, J. E. "System identification for building thermal systems under the presence of unmeasured disturbances in closed loop operation: Lumped disturbance modeling approach", *Building and Environment*, Vol. 107, (2016), 169-180. <https://doi.org/10.1016/j.buildenv.2016.07.007>

6. Ahmadi-Javid, A., Hoseinpour, P. "A location-inventory-pricing model in a supply chain distribution network with price-sensitive demands and inventory-capacity constraints", *Transportation Research Part E: Logistics and Transportation Review*, Vol. 82, (2015), 238-255. <https://doi.org/10.1016/j.tre.2015.06.010>
7. Ahmadzadeh, E., Vahdani, B. "A location-inventory-pricing model in a closed loop supply chain network with correlated demands and shortages under a periodic review system", *Computers and Chemical Engineering*, Vol. 101, (2017), 148-166. <https://doi.org/10.1016/j.compchemeng.2017.02.027>
8. Hajiaghaci-Keshтели, M., Fard, A. M. F. "Sustainable closed-loop supply chain network design with discount supposition", *Neural Computing and Applications*, Vol. 31, No.9, (2019), 5343-5377. <https://doi.org/10.1007/s00521-018-3369-5>
9. Mardan, E., Govindan, K., Mina, H., Gholami-Zanjani, S. M. "An accelerated benders decomposition algorithm for a bi-objective green closed loop supply chain network design problem", *Journal of Cleaner Production*, Vol. 235, (2019), 1499-1514. <https://doi.org/10.1016/j.jclepro.2019.06.187>
10. Yadegari, E., Alem-Tabriz, A., Zandieh, M. "A memetic algorithm with a novel neighborhood search and modified solution representation for closed-loop supply chain network design", *Computers and Industrial Engineering*, Vol. 128, (2019), 418-436. <https://doi.org/10.1016/j.cie.2018.12.054>
11. Yavari, M., Zaker, H. "An integrated two-layer network model for designing a resilient green-closed loop supply chain of perishable products under disruption", *Journal of Cleaner Production*, Vol. 230, (2019), 198-218. <https://doi.org/10.1016/j.jclepro.2019.04.130>
12. Saedinia, R., Vahdani, B., Etebari, F., Nadjafi, B. A. "Robust gasoline closed loop supply chain design with redistricting, service sharing and intra-district service transfer", *Transportation Research Part E: Logistics and Transportation Review*, Vol. 123, (2019), 121-141. <https://doi.org/10.1016/j.tre.2019.01.015>
13. Nayeri, S., Paydar, M. M., Asadi-Gangraj, E., Emami, S. "Multi-objective fuzzy robust optimization approach to sustainable closed-loop supply chain network design", *Computers and Industrial Engineering*, Vol. 148, (2020), 106716. <https://doi.org/10.1016/j.cie.2020.106716>
14. Prakash, S., Kumar, S., Soni, G., Jain, V., Rathore, A. P. S. "Closed-loop supply chain network design and modelling under risks and demand uncertainty: an integrated robust optimization approach", *Annals of Operations Research*, Vol. 290, No. 1, (2020), 837-864. <https://doi.org/10.1007/s10479-018-2902-3>
15. Fatollahi fard, A. M., Ahmadi, A., Al-e-hashem, S.m.j., "Sustainable Closed-loop Supply Chain Network for an Integrated Water Supply and Wastewater Collection System under Uncertainty", *Journal of Environmental Management*, Vol. 275, (2020), <https://doi.org/10.1016/j.jenvman.2020.111277>
16. Fazli-Khalaf, M., Hamidieh, A. "A Robust Reliable Forward-reverse Supply Chain Network Design Model under Parameter and Disruption Uncertainties", *International Journal of Engineering, Transactions C: Aspects*, Vol. 30, No. 8, (2017), 1160-1169. doi: 10.5829/ije.2018.31.12c.10
17. Hamidieh, A., Arshadikhamseh, A., Fazli-Khalaf, M. "A Robust Reliable Forward-reverse Supply Chain Network Design Model under Parameter and Disruption Uncertainties", *International Journal of Engineering*, Vol. 31, No. 4, (2018), 648-658.
18. Alshamsi, A., Diabat, A. "Large-scale reverse supply chain network design: An accelerated Benders decomposition algorithm", *Computers & Industrial Engineering*, Vol. 124, (2018), 545-559. <https://doi.org/10.1016/j.cie.2018.05.057>
19. Rad, R. S., Nahavandi, N. "A novel multi-objective optimization model for integrated problem of green closed loop supply chain network design and quantity discount", *Journal of Cleaner Production*, Vol. 196, (2018), 1549-1565. <https://doi.org/10.1016/j.jclepro.2018.06.034>
20. Fakhrazad, M. B., Talebzadeh, P., Goodarziyan, F. "Mathematical formulation and solving of green closed-loop supply chain planning problem with production, distribution and transportation reliability", *International Journal of Engineering*, Vol. 31, No. 12, (2018), 2059-2067.
21. Pourjavad, E., Mayorga, R. V. "Multi-objective fuzzy programming of closed-loop supply chain considering sustainable measures", *International Journal of Fuzzy Systems*, Vol. 21, No. 2, (2019), 655-673. <https://doi.org/10.1007/s40815-018-0551-y>
22. Polo, A., Peña, N., Muñoz, D., Cañón, A., Escobar, J. W. "Robust design of a closed-loop supply chain under uncertainty conditions integrating financial criteria", *Omega*, Vol. 88, (2019), 110-132. <https://doi.org/10.1016/j.omega.2018.09.003>
23. Ghahremani-Nahr, J., Ghodrattama, A., IzadBakhah, H. R., Tavakkoli Moghaddam, R. "Design of multi-objective multi-product multi period green supply chain network with considering discount under uncertainty", *Journal of Industrial Engineering Research in Production Systems*, Vol. 6, No. 13, (2019), 119-137. [10.22084/ier.2017.8877.1421](https://doi.org/10.22084/ier.2017.8877.1421)
24. Pourjavad, E., Mayorga, R. V. "An optimization model for network design of a closed-loop supply chain: a study for a glass manufacturing industry", *International Journal of Management Science and Engineering Management*, Vol. 14, No. 3, (2019b), 169-179. <https://doi.org/10.1080/17509653.2018.1512387>
25. Darestani, S. A., Hemmati, M. "Robust optimization of a bi-objective closed-loop supply chain network for perishable goods considering queue system", *Computers and Industrial Engineering*, Vol. 136, (2019), 277-292. <https://doi.org/10.1016/j.cie.2019.07.018>
26. Zhang, X., Zhao, G., Qi, Y., Li, B. "A robust fuzzy optimization model for closed-loop supply chain networks considering sustainability", *Sustainability*, Vol. 11, No. 20, (2019), 5726. <https://doi.org/10.3390/su11205726>
27. Fazli-Khalaf, M., Khalilpourazari, S., Mohammadi, M. "Mixed robust possibilistic flexible chance constraint optimization model for emergency blood supply chain network design", *Annals of Operations Research*, Vol. 283, No. 1, (2019), 1079-1109. <https://doi.org/10.1007/s10479-017-2729-3>
28. Alkhayyal, B. "Corporate social responsibility practices in the US: Using reverse supply chain network design and optimization considering carbon cost", *Sustainability*, Vol. 11, No. 7, (2019), 2097. <https://doi.org/10.3390/su11072097>
29. Ghahremani-Nahr, J., Nozari, H., Najafi, S. E. "Design a green closed loop supply chain network by considering discount under uncertainty", *Journal of Applied Research on Industrial Engineering*, Vol. 7, No. 3, (2020b), 238-266. [10.22105/jarie.2020.251240.1198](https://doi.org/10.22105/jarie.2020.251240.1198)
30. Jiang, G., Wang, Q., Wang, K., Zhang, Q., Zhou, J. "A novel closed-loop supply chain network design considering enterprise profit and service level", *Sustainability*, Vol. 12, No. 2, (2020), 544. <https://doi.org/10.3390/su12020544>
31. Gholizadeh, H., Fazlollahtabar, H., Khalilzadeh, M. "A robust fuzzy stochastic programming for sustainable procurement and logistics under hybrid uncertainty using big data", *Journal of Cleaner Production*, Vol. 258, (2020), 120640. <https://doi.org/10.1016/j.jclepro.2020.120640>
32. Pourmehdi, M., Paydar, M. M., Asadi-Gangraj, E. "Scenario-based design of a steel sustainable closed-loop supply chain network considering production technology", *Journal of Cleaner Production*, Vol. 277, (2020), 123298. <https://doi.org/10.1016/j.jclepro.2020.123298>
33. Mohtashami, Z., Aghsami, A., Jolai, F. "A green closed loop supply chain design using queuing system for reducing environmental impact and energy consumption", *Journal of*

- Cleaner Production*, Vol. 242, (2020), 118452. <https://doi.org/10.1016/j.jclepro.2019.118452>
34. Liu, Y., Ma, L., Liu, Y. "A novel robust fuzzy mean-UPM model for green closed-loop supply chain network design under distribution ambiguity", *Applied Mathematical Modelling*, Vol. 92, (2021), 99-135. <https://doi.org/10.1016/j.apm.2020.10.042>
 35. Zahedi, A., Salehi-Amiri, A., Hajiaghayi-Kesheteli, M., Diabat, A. "Designing a closed-loop supply chain network considering multi-task sales agencies and multi-mode transportation", *Soft Computing*, Vol. 25, No. 8, (2021), 6203-6235. <https://doi.org/10.1007/s00500-021-05607-6>
 36. Boronoo, M., Mousazadeh, M., Torabi, S. A. "A robust mixed flexible-possibilistic programming approach for multi-objective closed-loop green supply chain network design", *Environment, Development and Sustainability*, Vol. 23, No. 3, (2021), 3368-3395. <https://doi.org/10.1007/s10668-020-00723-z>
 37. Habib, M. S., Asghar, O., Hussain, A., Imran, M., Mughal, M. P., Sarkar, B. "A robust possibilistic programming approach toward animal fat-based biodiesel supply chain network design under uncertain environment", *Journal of Cleaner Production*, Vol. 278, (2021), 122403. <https://doi.org/10.1016/j.jclepro.2020.122403>
 38. Nasiri, M.M., Shakouhi, F., Jolai, F. "A fuzzy robust stochastic mathematical programming approach for multi-objective scheduling of the surgical cases", *Journal of the Operational Research Society of India*, Vol. 56, No. 3, (2019), 890-910. <https://doi.org/10.1007/s12597-019-00379-y>
 39. Pishvae, M. S., Kianfar, K., Karimi, B. "Reverse logistics network design using simulated annealing", *The International Journal of Advanced Manufacturing Technology*, Vol. 47, No. (1-4), (2010), 269-281.
 40. Davis, P. S., Ray, T. L. "A branch-bound algorithm for the capacitated facilities location problem", *Naval Research Logistics Quarterly*, Vol. 16, No. 3, (1969), 331-344. <https://doi.org/10.1002/nav.3800160306>
 41. Gen, M., Cheng, R., Lin, L. "Network models and optimization: Multiobjective genetic algorithm approach" Springer Science & Business Media. (2008).
 42. Mirjalili, S., Saremi, S., Mirjalili, S. M., Coelho, L. D. S. "Multi-objective grey wolf optimizer: a novel algorithm for multi-criterion optimization", *Expert Systems with Applications*, Vol. 47, (2016), 106-119. <https://doi.org/10.1016/j.eswa.2015.10.039>

Persian Abstract

چکیده

با توجه به اهمیت زنجیره تامین و مسائل زیست محیطی، این مقاله یک مدل ریاضی جدید برای شبکه زنجیره تامین حلقه بسته سبز با اهداف حداکثرسازی سود، حداکثر کردن تعداد مشاغل ایجاد شده و حداکثر کردن قابلیت اطمینان ارائه می دهد. به دلیل عدم قطعیت در برخی از پارامترها مانند تقاضا و هزینه حمل و نقل، از روش جدید مدل برنامه نویسی فازی استوار استفاده شده است. برای حل مسئله در سایزهای بزرگتر از الگوریتم های بهینه سازی گرگ خاکستری چندهدفه و الگوریتم ژنتیک مرتب سازی نامغلوب ۲ استفاده شده است. نتایج حاصل از مقایسه الگوریتم ها با در نظر گرفتن برخی معیارها از جمله میانگین توابع هدف، شاخص فاصله متریک، شاخص فاصله از نقطه ایده آل، بیشترین گسترش، تعداد جواب کارا و زمان محاسبه، همگرایی سریع و کارایی بالای الگوریتم بهینه سازی گرگ خاکستری چندهدفه را برای این مسئله نشان داد. در نهایت، پیاده سازی مدل برای مطالعه موردی واقعی در صنعت روغن موتور ایران، کارایی راه حل های به دست آمده را برای این شبکه نشان داد.



An Efficient Approach for Edge Detection Technique using Kalman Filter with Artificial Neural Network

D. Siddharth^a, D. K. J. Saini^{*b}, P. Singh^a

^a Department of CSE, Rama University, Kanpur, India

^b Department of Computer and Information Sciences, Himalayan School of Science and Technology Swami Rama Himalayan University (SRHU) Jolly Grant Dehradun

PAPER INFO

Paper history:

Received 24 July 2021

Received in revised form 13 August 2021

Accepted 04 September 2021

Keywords:

Grey Level Image

Edge Detection Filter

Kalman Filter Algorithm

Artificial Neural Network

ABSTRACT

Edge identification is a technique for recognizing and detecting sharper breaks in an image. The halt is caused by a rapid change in the value of the pixel force dark level. Convolving the picture with an administrator (Two-Directional channel) that is set to be noise sensitive is the standard approach for edge location. Edge finder is a method for locating precisely adjusted intensity esteem alterations that incorporate many significant neighborhoods image preparation methods. Edge recognition is a fundamental method in a wide range of image processing applications, including movement analysis, design identification, object recognition, clinical picture creation, and so on. It's recently shown up in a variety of edge detection systems, demonstrating both the advantages and disadvantages of these computations. The Kalman Filter with ANN method has two benefits that make it suitable for dealing with improvement issues: quicker merging and lower calculation rates. In this study, The ANN method was used to improve object localization accuracy. Kalman filtering is used to object coordinates acquired using the ANN method. Using ANN + Kalman Filtering increases localization accuracy and lowers localization error distances, according to the findings.

doi: 10.5829/ije.2021.34.12c.04

1. INTRODUCTION

One of the most challenging challenges in image processing is edge detection in advanced images. In image processing and computer vision, it is critical [1, 4]. Separating things from their experiences is one of the most difficult issues, equivalent to the usage of machine vision and example recognition. Edges define the zone of interest for items of interest, allowing them to be legally identified in low-level handling situations. Later stages of the processing were impacted by the precision with which the picture was appraised.

The ability of the edge detection approach to remove the precise edge line with great direction in the thought about image is a major characteristic of the technology, and much writing nerve identification has been disseminated in the last two decades. In any case, there

isn't currently a large enough execution file to evaluate the edge detection algorithms' presentation.

Many computer-aided imaging systems employ Artificial Neural Networks (ANN) [2]. In addition, picture segmentation and edge detection remain a significant issue for all imaging applications, with edge recognition and other approaches such as snake modeling, watershed, contour detection and area growth being required by every computer-assisted system [2]. ANN has also been used to achieve segmentation and edge detection by utilizing its learning capabilities and training methods to categories pictures into content consistent areas. Because various users have different criteria for the similar image, edge detection algo are always assessed subjectively.

Despite the development of various image recognition methods, both the processing cost and the abstract image quality may be improved. In this vein, the

*Corresponding Author Institutional Email: dilipsaini@gmail.com
(D. K. J Saini)

goal of research is to present a efficient Artificial Neural Network based edge detection solution for a variety of images. Here you'll find highlights with flat, vertical, and skewed contrasts. At that time, the preparation yield will be a cunning edge detector. Finally, as updated parameters, we'll get the number of concealed layers and the yield edge. In terms of computation time, several well-known methods such as Canny, Sobel, Prewitt, Roberts, and the Laplacian of Gaussian will be compared (LoG) [3]. The proposed approach, according to the findings, enhanced image quality while lowering preparation time by several times. Currently, we feel that the solution to a development problem will be referred to as a Kalman Filter, which will excel in a high-quality issue environment [4]. As a result, the Kalman Filter attracts a larger number of collaborators, allowing for a more thorough examination of the search space.

We provide a new edge detection technique with the use of Kalman Filter algo and an Artificial Neural Network in this paper, along with comparisons to the Canny [5], Sobel [6], LoG, and Prewitt [7] techniques.

1. 1. Kalman Filter Algorithm (KFA) Kalman filtering is used to filter noisy data, produce non-observable states, and forecast future states. Because many sensor outputs are too noisy to use directly, filtering noisy signals is required, and Kalman filtering allows you to account for the signal/uncertainty. State's one of the most common applications of creating non-observable states is estimating velocity. On various joints, position sensors (encoders) are commonly employed; however, isolating the position to get velocity produces noisy results. Kalman filtering may be used to compute velocity to rectify this. The Kalman filter can also be used to predict future occurrences. This is critical if your sensor feedback has significant time delays, since this might cause motor control system instability [8].

Kalman filters provide the best approximation for a linear system. As a result, a sensor or system must have (or be close to having) a linear response in order to use a Kalman filter. We will go through how to work with nonlinear systems in the next sections. The Kalman filter has the benefit of requiring no prior knowledge of a long state history because it just utilizes the most recent state and a covariance matrix to estimate the likelihood of the state being accurate [9].

Remember that a covariance is merely a measure of how two variables correlate (that is, how they change in relation to one another) (the values aren't always clear), and that a covariance matrix simply gives you the covariance for a particular row and column value.

Before we get into the mechanics of the filter, let's go through some terminology to make sure we're all on the same page. The positions/velocities/values associated with the system are known as states. The components that you may modify to impact the system are known as

actions or inputs. For the Kalman filter, there are two sorts of equations. The prediction equations are the first. Based on the prior state and the needed action, these equations predict the present state [10]. The update equations look at your input sensors, how much you trust each sensor, and how much you trust the overall state estimate in the second set of equations. This filter uses prediction equations to forecast the current state, and then uses update equations to assess how well it predicted. This procedure is repeated endlessly to maintain the existing condition [11].

The prediction equations are

$$X = Ax_{k-1} + Bu_{k-1} \quad (1)$$

$$p = PA^T + Q \quad (2)$$

And the update equations are

$$K = pH^T (HpH^T + R)^{-1} \quad (3)$$

$$x_k = X + K(z - HX) \quad (4)$$

$$P_{x_k} = (1 - KH)p \quad (5)$$

1. 2. Artificial Neural Network A neural network is a conceptual framework that uses connection weights to link important multi-processing features. The connection weights, which are changed throughout the training time, demonstrate understanding. The two forms of neural network training are unsupervised learning and supervised learning [12]. Both the input and target values must be used in the initial sample of the training set. Back propagation, which is employed in the Multi-Layer perceptron (MLP), is the most frequent technique in this category, although it also covers most of the training methods for thrust basis networks, recurrent neural networks (RNN) and time delay neural networks. When the objective pattern is not entirely understood, unsupervised learning is utilized [13].

2 PROPOSED METHOD

Traditional modeling methods, such as response surface technique, have been shown to be unsuccessful in

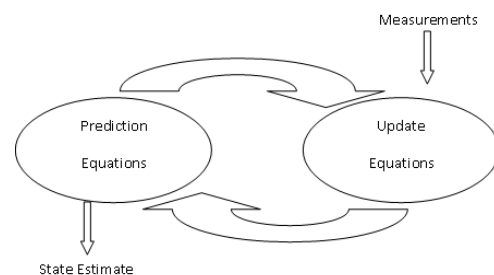


Figure 1. Kalman filter repeating process

accurately forecasting all QV values. For example, using a quadratic model to account for all interactions requires 44 terms, significantly complicating the procedure.

To complete the job, a multi-layer perceptron (MLP) artificial neural network (ANN) is used. After this phase, a recently found stochastic optimization technique must be used with the planned ANN to reduce QV and find the best set for each cutting condition [14].

2. 1. Artificial Neural Network A neural network is a logical structure made up of several processing units connected by connection weights. The connection weights, which are changed throughout the training time, demonstrate understanding. Unsupervised learning and supervised learning are the two methods for training a neural network. Both the input and target values must be used in the initial sample of the training set. Back propagation, which is employed in the Multi-Layer Perceptron (MLP), is the most frequent technique in this category, although it also covers most of the training techniques for time delay neural networks, thrust basis networks and recurrent neural networks [15]. When the objective pattern is not entirely understood, unsupervised learning is utilised [13].

2. 2. Kalman Filter Algorithm (KFA) The Kalman filter was created to address the problem of predicting the state of $x \in \mathbb{R}^n$, a discrete time regulated process using a linear differential equation as its controller. The process measurement connection is not linear in most real-world scenarios. Using something like the Taylor series, we may linear the estimation around the current estimate of the process and measurement functions of the non-linear process [16]. The process can be represented using a non-linear difference equation.

$$x_k = f(x_{k-1}, u_{k-1}, w_{k-1}) \tag{6}$$

with a measurement $z_k \in \mathbb{R}^m$ that is:

$$z_k = h(s_k, u_k) \tag{7}$$

Using w_{k-1} as the driving function, the measurement Equation (7) connects the w_{k-1} measurement and measurement noise. The measurement equation's non-

linear function h connects the state x_k to the measurement z_k . For this sort of edge detection challenge, a variety of filters have been investigated. For the past three decades, Kalman filters have been used to solve the problem of target tracking. In 1960, the Kalman filter was proposed for the first time as an optimum linear estimator [17].

The best aspect of a filter is calculating the gain using a minimal variance equation, which gives the highest weight to the data (observation or predicted data) with the least volatility. The Kalman filter is a linear predictor. The filter is optimal only when the process to be assessed is linear. In nonlinear circumstances, the Kalman filter works poorly. When missile velocity and range were lower, Kalman filters could manage the problem, but as technology has evolved, missile velocity and range have increased, and air drag has become a key factor. As a result, their voyage has taken an unexpected detour. Before the Kalman filter can be utilized for tracking, it must undergo several changes. Several filters have been created to solve non-linear tracking problems in various applications, and research is now continuing to identify the best filter performance [18].

The kalman filter offers the following benefits over another well-known filter.

1. Although the kalman filter method may be implemented on a digital computer, when it was initially presented, analogue circuitry was used to estimate and operate the kalman filter.
2. The kalman filter's stationary characteristics aren't necessary for deterministic dynamics or random processes. Non-stationary stochastic processes are used in many important applications.
3. The kalman filter may be used to design state space optical controllers for dynamic systems. It benefits both the estimation and control characteristics of these systems.
4. The kalman filter requires minimum additional mathematical instruction for a modern engineering student.
5. The kalman filter offers information for recognizing and rejecting abnormal data using mathematically accurate, statistically based decision-making approaches. The complete flowchart is given as follows,

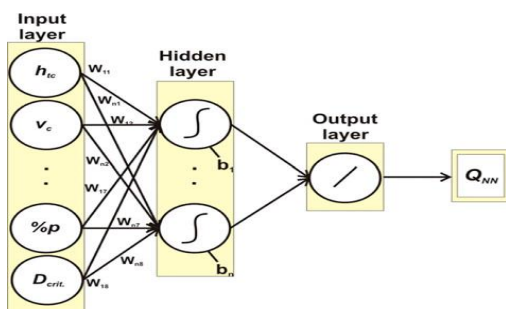


Figure 2. ANN architecture

3. EXPERIMENTAL RESULTS

In the figures below, you'll find comparisons of the performance of KFA and KFA+ANN on various pictures, as well as comparisons of the two approaches:

Figure 4(a) KFA edge detection is shown in (a), proposed method (KFA + ANN) edge detection is shown in Figure 4(b), and suggested algorithm (KFA + ANN) edge detection is shown in Figure 4(c).

The original grayscale image of "Modiji" is shown in Figure 5(a), whereas Figure 5(b) exhibits edge detect

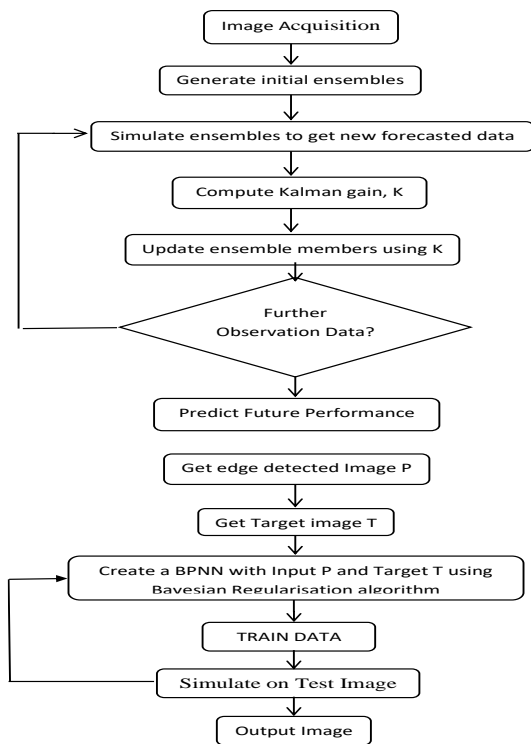


Figure 3. Proposed algorithm flow chart

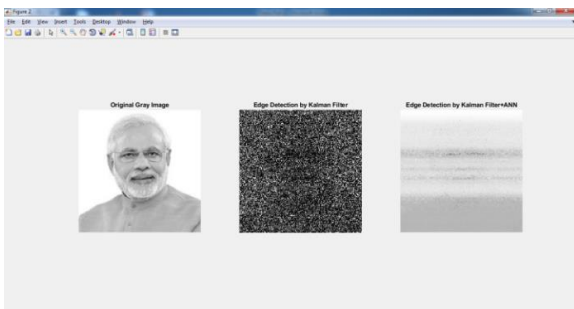


Figure 4. Edge detection using KFA and KFA+ANN

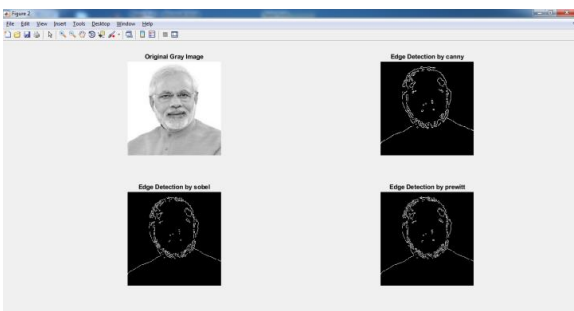


Figure 5. Result Comparison of classical edge detection methods and novel method

using the Canny method. The edge detect by the Sobel method is shown in Figure 5(c), whereas the edge detection by the Prewitt method is shown in Figure 5(d).

The original grayscale picture of 'Lena' is seen in Figure 6(a). Figure 6(b) KFA edge detection is shown, and Figure 6(c) recommended algorithm (KFA + ANN) edge detection is shown.

Figure 7 (a) depicts "Lena's" original grey picture, whereas Figure 7(b) depicts edge detection using the Canny method. The edge detection by the Sobel method is shown in Figure 7(c), whereas the edge detection by the Prewitt method is shown in Figure 7(d).

Figure 8 shows the grey image(a), KFA edge detection Figure 8(b), and proposed algorithm (KFA + ANN) edge detection Figure 8(c).

The original grey image of the 'building' is shown in Figure 9(a), whereas Figure 9(b) features Canny method. Figure 9(c) shows the edge detection by the Sobel method, whereas Figure 9(d) shows the edge detection by the Prewitt method Figure 9(d).

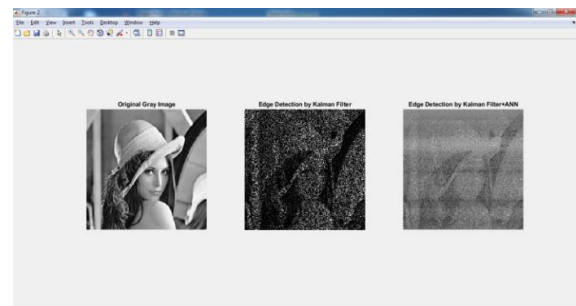


Figure 6. Edge detection using KFA and KFA+ANN

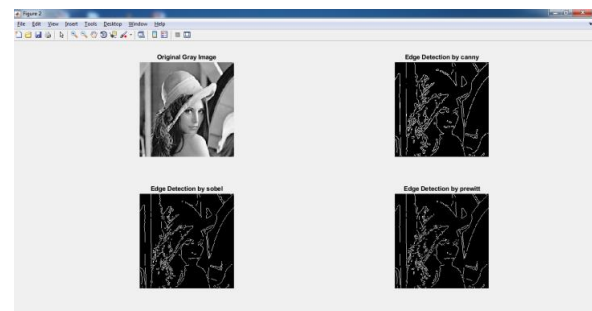


Figure 7. Result Comparison of classical edge detection methods and novel method

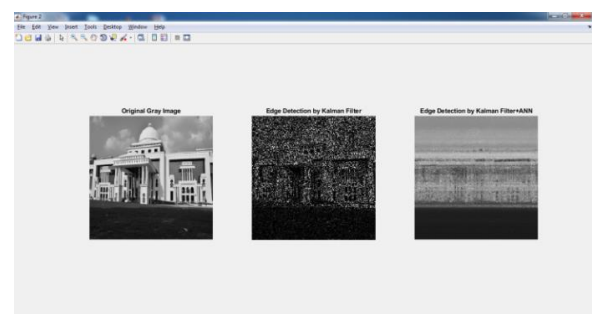


Figure 8. Edge detection using KFA and KFA+ANN

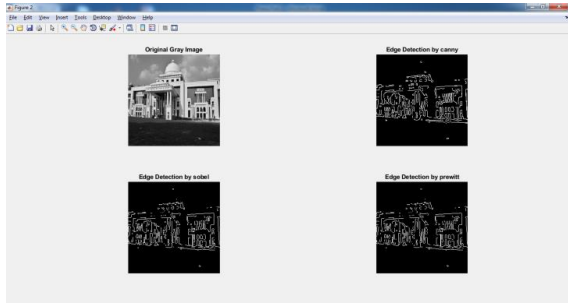


Figure 9. Result Comparison of classical edge detection methods and novel method

Figure 10(a) illustrates the ‘Baboon's' original grey picture, Figure 10(b) KFA edge detection, and Figure 10(c) recommended algorithm (KFA+ANN) edge detection.

Figure 11(a) depicts the 'Baboon's' original grey picture, whereas Figure 11(b) depicts edge detection using the Canny edge detector. The edge detection by the Sobel edge detector is shown in Figure 11(c), whereas the edge detection by the Prewitt edge detector is shown in Figure 11(d).

We utilized the peak signal to noise ratio (PSNR) approach to objectively evaluate our findings; the higher the PSNR value, the better the reconstructed picture quality.

$$PSNR = 10 \log_{10} \frac{(L-1)^2}{\frac{1}{MN} \sum_{r=0}^{M-1} \sum_{c=0}^{N-1} [E(r,c) - o(r,c)]^2} \quad (8)$$

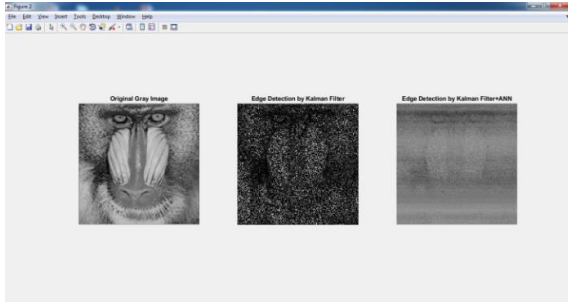


Figure 10. Edge detection using KFA and KFA+ANN

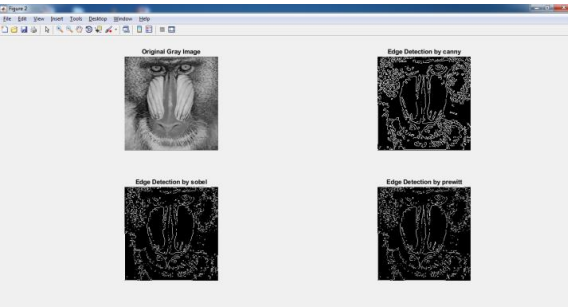


Figure 11. Result Comparison of classical edge detection methods and novel method

where $E(r,c)$ stands for the original image, $o(r,c)$ for the result, L for the number of grey levels equal to 256, $[M,N]$ for the number of rows and columns of pictures, and L for the number of grey levels equal to 256.

In addition, the root means square error (rmse) As seen below, the lower the rmse value, the higher the reconstructed picture quality:

$$RMSE = \sqrt{\frac{1}{MN} \sum_{r=0}^{M-1} \sum_{c=0}^{N-1} [E(r,c) - o(r,c)]^2} \quad (9)$$

Tables 1 and 2 show the results of the PSNR and RMSE methods used to analyse the image. The assessment findings reveal that in the great majority of situations, edge detected pictures are superior. It also demonstrated the suggested technique's capacity to identify edges.

4. PROS AND CONS

The "layers" of an ANN are rows of data points that all neurons in the same neural network share. ANN uses weights to learn. After each cycle across the neuron, the weights of ANN are changed. The weights are subsequently adjusted by ANN according to the accuracy assessed by a "cost function." Using the image input, several features are discovered and connected to the n-dimensional output. The user can then receive the classification output. To test the efficacy of the models created to improve learning, ANN methods employ error measures and epochs. A good approach for dealing with

TABLE 1. The recommended technique is compared to the Kalman Filter Algorithm, the 'Canny', 'Sobel', and 'Prewitt' approaches using PSNR and RMSE criteria

| PSNR | Proposed Work (KFA+ANN) | Kalman Algorithm | Canny | Sobel | Prewitt |
|--------|-------------------------|------------------|--------|--------|---------|
| Modiji | 13.4481 | 6.2853 | 4.8506 | 4.8475 | 4.8547 |
| Lena | 13.6274 | 9.1830 | 7.6232 | 7.6597 | 7.6595 |
| Aktu | 15.4916 | 9.5200 | 8.0088 | 7.9867 | 7.9977 |
| Baboon | 14.7841 | 8.2100 | 7.0728 | 6.9720 | 6.9676 |

TABLE 2. The recommended technique is compared to the Kalman Filter Algorithm, the 'Canny', 'Sobel', and 'Prewitt' approaches using RMSE criterion

| RMSE | Proposed Work (KFA+ANN) | Kalman Filter | Canny | Sobel | Prewitt |
|--------|-------------------------|---------------|--------|--------|---------|
| Modiji | 0.1330 | 0.3895 | 0.4831 | 0.4833 | 0.4828 |
| Lena | 0.1295 | 0.2522 | 0.3187 | 0.3170 | 0.3170 |
| Aktu | 0.0979 | 0.2398 | 0.3008 | 0.3018 | 0.3013 |
| Baboon | 0.1089 | 0.2919 | 0.3461 | 0.3514 | 0.3516 |

data-related difficulties is artificial neural networks (ANN). Forward-facing algorithms can be used to process image, text, and tabular data. You'll need to use a variety of data augmentation strategies to widen the scope of your data in order to achieve the same level of data processing accuracy as an ANN. Indirectly, ANN may discover complex nonlinear relationships between dependent and independent variables. ANN still reigns supreme in instances when there are few datasets and no requirement for image inputs.

5. CONCLUSION AND FUTURE SCOPE

In this paper, we used the Kalman Filter technique to provide a unique filter, KFA+ANN, for edge detection of grey level images. In the recommended approach, we employ a basic photo and its edge map to construct a new filter. The projected filter may be used on a range of images and evaluated using a number of different criteria. The obtained results, as well as subjective and objective assessments, indicate the usefulness of the recommended filter in edge detection. In this work, shown that using the ANN method, object localization accuracy was shown to improve. Kalman filtering is used to object coordinates acquired using the ANN method. Combining ANN with Kalman Filtering increases localization accuracy and decreases error distances, according to the findings.

Despite the fact that there are various methods for recognizing image edges, deciding which one is appropriate for the image content can be difficult due to the numerous elements that impact the selection. The proposed technique should be utilized to verify edge detection algorithms' evaluations if pictures with varying content have high criterion values and weights. More artificial neural network approaches will be used in the future to investigate the indoor localization of moving persons. To increase positioning accuracy even more, the object coordinates of these approaches will be subjected to Kalman filtering.

6. REFERENCES

1. D.-S. Lu and C.-C. Chen, "Edge detection improvement by ant colony optimization", *Pattern Recognition Letters*, Vol. 29, No. 4, 416-425, 2008.
2. T. Ashwini, Sapkal Mr. C. Bokhare and N. Z. Tarapore, Satellite Image Classification using the Back Propagation Algorithm of ANN, V. I. T. Pune, Reliance communication Mumbai.
3. C.-Y. Chang, "Contextual-based Hopfield neural network for medical image edge detection," *Optical Engineering*, Vol. 45, (2006), doi: 037006-037006-9.
4. P. Arbeláez, M. Maire, C. Fowlkes and J. Malik, "Contour detection and hierarchical image segmentation", *IEEE Transactions on Pattern Analysis and Machine Intelligence*, Vol. 33, No. 5, (2011), 898-916.
5. JW. Rong, Z. Li, W. Zhang and L. Sun, "An improved Canny edge detection algorithm," IEEE International Conference on Mechatronics and Automation, (2014), 577-582, doi: 10.1109/ICMA.2014.6885761.
6. N. Kanopoulos, N. Vasanthavada and R. L. Baker, "Design of an image edge detection filter using the Sobel operator," in *IEEE Journal of Solid-State Circuits*, Vol. 23, No. 2, 358-367, (1988), doi: 10.1109/4.996.
7. P. Nguyen, J. Cho and S. B. Cho, "An architecture for real-time hardware co-simulation of edge detection in image processing using Prewitt edge operator," International Conference on Electronics, Information and Communications (ICEIC), (2014), 1-2, doi: 10.1109/ELINFOCOM.2014.6914387.
8. Y. Yang, K. I. Kou and C. Zou, "Edge detection methods based on modified differential phase congruency of monogenic signal", *Multidimensional Systems and Signal Processing*, Vol. 29, No. 1, (2016), 339-359.
9. Alipoor, M., Imandoost, S, Haddadnia, J, "Designing Edge Detection Filters Using Particle Swarm Optimization", proceeding of ICEE, 2010
10. Ghosh, Chinmoy & Majumder, Suman & Ray, Sangram & Datta, Shrayasi & Nath, Satyendra & Ghosh, C. (2020). Different EDGE Detection Techniques: A Review. Doi: 10.1007/978-981-15-7031-5_84.
11. Akhilesh Pandey, Shashi Kant Shukla "Classification of Devnagari Numerals using Multiple Classifier" *International Journal of Computer Trends and Technology*, Vol. 12, No. 4 (2014).
12. Ding, Y. Xia and Y. Li, "Supervised segmentation of vasculature in retinal images using neural networks," International Conference on Orange Technologies, (2014), 49-52, doi: 10.1109/ICOT.2014.6954694.
13. Quiza, R. and Davim, J.P., Computational methods and optimization. In *Machining of Hard Materials*, (2011), 177-208, Springer, London.
14. M. Nikolic, E. Tuba and M. Tuba, "Edge detection in medical ultrasound images using adjusted Canny edge detection algorithm," 2016 24th Telecommunications Forum (TELFOR), (2016), 1-4, doi: 10.1109/TELFOR.2016.7818878.
15. M. A. Günen, Ü. H. Atasever and E. Beşdok, "A novel edge detection approach based on backtracking search optimization algorithm
16. (BSA) clustering", Proceedings of 8th International Conference on Information Technology (ICIT), (2017), 116-122.
17. X. Ma, S. Liu, S. Hu, P. Geng, M. Liu and J. Zhao, "SAR image edge detection via sparse representation", *Soft Compute*, Vol. 22, No. 8, (2018), 2507-2515,
18. Zhang, J.; Liu, Y.; Liu, H.; Wang, J. Learning Local-Global Multiple Correlation Filters for Robust Visual Tracking with Kalman Filter Redetection. *Sensors* 21, (2021), 1129.

Persian Abstract

چکیده

تشخیص لبه یک تکنیک برای تشخیص شکستگی های واضح تر در یک تصویر است. توقف ناشی از تغییر سریع مقدار سطح تاریک نیروی پیکسل است. متداول کردن تصویر با یک مدیر (کانال د جهته) که به نوبت حساس است رویکرد استاندارد برای مکان لوبه است. **Edge Finder** روشی برای مکان یابی تغییرات شدت و شدت تنظیم شده است که بسیاری از روشهای آماده سازی تصویر در محله های مهم را شامل می شود. تشخیص لبه یک روش اساسی در طیف گسترده ای از برنامه های پردازش تصویر از جمله تجزیه و تحلیل حرکت، شناسایی طراحی، تشخیص اشیاء، ایجاد تصویر بالینی و غیره است. اخیراً در انواع سیستم های تشخیص لبه نشان داده شده است که مزایا و معایب این محاسبات را نشان می دهد. فیلتر کالمن با روش ANN دارای دو مزیت است که آن را برای مقابله با مسائل بهبود مناسب می کند: ادغام سریعتر و نرخ محاسبه کمتر. در این مطالعه، از روش ANN برای بهبود دقت محلی سازی شی استفاده شد. فیلترینگ کالمن برای شیء مختصات به دست آمده با استفاده از روش ANN استفاده می شود. بر اساس یافته ها، استفاده از فیلتر ANN + Kalman دقت محلی سازی را افزایش می دهد و فاصله خطاهای محلی سازی را کاهش می دهد.



Experimental Study on Yttria Stabilized and Titanium Oxide Thermal Barrier Coated Piston Effect on Engine Performance and Emission Characteristics

V. Veda Spandana^a, G. Jamuna Rani^{a*}, K. Venkateswarlu^b, V. V. Venu Madhav^a

^a Department of Mechanical Engineering, VR Siddhartha Engineering College, Vijayawada, A.P, India

^b Department of Mechanical Engineering, Gokaraju Rangaraju Institute Engineering and Technology, India

PAPER INFO

Paper history:

Received 02 August 2021

Received in revised form 21 August 2021

Accepted 04 September 2021

Keywords:

Coating

Emissions

Engine

Piston

Performance Characteristics

Thermal Barrier

ABSTRACT

Most of the energy was being lost through the cooling system and exhaust gas, to utilize that energy and convert it to a useful job thermal barrier coatings is widely used. Tests were conducted on a four stroke, single cylinder diesel engine for which its piston crown was coated with a thickness of 100/100 microns YSZ/TiO₂ over 100 microns NiCr bond coat with plasma spray coating technology and then the results were juxtapose with uncoated piston. Thermal barrier coating was used for better performance, emission and combustion characteristics. The tests were performed at different load conditions using both the pistons and compared the results. At maximum load there is a rise in Brake Thermal Efficiency (BTE) and reduction in Brake Specific Fuel Consumption (BSFC), CO, hydrocarbons (HC) emissions compared to uncoated piston at maximum load. With use of coated piston NO_x emissions were increased and the smoke opacity is decreased compared to uncoated piston. Finally, the results convey that thermal barrier coated piston is more efficient than uncoated piston.

doi: 10.5829/ije.2021.34.12c.05

NOMENCLATURE

| | | | |
|-----------------|---------------------------------|------------------|---------------------------------------|
| BSFC | Brake Specific Fuel Consumption | TBC | Thermal Barrier Coated |
| BTE | Brake Thermal Efficiency | TiO ₂ | Titanium Oxide |
| HC | Hydrocarbons | YSZ | Yttria Stabilized Zirconia |
| CO | Carbon monoxide | HBP | Heat converted to useful Brake Power |
| NO _x | Nitrogen Oxide | HJW | Heat rejected to Jacket cooling Water |

1. INTRODUCTION

Environmental protection and fuel economy are the most important concerns especially in the transport sector with an increasing demand in usage of diesel engine vehicles [1-3]. In the internal combustion engines, combustion chamber walls and the piston absorb most of the heat generated at the process of combustion. This causes heat loss in walls and piston. Which lowers the generated power in engine and the performance. The temperature will be maintained in the combustion chamber to required level, unburnt gases will be burned which will reduce the polluted exhaust because of a decrease in heat loss in the piston [4,5]. In TB coating a bond coat and a top coat will be casted on piston. To improve the coating

union between TBC and substrate metal bond layer is used. TBC materials have some basic requirements like low thermal conductivity, low sintering rate of the porous microstructure, no phase transformation, high melting point, thermal expansion match with the metallic substrate, chemical inertness and good adherence to the metallic substrate. To enhance the performance, different TBC materials were used for IC engines by various researchers. It has an effective effect on exhaust emission and the power of the engine [6-8]. Yttria-stabilized zirconia of 400 microns was cast-off for top coat and NiCrAl of 100 microns was cast-off for bond coat. Holes were made of 2, 3, 4 and 5 mm diameter to the exterior of coating and temperature distribution was examined. Results appear that for coated piston there is a rise in

*Corresponding Author Institutional Email:

jamunarani@vrsiddhartha.ac.in (G. Jamuna Rani)

Please cite this article as: V. Veda Spandana, G. Jamuna Rani, K. Venkateswarulu, V.V. Venu Madhav, Experimental Study on Yttria Stabilized and Titanium Oxide Thermal Barrier Coated Piston Effect on Engine Performance and Emission Characteristics, International Journal of Engineering, Transactions C: Aspects Vol. 34, No. 12, (2021) 2611-2616

temperature of top exterior and drop in substrate. Extra raise in temperature of the top exterior appears when on coating surface holes are made, i.e. 9.5% raise and 2.7% drop with 2 mm diameter holes aimed at top and substrate temperature. With the enlargement of holes diameter, it can be noticed that substrate and top exterior temperatures are dropping. Thermal analysis was performed on an uncoated diesel piston on ANSYS, finished with aluminium silicon alloy and steel [9]. Again, on a piston coated with $MgZrO_3$, the results of 4 different pistons are compared with one another. The material with low thermal conductivity is appeared that the utmost surface with coated piston was improved around 48% for AlSi alloy and 35% for steel. The utmost surface temperature of base metal of coating piston for AlSi and steel are 261 °C and 326 °C [10]. TiO_2 of 100 microns thick was sprayed to the piston crown using a plasma spray method. There is 3% and 2% raise in brake thermal efficiency and mechanical efficiency and also fuel consumption is low compared to uncoated piston [11]. The Diesel engines combustion chamber was encased with mixture of 20% Lead Zirconate Titanate (PZT) and 60% Cyanate modified Epoxy system. Results appeared that 15.89% specific fuel consumption dropped due to the consequence of TB coatings on Diesel engine performance [12]. $FeCl_3$ as catalyst was used to diesel fuel and YSZ coating was encased on valves and piston crown. The outcomes they got were that $FeCl_3$ with a YSZ diesel engine raised the brake thermal efficiency to 2.7%, and has fallen brake specific fuel consumption to 8.3% and for 3-cylinder diesel engine there is 3-5% gain in thermal efficiency with 28.29% fall BSFC [13,14]. Fly ash with composition of silica (45%), alumina (30%), iron (10%) and magnesium (0.5%) were used as TBCs for cylinder head, piston crown, cylinder liner, inlet and exhaust valves for diesel engine. There was 3.4% raise in BTE and 10.3% drop in (Specific Fuel Consumption) SFC compared to uncoated [15]. Two different piston top coatings were used, $CeO_2/8YSZ$ and $Al_2O_3/8YSZ$ and bond coat as $CoNiCrAlY$. Results revealed brake thermal efficiency has raised to 3.37% and specific fuel consumption was 3.45% less in $CeO_2/8YSZ$ TBC coated engine than that of $Al_2O_3/8YSZ$ TBCs [16]. To investigate the temperature of the exterior built on coating thickness experiment was conducted by coating an aluminum piston crown with magnesia-stabilized zirconia. Tests were performed for different coating thicknesses from 0.2mm to 1.6 mm eliminating the bond coat layer. Maximum temperature at the crown center is 32.70%, 55.80%, 72.50% and 84.80% for 0.4 mm, 0.8 mm, 1.2 mm and 1.6 mm thick coating compared with the uncoated piston [17]. To calculate the temperature gradients a steady state thermal analysis was conducted in the two different partially stabilized ceramic coated pistons using Yttria Stabilized Zirconia (Y-PSZ), Magnesium Stabilized Zirconia (Mg-PSZ) compared with standard engine by using Abaqus finite element

(FE) software. Results display that there is 18% raise in temperature value of Y-PSZ coated piston and 48% raise in Mg-PSZ coated piston compared to the uncoated piston [18]. $CaZrO_3$ and $MgZrO_3$ were plasma sprayed on the base of the NiCrAl bond coat. The uncoated piston was tested at different loads and speed conditions then the combustion chamber, piston crown faces, valves and cylinder head were coated with thermal barrier coatings. The results at all load levels and engine speed, show a 2-7% reduction in bsfc and the effective efficiency development of about 2%, 5% and 3% at low, medium and full loads. It is known that the coating surface temperature rises with increasing thickness. Utmost temperature at 0.5 mm thick coating was established to be more in $MgZrO_3$ by 34% compared to uncoated piston. [19,20]. Motor tests were conducted using the MEZ VSETIN test bench with a DS 736-4/V DC dynamometer. In MAO-coated pistons inside temperature falls at least 45 °C when compared with non-MAO pistons. Comparing pistons with different thickness i.e. 76 and 108 microns of MAO layers finalizes that thickness will not have a major effect on thermal state of pistons [21]. Through plasma spray technique the piston top was coated with partially stabilized zirconia of thickness 125microns, following with alumina (Al_2O_3) and NiAl as bond coat. Finally the total thickness to achieve is 250 microns. Results observed a 4 bar increase in peak pressure, 4.6% raise in BTE, 12.6% in exhaust gas temperature and 15.67% increase in nitric oxide emission compared with uncoated piston in the engines [22]. 6-8% Yttria stabilized zirconia (YSZ) TBCs of different thicknesses (100, 125 and 150 μ m) on 50 to 75 μ thick NiAl bond coat was applied on Aluminium – silicon alloy flat plates. It was observed 40° to 48° C by 100 and 125 μ m thick coating and nearly 40% increase in the drop value i.e. 57 to 68° C was observed for just 25 μ m raise in coating thickness i.e. 150 μ m. It is observed that temperature drop raises with the thickness of YSZ coating. [23]. NiCr coating of 100 microns and Aluminium Oxide coating of 150 microns was covered on piston crown. Two different varieties of biodiesel combination (Lemongrass biodiesel and pongamia pinnata methyl ester) was used. At 100% load condition it was proved that the blend combination with TBC piston (i.e D80 PME 10 LGB 10), BTE is improved by 29.2%, BSFC also improved by 0.23 kg/kW-h. Whereas the emission characteristic was dropped in CO, HC and smoke, slightly raised in NOx emission. [24].

From the literature survey it is revealed that the performance of engines with thermal barrier coated pistons is improved. Few researchers worked with YSZ with different thickness ratios. In the present work, the performance and energy balance study of diesel engine is carried out using piston coated with YSZ + TiO_2 materials with 100mm thickness each and the results are discussed.

2. COATING PROCESS

Kirloskar TV1 alloy of aluminium piston of diameter 87.5mm with stroke length 110mm was coated using Plasma spray method used in this experiment. The piston was cleaned with kerosene to remove the dust particles. The coating specifications were shown in Table 1. Grit blasting was done with the help of compressed air at 3.5 kg/cm² pressure to create rough exterior on crown hence the mechanical bond in between substrate and coating remains strong. The nozzle used is of GH type and sprayed with distance of 2-3 inches. The process of coating is done with 490- 500amps current and 60-70 volts. To offer good bonding for coating material, NiCr of 100 microns was applied as a bond coat. TiO₂ is used as coating material which has low thermal conductivity of 4.8W/m-k. Then TiO₂ in powder form was sprayed with a gun on to the piston crown of thickness 100 microns and then 100 microns of Ytria stabilized zirconia was sprayed on TiO₂ layer. YSZ is casted as coating material for its low thermal conductivity, which is anticipated for substrate to diminish the thermal fatigue. Thermal conductivity is 2.2W/m-k for YSZ and it has good thermal insulation property, the stability is high at high temperature. The powder feed of YSZ and TiO₂ is 40-50g/min. Table 2 indicates the properties of YSZ and TiO₂. TiO₂ was sprayed at pressure of 100-120 psi and YSZ at pressure of 50 psi. The powder feed was 40-50 g/m. Coated and uncoated pistons before testing are shown in Figure 1 and coated piston after testing is shown in Figure 2.

TABLE 1. Specifications of coating parameters [14]

| Coating parameters | Specifications |
|---------------------------|-----------------------|
| Plasma gun | 3 MB plasma spray gun |
| Nozzle | GH type nozzle |
| Pressure of hydrogen gas | 50 psi |
| Flow rate of hydrogen gas | 15-20 SCFH |
| Pressure of argon gas | 100-120 psi |
| Flow rate of argon gas | 80-90 SCFH |
| Spraying distance | 2-3 inches |
| Powder feed rate | 40-50 g/m |

TABLE 2. Properties of YSZ and TiO₂ [11,14]

| Properties | YSZ | TiO ₂ |
|-------------------------------|----------|------------------|
| Allowable temperature °C | 1000 | 1840 |
| Density gm/cm ³ | 5.2-6.1 | 4.23 |
| Thermal Conductivity W/m-K | 2-3.8 | 4.8-11.8 |
| Specific heat J/kg-K | 400-700 | 683-697 |
| Thermal expansion coefficient | 8.0-11.4 | 8.4-11.8 |

3. EXPERIMENTAL PROCEDURE

Tests were conducted on Kirloskar TV1, 5.20 kW rated power at 1500 rpm, 1-cylinder, four stroke water cooled, loaded with eddy current dynamometer diesel engine.

The photograph of the engine used is shown in Figure 4 and specifications were listed in Table 3. Tests were conducted at varying the loads i.e. 25, 50, 75 and 100%. The parameters like BSFC, BTE were obtained and the emission parameters like CO, HC, NO_x and smoke opacity were studied. There is a possibility of ±0.1 % uncertainty in the results with the equipments used.

4. RESULTS AND DISCUSSION

4. 1. Brake Specific Fuel Consumption Figure 3 shows variation in BSFC for uncoated and coated piston at different loads. Decrease in BSFC was obtained with rise in brake power for both the pistons, but associated to uncoated piston there is 6.94% reduction in fuel consumption at higher load condition for coated piston. This is caused by high temperature increase in the combustion chamber walls leads to high fuel vaporization causes reduction in physical delay and BSFC drops with coated piston. i.e YSZ and TiO₂ is more efficient and against the exiting.

TABLE 3. Specifications of tested engine

| Type of the Engine | Kirloskar TV1 |
|---------------------|-------------------|
| Number of cylinders | 1 |
| Number of Stroke | 4 |
| Bore and stroke | 87.5mm, 110mm |
| Rated Power | 5.2 kW @ 1500 rpm |
| Compression Ratio | 17.5 :1 |



Figure 1. Uncoated and Coated Piston before testing



Figure 2. Coated piston after testing

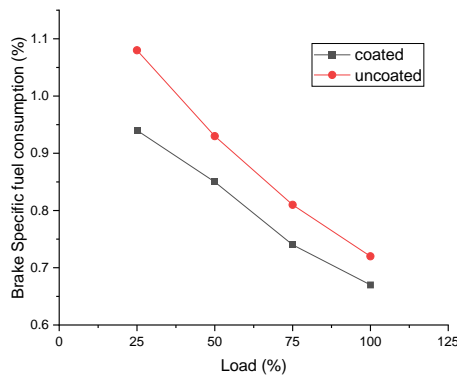


Figure 3. Variation in BSFC for coated and uncoated pistons

4. 2. Brake Thermal Efficiency The variation in BTE is shown in Figure 4 for both uncoated and coated pistons at various loads. It was observed that there is 3.128% raise in brake thermal efficiency compared to uncoated piston at higher load. This is due to the TBC on the piston i.e. YSZ of thermal conductivity 1.4 W/m c and TiO₂ of thermal conductivity 4.8W/m-K. which lowers the heat energy rejection and cannot be allowed to coolant and that energy is transformed as more available work and then BTE increased.

temperature. When increasing the load the fuel consumption is greater and there will be high combustion for thermal barrier coated piston.

4. 6. Smoke Opacity Figure 8 shows the variation of smoke opacity and it shows that the smoke opacity upsurges with load. But compared to uncoated piston the smoke opacity is lower for TBCoated piston. At higher load conditions there is a 12.4% decrease in smoke opacity for YSZ and TiO₂ coated piston. This is due to a steady increase in

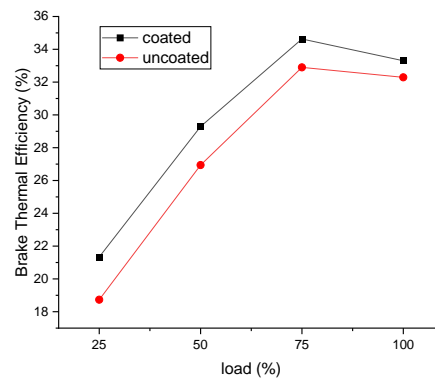


Figure 4. Variation in BTE for coated and uncoated piston

4. 3. HC Emission Figure 5 indicates the deviation in HC emissions in the thermal barrier coated piston and the uncoated piston at different loads. There is 16.92% decrease in the HC emission of the coated piston. In thermal barrier coatings the combustion temperature is higher and also the amount of oxygen. This reduces the hydro carbon emissions and reduces the heat loss going to coolant. The TBC raises the temperature of local heat high and leads to decomposition of fuel molecules. It is because of the presence of radicals, the combustion enhances

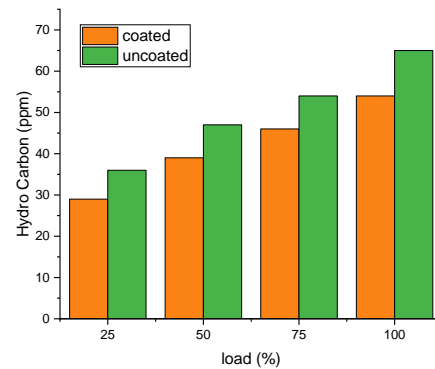


Figure 5. Variation in HC emissions for coated and uncoated pistons

4. 4. CO Emission At various load conditions the CO emissions are determined for both TBC piston and uncoated piston graphically is shown in Figure 6 and is observed that CO emission were decreased by 14.92% with growth in load compared to uncoated piston. In general incomplete combustion auses the formation of CO emissions and is more at higher loads. But TBC lowers the heat transfer and fuel combustion gets better which leads to decrease in CO emissions.

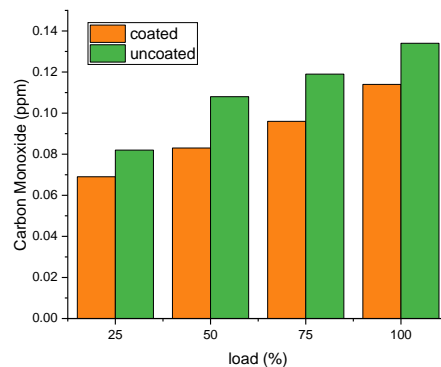


Figure 6. Variation in CO emissions for coated and uncoated pistons

4. 5. NOx Emissions Figure 7 indicates the variance in NOx emissions at different lods for both thermally coated engine and uncoated engine. The NOx emissions were visibly increased for both pistons with increasing load. But in TBC coated piston there is 6.93% raise in NOx emission associated with uncoated piston. This is because the combustion chamber has a high flame

combustion chamber temperature for thermally coated piston, and a great drop in smoke opacity

4. 7. Energy Balance Energy balance of coated and uncoated is shown in Figures 9 and 10. Due to TBC, the heat rejected to through the piston which is not useful to the engine was reduced. By the lower heat loss, more brake thermal energy is converted into useful work out as brake power.

There is an 8.2% raise in HBP compared to uncoated piston. The HJW difference was found by 14.64% drop in coated engine as the rejection of heat is cleared by temperature rise of the coolant. The decrease in thermal

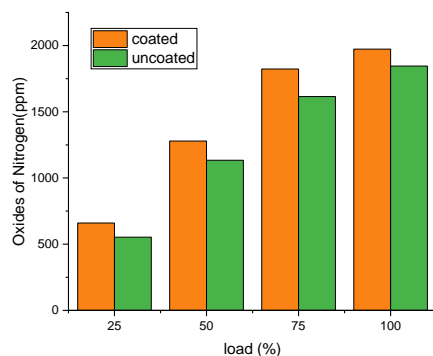


Figure 7. Variation in NOx emissions for coated and uncoated pistons

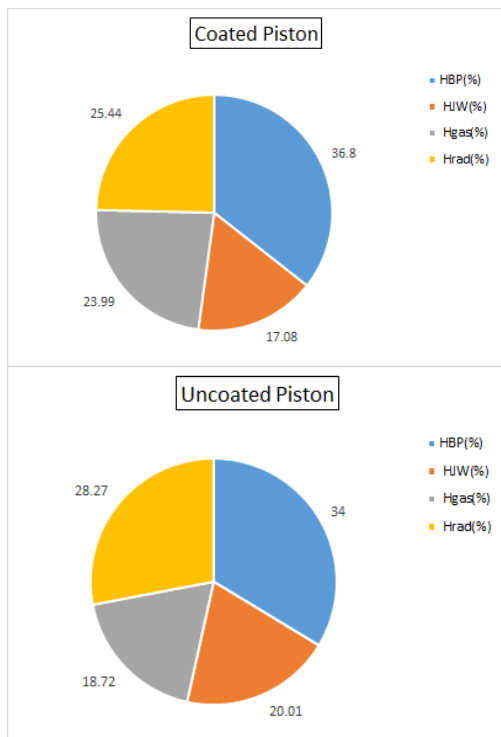


Figure 8. Energy balance for coated uncoated piston

rejection of loads leads to increase in exhaust gas temperature in coated engines, and hence there is 28.1% increase in exhaust gasses temperature. From the experiment the HRad (unaccounted losses) were decreased by 10% in coated piston compared to uncoated piston. Unaccounted losses mainly caused because of energy losses like radiation, conduction and convection removal of heat from the engine to atmosphere.

5. CONCLUSION

From the experimental work done on the diesel engine using YSZ and TiO₂ coated piston, and uncoated piston the following conclusions were observed.

- The TBC coated piston shows a great result of increase in brake thermal efficiency and decrease in brake specific fuel consumption compared to the uncoated piston.
- At higher load condition there is 3.12% increase in brake thermal efficiency in TBC coated piston compared to the uncoated piston.
- In TBC coated piston there is 6.94% decrease in brake specific fuel consumption when differentiated with uncoated piston.
- There was 14.9% and 16.9% drop in CO emission and HC emission in TBC coated piston whereas NOx emissions were increased by 6.93%.
- Smoke opacity is decreased by 12.4% in the TBC coated pistons.

6. REFERENCES

1. Jain, A., E. Porpatham, and S. S. Thipse., "Emission Reduction Strategies for Small Single Cylinder Diesel Engine Using Valve Timing and Swirl Ratio" *International Journal of Engineering, Transactions B: Applications*, Vol. 33, No. 8, (2020), 1608-1619. <https://dx.doi.org/10.5829/ije.2020.33.08b.19>.
2. Fekari, A., N. Javani, and S. Jafarmadar., "Experimental Study of Management Systems for Emission Reduction in Ignition Engines." *International Journal of Engineering, Transactions A: Basics*, Vol. 33, No. 7, (2020), 1347-1353, <https://dx.doi.org/10.5829/ije.2020.33.07a.22>
3. Jamuna Rani, G., YV Hanumantha Rao, and B. Balakrishna., "Fuel injection timing impact on diesel engine performance, combustion and emission characteristics of nano additive biodiesel blends." *International Journal of Ambient Energy*, (2020),1-8, <https://doi.org/10.1080/01430750.2020.1725119>.
4. Reddy, G. Vidyasagar, R. L. Krupakaran, Hariprasad Tarigonda, D. Raghurami Reddy, and N. Govindha Rasu. "Energy balance and emission analysis on diesel engine using different thermal barrier coated pistons." *Materials Today: Proceedings*, Vol. 43 (2021), 646-65. <https://doi.org/10.1016/j.matpr.2020.12.424>
5. Chan, S. H., and K. A. Khor. "The effect of thermal barrier coated piston crown on engine characteristics" *Journal of Materials Engineering and Performance* 9.1, (2000), 103-109. <https://doi.org/10.1361/105994900770346358>.
6. Taymaz, I., Kemal Çakır, and A. Mimaroglu "Experimental study of effective efficiency in a ceramic coated diesel engine" *Surface*

- and Coatings Technology* 200.1-4 (2005), 1182-1185 <https://doi.org/10.1016/j.surfcoat.2005.02.049>.
- Cao, X. Q., Robert Vassen, and Detler Stöver., "Ceramic materials for thermal barrier coatings." *Journal of the European Ceramic Society* 24.1, (2004), 1-10. [https://doi.org/10.1016/S0955-2219\(03\)00129-8](https://doi.org/10.1016/S0955-2219(03)00129-8)
 - Dhomne, Shailesh, and Ashish M. Mahalle. "Thermal barrier coating materials for SI engine." *Journal of Materials Research and Technology* 8.1, (2019), 1532-1537. <https://doi.org/10.1016/j.jmrt.2018.08.002>
 - Banka, Vaibhav Kumar, and M. R. Ramesh. "Thermal analysis of a plasma sprayed ceramic coated diesel engine piston." *Transactions of the Indian Institute of Metals* 71.2 (2018): 319-326. <https://doi.org/10.1007/s12666-017-1184-9>
 - Buyukkaya, Ekrem, and Muhammet Cerit. "Thermal analysis of a ceramic coating diesel engine piston using 3-D finite element method." *Surface and Coatings Technology* 202.2 (2007): 398-402 <https://doi.org/10.1016/j.surfcoat.2007.06.006>
 - Rupangudi, Suresh Kumar, C. S. Ramesh, Kavadike Veerabhadhrappa, and Ram Rohit V. "Study of Effect of Coating of Piston on the Performance of a Diesel Engine." *SAE International Journal of Materials and Manufacturing* 7.3, (2014), 633-637. <https://doi.org/10.4271/2014-01-1021>
 - Uchida, Noboru. "A review of thermal barrier coatings for improvement in thermal efficiency of both gasoline and diesel reciprocating engines." *International Journal of Engine Research*, (2020), 1468087420978016. <https://doi.org/10.1177%2F1468087420978016>.
 - Jena, Shakti P., Saroj K. Acharya, Harish C. Das, Pragyan P. Patnaik, and Shubhra Bajpai. "Investigation of the effect of FeCl₃ on combustion and emission of diesel engine with thermal barrier coating." *Sustainable Environment Research* 28.2, (2018), 72-78. <https://doi.org/10.1016/j.serj.2017.10.002>
 - Sivakumar, G., and S. Senthil Kumar. "Investigation on effect of Yttria Stabilized Zirconia coated piston crown on performance and emission characteristics of a diesel engine" *Alexandria Engineering Journal*, 53.4, (2014), 787-794. <https://doi.org/10.1016/j.aej.2014.08.003>
 - MohamedMusthafa, M., S. P. Sivapirakasam, and M. Udayakumar. "Comparative studies on fly ash coated low heat rejection diesel engine on performance and emission characteristics fueled by rice bran and pongamia methyl ester and their blend with diesel." *Energy* 36.5, (2011), 2343-2351 <https://doi.org/10.1016/j.energy.2010.12.047>
 - Venkadesan, Gnanamoorthi, and Jayaram Muthusamy. "Experimental investigation of Al₂O₃/8YSZ and CeO₂/8YSZ plasma sprayed thermal barrier coating on diesel engine" *Ceramics International*, 45, No. 3, (2019), 3166-3176, <https://doi.org/10.1016/j.ceramint.2018.10.218>
 - Cerit, Muhammet, and Mehmet Coban. "Temperature and thermal stress analyses of a ceramic-coated aluminum alloy piston used in a diesel engine." *International Journal of Thermal Sciences*, 77 (2014), 11-18. <https://doi.org/10.1016/j.ijthermalsci.2013.10.009>
 - Durat, Mesut, Murat Kapsiz, Ergun Nart, Ferit Ficici, and Adnan Parlak. "The effects of coating materials in spark ignition engine design." *Materials & Design* (1980-2015), 36, (2012), 540-545. <https://doi.org/10.1016/j.matdes.2011.11.053>
 - Taymaz, I., K. Cakir, Mesut Gur, and A. Mimaroglu "Experimental investigation of heat losses in a ceramic coated diesel engine." *Surface and Coatings Technology* 169 (2003): 168-170. [https://doi.org/10.1016/S0257-8972\(03\)00220-2](https://doi.org/10.1016/S0257-8972(03)00220-2)
 - Cerit, Muhammet. "Thermo mechanical analysis of a partially ceramic coated piston used in an SI engine." *Surface and Coatings Technology*, 205.11 (2011), 3499-3505. <https://doi.org/10.1016/j.surfcoat.2010.12.019>
 - Dudareva, N. Yu, RDa Enikeev, and V. Yu Ivanov. "Thermal protection of internal combustion engines pistons." *Procedia Engineering* 206, (2017), 1382-1387. <https://doi.org/10.1016/j.proeng.2017.10.649>
 - Abbas, S. Mohamed, A. Elayaperumal, and G. Suresh. "A study on combustion and performance characteristics of ceramic coated (PSZ/Al₂O₃) and uncoated piston-DI engine." *Materials Today: Proceedings* 45, (2021), 1328-1333
 - Reghu, V. R., Nikhil Mathew, Pramod Tilleti, V. Shankar, and Parvati Ramaswamy. "Thermal Barrier Coating Development on Automobile Piston Material (Al-Si alloy), Numerical Analysis and Validation." *Materials Today: Proceedings* 22, (2020), 1274-1284. <https://doi.org/10.1016/j.matpr.2020.01.420>
 - Prakash, S., M. Prabhakar, O. P. Niyas, Safavanul Faris, and C. Vyshnav. "Thermal barrier coating on IC engine piston to improve efficiency using dual fuel." *Materials Today: Proceedings* 33, (2020), 919-924. <https://doi.org/10.1016/j.matpr.2020.06.451>.

| |
|------------------|
| Persian Abstract |
|------------------|

| |
|-------|
| چکیده |
|-------|

| |
|--|
| <p>غالباً انرژی از طریق سیستم خنک کننده و گازهای خروجی از بین می رود، برای استفاده از این انرژی و تبدیل آن به یک کار مفید، پوشش های مانع حرارتی به طور گسترده ای مورد استفاده قرار می گیرد. آزمایشات بر روی موتور دیزلی تک سیلندر چهار زمانه انجام شد که تاج پیستونی آن با ضخامت ۱۰۰/۱۰۰ میکرون YSZ/TiO₂ با پوشش میکرومتر ۱۰۰ NiCr با فناوری پوشش پاشش پلاسما پوشش داده شد و سپس نتایج با پیستون بدون روکش کنار هم قرار گرفت. به پوشش حرارتی برای عملکرد بهتر، ویژگی های انتشار و احتراق استفاده شد. آزمایش ها در شرایط بار مختلف با استفاده از هر دو پیستون انجام شد و نتایج مقایسه گردید. در حداکثر بار افزایش BTE و کاهش انتشار HC, CO, BSFC در مقایسه با پیستون بدون روکش در حداکثر بار وجود دارد. با استفاده از پیستون پوشش داده شده، انتشار NOx افزایش یافته و کدورت دود در مقایسه با پیستون بدون روکش کاهش می یابد. در نهایت، نتایج نشان می دهد که پیستون با روکش حرارتی کارآمدتر از پیستون بدون روکش است.</p> |
|--|



Waviness Effect of Fiber on Buckling Behavior of Sisal/Carbon Nanotube Reinforced Composites Using Experimental Finite Element Method

P. Phani Prasanthi*^a, K. Sivaji babu^a, A. Eswar Kumar^b

^a Department of Mechanical Engineering, P.V.P. Siddhartha Institute of Technology, Kanuru, Vijayawada, Krishna District, A.P., India

^b K.L. deemed to be University, vaddeswaram, Gudur, Andhra Pradesh

PAPER INFO

Paper history:

Received 7 July 2021
Received in revised form 30 July 2021
Accepted 08 August 2021

Keywords:

Sisal Fibe
Waviness Effect
Hybrid Composite
Compressive Load
Buckling Load

ABSTRACT

Sisal fiber-reinforced composites have huge potential applications in many industries. Different defects during the production process of the composite may decrease the performance of these composites. In this work, one of the important defects such as the waviness of the sisal fiber was studied under compressive loading. Two types of composite materials were considered for this study. One is sisal fiber-reinforced polymer matrix composite and another one is hybrid composite i.e. sisal fiber and carbon nanotube reinforced polymer matrix composite. The sisal and hybrid sisal straight fiber composite specimens are prepared by using the hand lay-up technique. The buckling load of the sisal and sisal hybrid composites is estimated by conducting suitable experiments. Further, using the finite element method the effect of the waviness of sisal fiber on the buckling load is estimated. Two different wavy patterns such as Full Sine Waviness (FSW) and Half Sine Waviness (HSW) are considered for sisal fiber. The position effect of waviness of the fiber on the same property is also estimated by changing (A/λ) ratio from 0.1 to 0.35 and the amplitude of waviness from 5 to 17.5 mm (A) and maintaining the length of waviness (λ) to 100mm. The present study is used to design the buckling load of natural composite with waviness because the perfectly straight fibers are difficult to extract from plants.

doi: 10.5829/ije.2021.34.12C.06

1. INTRODUCTION¹

The biodegradability, as well as environmental concerns in the view of plastic usage, has awakened many researchers to replace the conventional composite with natural fiber-reinforced composites. Sisal, hemp, jute, banana fibers are the most used fibers in the place of man-made fiber-reinforced composites. Two important aspects in the usage of the natural composite are needed to be addressed while replacing the commercial composite with natural composite. The first one is the type of natural resource we are using in the form of fiber and their characterization. The second aspect are how to enhance the already used natural fibers to make them as a better competitor in place of man-made fibers.

From these perspectives, the work performed so far on natural and hybrid composite has been reported. The buckling characteristics of natural fiber reinforced polymer composite beams are studied experimentally [1]. In the view of lightweight structures, the compressive strength of flat plates and plain channel sections made with natural flax, jute and hemp have been studied [2-3]. The critical axial and lateral buckling loads of the composite material have been evaluated by conducting suitable experiments [4]. The extension in the buckling behavior was identified by preparing specimens with aluminium and polypropylene [5]. Woven flax-epoxy-laminated composite specimens are prepared and tested for in-plane and out-of-plane compressive behavior [6]. Rectangular and skew composite plates with embedded shape memory alloy wire are tested for thermal buckling

*Corresponding Author Institutional Email:

phaniprasanthi.parvathaneni@gmail.com (P. Phani Prasanthi)

Please cite this article as: P. Phani Prasanthi, K. Sivaji babu, A. Eswar Kumar, Waviness Effect of Fiber on Buckling Behavior of Sisal/Carbon Nanotube Reinforced Composites Using Experimental Finite Element Method, International Journal of Engineering, Transactions C: Aspects Vol. 34, No. 12, (2021) 2617-2623

[7]. A thin-walled open cross-section profile made of fiber metal laminates were tested for buckling response [8]. Compared to straight fiber, the sinusoidal curved fiber showed high buckling strength than straight fiber reinforced composite plate [9]. Composite I-beams are analyzed by adopting the refined beam theory supported by 3D Saint-Venant's solution [10]. Reinforcing the Carbon nanotubes with regular composite effects the bending and buckling properties because reinforcement of CNT's enhances the stiffness of the resulting composite [11]. Compressive and tensile mechanical behavior along with the properties of Flax-fiber reinforced-Epoxy composite is examined [12]. The large deflection, post-buckling of graphene nano platelets-reinforced multi-scale composite beams is studied through a theoretical study [13]. Critical buckling strength of natural fiber fabric, polymer composite beam is analyzed experimentally. [14]. Using the Micromechanics methodology, the plate thickness influence by using functional graded graphene reinforced composites are reported [15]. Buckling loads and corresponding failure modes are also presented [16]. The global buckling and wrinkling behavior of sandwich plates with anisotropic face sheets are investigated [17]. The buckling behaviour of composites with cenosphere and sisal fabric epoxy is discussed by Wang and Wang [18]. The waviness effect of sisal fiber reinforced composite on elastic properties are explored by using experimental and micromechanics [19]. Using the micromechanics, moisture effect of fiber reinforced composites are explored [20]. The debond effect of fiber reinforced nano based composite was addressed by Prasanthi et al. [21]. The waviness effect of fiber on the fatigue response is also explored [22]. Random waviness of fiber is also identified [23-27]. Carbon nanotube curviness and waviness effect on the longitudinal modulus is reported by Matveeva et al. [26]. Using the multiwall carbon nanotube reinforcement, buckling analysis performed on composite beams [28]. Using the buckling-restrained braces, the buckling failure load can be avoided [29]. From the above finding, the knowledge gap has been identified in relation to the natural fiber with waviness under compressive load.

The position effect of waviness of natural fiber with respect to the constraints (fixed and free end of the specimen) is not addressed so far. The buckling load of sisal fiber and carbon nanotube mixed epoxy composite is not performed yet. Considering the above factor, in this work, a complete study on buckling behavior of sisal fibers reinforced composite with waviness effect is reported using both experimental and analytical approaches. Two different waviness patterns such as Full Sine waviness (FSW) and Half Sine Wave (HSW) patterns are considered over a length of 100mm (λ) by varying the amplitude of waviness by changing (A/λ) ratio to 0.1 to 0.35.

2. MATERIALS AND METHODS

The aim of the current proposal is to recognize the buckling load of natural sisal fiber composite and carbon nanotube reinforced sisal fiber (Hybrid) composite by using wavy fibers as reinforcement subjected to compressive load. The buckling load is estimated with experimental and Finite Element studies. Mostly faced problems in the natural fiber is waviness and the effect of waviness on the compressive strength and enhancement of buckling strength by nano reinforcement is also addressed in this work.

To conduct experimental studies, the testing samples are manufactured by using the hand lay-up technique. For that, the fibers were purchased from Vruksha composites, Tamilnadu. These fibers were treated with NaOH solution for 24 hours to promote better bonding between these fibers and the polymer matrix. These treated fibers are used as reinforcement in the polymer matrix and the weight of the matrix is selected in such a way that the fiber weight fraction is 0.1, 0.2, 0.3, 0.4 and 0.5%, respectively. The testing sample dimensions are fixed according to ASTM specified standards. To maintain the accuracy of the results, four testing samples are manufactured and tested.

To create hybrid composites, the Nano carbon tubes are used as reinforcement along with sisal fibers. In this work hybrid composite means sisal fiber reinforced in CNT mixed epoxy matrix. The carbon tubes are mixed with polymer matrix using Ultra Sonication. The ultra sonicator ensures the uniform mixing of carbon tubes in the polymer matrix. The carbon nanotube-infused polymer matrix is used as a hosting medium to reinforce the sisal fibers. In this case, two types of reinforcements are using i.e sisal fiber and carbon nanotubes. The carbon nanotubes weight fraction is maintained at 0.1%. The sisal fiber weight fraction is the same fraction as considered for sisal composites. The specimens of sisal and hybrid composite are presented in Fig.1a-b.

Axial buckling samples were prepared according to the standards ASTM E2954 with a size of 200 mm length and 20 mm width and the thickness of the specimens is in the range of 2.5mm. Using a compression testing machine with 50KN loading capacity, the testing is performed by applying compressive load along the length of the fiber. The buckling load and corresponding elongation are estimated for sisal and hybrid composite. During the experiments, the specimens are fixed both from the bottom and top grips, the specimens are loaded in the axial direction (Figure 1a). Four samples are tested at each weight fraction, and the average value is considered as the final buckling load (Figure 1b).

2.1. Finite Element Method

To identify the waviness of sisal fiber composites on buckling load, the finite element method is used. The finite element models

are created by using ANSYS. Using the mechanics of material method, the buckling load is estimated for sisal and hybrid composite. Applying the assumption of the micromechanics approach that is considering the uniform distribution of fibers in the hosting medium and selecting one unit cell from the total array and by analyzing one unit cell under compressive load, the buckling load can be obtained. (Figure 2)

The unit cell dimensions are calculated based on the volume fraction of fiber. The volume fraction of fiber is changed from 10 to 50%. The Young's modulus of an epoxy matrix is 5.171 GPa, Poisson's ratio (ν) 0.35, sisal fiber modulus 190GPa, Poisson's ratio of sisal fiber 0.3 [20-21, 27]. The carbon nanotube mixed sisal fiber reinforced epoxy composite elastic properties are obtained from our previous research work [28]. To compute the buckling load, one end of the FE model is fixed (Figure 3a) and compressive elongation obtained from the experiments is applied at the opposite end of the FE model as shown in Figure 3a. The eigen buckling load is estimated by performing analysis for straight fibers. The finite element mesh on the FE model is presented in Figure 3b.

The buckling load obtained from the finite element model and experimental results are presented along with the percentage of error in the results and discussion section. Further, the buckling load is estimated for the

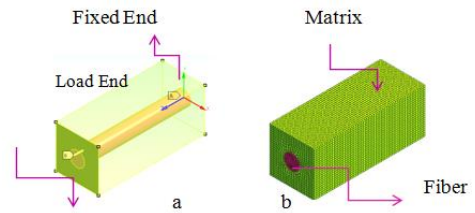


Figure 3. FE model and Finite element mesh

wavy fibers using finite element method ANSYS software. The fibers are modeled with waviness and the waviness is created at the center of the fiber. The length of the fiber (L) is 200mm, waviness length of the fiber (λ) and the amplitude (A) is changing according to the A/λ equal to 0.1, 0.2, 0.3 and 0.35. Figure 4 shows the Full Sign Waviness (FSW) and Half Sign Waviness (HSW) of FE models.

Further, the position of the waviness effect on the buckling load also studied by creating waviness at fixed end (Figure 5) and load end of the fiber (Figure 6). In all the cases, the waviness length in the fiber is fixed to 100 mm in the total length of 200 mm fiber and the amplitude of the waviness varies from 5 mm, 10mm, 15mm and 17.5mm. With these amplitude the (A/λ) becomes 0.1, 0.2, 0.3 and 0.35.

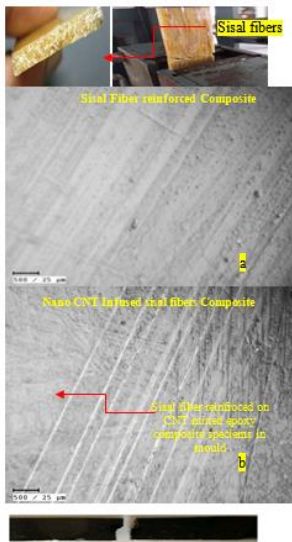


Figure 1. Sisal and hybrid composite and Microscopic view

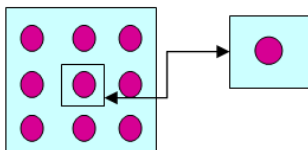


Figure 2. Micromechanics approach and unit cell

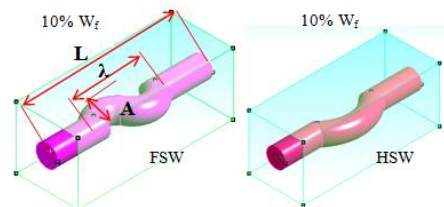


Figure 4. Finite Element models with fiber waviness

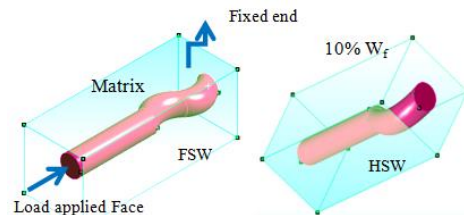


Figure 5. waviness at the fixed end of the fiber

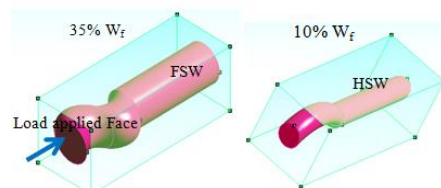


Figure 6. waviness at the Load end of the fiber

3. RESULTS AND DISCUSSIONS

Figure 7 shows the buckling load of sisal and hybrid composites. The buckling load is increased with increasing the weight content of sisal fibers up to 40% [9]. Later the buckling load is slightly decreased in case of sisal fiber composites due to improper load transmission between the fibers and matrix under compressive loading. That 40% is the threshold limit for this case [4]. The hybrid composite buckling load is also increased with increasing the weight fraction of sisal fiber. The buckling strength is more for hybrid composites due to the additional carbon nanotubes in the polymer matrix. From this it is observed that, addition of nano CNT will enhance the buckling load of the sisal fiber reinforced composite [11]. Standard deviation of the results also presented in Table 2.

Figure 8 shows the comparison of buckling load from experimental and FE results. To validate the finite element models, the buckling load of the composite plate is analysed, compared with the published results [25-26]. Table 2 presents the comparison of buckling loads of composite plate under uniaxial compression load with $[40^0/+40^0/90^0/0^0]_{2s}$ laminate lay-up and with two ends fixed support and two ends are simply supported. The results are obtained by performing the analysis with the same material properties, same geometrical data and same boundary conditions [25-26]. Good agreement is found between the present results and published results (Table 1).

At every volume fraction, the percentage of error between the experimental and analytical results is also presented. The correlation between the experimental and FE results are good at a lower weight fraction of sisal fiber. After validating the experimental and analytical results of buckling load, the waviness effect of sisal fiber on the buckling load is presented.

Figure 9 shows the buckling load of sisal and hybrid composites by considering waviness in the fiber in the center of the fiber. The buckling load increasing with increasing the weight fraction of sisal fiber and hybrid composite buckling load is more than the sisal fiber composite. Increasing the waviness ratio (A/λ) from 0.1 to 0.35, increases the buckling load. Increasing the (A/λ) means the amplitude of the full sine wave increasing that means the deviation of the fiber from the straight shape is increasing and the resulting buckling load is also

increasing. The reason for this behavior is that wavy pattern is created at the middle of the FE model and while transmitting a compressive force through the model, the fiber takes more loads. The penetrated fiber portions due

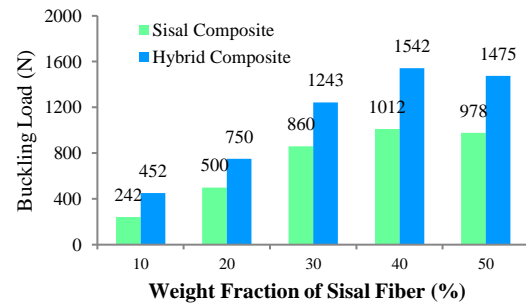


Figure 7. Buckling Load of sisal and Hybrid composites

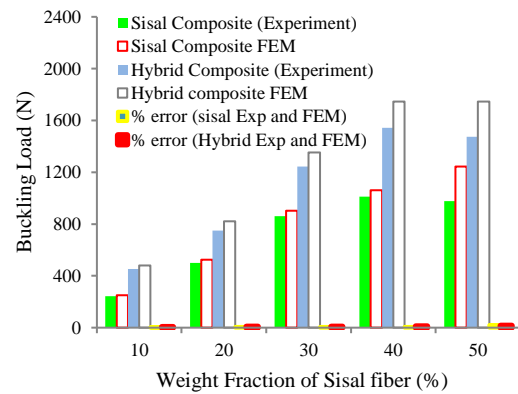


Figure 8. Buckling load from Experimental and FE results with percentage error

TABLE 2. Standard deviation of experimental results

| Sisal fiber reinforced composite | | | | | |
|----------------------------------|------|------|------|------|----------|
| S1 | S2 | S3 | S4 | Avg. | SD |
| 220 | 254 | 239 | 255 | 242 | 16.39105 |
| 512 | 480 | 492 | 516 | 500 | 16.97056 |
| 850 | 840 | 860 | 890 | 860 | 21.60247 |
| 998 | 1015 | 1021 | 1014 | 1012 | 9.831921 |
| 960 | 954 | 995 | 1003 | 978 | 24.58997 |
| Hybrid composite | | | | | |
| S1 | S2 | S3 | S4 | Avg. | SD |
| 451 | 442 | 457 | 458 | 452 | 7.348469 |
| 740 | 745 | 750 | 765 | 750 | 10.80123 |
| 1226 | 1222 | 1256 | 1268 | 1243 | 22.53886 |
| 1558 | 1554 | 1542 | 1514 | 1542 | 19.86622 |
| 1468 | 1502 | 1476 | 1454 | 1475 | 20.16598 |

TABLE 1. validation of buckling load with published results

| Buckling load (KN/cm) [25] | Buckling load (KN/cm) [26] | Buckling load (KN/cm) Present work | % Error |
|----------------------------|----------------------------|------------------------------------|---------|
| 2.4 | 2.4 | 2.294 | 4.41% |
| 3.3 | 3.2 | 3.1674 | 4.08% |

to waviness receive more load than a pure matrix, as a result, the deformation due to compressive load is less and buckling strength is more. Similar trend in the results are found for fiber with sine waviness [9]

Figure 10 shows the variation of buckling load with HSW of fiber at the center of its length. Compared to FSW of fiber, the buckling load is less for HSW of fiber. This is due to the reason that fiber penetration part into the matrix due to the waviness is less than FSW.

Figures 11 and 12 show the response of buckling load of sisal and hybrid composite with the waviness at the fixed end of the fiber. In this case, the waviness effect of fiber is negligible on the buckling load. Because the waviness of the fiber is located nearer to the fixed end. The fixed end restricts the movement as a result the buckling load is not effected with the waviness of fiber.

Figures 13 and 14 show the buckling load of sisal and hybrid composite with the waviness of fiber at the compressive load applied end. The buckling load is highly affected by waviness at load end in both cases (FSW and HSW). As the load applied on the composite is directly applied on the wavy part and later the load is passed through the straight part of the fiber.

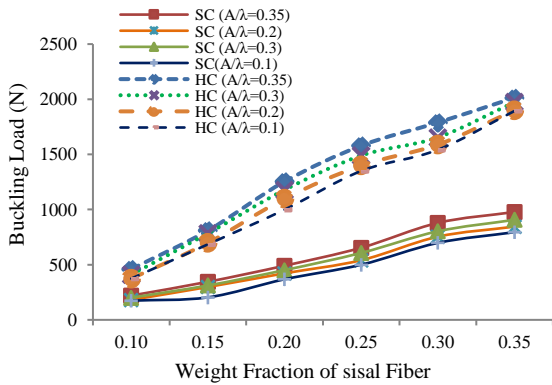


Figure 9. Buckling Load of FSW

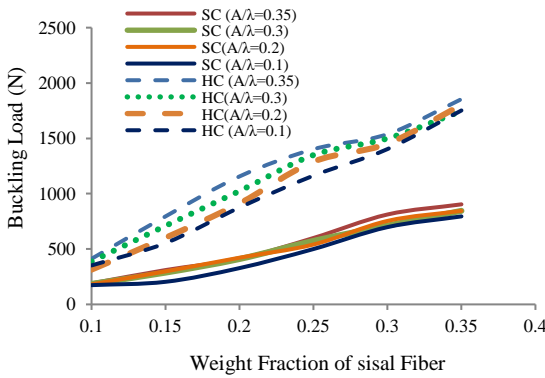


Figure 10. Buckling Load of HSW

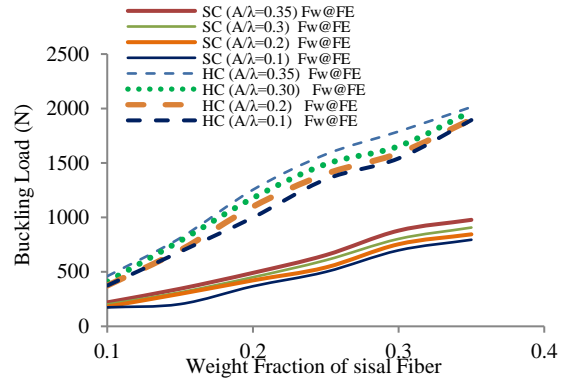


Figure 11. Buckling load of FSW at the fixed end

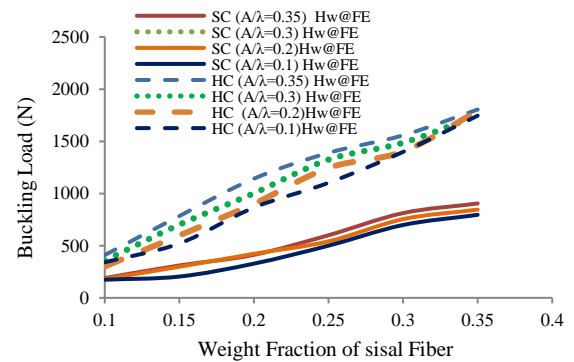


Figure 12. Buckling load of HSW at the fixed end

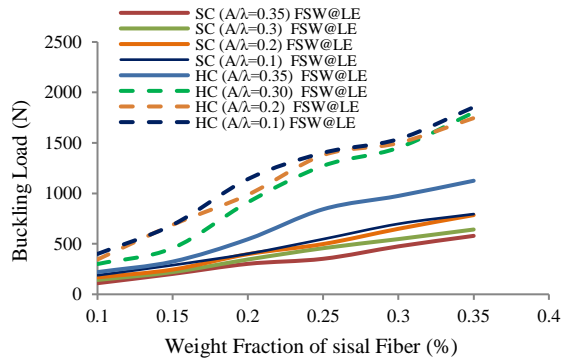


Figure 13. Buckling load of FSW at the Load end

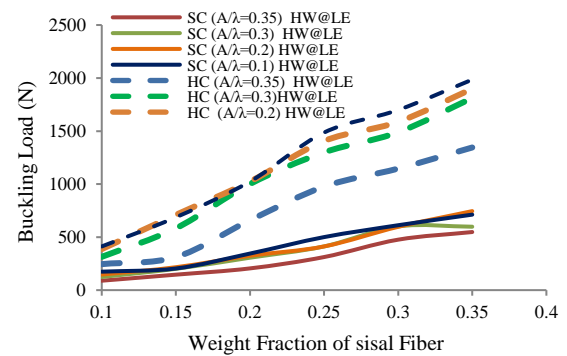


Figure 14. Buckling load of HSW at the Load end

3. CONCLUSIONS

As the fiber weight fraction increases, the buckling load increases up to 40% of weight fraction, later there is no improvement in the same property; but the hybrid composite buckling load increases even beyond 40% of fiber weight fraction due to the nano reinforcement.

Compared to FSW fiber reinforced composite, HSW fiber composite showed less buckling loads at all the waviness ratio (A/λ) considered for the study.

The waviness is located nearer to the fixed support will not influence the buckling load of wavy fiber reinforced composite. Whereas the waviness at the middle and nearer to the load ends, have a considerable influence on buckling load. In these cases, the waviness located at the load end having very high impact on buckling strength

6. REFERENCES

1. Sunil Waddar, Jeyaraj Pitchaimani, Mrityunjay Doddamani, Ever Barbero, "Buckling and vibration behaviour of syntactic foam core sandwich beam with natural fiber composite facings under axial compressive loads", *Composites Part B: Engineering*, Vol. 175, (2019), 107-133, <https://doi.org/10.1016/j.compositesb.2019.107133>.
2. M.R. Bambach, "Compression strength of natural fibre composite plates and sections of flax, jute and hemp", *Thin-Walled Structures*, Vol. 119, (2017), 103-113, <https://doi.org/10.1016/j.tws.2017.05.034>.
3. M.R. Bambach, "Geometric optimisation and compression design of natural fibre composite structural channel sections", *Composite Structures*, Vol. 185, (2018), 549-560, <https://doi.org/10.1016/j.compstruct.2017.11.065>.
4. Omer YavuzBozkurt, Mehmet Bulut, Ahmet Erklig, Waleed Ahmed Faydh, "Axial and lateral buckling analysis of fiber reinforced S-glass/epoxy composites containing nano-clay particles", *Composites Part B: Engineering*, Vol. 158, (2019), 82-91, <https://doi.org/10.1016/j.compositesb.2018.09.043>.
5. Shunfeng Gong, Xipeng Wang, Tao Zhang, Chengbin Liu, "Buckle propagation of sandwich pipes under external pressure", *Engineering Structures*, Vol. 175, (2018), 339-354, <https://doi.org/10.1016/j.engstruct.2018.08.033>.
6. Jianxing Hu, Sha Yin, T.X. Yu, Jun Xu, "Dynamic compressive behavior of woven flax-epoxy-laminated composites", *International Journal of Impact Engineering*, Vol. 117, (2018), 63-74, <https://doi.org/10.1016/j.ijimpeng.2018.03.004>.
7. S. Kamarian, M. Shakeri, "Thermal buckling analysis and stacking sequence optimization of rectangular and skew shape memory alloy hybrid composite plates", *Composites Part B: Engineering*, Vol. 116, (2017), 137-152, <https://doi.org/10.1016/j.compositesb.2017.01.059>.
8. Radoslaw J. Mania, Christopher Bronn York, "Buckling strength improvements for Fibre Metal Laminates using thin-ply tailoring", *Composite Structures*, Vol. 159, (2017), 424-432, <https://doi.org/10.1016/j.compstruct.2016.09.097>.
9. M. D. Pandey, "Effect of Fiber Waviness on Buckling Strength of Composite Plates", *Journal of Engineering Mechanics*, 1999, 125(10), 1173-1179
10. Fares Naccache, Rached El Fatmi, "Buckling analysis of homogeneous or composite I-beams using a 1D refined beam theory built on Saint Venant's solution", *Thin-Walled Structures*, Vol. 127, (2018), 822-831, <https://doi.org/10.1016/j.tws.2018.02.028>.
11. Ahmadi, Masoud & Ansari, Reza & Rouhi, H. Multi-scale bending, buckling and vibration analyses of carbon fiber/carbon nanotube-reinforced polymer nanocomposite plates with various shapes. *Physica E: Low-dimensional Systems and Nanostructures*, Vol. 93, (2017) doi: 10.1016/j.physe.2017.05.009.
12. Zia Mahboob, Ihab El Sawi, Radovan Zdero, ZouheirFawaz, HabibaBougherara, "Tensile and compressive damaged response in Flax fibre reinforced epoxy composites", *Composites Part A: Applied Science and Manufacturing*, Vol. 92, (2017), 118-133, <https://doi.org/10.1016/j.compositesa.2016.11.007>.
13. M. Rafiee, F. Nitzsche, M.R. Labrosse, "Modeling and mechanical analysis of multiscale fiber-reinforced graphene composites: Nonlinear bending, thermal post-buckling and large amplitude vibration", *International Journal of Non-Linear Mechanics*, Vol. 103, (2018), 104-112, <https://doi.org/10.1016/j.ijnonlinmec.2018.05.004>.
14. M. Rajesh, JeyarajPitchaimani, "Experimental investigation on buckling and free vibration behavior of woven natural fiber fabric composite under axial compression", *Composite Structures*, Vol. 163, (2017), 302-311, <https://doi.org/10.1016/j.compstruct.2016.12.046>.
15. Hui-ShenShen, Y. Xiang, Feng Lin, D. Hui, "Buckling and postbuckling of functionally graded graphene-reinforced composite laminated plates in thermal environments", *Composites Part B: Engineering*, Vol. 119, (2017), 67-78, <https://doi.org/10.1016/j.compositesb.2017.03.020>.
16. MariuszUrbaniak, Adrian Gliszczynski, LukaszBorkowski, "Numerical studies on stability and load capacity of compressed channel section columns made of composite reinforced with flax fibers", *Composite Structures*, Vol. 206, (2018), <https://doi.org/10.1016/j.compstruct.2018.07.123>.
17. Riccardo Vescovini, Michele D'Ottavio, Lorenzo Dozio, Olivier Polit, "Buckling and wrinkling of anisotropic sandwich plates", *International Journal of Engineering Science*, Vol. 130, (2018), 136-156, <https://doi.org/10.1016/j.ijengsci.2018.05.010>.
18. K.F. Wang, B.L. Wang, "A mechanical degradation model for bidirectional natural fiber reinforced composites under hydrothermal ageing and applying in buckling and vibration analysis", *Composite Structures*, Vol. 206, (2018), 594-600, <https://doi.org/10.1016/j.compstruct.2018.08.063>.
19. P. Phani Prasanthi, K. SivajiBabu, M. S. R. Niranjan Kumar & A. Eswar Kumar, "Analysis of Sisal Fiber Waviness Effect on the Elastic Properties of Natural Composites Using Analytical and Experimental Methods", *Journal of Natural Fibers*, <https://doi.org/10.1080/15440478.2019.1697987>
20. P Phani Prasanthi, K SivajiBabu, M S R Niranjan Kumar, G Raja Vamsi and N Raghu Ram, "Analysis of hybrid composite with moisture defects using finite element method and micromechanics", *Materials Research Express*, Vol. 4, (2017), <https://doi.org/10.1088/2053-1591/aa8d2f>
21. P. Prasanthi, G. SambasivaRao B. UmamaheswarGowd "Mechanical performance of Buckminster fullerene-reinforced composite with interface defects using finite element method through homogenization techniques", *Composite Interfaces*, 22:4, (2015) 299-314, DOI: 10.1080/09276440.2015.1021223
22. F. Schmidt and M. Rheinfurth and P. Horst and G. Busse, "Effects of local fibre waviness on damage mechanisms and fatigue behaviour of biaxially loaded tube specimens", *Composites Science and Technology*, Vol. 72, (2012), 1075-1082, <https://doi.org/10.1016/j.compscitech.2011.09.012>

23. M.P.F. Sutcliffe, "Modelling the effect of size on compressive strength of fibre composites with random waviness", *Composites Science and Technology*, Vol. 88, (2013), 142-150, <https://doi.org/10.1016/j.compscitech.2013.09.002>.
24. Bradshaw, R. D., F. T. Fisher, and L. C. Brinson. "Fiber waviness in nanotube-reinforced polymer composites—II: modeling via numerical approximation of the dilute strain concentration tensor." *Composites Science and Technology*, Vol. 63, 1705-1722. (2003). [https://doi.org/10.1016/S0266-3538\(03\)00070-8](https://doi.org/10.1016/S0266-3538(03)00070-8).
25. Narayana, A. Lakshmi, Krishnamohana Rao, and R. Vijaya Kumar. "Buckling analysis of rectangular composite plates with rectangular cutout subjected to linearly varying in-plane loading using fem." *Sadhana*, Vol. 39, (2014), 583-596, <https://doi.org/10.1007/s12046-014-0250-9>
26. Anna Y. Matveeva, Sergey V. Pyrlin, Marta M.D. Ramos, Helmut J. Böhm, Ferrie W.J. van Hattum, "Influence of waviness and curliness of fibres on mechanical properties of composites", *Computational Materials Science*, Vol. 87, (2014), 1-11, <https://doi.org/10.1016/j.commatsci.2014.01.061>.
27. P. Phani Prasanthi, K. Sivaji Babu, M. S. R. Niranjan Kumar and A. Eswar Kumar, "Comparison of elastic properties of different shaped particle reinforced composites using micromechanics and finite element method", *International Journal of Computational Materials Science and Engineering* Vol. 09, No. 02, 2050011 (2020), <https://doi.org/10.1142/S2047684120500116>
28. I. Arun Babu, B. Raghu Kumar, P. Phani Prasanthi, A. Eswar Kumar, Ch. Vidya, "Fatigue Characterization of Sisal Fiber Reinforced Composites Using Experimental and Finite Element Method", *International Journal of Innovative Technology and Exploring Engineering*, Vol. 8, (2019).
29. B. Pordel Maragheha, A. Jalalia,b, S.Mohammad Mirhosseinia "Evaluating the Effect of Buckling-Restrained Braces in Steel Buildings Against Progressive Failure using Different Simulation Strategies", *International Journal of Engineering, Transactions A: Basics*, Vol. 34, No. 10, (2021), 2248-2258, doi: 10.5829/IJE.2021.34.10a.06

Persian Abstract

چکیده

کامپوزیت های تقویت شده با الیاف سیزال کاربردهای بالقوه عظیمی در بسیاری از صنایع دارند. نقص های مختلف در طول فرآیند تولید کامپوزیت ممکن است عملکرد این کامپوزیت ها را کاهش دهد. در این کار، یکی از نقص های مهم مانند موج دار بودن الیاف پایان نامه تحت بار فشاری مورد مطالعه قرار گرفت. دو نوع مواد کامپوزیتی برای این مطالعه در نظر گرفته شد. یکی کامپوزیت ماتریس پلیمری تقویت شده با فیبر سیزال و دیگری کامپوزیت ترکیبی یعنی فیبر سیزال و کامپوزیت ماتریس پلیمری تقویت شده با نانولوله های کربنی. نمونه های کامپوزیت سیزال و هیبرید سیزال با استفاده از تکنیک چیدن دست آماده می شوند. بار کمانش کامپوزیت های سیزال و سیزال با انجام آزمایشات مناسب برآورد می شود. علاوه بر این، با استفاده از روش اجزای محدود، اثر موج الیاف سیزال بر بار کمانش برآورد می شود. دو الگوی موج دار مختلف مانند موج سینوسی کامل (FSW) و موج نیمه سینوسی (HSW) برای فیبر سیزال در نظر گرفته شده است. اثر موقعیت موج دار شدن الیاف بر روی همان ویژگی نیز با تغییر نسبت (A/λ) از 0.1 به 0.35 و دامنه موج از 5 تا 17.5 میلی متر (A) و حفظ طول موج (λ) تا 100 میلی متر مطالعه حاضر برای طراحی بار کمانش کامپوزیت طبیعی با موج استفاده می شود. زیرا استخراج الیاف کاملاً مستقیم از گیاهان دشوار است.



Effect of Motivation, Opportunity and Ability on Human Resources Information Security Management Considering the Roles of Attitudinal, Behavioral and Organizational Factors

L. Bahrami^a, N. Safaie^{*a}, H. Hamidi^b

^a Faculty of Industrial Engineering, K. N. Toosi University of Technology, Tehran, Iran

^b Department of Information Technology, Faculty of Industrial Engineering, K. N. Toosi University of Technology, Tehran, Iran

PAPER INFO

Paper history:

Received 10 July 2021

Received in revised form 26 August 2021

Accepted 30 August 2021

Keywords:

Information Security

Human Resources Behavior

Motivation Opportunity Ability Model

Norm Activation Model

Planned Behavior Theory

ABSTRACT

Information security is a vital issue currently faced by organizations around the world. There is a huge flood of cyber-attacks and security threats due to the negligence of human agents, which doubles the importance of human resource behavior in the organization. This study provides an integrated framework of motivation opportunity-ability (MOA) that includes social psychological factors from the norm activation model (NAM) model and planned behavior (PB) theory to examine the variables that determine security behaviors in a well-founded university in Tehran. For this purpose, data were collected and analyzed by distributing 141 questionnaires among the staff of this university. The research hypotheses have been tested by structural equation modeling (SEM) using SPSS and Lisrel software. The results show that the ability has the greatest impact on information security behaviors, followed by opportunity and motivation, which have a direct and significant impact on behavior. In addition, motivation mediates the impact of opportunity and ability. Finally, recommendations are provided for designers of effective information security strategies based on the constraining factors of human resources behavior in the organization.

doi: 10.5829/ije.2021.34.12C.07

1. INTRODUCTION

Today, Modern organizations have broad range of information resources that are heavily dependent on their human resources factors, and this dependency has made them vulnerable to events that could jeopardize their information systems [1]. Information leakage has serious consequences for organizations, including reputation damages, loss of intellectual property, reduced productivity, loss of competitive advantage, and, worst of all, and bankruptcy. In another words, organizations have identified people as a significant liability to information security governance [2], security and risk, economics and technology, which is among the industries rapidly growing and developing [3]. Therefore, the role of information security is essential in

organizations to protect data and ensure that services and projects are categorized and successfully performed without disclosing information [4] and which has become an overwhelming challenge [5].

Evidence shows that the number and severity of information security breaches is increasing and has been a major concern for users and organizations. According to Karjalainen et al. [6], the average cost of cybercrime has increased by 62% over the past 5 years. Lloyd's, the British insurance company, stated in a report that its annual loss would be \$ 400 billion in the absence of cybersecurity mechanisms [7]. DBIR Research Center claims that occurrence of 60% of information security threats can seriously endanger organizations within minutes. In this report, 55% of information security incidents are the result of the workings of human resources inside organizations [8]. The IBM Cyber Security Information Index also reported that 95% of

* Corresponding Author Institutional Email: nsafaie@kntu.ac.ir (N. Safaie)

information security incidents were related to human error [9].

Intentionally or unintentionally, employees make up a significant portion of threats to organizations' information assets. According to the findings and after analyzing two case studies, public and private sector organizations participating in these studies stated that 92.5% and 51% of the recorded information security incidents have been related to human error, respectively [10]. According to a research report by the Ponemon Institute on the cost of cyber security attacks, internal threats are of the highest costs, the impact of which is not limited to financial losses, but may also endanger the security of individuals and the organization [11]. In the literature, several theories postulated after investigations by researchers and reported human factors to have had an impact on user behavior, both negative and positive which is mentioned by researchers and security experts have reported that the "weakest link" in any security chain is human behavior; because any technical security solution is still prone to failures due to human error [12]. From a practical perspective, understanding such behaviors is important; if users do not comply with information security solutions; however, technically sophisticated, lose their effectiveness [13]. Therefore, it is recognized that in the field of information security, reducing the risk requires attention to human aspects along with technological aspects. Domestic staff does not require much effort and time to access targeted information compared to foreign attackers. Organizations often trust their employees, and anonymity is a feature that can reduce the risk of identifying them. Due to their constant involvement with highly complex security systems and a wide range of other job requirements, domestic staff may easily ignore unlikely information security threats or take no action on them, because they neither have the time, nor do they have enough skills to respond to these threats. As a result, the potential harms of domestic staff are increasing.

In order to understand the main factors of human resources security behaviors in organizations, the question of the present study is as follows: What are the determinants of human resources security behaviors in the field of organizational information? The results of this study can be effective in improving the information security behaviors of human resources of organizations by helping managers apply appropriate strategies in accordance with the characteristics of employees. In the following, while reviewing the background of the studies, the theoretical foundations, conceptual model and also the research method are provided. The results are analyzed in a well-founded university in Tehran and finally, the conclusion and key factors affecting the information security of human resources in the organization are presented.

Therefore, according to experts, the "weakest link" in any security chain is human behavior because any technical security solution is still subject to failures resulting from human errors. Hence, the risk reduction in information security area involves paying attention to aspects of human being along with technological aspects. As a result, one of the main motives of this study is investigating the factors affecting the security behaviors of human resources in the organization. the purpose of this study is to determine the relationship between attitudinal, behavioral and organizational factors with empirical support from three theoretical frameworks including Theory of planned behavior, the norm activation model (NAM) and motivation model with the interdisciplinary approach, in the integration form.

The structure of this paper consists of follow sections; in the second section, the literature of the research is reviewed and in the third section, the research model and hypotheses are presented. Section fourth provides research method and results, and section fifth devoted to findings and conclusions. In the final section, limitations of the research and suggestions for future research are presented.

2. LITERATURE REVIEW

2. 1. Norm Activation Model (NAM)

The NAM theory, first developed by Schwartz [14], is a social-friendly theory to explain the purpose of humanitarian behaviors. The theory states that personal norms are an essential prerequisite for each individual's behavior [15]. The theory also argues that people engage in humane behaviors for the benefit of society, even if the behaviors sometimes cause them inconvenience. There are three main variables in NAM: Personal Norms (PN), Awareness of Consequences (AC), and Ascription of Responsibility (AR). A personal norm is a "moral obligation to perform or refrain from certain [16]. The term awareness of consequences means, "One is aware of the impact of the consequences of one's behavior on others." Ascription of Responsibility is also described as "one's personal feeling about whether or not s/he is responsible for the negative consequences of not engaging in the desired social behaviors" [17].

Although following the personal norms may increase self-confidence and prevent self-blame, it can also lead to costs, such as extra time and effort. If the benefits of the behavior outweigh its costs to the individual, it is likely that the behavior will be performed. However, if the costs outweigh the benefits, or the costs and benefits are not clear, the person may be hesitant to make a decision. To reduce this skepticism, one may redefine one's understanding of the situation

and use defense mechanisms to undermine one's sense of moral commitment. Denying the consequences of not performing such behaviors, which involves underestimating the negative consequences of an action, as well as denying personal responsibility for the behavior, which involves considering it as something beyond control or outside the realm of personal responsibility, are common defense mechanisms in this field [18]. The full implementation of these defense mechanisms neutralizes the individual's moral obligation without imposing punishments on him/her [19]. Two conditions are necessary to overcome such defense mechanisms. First, one must understand that one's behavior affects the well-being of others. Second, the individual must accept personal responsibility for the consequences of his behavior [20]. When these conditions are met, defense mechanisms have less of an impact on his/her performance, and personal norms are more likely to be activated, creating a sense of personal commitment to regulate behavior [21].

2. 2. Theory of Planned Behavior (TPB) The theory of TPB, developed by Azjen [8] is one of the most important and documented frameworks of a socio-psychological theory that tries to logically explain and understand the reason for certain behaviors by individuals [22]. TPB is a generalization of Theory of Reasoned Action (TRA) and has been widely used in the study of ethical behaviors in the information security systems and individual decision-making to adopt acceptable computer security measures and ISSP-compliant behaviors as well as in the field of information security [23].

Azjen [8] stated that a large part of committing a behavior results from a strong decision to do it. The stronger the decision to perform a particular behavior, the more likely a person is to perform that behavior. The TPB theory believes that an individual's decision to engage in behavior is influenced by three psychosocial factors. By carefully considering these three factors, we can predict the likelihood of a particular behavior by the individual. These three factors are a person's attitude toward behavior, perceived behavioral control (PBC), and mental norms.

Attitude is defined as an individual's overall assessment of an object, person, or place, and his or her positive or negative feelings about performing a particular behavior [24]. The more positive a person's attitude toward a behavior, the stronger his or her decision to engage in that behavior. Therefore, attitude can be examined as a fundamental factor in relation to the probability of performing the desired behavior in an individual [25]. However, identifying and extracting a person's attitudes and beliefs is not an easy task. For this reason, there are other variables that affect TPB-related factors. Previous studies have shown that when the

behavior in question has an ethical dimension, the individual's norms should be included in the TPB model [26]. Therefore, since ethical dimensions play an important role in conducting behaviors that conform to information security practices, it seems appropriate to pay attention to personal norms in the TPB theory. Mental norms refer to the influence exerted by important people in the individual's life (family, friends, etc.) on his or her behavioral decisions [27]. Getting approval from the important people in a person's life for a behavior has a great impact on motivating him/her to make stronger decisions. Thus, having a high understanding of the associated mental norm can increase the likelihood of a person performing a particular behavior [28]. In addition to examining the reasoned variables that influence a behavior, that is, attitudes toward something and the influence of other people, TPB theory also considers whether a person is fully capable of performing the desired behavior. Each individual has a different capacity to perform planned behaviors, so different default variables may affect his/her planned behavior. PBC is the third component of TPB theory, which defines an individual's perception of the ease or difficulty of performing a particular behavior. Individuals' serious decision to perform a certain behavior is due to the person's high control over himself [29].

In short, the TPB theory predicts that to perform a behavior, people with a more positive attitude toward that behavior, increased approval of others, and more control over the perceived behavior, will make a stronger decision to perform it. The stronger the decision to perform a certain behavior, the more likely a person is to perform that behavior [30].

2. 3. Motivation-Opportunity-Ability (MOA) Model

The MOA model was first developed and used to understand consumers' brand information processing methods and their shopping-related behavior [31], which has recently been used extensively in existing studies to explain different types of behavior. In the context of MOA, three main factors influence an individual's behavior, which include "motivation", "necessary skills and abilities" and "opportunities provided" to perform the desired behavior [32]. Motivation examines a person's incentives, concerns, and participation in maintaining information security. Opportunity involves environmental (such as organizational support) and interpersonal (e.g., peer pressure) factors that affect an individual's compliance with information security necessities. Ability examines prior knowledge of information security and skills in interpreting received information [33].

Despite the capacity of the MOA framework for understanding the factors influencing information security compliance behaviors in the workplace, there

are many limitations. Admittedly, first, direct measurement of motivation, which is the concern and willingness to comply with information security points, is not possible without taking into account broader dimensions of motivation such as perceived consequences and individual responsibility (NAM theory factors). Second, for the “opportunity” factor, analyzing the effect of peer pressure on individual behavior requires considering a combination of descriptive norms and individual mental norms from TPB theory, which makes it easier to describe interpersonal factors affecting security behaviors. Third, to generalize the concept of ability, it is necessary to examine variables such as actual knowledge (AK) and perceived knowledge of the individual (PK) as well as PBC (from the TPB theory). Therefore, one of the important goals of this study is to integrate the important variables of NAM and TPB theories to strengthen the MOA framework. These proposed variables not only predict information security behaviors, but also inherently complement motivation, opportunity, and ability by definition.

2. 4. Conceptual Model and Research Hypotheses

This study is an integrated MOA framework for analyzing the factors affecting behaviors related to human resources information security in the organizational environment, which has been prepared by considering the socio-psychological factors in the model. In the context of MOA, the three main factors, namely motivation, opportunity and ability, are indirect factors affecting behaviors that are not directly observed in this survey but are inferred from other variables. In order to examine the complexity of human behaviors, researchers have recently emphasized the importance of integrating different theories and models for synergistic studies [34]. There is a high potential for using interdisciplinary research approaches, and the knowledge gained in this field can provide new insights into the management of human resource security behaviors in organizations. Many researchers have emphasized that TPB theory is a logical paradigm that ignores the role of irrational and emotional motivations in shaping behavior. In addition, normative activation theory (NAM) is derived only from the heart and states that a person's socializing behavior is due to the activation of his or her personal norms. Accordingly, it seems that TPB and NAM alone may not be sufficient to explain human resource security behaviors [35]. Therefore, in this study, to prepare clear and measurable components for each MOA factor, structures of NAM and TPB theories as well as other variables, identified as indicators of MOA factors in existing models, have been used. It considers the personal and internal goal of the individual to perform the behavior, the external influencing factors and the effects of the external social

environment (mental norms) on the individual's behavior. The conceptual model of the present study is shown in Figure 1.

To emphasize the socio-psychological causes affecting the “motivation” factor, the present study considers the three main structures of NAM theory as three indicators of motivation. People usually go through a series of cognitive processes related to their motivation before deciding to start, maintain, or cancel an effort, and all three indices of AC, AR, and PN play an important role in this cognitive dimension of the motivation factor [35, 36]. Attitude - from the TPB theory - is also accepted as the fourth indicator of motivation. Thøgersen [37] also considers attitude as one of the motivational factors in setting behavioral goals. The four dimensions identified are the variables that motivate security behaviors.

The opportunity factor in this study broadly includes all environmental and interpersonal factors that are outside the realm of individual. Therefore, it also includes mental and descriptive norms. In this case, if employees can predict that they can achieve social rewards by accepting social norms, then social norms should be considered as an opportunity [38]. Norms include the social influences that are prevalent in the organizational environment. These social influences can reinforce or inhibit the decision to engage in a behavior, resulting in a situation that is beyond the individual's control. Therefore, norms are considered as constructive variables of the opportunity factor. This study considers three social norms that are consistent with human resource information security practices and affect behaviors. First, subjective norms (SNs), which are a type of emphatic norm in TPB theory and reflect the expectations of others about one's behavior (for example, the majority of co-workers expect employees to turn off their computers when leaving it), include two other important socio-psychological factors, i.e., descriptive norms (DN) and organizational norms (ON). Descriptive norms are observing and understanding the behavior of others in the real world (for example, observing and perceiving whether, in real situations, co-workers behave in accordance with information security practices); Organizational norms also reflect the organization's expectations of the individual's behavior and the degree of commitment or encouragement of the organization to promote the desired behavior (for example, the organization rewards its human resources for observing information security tips). Studies have shown that participation of human resources in community-friendly behaviors is positively associated with organizational support [39]. Positive social norms enhance the perceived opportunity of the individual through social interaction with colleagues. Negative social norms can also limit the individual's ability to engage in behaviors that conform to information

security practices. For example, an employee may not feel comfortable observing information security tips due to selfish coworkers who are unwilling to be bothered to protect customer and organization information. To examine the ability factor, three indicators have been considered, including the individual's perceived knowledge, the individual's actual knowledge and PBC from the TPB theory. A person's perceived knowledge refers to his or her personal understanding of his or her knowledge of data protection (for example, updating his or her information about cyber-attacks). In fact, it shows the background knowledge necessary to achieve the desired result. Actual knowledge examines an individual's understanding of information security facts, including that "a website address that starts with http has information security." Perceived knowledge is not always accurate and is also often judged subjectively. Therefore, a standard and correct survey (i.e., actual knowledge) is included in the model. Employees of human resources, like other employees, need training, information systems, coordination, and performance management. Therefore, in order to provide the expected value of business units, the employees of this unit also need training and acquisition of new skills [39, 40]. In addition, PBC complements a person's physical ability with perceived ease to perform a behavior. Based on the research background, we provide hypotheses for MOA framework factors (H1, H2, H3) and for the impact of MOA factors on human resources information security behaviors (H4, H5, H6), which are listed in Table 1. The present study hypothesizes that ability and opportunity are most important if they can be internalized in an individual's motivation, which shows the mediating effect of motivation on the behaviors suggested in previous studies [41].

TABLE 1. Research Hypotheses

| Hypothetical structures of MOA variables | |
|--|--|
| H ₁ | Motivation factor includes the following indicators: a- Attitude (AT), b- Awareness of consequences (AC), c- Ascription of responsibility (AR) and d- Personal norms (PN). |
| H ₂ | Opportunity factor includes the following indicators: a- Subjective norms (SN), B- Descriptive norms (DN) and c- Support for organizational norms (ON). |
| H ₃ | The ability factor includes the following indicators: a- Perceived knowledge (PK), B) Actual knowledge (AK) and c) Perceived behavioral control (PBC). |
| H ₄ | Motivation factor has a positive and direct effect on information security behaviors. |
| H ₅ | Opportunity factor has a positive and direct effect on information security behaviors. |
| H ₆ | Ability factor has a positive and direct effect on information security behaviors. |
| H ₇ | Opportunity factor has a positive and direct effect on motivation. |
| H ₈ | Ability factor has a positive and direct effect on motivation. |

Based on the MOA model, the proposed conceptual model consists of three hidden factors of motivation, opportunity and ability as well as 10 variables. This model includes 8 hypotheses that were described earlier. The proposed conceptual model is shown in Figure 1. According to this model, opportunity and ability (each with 3 variables) play the role of independent factors and motivation (with 4 variables) plays the role of mediator, and behavior plays the role of dependent factor.

3. METHODOLOGY

3. 1. Samples and Data Collection In this study, a quantitative approach has been used to investigate the impact of MOA factors on behaviors consistent with human resources information security in organizations. The target population of this research is professors and staff from K. N. Toosi University of Technology in Tehran, who deal with students and university information and the Internet more than other staff. One of the reasons for choosing of this university as a statistical population is the lack of integration of university colleges in one place, and attention to human factors can play an effective role in information security of students and university documents.

This survey was conducted in November 2019 by distributing a paper questionnaire among a sample of 200 people, three quarters of whom were professors and staff of various faculties of the university and one third included the staff of the central building of the university. A total of 160 responses were collected. In the process of data pruning, responses with missing values in terms of information security behaviors were deleted. As a result, 141 responses were retained for review.

The final questionnaire consists of 7 items related to demographic characteristics and 33 items related to the conceptual model of the study (motivation, opportunity, ability, security behaviors). Most of these questions have been collected using previous studies related to the subject of research, and some of them have been slightly

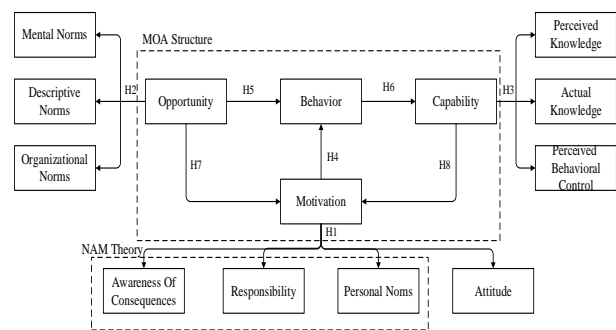


Figure 1. Conceptual model of the study

changed according to the conditions and culture of the community as well as the study environment to be tangible for the respondents. Responses were collected using a 5-point Likert scale with a minimum of 1 and a maximum of 5 and were analyzed by SPSS and LISREL software. Statistics on respondents' demographic characteristics are shown in Table 2.

4. DATA ANALYSIS

The analysis of research hypotheses is performed through second-order structural equation modeling (SEM), in which the structural model describes the relationship between latent variables [42], in which each second-order factor (i.e., motivation, opportunity, and ability) is a combination of several first-order factors (e.g., attitude, awareness of consequences, and personal norms). In this hierarchical structure, first-order factors can be considered as various indicators of second-order ones, and therefore help to understand which specific aspect (i.e., first-order factor) is involved in motivation, opportunity and ability.

TABLE 2. Demographic characteristics of the statistical population of the study

| Demographic info | Number | (%) | |
|---|--------------------|-----|----|
| Gender | Male | 70 | 49 |
| | Female | 71 | 50 |
| Marital status | Single | 29 | 20 |
| | Married | 112 | 80 |
| Education level | Diploma and lower | 4 | 2 |
| | Associate degree | 5 | 3 |
| | Master's degree | 44 | 32 |
| | Masters and above | 88 | 63 |
| Work experience | Under 5 years | 14 | 10 |
| | 5-10 years | 18 | 12 |
| | 11-15 years | 46 | 33 |
| | 16 years and older | 63 | 45 |
| Age | 20-30 years | 15 | 11 |
| | 31-40 years | 62 | 44 |
| | 41-50 years | 40 | 28 |
| | 51 years and older | 24 | 17 |
| English language literacy | Beginner | 22 | 16 |
| | Average | 79 | 56 |
| | Advanced | 40 | 28 |
| Level of experience in working with computer/ internet | Beginner | 7 | 5 |
| | Average | 78 | 55 |
| | Advanced | 56 | 40 |

According to Table 3, the average of all first-order factors is higher than the median. In addition, the values of skewness and kurtosis of the factors, which are a measure of the normality of the data, are in the range of -0.44 and -0.98.

To fit the measurement model, reliability and validity criteria must be investigated. Reliability of the measurement model is investigated by criteria such as Cronbach's alpha, composite reliability and factor loads. Validity is also two types, convergent validity and diverging validity. Convergent validity is investigated by criteria such as the average variance extracted and divergent and composite reliability with Fornell-Larcker test. The conceptual model fitting algorithm is in Figure 2.

According to Table 4, the average of all second-order factors is higher than the median. In addition, the values of skewness and kurtosis of the factors, which are a measure of the normality of the data, are in the range of -43.0 and -0.97. According to Briz-Ponce [10], the normality of data is confirmed in conditions where the values of skewness and kurtosis are in the range of 1 and -1, so, this condition is confirmed for first and second order factors.

4. 1. Validity and Reliability

Cronbach's alpha, factor loads and Combined reliability (CR) are the criteria for measuring reliability. Also, the average variance extracted (AVE) and CR were considered as criteria for convergent validity and Fornell-Larcker test for divergent validity. Second-order confirmatory factor analysis was performed to assess: (1) the convergent validity of each first-order factor and (2) whether each of the first-order factors, as assumed in H1, H2, and H3, is a significant portion of its second-order factor (Motivation, opportunity or ability). Factors with a factor load of less than 0.5 were excluded from the hypothetical model [9]. SPSS software was used to

TABLE 3. Descriptive statistics of first-order factors

| First-order factor | Mean | Standard deviation | Skewness | Kurtosis |
|--------------------|------|--------------------|----------|----------|
| AT | 3,54 | 1,22 | -0,69 | 0.99 |
| AC | 3,48 | 1,13 | -0,62 | 0.97 |
| AR | 3,52 | 1,23 | -0,61 | 0.98 |
| PN | 3,52 | 1,30 | -0,71 | 0.95 |
| DN | 3,19 | 0,83 | -0,59 | 0.96 |
| SN | 3,13 | 0,71 | -0,75 | -0,43 |
| ON | 3,10 | 0,73 | -0,50 | 0.96 |
| PK | 3,42 | 1,11 | -0,50 | 0.98 |
| AK | 3,40 | 1,20 | -0,54 | 0.97 |
| PBC | 3,29 | 1,04 | -0,44 | 0.96 |

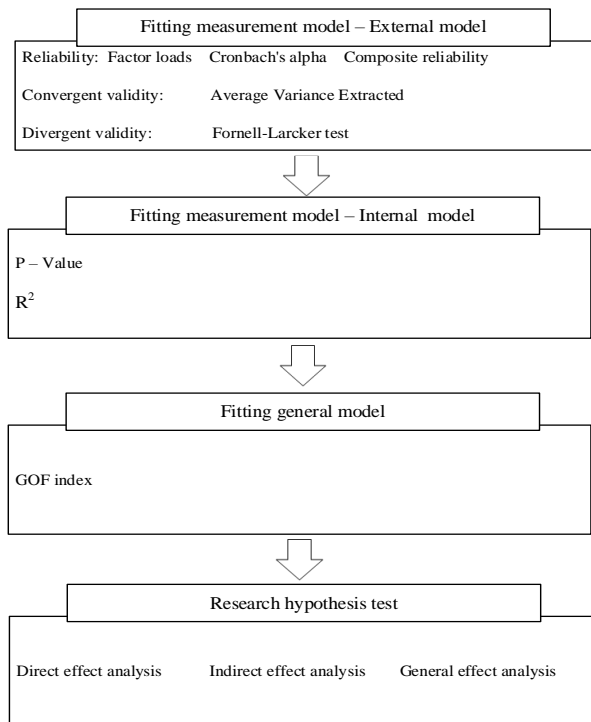


Figure 2. Conceptual model fitting algorithm

TABLE 4. Descriptive statistics of second-order factors

| Second-order factor | Mean | Standard deviation | Skewness | Kurtosis |
|---------------------|-------|--------------------|----------|----------|
| Motivation | 42.18 | 14.19 | 0.96 | -0.70 |
| Opportunity | 28.25 | 6.63 | 0.95 | -0.64 |
| Ability | 30.30 | 9.70 | 0.97 | -0.53 |
| Behavior | 10.82 | 3.33 | -0.46 | 0.97 |

calculate Cronbach's alpha, CR and AVE and the Laser software was used to calculate factor loads. The minimum acceptable value for Cronbach's alpha coefficient is 0.7 [25]. The third step in examining convergent reliability is to calculate the Composite reliability. The minimum accepted value for Composite reliability is also considered to be 0.7 [26]. According to

Fornell and Larcker [15], the AVE of any structure must be greater than 0.5. The results of convergent reliability and validity calculations are shown in Tables 5 to 9. As the results of convergent reliability and validity calculations show that the factor load of all items is more than 0.5 and Cronbach's alpha coefficient of all factors is higher than 0.7. Therefore, the reliability of the present study is supported. In the convergent validity test, for all first-order factors, AVE is higher than the suggested threshold (from 0.61 to 0.88) and CR is satisfactory (from 0.80 to 0.98), and AVE and CR are also acceptable for second-order factors (Table 9), which supports the convergent validity of the study. Divergent validity is also supported because the value of the AVE root of the latent variables in the major diameter of the matrix is greater than the value of the correlation between them in the lower and left cells of major diameter (according to Table 10). According to these results, it can be said that convergent reliability and validity have been confirmed.

Table 5 statistics of fit of hidden variable and survey items related to motivation factor, Table 6 statistics of fit of hidden variable and survey items related to opportunity factor, Table 7 statistics of fit of hidden variable and survey items related to ability factor, are available in appendix section.

As shown in the results of convergent reliability and validity calculations, according to Table 9, the factor load of all second-order factors are greater than 0.5 and the Cronbach's alpha coefficient of all factors is higher than 0.7. Therefore, the reliability of the present study is supported. For the second-order factors, AVE and CR are also acceptable in the convergent validity test, which supports the convergent validity of the study.

To calculate the Fornell-Larcker index, the value of the AVE root of the latent variables in the major diameter of the matrix must be greater than the correlation between those arranged in the lower and left cells of the original diameter [14]. In this study, the value of the AVE root of the hidden variables in the major diameter of the matrix is greater than the correlation value between them in the lower and left cells of the major diameter (Table 8).

TABLE 8. Statistics of fit of hidden variable and survey items related to behavior factor

| Hidden variables | Item | standard deviation SD | Factor load | AVE | Combined reliability | Cronbach's alpha |
|--------------------------------|---|-----------------------|-------------|------|----------------------|------------------|
| Information security behaviors | Because forgetting multiple passwords is probable, I use the same password for all my accounts. | 1.01 | 0.92 | 0.86 | 0.98 | 0.95 |
| | When someone sends me a link, I open it without making sure the link is valid. | 1.28 | 0.93 | | | |
| | I will create a backup of my important information. | 1.19 | 0.94 | | | |

TABLE 9. Statistics of fit of second-order factors

| Second-order factor | First-order factor | Factor load | AVE | Combined reliability | Cronbach's alpha |
|---------------------|--------------------|-------------|------|----------------------|------------------|
| Motivation | AT | 0.98 | 0.92 | 0.99 | 0.98 |
| | AC | 0.94 | | | |
| | AR | 0.95 | | | |
| Opportunity | PN | 0.97 | 0.89 | 0.98 | 0.96 |
| | DN | 0.97 | | | |
| | SN | 0.92 | | | |
| Ability | ON | 0.96 | 0.90 | 0.99 | 0.96 |
| | PK | 0.95 | | | |
| | AK | 0.97 | | | |
| | PBC | 0.91 | | | |

TABLE 10. Divergent validity by Fornell-Larcker test

| Factor | AT | AC | AR | PN | DN | SN | ON | PK | AK | PBC |
|--------|-------|-------|-------|-------|-------|-------|-------|-------|-------|------|
| AT | 0.90 | | | | | | | | | |
| AC | 0.788 | 0.91 | | | | | | | | |
| AR | 0.788 | 0.90 | 0.93 | | | | | | | |
| PN | 0.789 | 0.789 | 0.91 | 0.92 | | | | | | |
| DN | 0.788 | 0.785 | 0.786 | 0.787 | 0.99 | | | | | |
| SN | 0.785 | 0.783 | 0.784 | 0.785 | 0.787 | 0.98 | | | | |
| ON | 0.787 | 0.785 | 0.785 | 0.785 | 0.788 | 0.787 | 0.90 | | | |
| PK | 0.787 | 0.787 | 0.788 | 0.785 | 0.787 | 0.785 | 0.787 | 0.91 | | |
| AK | 0.788 | 0.786 | 0.789 | 0.787 | 0.788 | 0.786 | 0.789 | 0.90 | 0.94 | |
| PBC | 0.781 | 0.783 | 0.782 | 0.781 | 0.786 | 0.783 | 0.785 | 0.788 | 0.788 | 0.90 |

4. 2. Structural Model Analysis The internal model describes the relationship between the hidden variables. To evaluate the internal model, the path coefficient, t-statistic and coefficient R² (variance of each factor) must be calculated. In the present study, all the criteria required for structural model analysis have been calculated by SPSS software. Path coefficients represent the overlap level between the two hidden variables. In other words, the path coefficient indicates the existence of a linear causal relationship and the intensity and direction of this relationship between the two hidden variables. The path correlation coefficient is a number between +1 and -1. A value of zero means that there is no linear relationship between the two hidden variables. According to Table 11, the magnitude of the significance coefficients t for all relations in the model is greater than 1.96, which means that the path coefficient is accepted at the significance level of 95%. Also, since the value of p statistic for all available relations is less than 0.05, all hypotheses are confirmed.

TABLE 11. Hypotheses of the internal model

| Number | Hypotheses | Path correlation | T statistic | P value | Confirmed? |
|--------|--------------------------|------------------|-------------|---------|------------|
| 1 | Motivation → Behavior | 0.040 | 32.597 | 0.000 | yes |
| 2 | Opportunity → Behavior | 0.061 | 52.330 | 0.000 | yes |
| 3 | Ability → Behavior | 0.846 | 34.648 | 0.000 | yes |
| 4 | Opportunity → Motivation | 0.446 | 19.23 | 0.000 | yes |
| 5 | Ability → Motivation | 0.495 | 21.29 | 0.000 | yes |

The coefficient R² is a criterion used to correlate the measurements and the structural equation modeling and shows the effect of an independent variable on a dependent variable (Table 12). The higher the coefficient of determination related to the dependent variables of a model, the better the model fits. Three values of 0.25, 0.5 and 0.75 are considered as the criterion values for weak, medium and strong values of R² [14, 15].

5. DISCUSSION

In this study, which was based on the MOA model, the results confirm that awareness of consequences, ascription of responsibility, personal norms and attitudes play a role in creating the motivating factor. Subjective norms, descriptive norms, and organizational norms help create the opportunity factor. Perceived behavioral control, perceived knowledge, and actual knowledge play a role in creating the ability factor. It can also be concluded that ability, opportunity and motivation directly affect the information security behaviors of organizational human resources, where, the effect of ability is more than opportunity and that of opportunity more than motivation. Also, the two factors of opportunity and ability affect the behavior of organizational human resources indirectly and through the motivation mediatory factor. According to the results, the mediating effect of motivation in the relationship between the ability and behavior is less than

TABLE 12. Coefficients of determination of dependent variables

| Dependent variable | Coefficient of determination (R ²) |
|--------------------|--|
| Behavior | 0.883 |
| Motivation | 0.858 |

8%, which is ignorable. According to the VAF concept proposed by Zhao et al. [41], it can be inferred:

- Considering the coefficient of 0.079 as the total effect of the opportunity factor on the behavior factor, 23% of the total effect is indirect, going through the following path: opportunity → motivation → behavior ($0.079 \div 0.040 \times 0.446$).
- 77% of the total effect of opportunity factor on behavior is a direct effect, going through the path: opportunity → behavior ($0.079 \div 0.061$).
- Considering the coefficient of 0.866 as the total effect of the ability factor on the behavior factor, 3% of the total effect is indirect, going through the following path: ability → motivation → behavior ($0.866 \div 0.040 \times 0.495$).
- 97% of the total effect of ability factor on behavior is a direct, going through the following path: ability → behavior ($0.866 \div 0.846$).

Considering these values and the prominent effect of “ability” in human resource security behaviors, it can be concluded that holding the necessary training courses to enhance information level and employees' abilities for information security can motivate people to maintain security and also improve their security behaviors. In addition, creating organizational norms in the form of financial and social rewards for observing information security tips in the organization as well as creating a demanding culture among employees (for example, if your colleague does not pay attention to information security tips, ask him to reconsider his behavior), can be useful strategies to improve perceived employee opportunities, which in turn improves security motivation and behaviors. Organizational efforts can also focus on exerting beneficial normative influence in the organization to increase social norms. Conducting personality tests on employees can also help managers (especially human resources managers) to plan and implement appropriate strategies correspondent to personal differences in order to know the employees' subjective norms, personal norms and to some extent, their attitude and responsibility in order to maintain the security of the organization's information as much as possible.

5. 1. Research Limitations and Recommendations for Future Research

In carrying out any research project, obstacles and limitations emerge on the way. This study is no exception and therefore, we indicate the existing barriers and limitations. One of these limitations is the measurement tool used in this study, because in this study, a questionnaire was used to collect data, the inherent limitations of the questionnaire, such as superficial consideration of real events and scalability can prevent attaining real results and the respondents have encountered perceptual errors in answering the questions. Accordingly, new methods

can be used for data collection in future research. Also, in this study, a total of 141 questionnaires have been analyzed for data collection. Naturally, increasing the number of questionnaires and consequently increasing the number of available data can increase the consistency and validity of the results. It should also not be overlooked that the moderator variable was not used in this study. In general, the use of adjusting variables such as gender, age, work experience, etc. could provide more comprehensive and accurate results. With the variables defined in each of the MOA factors, this framework can be used as a diagnostic tool to identify the limiting factors of information security behaviors in a particular organization and can become the basis for future studies to identify the right strategies in order to maintain information security and thus help decision makers to create more efficient and targeted executive programs to promote behavior change.

6. REFERENCES

1. Hoffmann R., Napiórkowski J., Protasowicki T., Jerzy Stanik, “Measurement Models of Information Security Based on the Principles and Practices for Risk-Based Approach”, 1st International Conference on Optimization-Driven Architectural Design, (2020), <https://doi.org/10.1016/j.promfg.2020.02.244>.
2. Zare M. R., Aghaie A., Samimi Y., A. Hadad Asl, “A Novel Excellence Model of the Information and Communications Technology Industry: Case Study on Telecommunications Backbone Network of Iran”, *International Journal of Engineering, Transactions A: Basics*, Vol. 33, No. 10, (2020) 2016-2029, <https://doi.org/10.5829/ije.2020.33.10a.20>.
3. Roberts D. J., An Analysis of employee information security policy compliance behaviour: A generic qualitative inquiry, Capella University, 2021.
4. Jeyanthi N., Shabeeb H., M. Saleem A. Durai, Thandeewaran R., “Reputation Based Service for Cloud User Environment”, *International Journal of Engineering, Transactions B: Applications*, Vol. 27, No. 8, (2014), 1179-1184, <https://doi.org/10.5829/idosi.ije.2014.27.08b.03>.
5. Kwesi Hughes-Lartey, Meng Li, Francis E. Botchey, Zhen, “Human factor, a critical weak point in the information security of an organization's Internet of things”, *Heliyon*, (2021), <https://doi.org/10.1016/j.heliyon.2021.e06522>.
6. Karjalainen M., Siponen M., Sarker S., “Toward a stage theory of the development of employees' information security behaviour”, *Computers & Security*, (2020) <https://doi.org/10.1016/j.cose.2020.101782>.
7. Bagheri Z., Safaie N., Strategic planning of human resources based on BSC model, *Quarterly Journal of Human Resource Management Research*, Imam Hossein University, 8th year, consecutive issue 25, 159-181. (2016).
8. Azjen, I. The theory of Planned Behavior. *Organizational Behavior and Human Decision Processes*, 50(2), 179–211, (1991). [https://doi.org/10.1016/0749-5978\(91\)90020-T](https://doi.org/10.1016/0749-5978(91)90020-T).
9. Bagozzi, R. P., & Yi, Y. “Specification, evaluation, and interpretation of structural equation models” *Journal of the Academy of Marketing Science*, 40, No. 1, 8-34, (2012), <https://doi.org/10.1007/s11747-011-0278-x>.
10. Briz-Ponce, L., Pereira, A., Carvalho, L., Juanes-Méndez, J. A., & García-Peñalvo, F. J. Learning with mobile technologies—Students' behavior. *Computers in Human Behavior*, Vol. 72, 612-620, (2017). <https://doi.org/10.1016/j.chb.2016.05.027>.

11. Carlton M., Levy Y., "Expert assessment of the top platform independent cybersecurity skills for non-IT professionals." *SoutheastCon*, IEEE. (2015), <https://doi.org/10.1109/SECON.2015.7132932>.
12. Evans, M. "Evaluating information security core human error causes (IS-CHEC) technique in public sector and comparison with the private sector." *International Journal of Medical Informatics*, Vol. 127 109-119, (2019), <https://doi.org/10.1016/j.ijmedinf.2019.04.019>.
13. Hamidi, H., Vafaei, A. and Monadjemi, S.A. (2012). Analysis and Evaluation of a New Algorithm Based Fault Tolerance for Computing Systems. *International Journal of Grid and High Performance Computing (IJGHPC)*, Vol. 4, No. 1, 37-51. doi:10.4018/jghpc.2012010103
14. Schwartz, Shalom H., "Normative influences on altruism." *Advances in Experimental Social Psychology*, Vol. 10. Academic Press, 221-279, (1977), [https://doi.org/10.1016/S0065-2601\(08\)60358-5](https://doi.org/10.1016/S0065-2601(08)60358-5).
15. Fornell, C., & Larcker, D. F. Evaluating structural equation models with unobservable variables and measurement error. *Journal of Marketing Research*, 18, (1), 39-50, (1981), <https://doi.org/10.1177/002224378101800104>.
16. Gao, L., "Application of the extended theory of planned behavior to understand individual's energy saving behavior in workplaces." *Resources, Conservation and Recycling*, 127, 107-113, (2017) <https://doi.org/10.1016/j.resconrec.2017.08.030>.
17. Gandel, Lloyd's CEO: Cyber-attacks cost companies 400 billion every year, (2015). <http://fortune.com/2015/01/23/cyber-attack-insurancelloyds/>(accessed 03 October 2018).
18. Gratian, M., Bandi S., Cukier M., Dykstra J., Ginther A., "Correlating human traits and cyber security behavior intentions." *Computers & Security*, 73, 345-358, (2018) <https://doi.org/10.1016/j.cose.2017.11.015>.
19. Hair, J. F., Ringle, C. M., & Sarstedt, MPLS-SEM, "Indeed a silver bullet". *Journal of Marketing theory and Practice*, Vol. 19, No. 2, (2011), 139-152, <https://doi.org/10.2753/MTP1069-6679190202>.
20. Altabash K., Happaa b., "Insider-threat detection using gaussian mixture models and sensitivity profiles." *Computers & Security* 77, 838-859., (2018) <https://doi.org/10.1016/j.cose.2018.03.006>.
21. Ifinedo, P., "Understanding information systems security policy compliance: An integration of the theory of planned behavior and the protection motivation theory." *Computers & Security* 31.1.83-95, (2012), <https://doi.org/10.1016/j.cose.2011.10.0076>.
22. Kuru, Damla, and Sema Bayraktar, "The effect of cyber-risk insurance to social welfare." *Journal of Financial Crime* 24.2 ,329-346, (2017), <https://doi.org/10.1108/JFC-05-2016-0035>.
23. Xu, X., Chen C., Menassa C., "Understanding energy-saving behaviors in the American workplace: A unified theory of motivation, opportunity, and ability." *Energy Research & Social Science* 51, 198-209, (2019), <https://doi.org/10.1016/j.erss.2019.01.020>.
24. Malekinezhad, F., Bin H. L. Investigation into University Students Restoration Experience: The Effects of Perceived Sensory Dimension and Perceived Restrictiveness, (2017), <https://doi.org/doi:10.20944/preprints201708.0085>.
25. Michie S., Stralen, M., West, R., "The behaviour change wheel: a new method for characterising and designing behaviour change interventions." *Implementation Science* 6.1, 42, (2011), <https://doi.org/10.1186/1748-5908-6-42>.
26. Nunnally, J., *Psychometric Theory*. McGraw-Hill, Retrieved from. 1978.
27. Osterhus, Thomas L., "Pro-social consumer influence strategies: when and how do they work? " *Journal of Marketing* 61.4,16-29, (1997), <https://doi.org/10.1177/002224299706100402>.
28. Hamidi, H., Vafaei, A., and Monadjemi, A. H., "Algorithm Based Fault Tolerant and Check Pointing for High Performance Computing Systems", *Journal of Applied Sciences*, vol. 9, no. 22, 3947-3956, 2009. doi:10.3923/jas.2009.3947.3956.
29. Hamidi, H., & Mohammadi, K. (2006). Modeling Fault Tolerant and Secure Mobile Agent Execution in Distributed Systems. *International Journal of Intelligent Information Technologies (IJIT)*, 2(1), 21-36. doi:10.4018/jiit.2006010102
30. Rezaei, R., "Drivers of farmers' intention to use integrated pest management: Integrating theory of planned behavior and norm activation model." *Journal of Environmental Management*, Vol. 236, 328-339, (2019) <https://doi.org/10.1016/j.jenvman.2019.01.097>.
31. Sohrabi Safaab N., Maplea C., Watson T., Von Solms B., (2018), "Motivation and opportunity-based model to reduce information security insider threats in organisations." *Journal of Information Security and Applications*, Vol. 40, 247-257, (2018), <https://doi.org/10.1016/j.jisa.2017.11.001>.
32. Schwartz, Shalom H., "Normative explanations of helping behavior: A critique, proposal, and empirical test." *Journal of Experimental Social Psychology* 9.4, 349-364, (1973), [https://doi.org/10.1016/0022-1031\(73\)90071-1](https://doi.org/10.1016/0022-1031(73)90071-1).
33. Schmidt, K., "Predicting the consumption of expired food by an extended Theory of Planned Behavior" *Food Quality and Preference*, 78, 103746, (2019), <https://doi.org/10.1016/j.foodqual.2019.103746>.
34. Shan, J., Jingmei, L., and Zhihua, X., "Estimating ecological damage caused by green tides in the Yellow Sea: A choice experiment approach incorporating extended theory of planned behavior" *Ocean & Coastal Management*, 181, 104901, (2019), <https://doi.org/10.1016/j.ocecoaman.2019.104901>.
35. Hamidi, H., Vafaei, A. and Monadjemi, S.A., Analysis and design of an ABFT and parity-checking technique in high performance computing SYSTEMS. *Journal of Circuits, Systems and Computers*, Vol. 21, No. 03, 1250017 (2012) , <https://doi.org/10.1142/S021812661250017X>
36. Sohrabi Safa N., Solms R., Fitcher, L., " Human aspects of information security in organisations". *Computer Fraud & Security* 2, 15-8, (2016), [https://doi.org/10.1016/S1361-3723\(16\)30017-3](https://doi.org/10.1016/S1361-3723(16)30017-3).
37. Thøgersen, J., "Understanding of consumer behaviour as a prerequisite for environmental protection." *Journal of Consumer Policy* 18, No. 4, 345-385, (1995), <https://doi.org/10.1007/BF01024160>.
38. Wilson, C., and Melissa R., "Insights from psychology about the design and implementation of energy interventions using the Behaviour Change Wheel." *Energy Research & Social Science*, 19, 177-191, (2016), <https://doi.org/10.1016/j.erss.2016.06.015>.
39. Wolske, K. S., Paul, C., and Thomas, D., "Explaining interest in adopting residential solar photovoltaic systems in the United States: Toward an integration of behavioral theories" *Energy Research & Social Science*, 25, 134-151, (2017).
40. Yazdanmehr, A., and Jingguo W. "Employees' information security policy compliance: A norm activation perspective." *Decision Support Systems*, 92, 36-46, (2016), <https://doi.org/10.1016/j.erss.2016.12.023>.
41. Zhao, X., Lynch Jr, J. G., & Chen, Q., "Reconsidering Baron and Kenny: Myths and truths about mediation analysis". *Journal of Consumer Research*, 37(2), 197-206, (2010) <https://doi.org/10.1086/651257>.
42. Torabi, A., Hamidi, H., Safaie, N., "Effect of Sensory Experience on Customer Word-of-mouth Intention, Considering the Roles of Customer Emotions, Satisfaction, and Loyalty", *International Journal of Engineering, Transactions C: Aspects*, Vol. 34, No. 3, (2021), 682-699, <https://doi.org/10.5829/ije.2021.34.03c.13>.

7. APPENDIX

TABLE 5. Statistics of fit of hidden variable and survey items related to motivation factor

| Hidden variables | Item | Standard deviation SD | Factor load | AVE | Combined reliability | Cronbach's alpha |
|-----------------------------------|---|-----------------------|-------------|------|----------------------|------------------|
| Attitude (AT) | Adherence to workplace information security tips is essential. | 1,20 | 0,90 | 0,82 | 0,96 | 0,93 |
| | Holding information security training courses for the organization's employees is a waste of time and money. | 1,35 | 0,92 | | | |
| Awareness of Consequences (AC) | Accomplishing a project in less time and with lower information security levels is better than accomplishment of the project in more time but with higher information security. | 1,34 | 0,90 | 0,83 | 0,96 | 0,93 |
| | Observance of workplace information security tips will have positive consequences for the organization. | 1,16 | 0,92 | | | |
| | By observing the information security of the workplace, I will play a beneficial role for my organization. | 1,20 | 0,91 | | | |
| Ascription of Responsibility (AR) | Non-observance of workplace information security tips will have adverse consequences for the organization's customers. | 1,24 | 0,90 | 0,86 | 0,97 | 0,95 |
| | Because my involvement in information security is ignored by the organization, I do not feel responsible for complying with my workplace security tips. | 1,38 | 0,95 | | | |
| | The responsibility for information security of my workplace lies with the organization itself, not me. | 1,32 | 0,94 | | | |
| Personal norms (PN) | I feel responsible for adhering to workplace information security tips. | 1,16 | 0,89 | 0,85 | 0,97 | 0,95 |
| | I feel guilty when I do not follow the information security tips in performing my duties. | 1,34 | 0,91 | | | |
| | No matter how others behave, I feel morally obligated to follow the information security tips of my workplace. | 1,41 | 0,94 | | | |
| | I feel good when I follow the information security tips. | 1,35 | 0,92 | | | |

TABLE 6. Statistics of fit of hidden variable and survey items related to opportunity factor

| Hidden variables | Item | Standard deviation SD | Factor load | AVE | Combined reliability | Cronbach's alpha |
|---------------------------|--|-----------------------|-------------|------|----------------------|------------------|
| Descriptive norms (DN) | My colleagues are concerned about workplace security vulnerabilities. | 0,92 | 0,93 | 0.80 | 0.94 | 0.92 |
| | My colleagues pay attention to information security in the performance of their duties. | 0,94 | 0,94 | | | |
| | My colleagues work to ensure the safety of workplace information. | 0,84 | 0,79 | | | |
| Subjective norms (SN) | My colleagues expect me to lock or shut down my system when it leaves. | 0,82 | 0,78 | 0.61 | 0.80 | 0.82 |
| | My colleagues expect me to be aware of the presence of strangers when giving confidential information. | 0,83 | 0,79 | | | |
| | My colleagues expect me not to connect my personal communication devices such as cell phones, flash memories, etc. to workplace systems. | 0,83 | 0,78 | | | |
| Organizational norms (ON) | My organization rewards its employees (in various ways) for adhering to information security tips. | 0,84 | 0,78 | 0.64 | 0.84 | 0.85 |
| | Observing information security tips in my workplace is defined as an organizational culture and value. | 0,83 | 0,81 | | | |
| | The leadership and management of my organization strive to provide in-house training courses to increase employee awareness of information security. | 0,85 | 0,82 | | | |

TABLE 7. Statistics of fit of hidden variable and survey items related to ability factor

| Hidden variables | Item | Standard deviation SD | Factor load | AVE | Combined reliability | Cronbach's alpha |
|------------------------------------|---|-----------------------|-------------|------|----------------------|------------------|
| Perceived Knowledge (PK) | I'm constantly updating my knowledge of cyberattack malware and data theft methods. | ۱,۰۲ | ۰,۹۰ | | | |
| | I know how to use the firewall and update my system security software. | ۱,۱۸ | ۰,۸۹ | ۰,۸۳ | ۰,۹۶ | ۰,۹۳ |
| | I how to make the deleted files irrecoverable. | ۱,۳۲ | ۰,۹۵ | | | |
| | The website address that starts with http guarantees information security. | ۱,۴۳ | ۰,۹۲ | | | |
| Actual Knowledge (AK) | I am familiar with more than three of the following concepts. -Phishing attacks -Social engineering attacks - DDOS attacks -Cloud database -Multi-factor authentication | ۰,۹۷ | ۰,۹۹ | ۰,۸۸ | ۰,۹۸ | ۰,۹۴ |
| | Before downloading a file, it can be checked to see if it's a virus. | ۱,۳۴ | ۰,۹۱ | | | |
| Perceived Behavioral Control (PBC) | I'm sure I can follow my workplace information security tips if I want to. | ۰,۹۸ | ۰,۸۵ | | | |
| | It's entirely up to me whether I follow my job security tips. | ۱,۰۹ | ۰,۸۷ | ۰,۸۱ | ۰,۹۴ | ۰,۹۲ |
| | Applying information security methods in my workplace is completely under my control. | 1.27 | ۰,۹۷ | | | |

Persian Abstract

چکیده

امنیت اطلاعات یک مسأله حیاتی است که امروزه سازمان‌ها در سراسر دنیا با آن روبرو هستند. در حال حاضر سیل عظیمی از حملات سایبری و تهدیدات امنیتی ناشی از سهل‌انگاری عوامل انسانی اتفاق می‌افتد که این امر اهمیت رفتار منابع انسانی در سازمان را دوچندان می‌کند. پژوهش حاضر چارچوبی یکپارچه از انگیزه فرصت-توانایی (MOA) را ارائه می‌دهد که شامل عوامل روانشناختی اجتماعی از مدل NAM و نظریه TPB برای بررسی متغیرهای تعیین‌کننده رفتارهای امنیتی در یکی از دانشگاه‌های معتبر تهران است. برای این منظور اطلاعات با توزیع ۱۴۱ پرسشنامه بین کارکنان این دانشگاه، جمع‌آوری شده و مورد تحلیل قرار گرفته است. فرضیه‌های تحقیق، از روش مدل‌سازی معادلات ساختاری (SEM) و با استفاده از نرم‌افزار SPSS و Lisrel مورد بررسی و آزمون قرار گرفته است. نتایج حاصله نشان می‌دهد که توانایی بیشترین تأثیر را در رفتارهای امنیت اطلاعات دارد و به دنبال آن فرصت و انگیزه، به ترتیب تأثیر مستقیم و معناداری بر رفتار دارند. علاوه بر این، انگیزه، میانجی‌گر تأثیر فرصت و توانایی است. در انتها پیشنهادهایی برای طراحان استراتژی‌های مؤثر امنیت اطلاعات بر اساس عوامل محدودکننده رفتار منابع انسانی در سازمان ارائه گردیده است.



Effect of Wetting Progress on the Potential Collapse of Gypseous Sand using Modified Oedometer

M. J. Abraham, M. S. Mahmood*

Civil Engineering Department, University of Kufa, Al-Najaf, Iraq

PAPER INFO

Paper history:

Received 03 June 2021

Received in revised form 13 September 2021

Accepted 23 September 2021

Keywords:

Unsaturated Tests

Gypseous Soils

Matric Suctions

Najaf City

Sandy Soils

ABSTRACT

Gypsum is a soluble material, and it is one of the problematic components in the soil in the west of Iraq. Al-Najaf is one of the governorates in Iraq which suffers from the gypsum content in different levels. The soil of the city is mainly sand-sized particles bonded by different percentages of gypsum. The main problem of this component is the dissolution upon the wetting process in unsaturated conditions. This paper investigates the effect of decreasing the matric suction (wetting) on soil deformation under a specific stress level. A modified Oedometer setup is used to perform the tests, including the application of air and water pressures up to achieve the specific matric suctions. The investigation includes three matric suctions of (50, 20, and 0 kPa) and each under three net normal stresses of 221 kPa, 442 kPa and 885 kPa respectively. The soil specimens are remolded to 95% of the maximum dry density from the proctor test. The results revealed that the highest value of collapse potential (CP) is under the stress of 221kPa. The greatest part of the CP is achieved before the saturation of the soil. This issue must be considered in the analysis and design of the foundation in unsaturated gypseous sandy soils as an improvement issue.

doi: 10.5829/ije.2021.34.12c.08

NOMENCLATURE

| | | | |
|-----|----------------------------------|--------------|------------------------------------|
| Cu | Soil water characteristics curve | USCS | Unified soil classification system |
| Cc | Initial void ratio | Sp | Sand poorly-graded |
| Wn | Natural moisture content | ρ_{dry} | dry density |
| Ua | Pore air pressure | θ | Volumetric water content |
| Uw | Pore water pressure | Gs | Specific gravity |
| owc | Optimum water content | Sm | Matric suction |

1. INTRODUCTION

Al-Najaf city is an important city in Iraq due to its religious value, and there are many preserved and architectural heritage buildings which may be faced by the risk of conservation. The city soil consists of more than 70% of sand to a depth of 14m with gypsum content varied from 10 to 30% in the upper 2m depth [1, 2]. The spatial arrangement of sand, silt and clay grains, pore geometry, size distribution and network connectivity allows both capillary condensation and effective capillary transport of water [3]. Granular materials have a very low air-entry value. Besides, capillary forces

induced by suction increase the inter-particle stresses resulted in a decrease in void ratio and increase of dry unit weight [4]. Metastable characteristics of soils due to high porosity and kind of cementation present a temporally unstable structure when undergoing an increase of wetting and/or variation of the stress state [5].

Gypseous soil is collapsible soil that causes problems to buildings and structures constructed on them due to a significant decrease in the shear strength as they are exposed to wetting [6, 7]. This collapse depends on many factors, such as the wetting process [8-11], higher gypsum content, void ratio, permeability [12], initial degree of saturation [13, 14] and soil time-based wetting

*Corresponding Author Institutional Email:
mohammedsh.alshakarchi@uokufa.edu.iq (M. S. Mahmood)

prior loading [15-17]. Gypseous soils experience numerous changes in their physical and mechanical characteristics due to their exposure to continuous mass loss [18]. The soils' bearing capacity is decreased by about 50% due to the soaking process [19]. The shear strength of the soil can be improved by advancing the soaking time (long term) before shearing [20, 21]. The settlement of the gypseous soils is increased and continued relating to the increase of the gypsum content due to wetting [17]. The shape and dimensions of remolded soil specimens affect the reliability of the deformation results, and the Oedometer cell (cylindrical) gave a clear trend of results compared to other specimen shapes (rectangular) [22].

The unsaturated state always presents in collapsible soils where large collapse occurs with a decrease in the matric suction ($u_a - u_w$) [18]. During wetting in the sand, a sudden reduction in volume occurs, as observed by means of granulometry, porosimetry, permeability, optical and ESEM-EDS microscopy, thermogravimetry and XR diffractometry, electric conductivity, and ionic chromatography [19]. Unsaturated soil changes its volume when the magnitude of the " $u_a - u_w$ " or the net normal stress changes, and this leads to the occurrence of the phenomenon of collapse [23, 24]. Richards' equation is a nonlinear constitutive relation that described the water flow in an unsaturated porous medium [25]. The bearing capacity increased nonlinearly from 2.55 to 3.95 times as the suction increased [26]. The more increase of the nano-clay to the gypseous soil sample, the more decrease in collapse potential [27].

This paper investigates the effect of matric suction on the deformation of sandy soil with high gypsum content in Al-Najaf city, Iraq. This investigation is performed under different net normal stresses to represent the case of wetting progression under a certain construction load. The investigation is done using a modified Oedometer cell which controls the air and water pressures.

2. MATERIALS, TOOLS AND METHODOLOGY

The tests are performed on a soil sample from Al-Najaf city, Iraq. The sample was disturbed and collected in a plastic bag to maintain the natural water content. The soil sample is mainly sand. Table 1 summarizes the main soil identification properties and classification.

The natural water content is low (3%), and the soil may act as a dry behavior. The low G_s is related to the high gypsum content (29%), as to be stated in the literature. The higher dry density in the field (1.829 gm/cm³) with lower water content may be attributed to the bonding condition by gypsum material. Figures 1 and 2 illustrate the grain size distribution and standard Proctor tests results.

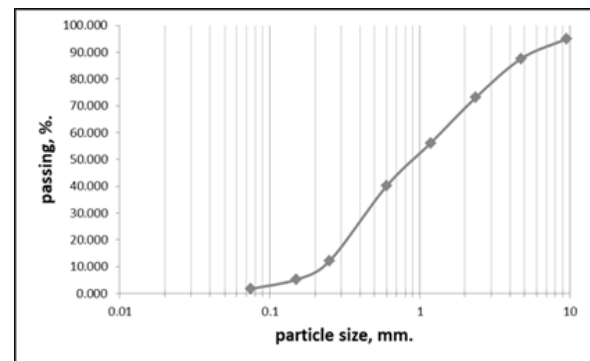


Figure 1. The particles size distribution of the soil sample

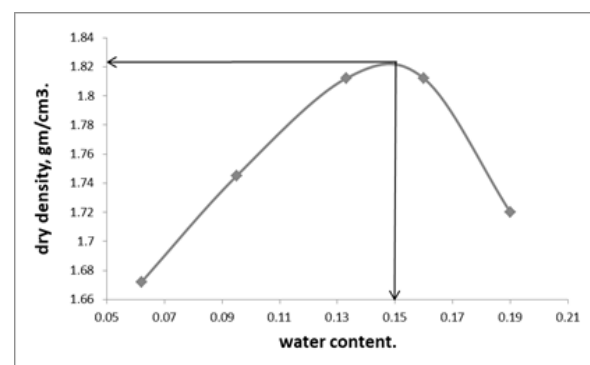


Figure 2. The results of standard Proctor test.

TABLE 1. The results of soil sample identification and classification tests..

| Test name | Specification | Value |
|--|---------------|----------------|
| Sand, % | ASTM D422 | 86% |
| Fine, % | ASTM D422 | 1.74% |
| D ₁₀ , D ₃₀ and D ₆₀ , mm | ASTM D422 | 0.22,0.47,1.45 |
| Cu | ASTM D422 | 6.6 |
| Cc | ASTM D422 | 0.703 |
| USCS | ASTM D422 | SP |
| G _s | ASTM D854 | 2.38 |
| Gypsum content, % | ASTM C25-99 | 29 |
| W _n , % | ASTM D2216 | 3 |
| O.W.C., % | ASTM D698 | 15 |
| ρ_{dry} , gm/cm ³ | ASTM D698 | 1.825 |

3. TOOLS AND EQUIPMENT

Figure 3 represents the scheme of the equipment and tools that have been used in the tests. The modified Oedometer is divided into three main categories. First, the modified cell, second, the control board (system of

the pressure application) and third, the data logger. The following paragraphs illustrate the details of each part:

3. 1. Modified Oedometer Cell A modified Oedometer cell was adopted to apply a specific matric suction in unsaturated testing (wetting process) by controlled application of air and water pressures. The modified Oedometer consists of a top cap, a grooved base plate, a High Air Entry ceramic disc (HAE), an inner cell and an outer cell. The 5 cm diameter HAE disc is installed on the base plate (by screws), and the grooves in the base plate are acting as canals to drain the air bubbles out through the flush valve before the work begins. The pore air pressure (u_a) is controlled and applied through the top cap, while the pore water pressure (u_w) is exerted through the HAE ceramic disc and an O-ring (outer ring) to avoid water leakage. The soil specimen is remolded to the specific density in the inner cell. Plate 1 illustrates the final setup of the modified oedometer test.

3. 2. Control Board Plate 2 shows the control board through which the test is operated. The control board consists of a compressor with a pressure capacity of 11 bar (1100 kPa) to control the whole system, a cylindrical container is filled with water to use in the application of water pressure before the start of the test, non-stretching tubes of 6 cm in diameter, regulators that

can regulate the pressure up to 30 bar, a ruler to measure the change in the water volume and sensors connected to a data logger to read the specific pressures. For the safety of the control board system, another regulator is connected to the compressor to maintain the pressure within suitable air pressure (3 bar) to the system.

3. 3. Datalogger and Software Plate 3 illustrates the data logger, which consists of eight channels that enable to perform more than one test. The data logger is connected to a computer and to the control board by sensors to read the applied water and air pressures. A linear variable differential transformer (LVDT), 0.01 mm, to calculate the axial vertical displacement of the specimen throughout the test. The software is a program that is installed on the computer, through which the readings of the settlement, the air and water pressure are recorded per second or even milliseconds. The results are also recorded on the excel sheet.

4. METHODOLOGY

For analysis, three soil specimens were prepared and remolded into an Oedometer cell of 19.38 mm in height

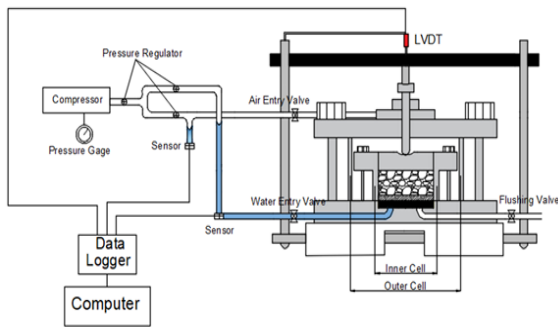


Figure 3. The scheme of the used tools and equipment.

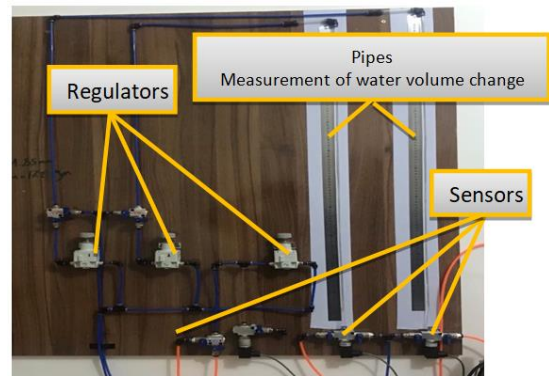


Plate 2. The control board

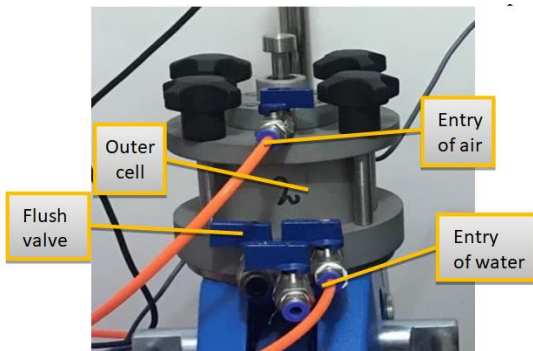


Plate 1. The modified Oedometer cell.

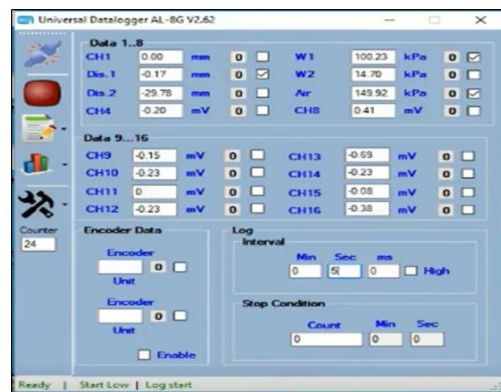


Plate 3. Setup of the computer software

and 50.31 mm in diameter, where the soil specimen was stacked in four layers, each layer having a height of 4.85 to achieve the required density. The dry density is 95% of the maximum dry density from the proctor test with 3% by weight water content.

The initial volumetric water content is around 2%, and concerning the soil water characteristics curve (SWCC) of the selected site, the initial matric suction (S_m) is 50kPa. The initial matric suction of 50kPa is selected depending on the natural water content of the soil sample and using the soil water characteristics curve (SWCC) [1].

A 1 bar (max difference between air and water pressure is 100 kPa) HAE ceramic disc was selected based on the natural water content that suited the 50 kPa matric suction (as initial matric suction) from the SWCCs, then, the matric suction is decreased up to saturation condition (zero matric suction). Three matric suction values (S_m) were selected to perform the tests, initial (50kPa), intermediate (20kPa) and zero matric suction (saturated). The change in matric suction is performed by maintaining the pore air pressure ($u_a=150$ kPa) and increase the pore water pressure ($u_w=100, 130$ and 150 kPa). Each of the three specimens initially was subjected to the initial matric suction ($S_m=50$ kPa), then a gradual net normal stress was applied (55, 111, 221, ... kPa) until reaching the specific stress level, then a change in matric suction is applied (decreasing). These stress levels are selected to draw the e - $\log \sigma$ within the below and upper designed bearing capacity limit of the site soil. Table 2 illustrates the tests program.

5. RESULTS AND DISCUSSION

5.1. Effect of Matric Suction Figures 4, 5 and 6 show the settlement in terms of void ratio versus log net

normal stress for different matric suctions (50, 20, 0 kPa). Under all the investigated net normal stresses, there is a clear decrease in the void ratio due to the wetting process at matric suction of 20kPa, while this decrease is smaller at matric suction of 0kPa (saturation). This phenomenon may be caused by first; the potential settlement is completely achieved due to the stress level and

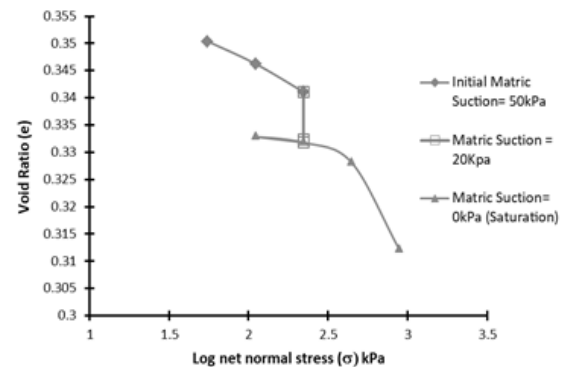


Figure 4. The void ratio versus the log net normal stress for different matric suction under a stress level of 221 kPa.

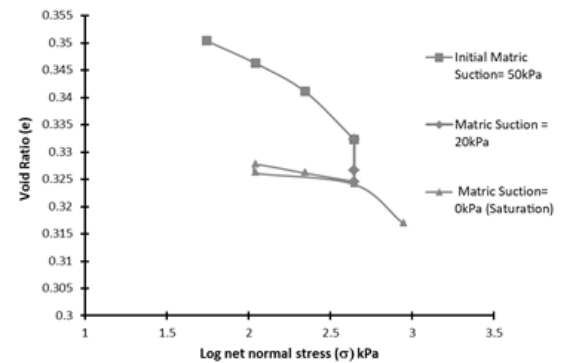


Figure 5. The void ratio versus log net normal stress for different matric suction under stress level of 442 kPa.

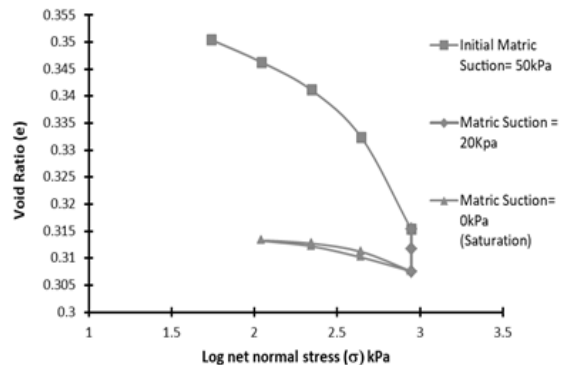


Figure 6. The void ratio versus log net normal stress for different matric suction under stress level of 885 kPa.

TABLE 2. Tests program

| Sm, kPa. | Net Normal Stress, kPa | | |
|----------|------------------------|-----------------------|----------------------------|
| | Wetting at 221 kPa | Wetting at 442 kPa | Wetting at 885 kPa |
| 50 | 55, 111 then 221 | 55, 111, 221 then 442 | 55, 111, 221, 442 then 885 |
| 20 | 221 | 442 | 885 |
| 0 | 221 | 442 | 885 |
| 0 | 111* | 221* | 442* |
| 0 | 221** | 111* | 221* |
| 0 | 442 | 221** | 111* |
| 0 | 885 | 442** | 221** |
| 0 | | 885 | 442** |
| 0 | | | 885** |

* unloading stage

** reloading stage

dissolution of the gypsum, or, second, the lack of time, whereas the specimen needed a longer time to reach the matric suction of 20kPa than the 0kPa.

Table 3 displays the collapse potential (CP) for each level of the net normal stress and the matric suction, according to Jennings & Knight modified method [18, 28]. Obviously, the highest CP (0.677) is under the net normal stress of 221 kPa, and the highest part (0.639) of the CP is due to wetting progress at matric suction of 20 kPa. With increasing the net normal stress, the CP is decreased at 20 kPa of matric suction and increased in saturation, and this can be explained due to the effect of loading and gypsum dissolution interaction. This certifies that the stress level of 200 kPa is an effective level to evaluate the soil collapse, as indicated in the Jennings & Knight modified method. All values of CP are within the "no problem" category according to the classification of severity by Jennings & Knight modified method, and these values are within collapse degree of "slight" according to ASTM D5333. These results may be attributed to the high initial density of the specimen (95% of the maximum dry density).

5. 2. Effect of Loading To investigate the effect of net normal stress level on the behavior of the soil specimen, two other specimens prepared from the same sample are subjected to other levels of stress, 442 kPa and 885 kPa. Figures 5 and 6 show the results under the stress levels of 442 kPa and 885 kPa, respectively.

With higher initial settlement (initial $S_m=50$ kPa), the trends of the deformation versus time are close to that under net stress of 221 kPa. With an initial higher stress level, the effect of the wetting process is low. The settlement ratio increases with $S_m=20$ kPa is 1.1404 under the stress of 442 kPa, while the settlement ratio increase is 1.0629 under the stress of 885kPa.

In higher stress levels, there is an increase in the time required to achieve both the specific matric suction and the total settlement, and this may be attributed to the restriction of the stress on the water volume change in the soil voids. The settlement ratio increases with $S_m=0$ kPa is 1.0448 under the stress of 442 kPa, while the settlement ratio increase is 1.0676 under the stress of 885 kPa.

TABLE 3. The Collapse potential under different net normal stresses and matric suction.

| Net normal stress, kPa | Collapse potential (CP) | | |
|---------------------------|-------------------------|----------|-------|
| | $\Psi=20$ | $\Psi=0$ | Total |
| 221 | 0.639 | 0.038 | 0.677 |
| 442 | 0.413 | 0.150 | 0.564 |
| 885 | 0.263 | 0.301 | 0.564 |

6. CONCLUSIONS

The recent paper investigates the effect of wetting progression due to different matric suction (50, 20 and 0kPa) in unsaturated gypseous sand using a modified Oedometer. This investigation is performed under three different levels of net normal stresses (221, 442 and 885 kPa). From the current investigation, the following points can be concluded:

- With decreasing in the matric suction (wetting), there is an increase in soil settlement under the different net normal stress levels.
- From the investigation, the net normal stress level of 221 kPa is dominated in the calculation of collapse potential (CP), where the related CP is the highest during wetting advancement in the unsaturated soils.
- The main part of the collapse is before the saturation (matric suction = 0 kPa) in unsaturated soils, which is the most important issue to be considered in the analysis and design of foundations in unsaturated gypseous sandy soils.
- It is recommended to investigate the effect of different stress levels, matric suction, and initial soil properties on the stability of the structures.

7. REFERENCES

1. Al-Shakerchy, M.S., "Geotechnical properties of al najaf city soil with emphasis on the infiltration and strength characteristics", (2007),
2. Al-Saoudi, N.K. and Al-Shakerchy, M.S.M., "Statistical analysis of some geotechnical properties of najaf city", in Proceedings of International Geotechnical Conference. Vol. 3, (2010), 1173-1180.
3. Scaffaro, R., Lopresti, F., Botta, L., Rigogliuso, S. and Ghersi, G., "Integration of pcl and pla in a monolithic porous scaffold for interface tissue engineering", *Journal of the Mechanical Behavior of Biomedical Materials*, Vol. 63, (2016), 303-313, doi: <https://doi.org/10.1016/j.jmbbm.2016.06.021>
4. Chekired, M., "A modified oedometer apparatus for experimentally obtaining the soil-water retention curve", Proceedings of: Geovancouver Conference, (2016).
5. Ruge, J., Cunha, R. and Mašin, D., "Results of unsaturated tests on metastable soils", in Proceedings 1st Pan-American Conference on Unsaturated Soils, PanAmUNSAT. (2013), 469-474.
6. Aldaood, A., Bouasker, M. and Al-Mukhtar, M., "Effect of long-term soaking and leaching on the behaviour of lime-stabilised gypseous soil", *International Journal of Pavement Engineering*, Vol. 16, No. 1, (2015), 11-26,
7. Asghari, S., Ghafouri, M. and Tabatabai, S.S., "Changes in chemical composition and engineering properties of gypseous soils through leaching: An example from mashhad, iran", *Bulletin of Engineering Geology and the Environment*, Vol. 77, No. 1, (2018), 165-175.
8. Haeri, S.M., Beigi, M., Saberi, S. and Garakani, A.A., "Study on the stress path dependency of collapse behavior of gorgan loess implementing unsaturated oedometer devices", in E3S Web of Conferences, EDP Sciences. Vol. 9, (2016), 14019.

9. Abdalhusein, M.M., Akhtarpour, A. and Mahmood, M.S., "Effect of soaking on unsaturated gypseous sand soils", *International Journal of Civil Engineering and Technology*, Vol. 10, No. 5, (2019), 550-558.
10. Abdalhusein, M.M. and Ali Akhtarpour, M.S., "Effect of wetting process with presence of matric suction on unsaturated gypseous sand soils", *Journal of Southwest Jiaotong University*, Vol. 54, No. 5, (2019).
11. Liu, C., He, P. and Huang, Q., "Influence of matrix suction on engineering properties of unsaturated soil", in 2011 Second International Conference on Mechanic Automation and Control Engineering, IEEE. (2011), 2250-2253.
12. Fattah, M.Y., Al-Shakarchi, Y.J. and Al-Numani, H.N., "Long term deformation of some gypseous soils", *Engineering and Technology Journal*, Vol. 26, No. 12, (2008), 1461-1483, doi.
13. Fattah, M.Y., Al-Ani, M.M. and Al-Lamy, M.T., "Studying collapse potential of gypseous soil treated by grouting", *Soils and Foundations*, Vol. 54, No. 3, (2014), 396-404, doi: 10.1016/j.sandf.2014.04.008.
14. Mahmood, M., "Effect of soaking on the compaction characteristics of al-najaf sand soil", *Kufa Journal of Engineering*, Vol. 9, No. 2, (2018), 1-12, doi: 10.30572/2018/kje/090201.
15. Mahmood, M.S., Akhtarpour, A., Almahmodi, R. and Husain, M.M.A., "Settlement assessment of gypseous sand after time-based soaking", in IOP Conference Series: Materials Science and Engineering, IOP Publishing. Vol. 737, No. 1, (2020), 012080.
16. Mahmood, M.S., Aziz, L.J. and Al-Gharrawi, A., "Settlement behavior of sand soil upon soaking process", *International Journal of Civil Engineering and Technology, India*, Vol. 9, No. 11, (2018), 860-869.
17. Mahmood, M.S., "Prediction of discrepancy settlement behaviour of sand soils", *Applied Research Journal, Iran*, Vol. 4, No. 2, (2018), 30-37.
18. Mahmood, M.S. and Abraham, M.J., "A review of collapsible soils behavior and prediction", in IOP Conference Series: Materials Science and Engineering, IOP Publishing. Vol. 1094, No. 1, (2021), 012044.
19. Zimbaro, M., Ercoli, L. and Megna, B., "The open metastable structure of a collapsible sand: Fabric and bonding", *Bulletin of Engineering Geology and the Environment*, Vol. 75, No. 1, (2016), 125-139, doi: <https://doi.org/10.1007/s10064-015-0752-7>
20. Mahmood, M.S., "Effect of time-based soaking on shear strength parameters of sand soils", *Applied Research Journal*, Vol. 3, No. 5, (2017), 142-149.
21. Mahmood, M.S., Al-Baghdadi, W.H., Rabee, A.M. and Almahbobi, S.H., "Reliability of shear-box tests upon soaking process on the sand soil in al-najaf city", in Key Engineering Materials, Trans Tech Publ. Vol. 857, (2020), 212-220.
22. Mahmood, M., Almahbobi, S., Rabee, A., Rahim, A., Naama, M. and Mohammed, M., "Reliable prediction of structure settlement in al-najaf city using laboratory testing", in IOP Conference Series: Materials Science and Engineering, IOP Publishing. Vol. 888, No. 1, (2020), 012013.
23. Lloret, A. and Alonso, E., "Consolidation of unsaturated soils including swelling and collapse behaviour", *Géotechnique*, Vol. 30, No. 4, (1980), 449-477.
24. Fredlund, D.G. and Rahardjo, H., "Soil mechanics for unsaturated soils, John Wiley & Sons, (1993).
25. ISLAM, M., "Selection of intermodal conductivity averaging scheme for unsaturated flow in homogeneous media", *International Journal of Engineering*, Vol. 28, No. 4, (2015), 490-498, doi: 10.5829/idosi.ije.2015.28.04a.01.
26. Safarzadeh, Z. and Aminfar, M.H., "Experimental and numerical modeling of the effect of groundwater table lowering on bearing capacity of shallow square footings", *International Journal of Engineering*, Vol. 32, No. 10, (2019), 1429-1436, doi: 10.5829/ije.2019.32.10a.12.
27. Hayal, A., Al-Gharrawi, A. and Fattah, M., "Collapse problem treatment of gypseous soil by nanomaterials", *International Journal of Engineering*, Vol. 33, No. 9, (2020), 1737-1742, doi: 10.5829/ije.2020.33.09c.06.
28. Pells, P., Robertson, A., Jennings, J. and Knight, K., *A guide to construction on or with materials exhibiting additional settlement due to "collapse" of grain structure*. 1975.

Persian Abstract

چکیده

گچ یک ماده مجلول است و یکی از اجزای مشکل ساز خاک در غرب عراق است. نجف یکی از استان های عراق است که از سطوح گچی در سطوح مختلف رنج می برد. خاک شهر عمدتاً از ذرات به اندازه ماسه است که با درصد های گچی به هم متصل شده اند. مشکل اصلی این جزء انحلال در فرآیند خیس شدن در شرایط غیر اشباع است. این مقاله به بررسی تأثیر کاهش مکش ماتریک (خیس شدن) بر تغییر شکل خاک تحت یک سطح تنش خاص می پردازد. برای انجام آزمایشات، از جمله اعمال فشار هوا و آب به منظور دستیابی به مکش های ماتریک خاص، از یک تنظیم کننده اندازه گیری شده استفاده می شود. این تحقیق شامل سه مکش ماتریکی (۵۰، ۲۰ و ۰ کیلو پاسکال) و هر یک تحت سه تنش نرمال خالص به ترتیب ۲۲۱ کیلو پاسکال، ۴۴۲ کیلو پاسکال و ۸۸۵ کیلو پاسکال است. نمونه های خاک در آزمایش پروکتور تا ۹۵ درصد حداکثر چگالی خشک مجدداً بازسازی می شوند. نتایج نشان داد که بیشترین مقدار پتانسیل فروپاشی (CP) تحت فشار ۲۲۱ kPa است. بیشترین مقدار CP قبل از اشباع خاک به دست می آید. این مسئله باید در تجزیه و تحلیل و طراحی فونداسیون در خاکهای شنی گچی غیر اشباع به عنوان یک مساله بهبودیافته مورد توجه قرار گیرد.



Optimization of Travelling Salesman Problem on Single Valued Triangular Neutrosophic Number using Dhouib-Matrix-TSP1 Heuristic

S. Dhouib*

Department of Industrial Management, Higher Institute of Industrial Management, University of fax, Tunisia

PAPER INFO

Paper history:

Received 25 July 2021

Received in revised form 29 August 2021

Accepted 20 September 2021

Keywords:

Artificial Intelligence

Combinatorial Optimization

Dhouib-Matrix-TSP1 Heuristic

Fuzzy Number

Neutrosophic Number

Operational Research

Travelling Salesman Problem

ABSTRACT

The Travelling Salesman Problem (TSP) is one of the fundamental operational research problems where the objective is to generate the cheapest route for a salesman starting from a given city, visiting all the other cities only once and finally returning to the starting city. In this paper, we study the Travelling Salesman Problem in uncertain environment. Particularly, the single valued triangular neutrosophic environment is considered viewing that it is more realistic and general in real-world industrial problems. Each element in the distance matrix of the Travelling Salesman Problem is presented as a single valued triangular neutrosophic number. To solve this problem, we enhance our novel column-row heuristic Dhouib-Matrix-TSP1 by the means of the center of gravity ranking function and the standard deviation metric. In fact, the center of gravity ranking function is applied for defuzzification in order to convert the single valued triangular neutrosophic number to crisp number. A stepwise application of several numerical Travelling Salesman Problems on the single valued triangular neutrosophic environment shows that the optimal or a near optimal solution can be easily reached; thanks to the Dhouib-Matrix-TSP1 heuristic enriched with the center of gravity ranking function and the standard deviation metric.

doi: 10.5829/ije.2021.34.12c.09

1. INTRODUCTION

In 1995, Smarandache [1] introduced the philosophy of neutrosophic which covers wide concepts more than the intuitionistic (that can handle only the incomplete information); which consists of: set, probability, statistics, logic and theory. The neutrosophic number can handle three independent memberships: Truth (T), Indeterminacy (I) and Falsity (F), where T , I and F are subsets of $[0, 1^+]$.

Several recent research papers deal with the application of neutrosophic concept. Ibrahim et al. [2] developed a neutrosophic analytical hierarchy process model to measure the degree of credit risk for a private Bank. Khalifa Abd El-Wahed and Kumar [3] solved the neutrosophic assignment problem where the matrix elements; they presented as interval-valued trapezoidal neutrosophic number using the order relations technique. Moreover, Hamiden [4] used the weighting Tchebycheff

technique to generate a relative weights and ideal targets for the multi-objective assignment problem in the neutrosophic trapezoidal fuzzy situation. Prabha and Vimala [5] optimized the triangular fuzzy neutrosophic assignment problem is using the branch and bound technique and the efficiency is illustrated on a real-world agricultural problem. Chakraborty et al. [6] deigned a new score and accuracy technique is to convert the pentagonal neutrosophic fuzzy numbers into crisp numbers for the transportation problem in pentagonal neutrosophic environment.

Subasri and Selvakumari [7] solved the travelling salesman problem in neutrosophic environment with trapezoidal fuzzy distance via the branch and bound method. In addition, Subasri and Selvakumari [8] optimized the TSP in neutrosophic domain using triangular fuzzy distance through the ones assignment method.

Obviously, the TSP is an NP-complete problem [9].

*Corresponding Author Institutional Email:
dhouib.matrix@gmail.com (S. Dhouib)

Its objective is to find the cheapest route of a salesman starting from a given city, visiting all the other cities only once and finally returning to the starting city. This problem has been formulated by Equation (1):

$$\begin{aligned} & \sum_{i=1}^n \sum_{j=1}^n d_{ij} p_{ij} \\ & \sum_{j=1}^n p_{ij} = 1, \quad i=1, \dots, n \\ & \sum_{i=1}^n p_{ij} = 1, \quad j=1, \dots, n \\ & p_{ij} = 0 \text{ or } 1, \quad i=1, \dots, n, \quad j=1, \dots, n \end{aligned} \tag{1}$$

Where p_{ij} is a binary variable (if city i and city j are not connected then $p_{ij} = 0$ else $p_{ij} = 1$) and d_{ij} denotes the distance between city i and city j .

Our investigation shows that all of the research papers in the field of neutrosophic theory in operational research were intensive on the transportation problem and the assignment problem. Likewise, very limited number of research papers focused on solving the TSP in neutrosophic environment. Motivated by the above-mentioned problem, this paper proposes the first resolution of the TSP in single valued triangular neutrosophic environment with center of gravity score function. In fact, each element d_{ij} in the TSP distance matrix is considered as a single valued triangular neutrosophic distance and defuzzied to crisp number using the center of gravity score function. Hence, this TSP is optimized by our recently invented heuristic [10] entitled Dhouib-Matrix-TSP1 (DM-TSP1). Moreover, this paper presents the first application of the DM-TSP1 to the neutrosophic domains.

The rest of this paper is structured as follows. In section 2, we study the neutrosophic number concept. In section 3, we present the proposed DM-TSP1 heuristic enriched with the center of gravity ranking function. In section 4, we illustrate the resolution by applying the adapted DM-TSP1 technique on several numerical examples. Finally, in section 5 we present the conclusion and our further research work.

2. THE TRINAGULAR NEUTROSOPHIC NUMBER

This section gives a brief overview of the triangular neutrosophic concept [11, 12]. The triangular fuzzy number \tilde{Y} is denoted by $\tilde{Y} = (y_a, y_b, y_c)$ where y_a, y_b and y_c are real numbers with $y_a \leq y_b \leq y_c$. Let's consider X a space of points where the generic elements in X are denoted by x .

The single valued triangular neutrosophic number Y^N over X has the form of $Y^N = \{ \langle x : T_{Y^N}(x), I_{Y^N}(x), F_{Y^N}(x) \rangle, x \in X \}$ where the

functions $T_{Y^N}, I_{Y^N}, F_{Y^N} : X \rightarrow]0, 1^+ [$ with the condition $0 \leq T_{Y^N}(x) + I_{Y^N}(x) + F_{Y^N}(x) \leq 3^+$.

The truth (T), indeterminacy (I) and falsity (F) membership functions for the single valued triangular neutrosophic number $Y^N = \langle [y_a, y_b, y_c]; (\mu_{Y^N}, \nu_{Y^N}, \lambda_{Y^N}) \rangle$ are defined by Equation (2):

$$\begin{aligned} T_{Y^N}(x) &= \begin{cases} \frac{(x - y_a)\mu_{Y^N}}{y_b - y_a}, & y_a \leq x \leq y_b \\ \frac{(y_c - x)\mu_{Y^N}}{y_c - y_b}, & y_b \leq x \leq y_c \\ 0, & \text{otherwise} \end{cases} \\ I_{Y^N}(x) &= \begin{cases} \frac{y_b - x + (x - y_a)\nu_{Y^N}}{y_b - y_a}, & y_a \leq x \leq y_b \\ \frac{x - y_b + (y_c - x)\nu_{Y^N}}{y_c - y_b}, & y_b \leq x \leq y_c \\ 0, & \text{otherwise} \end{cases} \\ F_{Y^N}(x) &= \begin{cases} \frac{y_b - x + (x - y_a)\lambda_{Y^N}}{y_b - y_a}, & y_a \leq x \leq y_b \\ \frac{x - y_b + (y_c - x)\lambda_{Y^N}}{y_c - y_b}, & y_b \leq x \leq y_c \\ 0, & \text{otherwise} \end{cases} \end{aligned} \tag{2}$$

3. THE PROPOSED METHOD: Dhouib-Matrix-TSP1 (DM-TSP1)

We designed and developed a novel column-row method namely DM-TSP1 to solve the TSP [10]. Then, we adapted the DM-TSP1 heuristic for the case of: the trapezoidal fuzzy TSP [13] and the octagonal fuzzy TSP [14]. Moreover, a stochastic version of DM-TSP1 named DM-TSP2 was performed [15]. More recently, we invent a simple heuristic, entitled Dhouib-Matrix-TP1, in order to optimize the transportation problem [16]. This paper introduces the first resolution of the TSP in single valued triangular neutrosophic environment. Furthermore, this paper also presents the first application of our DM-TSP1 heuristic on the neutrosophic environment.

The DM-TSP1 heuristic starts by the defuzzification of the single valued triangular neutrosophic number to crisp value using the center of gravity (COG) ranking

function described by Broumi et al. [17]. For a triangular fuzzy distance $\tilde{Y} = [y_a, y_b, y_c]$ with $y_a \leq y_b \leq y_c$, the COG is computed as Equation (3):

$$COG(\tilde{Y}) = \frac{1}{4}[y_a + 2 \times y_b + y_c] \tag{3}$$

Thus, the score and the accuracy functions for the single valued triangular neutrosophic number $Y^N = \langle [y_a, y_b, y_c]; (\mu_{y^N}, \nu_{y^N}, \lambda_{y^N}) \rangle$ are defined as follows:

$$S(Y^N) = COG(Y^N) \times \frac{2 + \mu_{y^N} - \nu_{y^N} - \lambda_{y^N}}{3} \tag{4}$$

$$a(Y^N) = COG(Y^N) \times \frac{2 + \mu_{y^N} - \nu_{y^N} + \lambda_{y^N}}{3}$$

Here is an example of single valued triangular neutrosophic number $Y^N = \langle (3, 6, 9), 0.9, 0.5, 0.1 \rangle$ which can be converted into a crisp number (with the value equal to 4.60) by the means of Equations (3) and (4):

$$COG(Y^N) = \frac{1}{4}[3 + 2 \times 6 + 9] = 6$$

And

$$S(Y^N) = 6 \times \frac{2 + 0.9 - 0.5 - 0.1}{3} = 4.60$$

Figure 1 depicts the graphical representation of the single valued triangular neutrosophic number $Y^N = \langle (3, 6, 9), 0.9, 0.5, 0.1 \rangle$.

The DM-TSP1 is composed of four steps iterated in a sequential manner as described in Figure 2.

The DM-TSP1 heuristic is developed using the Python programming language in a sequential structure. However, we will look in a further research to insert the DM-TSP1 in a multi-agent structure as reported in

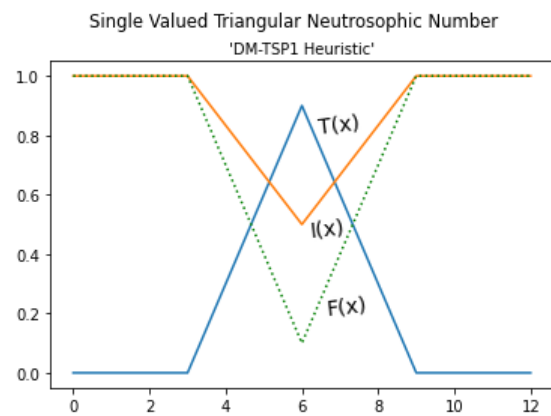


Figure 3. Graphical representation of the single valued neutrosophic number

Step 1

- Compute the standard deviation for each row and write it on the right-hand side of the matrix. Next, find the minimum standard deviation value and select its row. Then, select the smallest element in this row which will specify the two first cities x and y . Finally, discard the respected columns of city x and city y .

Step 2

- Find the minimum element for city x and for city y and select the smallest distance which will indicate city z .

Step 3

- Add city z to the list *List-cities* and discard its column. Next, go to step 2 if there is not a discarded column otherwise go to step 4.

Step 4

- Modify the realizable solution in *List-cities* in order to generate a cycle (the starting city in the cycle has to be also the last one). First, to ensure that the starting city will be at the first position, translate all the cities (one by one) before the starting one at the end of the list. Second, duplicate the starting city at the last position.

Figure 2. The four steps of the DM-TSP1 heuristic

literature [18, 19, 20] using different metric functions (Min, Max, Standard Deviation) in each agent.

4. COMPUTATIONAL RESULTS

Three numerical examples are used to prove the performance of the proposed DM-TSP1 heuristic.

4. 1. Numerical Example 1 Consider the following symmetric TSP with single valued triangular neutrosophic distance (see Figure 3).

Where:

$$d_{12} = \langle (4, 6, 10); 0.8, 0.4, 0.2 \rangle, d_{13} = \langle (2, 5, 9); 0.7, 0.6, 0.3 \rangle$$

$$d_{14} = \langle (4, 7, 9); 0.6, 0.6, 0.3 \rangle, d_{21} = \langle (4, 6, 10); 0.8, 0.4, 0.2 \rangle$$

$$d_{23} = \langle (1, 5, 8); 0.8, 0.5, 0.2 \rangle, d_{24} = \langle (2, 7, 9); 0.8, 0.5, 0.4 \rangle$$

$$d_{31} = \langle (2, 5, 9); 0.7, 0.6, 0.3 \rangle, d_{32} = \langle (1, 5, 8); 0.8, 0.5, 0.2 \rangle$$

$$\begin{pmatrix} \infty & d_{12} & d_{13} & d_{14} \\ d_{21} & \infty & d_{23} & d_{24} \\ d_{31} & d_{32} & \infty & d_{34} \\ d_{41} & d_{42} & d_{43} & \infty \end{pmatrix}$$

Figure 3. The single valued triangular neutrosophic distance matrix

$$d_{34} = \langle (1, 5, 10); 0.8, 0.3, 0.1 \rangle, d_{41} = \langle (4, 7, 9); 0.6, 0.6, 0.3 \rangle$$

$$d_{42} = \langle (2, 7, 9); 0.8, 0.5, 0.4 \rangle, d_{43} = \langle (1, 5, 10); 0.8, 0.3, 0.1 \rangle$$

For all single valued triangular neutrosophic distance in the TSP distance matrix will be converted into crisp numbers by using Equations (3) and (4). Here is an example, the single valued triangular neutrosophic distance $\langle (4, 6, 10); 0.8, 0.4, 0.2 \rangle$ in the element d_{12} is converted into the crisp distance equal to 4.76 by:

$$COG(d_{12}) = \frac{1}{4} [4 + 2 \times 6 + 10] = 6.50$$

and

$$S(d_{12}) = 6.50 \times \frac{2 + 0.8 - 0.4 - 0.2}{3} = 4.77$$

Similarly proceeding for all single valued triangular neutrosophic distance we get the crisp distance matrix (see Figure 4).

Now, from the given crisp distance matrix the standard deviation for each row is computed and the smallest standard deviation value is selected which is 1.59 in row 3 (see Figure 5) and finding its minimal element (at position d_{31}).

Insert cities 3 and 1 in the *List-cities* {3-1} and discard their columns. Next, select the smallest values for row 3 and row 1 (see Figure 6).

The smallest value in row 3 is at position d_{32} . Thus, insert city 2 at the left side (because it is generated from city 3) in the *List-cities* {2-3-1} and discard column 2 (see Figure 7).

Similarly, select the smallest element in rows 1 and 2, which is 3.83 at position d_{14} . Then, insert city 4 at the right side (because it is generated from city 1) in the *List-cities* {2-3-1-4} and discard column 4 (see Figure 8).

Finally, if there is no more columns to select so the last step is to generate a cycle from the *List-cities* {2-3-1-4}. Starts by translating the city from left position to

$$\begin{pmatrix} \infty & 4.77 & 3.15 & 3.83 \\ 4.77 & \infty & 3.33 & 3.96 \\ 3.15 & 3.33 & \infty & 4.20 \\ 3.83 & 3.96 & 4.20 & \infty \end{pmatrix}$$

Figure 4. The crisp distance matrix

$$\begin{bmatrix} \infty & 4.77 & 3.15 & 3.83 \\ 4.77 & \infty & 3.33 & 3.96 \\ 3.15 & 3.33 & \infty & 4.20 \\ 3.83 & 3.96 & 4.20 & \infty \end{bmatrix} \begin{matrix} 1.79 \\ 1.81 \\ 1.59 \\ 1.74 \end{matrix}$$

Figure 5. Select the element d_{31}

$$\begin{bmatrix} \infty & 4.77 & 3.15 & 3.83 \\ 4.77 & \infty & 3.33 & 3.96 \\ 3.15 & 3.33 & \infty & 4.20 \\ 3.83 & 3.96 & 4.20 & \infty \end{bmatrix}$$

Figure 6. Discard columns 3 and 1

$$\begin{bmatrix} \infty & 4.77 & 3.15 & 3.83 \\ 4.77 & \infty & 3.33 & 3.96 \\ 3.15 & 3.33 & \infty & 4.20 \\ 3.83 & 3.96 & 4.20 & \infty \end{bmatrix}$$

Figure 7. Discard column 1

$$\begin{bmatrix} \infty & 4.77 & 3.15 & 3.83 \\ 4.77 & \infty & 3.33 & 3.96 \\ 3.15 & 3.33 & \infty & 4.20 \\ 3.83 & 3.96 & 4.20 & \infty \end{bmatrix}$$

Figure 8. Discard column 4

the right one until the city number 1 will be at the first position: so, translate city 2 to the last position to obtain {3-1-4-2}; hence, translate city 3 to the last position to get {1-4-2-3}. Finally, add city 1 to the last position to obtain the cycle {1-4-2-3-1}. Therefore, the crisp optimal solution found by the DM-TSP1 heuristic using the center of gravity ranking function is {1-4-2-3-1} = 3.83 + 3.96 + 3.33 + 3.15 = 14.27.

4. 2. Numerical Example 2

Here is a second example, let us consider the following 5x5 distance matrix with single valued triangular neutrosophic number. Where:

$$d_{12} = \langle (1, 9, 20); 0.9, 0.4, 0.1 \rangle, d_{13} = \langle (2, 9, 25); 0.8, 0.5, 0.1 \rangle$$

$$d_{14} = \langle (5, 7, 9); 0.9, 0.7, 0.1 \rangle, d_{15} = \langle (2, 9, 19); 0.4, 0.4, 0.3 \rangle$$

$$d_{21} = \langle (1, 9, 20); 0.9, 0.4, 0.1 \rangle, d_{23} = \langle (3, 9, 14); 0.7, 0.3, 0.3 \rangle$$

$$d_{24} = \langle (5, 8, 13); 0.6, 0.2, 0.4 \rangle, d_{25} = \langle (7, 9, 18); 0.4, 0.1, 0.1 \rangle$$

$$d_{31} = \langle (2, 9, 25); 0.8, 0.5, 0.1 \rangle, d_{32} = \langle (3, 9, 14); 0.7, 0.3, 0.3 \rangle$$

$$d_{34} = \langle (4, 8, 17); 0.8, 0.5, 0.2 \rangle, d_{35} = \langle (5, 9, 15); 0.9, 0.6, 0.1 \rangle$$

$$d_{41} = \langle (5, 7, 9); 0.9, 0.7, 0.1 \rangle, d_{42} = \langle (5, 8, 13); 0.6, 0.2, 0.4 \rangle$$

$$d_{43} = \langle (4, 8, 17); 0.8, 0.5, 0.2 \rangle, d_{45} = \langle (1, 9, 16); 0.7, 0.4, 0.3 \rangle$$

$$d_{s_1} = \langle (2, 9, 19); 0.4, 0.4, 0.3 \rangle, d_{s_2} = \langle (7, 9, 18); 0.4, 0.1, 0.1 \rangle$$

$$d_{s_3} = \langle (5, 9, 15); 0.9, 0.6, 0.1 \rangle, d_{s_4} = \langle (1, 9, 16); 0.7, 0.4, 0.3 \rangle$$

Figure 9 depicts the five steps needed to solve the 5x5 distance matrix with single valued triangular neutrosophic number.

4. 3. Numerical Example 3 Let us consider the following 5x5 distance matrix where the distance d_{ij} are presented as follows:

$$d_{12} = \langle (2, 8, 18); 0.8, 0.3, 0.2 \rangle, d_{13} = \langle (1, 9, 24); 0.9, 0.6, 0.2 \rangle$$

$$d_{14} = \langle (4, 9, 15); 0.6, 0.5, 0.2 \rangle, d_{15} = \langle (3, 6, 13); 0.6, 0.3, 0.3 \rangle$$

$$d_{21} = \langle (2, 8, 18); 0.8, 0.3, 0.2 \rangle, d_{23} = \langle (6, 9, 19); 0.9, 0.4, 0.1 \rangle$$

$$d_{24} = \langle (1, 7, 12); 0.9, 0.1, 0.2 \rangle, d_{25} = \langle (5, 9, 18); 0.9, 0.8, 0.2 \rangle$$

$$d_{31} = \langle (1, 9, 24); 0.9, 0.6, 0.2 \rangle, d_{32} = \langle (6, 9, 19); 0.9, 0.4, 0.1 \rangle$$

$$d_{34} = \langle (3, 8, 23); 0.7, 0.1, 0.1 \rangle, d_{35} = \langle (2, 8, 32); 0.6, 0.5, 0.4 \rangle$$

$$d_{41} = \langle (4, 9, 15); 0.6, 0.5, 0.2 \rangle, d_{42} = \langle (1, 7, 12); 0.9, 0.1, 0.2 \rangle$$

$$d_{43} = \langle (3, 8, 23); 0.7, 0.1, 0.1 \rangle, d_{45} = \langle (2, 5, 11); 0.9, 0.3, 0.1 \rangle$$

$$d_{51} = \langle (3, 6, 13); 0.6, 0.3, 0.3 \rangle, d_{52} = \langle (5, 9, 18); 0.9, 0.8, 0.2 \rangle$$

$$d_{53} = \langle (2, 8, 32); 0.6, 0.5, 0.4 \rangle, d_{54} = \langle (2, 5, 11); 0.9, 0.3, 0.1 \rangle$$

Figure 10 depicts the five steps needed to solve the 5x5 distance matrix with single valued triangular neutrosophic number.

5. CONCLUSIONS

The Travelling Salesman Problem aims to generate the shortest cycle among all cities where each city is visited only once except the first city which should be revisited at the end.

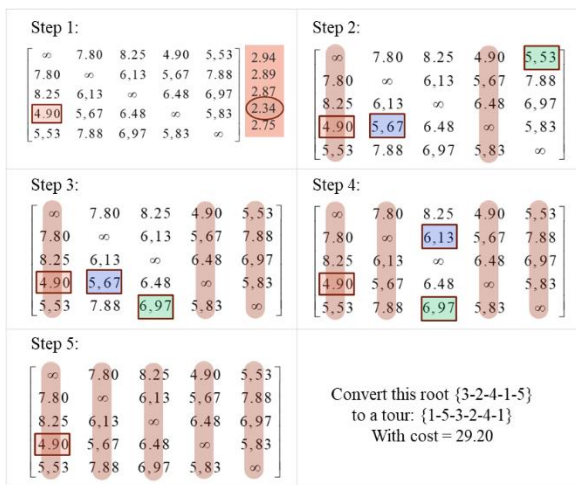


Figure 9. Just 5 steps to solve the 5x5 distance matrix

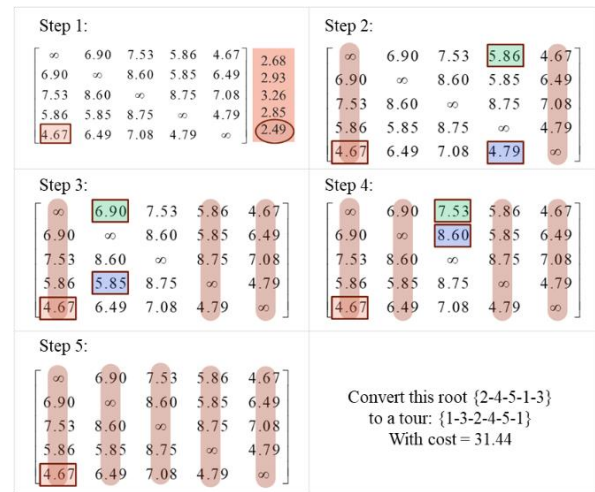


Figure 10. Just 5 steps to solve the 5x5 distance matrix

Neutrosophic philosophy can be used to solve many real-life problems like the travelling salesman problem. In this research work, the Dhoub-Matrix-TSP1 heuristic is proposed for solving the neutrosophic triangular fuzzy travelling salesman problem using center of gravity ranking function. The efficiency of this heuristic was proved by solving several numerical case studies.

Our further research work will be focused on adapting the Dhoub-Matrix-TSP1 heuristic to solve other neutrosophic forms (trapezoidal, octagonal, etc.) using different score functions and on enhancing the Dhoub-Matrix-TSP1 to solve the neutrosophic environment in the multi-objective travelling salesman problem widely occurred in real life industrial situations.

6. REFERENCES

1. Smarandache F., "A Unifying Field in Logics: Neutrosophic Logic. Neutrosophy, Neutrosophic Set, Neutrosophic Probability and Statistics", *Infinite Study*, (2005), DOI: 10.5281/zenodo.8792.
2. Ibrahim A. N., Elghareeb H., Farahat F. F. and AboElfotouh A., "Comparative Mathematical Model for Predicting of Financial Loans Default using Altman Z-Score and Neutrosophic AHP Methods", *Neutrosophic Sets and Systems*, Vol. 43, (2021), DOI: 10.5281/zenodo.4914802.
3. Khalifa Abd El-Wahed H. and Kumar P., "A Novel Method for Solving Assignment Problem by Using Interval-Valued Trapezoidal Neutrosophic Number", *Neutrosophic Sets and Systems*, Vol. 36, (2020), 24-36, DOI: 10.5281/zenodo.4065363.
4. Hamiden Khalifa, "An Approach to The Optimization of Multi-Objective Assignment Problems with Neutrosophic Numbers", *International Journal of Industrial Engineering & Production Research*, Vol. 31, No. 2, (2020), 287-294, DOI: 10.22068/ijiepr.31.2.287.
5. Prabha K. S. and Vimala S., "Neutrosophic Assignment Problem via BnB Algorithm", *Advances in Algebra and Analysis, Trends in Mathematics*, (2019), 323-330, DOI: 10.1007/978-3-030-01120-8_37.

6. Chakraborty A., Broumi S. and Singh K. P., "Some properties of Pentagonal Neutrosophic Numbers and its Applications in Transportation Problem Environment", *Neutrosophic Sets and Systems*, Vol. 28, (2019), 200-215, DOI: 10.5281/zenodo.3382542.
7. Subasri S. and Selvakumari K., "Neutrosophic Travelling Salesman Problem in Trapezoidal Fuzzy number using Branch and Bound Technique", *Journal of Physics: Conference Series*, (2019), DOI:10.1088/1742-6596/1362/1/012098.
8. Subasri S. and Selvakumari K., "Solving Neutrosophic Travelling Salesman Problem in Triangular Fuzzy Number Using Ones Assignment Method", *Eurasian Journal of Analytical Chemistry*, Vol. 13, (2018), 285-291, DOI: 10.5281/zenodo.3133798.
9. Abbasi M. and Rafiee M., "Efficient Parallelization of a Genetic Algorithm Solution on the Traveling Salesman Problem with Multi-core and Many-core Systems", *International Journal of Engineering, Transactions A: Basics*, Vol. 33, No. 7, (2020), 1257-1265, DOI: 10.5829/ije.2020.33.07a.12.
10. Dhoubi S., "A New Column-Row Method for Traveling Salesman Problem: The Dhoubi-Matrix-TSP1", *International Journal of Recent Engineering Science*, Vol. 8, No. 1, (2021), 6-10, DOI: 10.14445/23497157/IJRES-V8I1P102.
11. Deli I., and Şubaş Y., "A ranking method of single valued neutrosophic numbers and its applications to multi-attribute decision making problems", *International Journal of Machine Learning and Cybernetics*, Vol. 8, (2017), 1309-1322, DOI: 10.1007/s13042-016-0505-3.
12. Wang H., Smarandache F., Zhang Y. and Sunderraman R., "Single valued neutrosophic sets", *Technical Sciences and Applied Mathematics*, Vol. 4, (2010), 10-14, DOI: 10.1007/s13042-016-0505-3.
13. Dhoubi Sa. and Dhoubi S., "Optimizing the Trapezoidal Fuzzy Travelling Salesman Problem Through Dhoubi-Matrix-TSP1 Method Based on Magnitude Technique", *International Journal of Scientific Research in Mathematical and Statistical Sciences*, Vol. 8, No. 2, (2021), 1-4, DOI: 10.26438/ijrms/v8i2.14.
14. Miledi M., Dhoubi S. and Loukil T., "Dhoubi-Matrix-TSP1 Method to Optimize Octagonal Fuzzy Travelling Salesman Problem Using α -Cut Technique", *International Journal of Computer and Information Technology*, Vol. 10, No. 3, (2021), 130-133, DOI: 10.24203/ijcit.v10i3.105.
15. Dhoubi S., "Minimizing the Total Distance for the Supply Chain Problem Using Dhoubi-Matrix-TSP2 Method", *International Journal of Advanced Research in Engineering and Technology*, Vol. 12, No. 5, (2021), 1-12, DOI: 10.34218/IJARET.12.5.2021.001.
16. Dhoubi S., "A Novel Heuristic for the Transportation Problem: Dhoubi-Matrix-TP1", *International Journal of Recent Engineering Science*, Vol. 8, No. 4, (2021), 1-5, DOI: 10.14445/23497157/IJRES-V8I4P101.
17. Broumi S., Nagarajan D., Bakali A., Talea M., Smarandache F. and Lathamaheswari M., "The shortest path problem in interval valued trapezoidal and triangular neutrosophic environment", *Complex & Intelligent Systems*, Vol. 5, (2019), 391-402, DOI: 10.1007/s40747-019-0092-5.
18. Habibia M., Broumandnia A. and Harounabadic A., "Improvement of Multi-agent Routing Guidance with an Intelligent Traffic Light Scheduling and the Ability to Select Intermediate Destinations", *International Journal of Engineering, Transactions A: Basics*, Vol. 34, No. 4, (2021), 854-862, DOI: 10.5829/ije.2021.34.04a.11.
19. Dhoubi S., Kourraichi S., Loukil T. and Chabchoub H., "An Interactive Simulated Annealing Multi-agents platform to solve Hierarchical Scheduling Problems with Goals", *Studies in Computational Intelligence: Springer-Verlag*, Vol. 236, (2009), 177-187, DOI: 10.1007/978-3-642-03211-0_15.
20. Dhoubi S., "A threshold accepting framework to optimize discrete and continuous search space", *International Journal of Innovative Computing and Applications*, Vol. 2, No.3, (2010), 178-187, DOI: 10.1504/IJICA.2010.033649.

Persian Abstract

چکیده

مشکل فروشنده مسافر یکی از مشکلات اساسی تحقیقاتی عملیاتی است که هدف آن ایجاد ارزان ترین مسیر برای فروشنده ای است که از یک شهر شروع می شود، تنها یک بار از همه شهرهای دیگر دیدن کرده و در نهایت به شهر شروع باز می گردد. در این مقاله، مشکل فروشنده مسافر را در محیط نامشخص مطالعه می کنیم. به ویژه، محیط نوتروسوفی مثلثی با ارزش واحد در نظر گرفته می شود که در مشکلات صنعتی در دنیای واقعی واقع بینانه تر و کلی تر است. هر عنصر در ماتریس فاصله مسئله فروشنده مسافر به عنوان یک عدد نوتروسوفی مثلثی با ارزش واحد ارائه شده است. برای حل این مشکل، ما با استفاده از تابع رتبه بندی مرکز ثقل و معیار انحراف استاندارد، رمان ستون-ردیف ابتکاری Dhoubi-Matrix-TSP1 خود را افزایش می دهیم. در واقع، تابع رتبه بندی مرکز ثقل برای کوره زدایی به منظور تبدیل عدد نوتروسوفی مثلثی با ارزش واحد به عدد ترد استفاده می شود. استفاده گام به گام از نمونه های آزمایشی عددی بر روی محیط نوتروسوفی مثلثی با ارزش تنها نشان می دهد که راه حل مطلوب یا تقریباً مطلوب و همچنین هزینه کل واضح و فازی را می توان به راحتی به لطف روش ابتکاری Dhoubi-Matrix-TSP1 با مرکز غنی سازی به دست آورد. تابع رتبه بندی گرانس و معیار انحراف استاندارد بدست آورد.



A Two-level Semi-supervised Clustering Technique for News Articles

S. M. Sadjadi, H. Mashayekhi*, H. Hassanpour

Faculty of Computer Engineering, Shahrood University of Technology, Shahrood, Iran

PAPER INFO

Paper history:

Received 26 July 2021

Received in revised form 11 September 2021

Accepted 20 September 2021

Keywords:

News Clustering

Two-level Clustering

Semi-supervised

Word Embedding

Document Clustering

ABSTRACT

The web and social media are overcrowded with news pieces in terms of amount and diversity. Document clustering is a useful technique that is widely used in organizing and managing data into smaller groups. One of the factors influencing the quality of clustering is the way documents are represented. Some traditional methods of document representation depend on word frequencies and create sparse and large-sized document vectors. These methods cannot preserve proximity information between documents. In addition, neural network-based methods that preserve proximity information suffer from poor interpretability. Conceptual text representation methods have overcome the shortcomings of previous methods, but semi-supervised text clustering does not currently use concept-based document representation. This paper presents a two-level semi-supervised text clustering method that uses labeled and unlabeled data simultaneously to achieve higher clustering quality. In the first level, documents are represented based on the concepts extracted from the raw corpus. Second, the semi-supervised clustering process applies unlabeled data to capture the overall structure of the clusters and a small amount of labeled data to adjust the center of the clusters. Experiments on the Reuters-21578 and BBC News data collections show that the proposed model is superior to other semi-supervised approaches in both text classification and text clustering.

doi: 10.5829/ije.2021.34.12c.10

1. INTRODUCTION

News documents on web pages as well as social networks are the main source of textual data due to the widespread use of Internet [1]. News articles flood the web every day through many major or minor news portals around the world. As the amount of online information resources increases rapidly, so does the content of available online news [2]. To analyze a large number of documents, text clustering is applied, which is a method of dividing a group of documents into different clusters based on content similarity [3]. This method has many applications in news recommender systems [4-5], news classification, emotion analysis [6], text summarization [7], etc.

The clustering function relies mainly on the representation of documents that aims to convert raw

documents into numerical vectors. The most common way to represent a document, known for its interpretability and intuition, is the Bag-of-Words method [8], which represents a document vector with its word frequencies. However, although it is easy to interpret, it suffers from unreasonable dimensions. Deep neural network methods such as Convolutional Neural Networks (CNNs) [9] and Doc2Vec [10] create reasonable dimensional vectors to represent documents. Nevertheless, the resulting representations are not easy to interpret because the constituent values of the document vector are calculated through complex neural network weight structures.

Clustering is a primary method for discovering the natural structure of unlabeled data [11]. One of the newest methods is the use of labeled data to improve the performance of unsupervised clustering [12]. The basic

*Corresponding Author Institutional Email:

hmashayekhi@shahroodut.ac.ir (H. Mashayekhi)

idea is that unlabeled data form the overall structure of the clusters, and some labeled data set the center of the clusters. This method uses both labeled and unlabeled data, called semi-supervised clustering [13]. Nowadays many semi-supervised clustering methods have been proposed for various applications. In clustering methods such as SOM [14] and Naïve Bayes Expectation-Maximization [15], unlabeled data is first labeled, and then these new labeled data and the original labeled data train the model. But it is not clear how much data needs to be re-labeled and how reliable it is.

To solve these problems, we introduce a new two-level method for semi-supervised documents clustering, which makes full use of labeled and unlabeled data, while maintaining proximity information and high interpretability of documents. The words are represented in vectors using the Word2Vec [16] algorithm to utilizing the semantic similarity of the continuous space. In the first level, similar word vectors are grouped into clusters. In the second level, documents are represented based on these clusters. This proposed method can obtain the underlying components of documents while maintaining their interpretability. A semi-supervised clustering algorithm is applied on the documents in the new space to obtain the final document clusters. Because the model is explicable, it provides humans deeper understandings of texts and more explicit operation logic for reasoning.

This paper is organized as follows. In section 2, some related works of document representation and semi-supervised clustering are reviewed. Our proposed concept-based model for semi-supervised document clustering is presented in section 3. Section 4 presents the datasets used and the experimental results, and detailed analyses are presented in section 5. Ultimately, our work is concluded in section 6.

2. RELATED WORKS

2.1. Text Representation The Bag-of-Words (BoW) method has limitations such as large dimensionality and suffering from sparsity. Some succeeding representation techniques, such as Latent Semantic Analysis (LSA) [17] diminishes the term-document matrix into a low dimension matrix. Although it works more efficiently than the BoW method, it diminishes the matrix in linear space and fails to identify the non-linear semantic similarities between the words. The Word2Vec [18], a two-layer neural network, is a model for transforming large text into a multidimensional vector space. As the name implies, by training neural network weights, each word in the raw corpus is represented as a unique vector that can maintain

a semantic similarity between words. One of the most important contributions of Word2Vec is that words that occurred in a similar context will be close in embedded space and will preserve the semantic similarities between the words. Also, while high dimensions and sparsity are weaknesses of BoW, the vectors produced by Word2Vec have reasonable, optimal, and dense dimensions. For this reason, many machine learning and text data mining problems can be solved through Word2Vec [19].

Le et al. [10] proposed the Doc2Vec model, which utilizes textual information from words and paragraphs mutually to obtain the representation of texts in a continuous vector space. Due to the fewer dimensions of the produced document vectors, it is more effective than BoW. In addition, research has shown that Doc2Vec is more effective than Word2Vec in solving clustering problems [20]. Nevertheless, low interpretability and unclear logic behind document vectors' generation procedure are the problems of the Doc2Vec method.

In this study, the documents are represented based on the concepts in the text. In this regard, Kim et al. [16] proposed the Bag-of-Concepts (BoC) method. It creates concepts through clustering word vectors generated by Word2Vec. Then, the document vector is formed considering the frequency of concepts in the documents. But this method does not suggest a solution for text clustering. Jia et al. [21] used the concept decompositions method to cluster short texts. They presented a decomposition approach to obtain concept vectors that generate by identifying the semantics of word communities in a weighted word co-occurrence network extracted from the short text set.

Lee et al. [22] proposed a new way for representing documents. Their method is based on concepts that automatically receive appropriate conceptual knowledge from an external knowledge base and then conceptualizes the words and terms of the documents with a probabilistic approach. Their method, using an external knowledge base, provides a better understanding of document representation for humans. They also diminish concept ambiguity through clustering concepts with related meanings to improve the BoC algorithm. To evaluate the performance of the proposed method, their model is evaluated in the field of document classification.

2.2. Semi-Supervised Clustering Semi-supervised clustering is considered an alternative to conventional unsupervised methods. A complete review of some semi-supervised clustering algorithms is presented by Zhu et al. [23].

In a study, Dara et al. [14] used self-organizing map (SOM) for semi-supervised clustering of texts. First,

unlabeled texts are labeled, and then these texts, along with the previously labeled texts, are used to train the classifiers. However, their proposed method does not specify how much re-tagging of unlabeled data is required, which is one of the disadvantages of this method. A combination of Naive Bayes and Expectation Maximization (NBEM) algorithms for semi-supervised clustering was also presented [15]. This model repeatedly tags unlabeled data in a loop and uses this newly labeled data to retrain the model. Basu et al. [24] suggested MCP KMEANS, a method that merges two similarity-based and search-based clustering approaches. Although a combination of these two approaches may enhance clustering quality, their objective function may fall to a local minimum. Zhang et al. [25] designed an algorithm named TESC for text classification using semi-supervised clustering. The main difference between this method and other semi-supervised methods is that this method uses labeled and unlabeled documents together. The TESC algorithm assumes that the document set consists of several components and uses a clustering process to obtain these text components. After clustering, the process of classifying test documents is based on calculating the distance to the clusters' centroids.

Lee et al. [26] proposed a distributed method for semi-supervised documents clustering similar to the TESC algorithm. The difference between this method and the TESC method is that clustering is distributed and performed by several sub-algorithm simultaneously. The results are then collected from sub-clusters. The advantage of this method is higher speed and accuracy that can compete with the TESC method. Gan et al. [27] state that prior knowledge can reduce the quality of semi-supervised clustering if incorrectly collected. The basic premise is that when the label of a labeled sample is identified as risky, the predictions of the labeled instance and the nearest homogeneous unlabeled instances should be similar. This is performed through unsupervised clustering then creating a local graph to model the similarities between the labeled and the nearest unlabeled instances.

In another algorithm, document clustering using automatic generation constraints is applied to classify documents [28]. The intrinsic structure of the text data is analyzed using a partial clustering algorithm. The clustering algorithm allows reaching a set of must-link/cannot-link constraints that can be applied in semi-supervised clustering. Constraints are then considered as a semi-supervision factor in a hierarchical clustering algorithm.

Lu et al. proposed a method that uses concept factorization to improve document clustering performance with supervisory data [29]. This approach involves pairwise penalty and reward constraints on conceptual

factorization, which can guarantee that the data points of a cluster in the main space are still in the same cluster in the converted space.

In this paper, we present a method that uses labeled and unlabeled data simultaneously; however, our method is different from earlier approaches as well as the TESC method. In the TESC method, most data are labeled and only less than 3% of the data are unlabeled. In the proposed method of this research, large fractions of data are unlabeled and only a limited number of labeled data are used. This difference significantly reduces the cost of data tagging in real-world applications. In addition, most of the mentioned semi-supervised document clustering methods neglect the issue of document representation, which can greatly affect the clustering results. In this paper, a semi-supervised document clustering algorithm based on the conceptual representation of documents is presented that can be used in a variety of applications.

3. THE PROPOSED METHOD

This paper introduces an innovative semi-supervised clustering approach for news documents based on their conceptual representation. It is assumed that the input document set is split into unlabeled and labeled documents. Each document is constituted of a set of words. The purpose is to reach a clustering model $C = \{C_1, \dots, C_m\}$ of the documents, such that $\bigcup_{1 \leq i \leq m} C_i = D$ and $C_i \cap C_j = \emptyset$ ($1 \leq i \neq j \leq m$), where (D) = Document set.

Figure 1 presents the complete training procedure of the suggested model, expressed in terms of three steps: preprocessing, document representation, and clustering. This method, which represents documents based on their constituent concepts, takes advantage of the simultaneous use of both labeled and unlabeled data types for document clustering. In the following sections, we describe in detail all three steps of the proposed model.

3.1. Text Preprocessing

Initially, documents are tokenized after removing stop-words and pre-processing the texts. The word embedding model Word2Vec [30] is utilized to train word relationships from the input document set. The tokenized words of documents set are employed as an input for training the Word2Vec model. Consequently, each token in the words set (W) is: represented with a dense vector in the embedded space. The most notable contribution of the Word2Vec neural network model is that words that occur in a similar text are placed close to each other in the embedded space, after clustering these embedded words, words with related meanings are

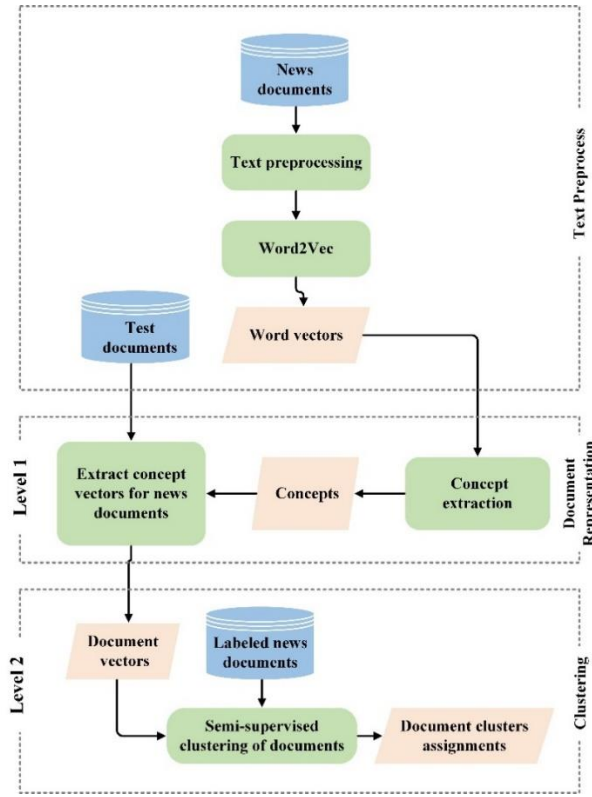


Figure 1. Proposed document clustering model

placed in the same cluster and concept, which helps to maintain semantic relationships between words.

3. 2. Documents Representation

Documents representation is based on the concepts extracted from the data corpus. In the document representation stage, firstly a set of concepts are extracted from the set of words W , such that each concept consists of an exclusive set of words. The main idea for deriving concepts is to implement a clustering algorithm on a set of words (W) to group it into several clusters, each of which represents a concept. Following the construction of the concepts, each document is represented by a vector formed by concepts (\vec{d}).

The Spherical K-Means clustering algorithm employing the cosine distance is applied to cluster word vectors. The procedure of the Spherical K-Means algorithm is the same as the K-Means clustering algorithm and it assigns each data to a cluster with a predetermined value for the number of clusters, and updates each cluster center according to the cluster data membership in the previous iteration. Since Word2Vec maximizes the cross-product of embedded vectors and context vectors, the cosine distance has been used as the proper criterion for clustering nearby

word vectors into a common cluster and measuring distances between word vectors in semantic space.

Each cluster created by Spherical K-Means clustering is considered as a concept. Document vectors are constructed using these concepts. Words with similar meanings are divided into the same cluster according to the clustering efficiency and semantic space trained by the Word2Vec. Therefore, each word in the text corpus will be regarded as a concept's member. Because each word may be present in many documents, it is not a proper discriminator for machine learning applications [31], so Concept Frequency - Inverse Document Frequency (CF-IDF) Equation (1) is applied to the produced word vectors to eliminate the unfavorable effects of common words between concepts.

$$CF-IDF(c_i, d_j, D) = CF(c_i, d_j) \times \log \frac{|D|}{|d \in D; c_i \in D|} \quad (1)$$

where $(c_i, d_j, D) = (Concept_i, Document_j, Corpus)$

The number of concepts and consequently the length of document vectors are arbitrary and defined by the user considering the processing complexity and storage constraints. It may also be determined experimentally according to the dataset. In this regard, the clustering accuracy may be evaluated for an increasing number of concept. As reported later in the experiments, it is observed that after a certain value, the accuracy does not change significantly. This value can determine number of concepts. After extracting the document vectors, it is time to cluster the documents. For this purpose, the clustering algorithm is implemented on the conceptual vectors of documents.

3. 3. Semi-supervised Clustering

Once the documents have been created based on the conceptual representation, it is time to cluster the constructed document vectors. In the clustering process, two documents with similar concepts are expected to have the same vectors. In this step, which uses both unlabeled and labeled data types, labeled documents are used as supervisors of the clustering process. Labeled and unlabeled document vectors are entered as input to the semi-supervised clustering algorithm. Spherical K-Means clustering is used to partition vectors. The resulting clusters may contain data from several different labels, so in a purification process described below, the gross clusters are broken down into smaller pure clusters.

Based on the data labels in each cluster, the proposed algorithm decides whether the cluster needs to be purified or is already pure. Also, the decision on how many smaller clusters to break the gross cluster is one of the tasks of the clustering algorithm, which is performed according to the

following purification procedure which is repeated until all clusters have a label:

1. The cluster contains data from only one label: the cluster is transferred to the final clustering result.

2. The cluster contains both unlabeled data and data from one label: The label of labeled data is selected as the cluster label.

3. The cluster contains several different labels: The cluster is divided into the number of labels and each of these sub-clusters contains only one type of data label.

4. The cluster contains several labels and unlabeled data: Purification is performed according to procedure 3, with the difference that unlabeled data will also have a separate sub-cluster.

5. The cluster is composed entirely of unlabeled data: Using the cosine distance, the nearest center of the labeled cluster is selected and its label is assigned as the label of this unlabeled cluster.

Once the purification is complete, all clusters will have an appropriate label.

After the document vectors are clustered using the semi-supervised clustering described in Figure 1, the document output clusters are identified as components of the text corresponding to the document categories. Each of these clusters is labeled and can be used in the test data clustering process. Each test data uses the cosine distance to find the nearest center of the cluster and chooses the label of that cluster as its label.

The method proposed in this research has the following contributions:

Previous methods of document representation have disadvantages such as not maintaining non-linear semantic relationships between words. Also, neural network-based methods such as Doc2Vec suffer from low interpretability. The method proposed in this paper is based on the conceptual representation of documents, in addition to maintaining non-linear relationships, has high interpretability and intuition. Since the proposed method is a semi-supervised clustering method, large amounts of data can be clustered and categorized with acceptable accuracy with low overhead and low cost. This point is beneficial in the application of social networks and stream data where the amount of unlabeled data is large. One of the most important advantages of this method over deep learning methods is that, unlike deep learning networks, the logic of the proposed method is clear, and with the addition of new data, there is no need to re-train the model.

3. 4. Complexity Analysis Since the proposed model consists of two levels, the time complexity of each level is calculated separately and the training total time complexity is obtained from the sum of these two values. At the first stage, to form the concept vectors of documents, due to the

existence of the Word2Vec model, the time complexity value is equal to $O(N * \log(V))$, where N is the total corpus size and V is the unique-words vocabulary count [17]. Also, the time complexity of the concept extraction part is equal to $O(tkV)$, where t is the number of iterations of the algorithm, and k is the number of concepts.

In the second step, the semi-supervised clustering algorithm is calculated with time complexity $O(t'mN + N)$, where t' is the number of iterations of the algorithm, and m is the number of final clusters. As a result, the overall time complexity of the architecture presented in this method is a maximum of $O(N * \log(V) + tkV + t'mN)$.

4. DATASET

In this paper, two datasets consisting of news documents are used to evaluate the proposed model. The Reuters-21578 news dataset includes a collection of news items published on the news agencies' websites. The Reuters-21578 set of documents is related to the news that was published on the Reuters website in 1987, which was collected by Reuters' staff in 1991. In this study, 2110 documents from four different categories are chosen as "agriculture" (571 documents), "crude" (580 documents), "trade" (483 documents), and "interest" (476 documents) are randomly selected after deleting the uncommon words.

The second dataset is the BBC News documentation, which includes 2,225 news documents published from 2004 to 2005, and was compiled in five categories in 2006. In this study, all 2225 documents from five different categories are chosen as follows: "tech" (401 documents), "sport" (511 documents), "politics" (417 documents), "entertainment" (386 documents), and "business" (510 documents).

Some common natural language pre-processing tasks, such as case folding (converting uppercase to lowercase letters), removing punctuations, removing stop-words, and tokenization, are applied to the document collection. For fast Word2Vec training, words that have occurred less than 5 times in the entire datasets are removed.

5. EXPERIMENTS

Various experiments have been designed and performed to observe the performance of the proposed model. The proposed model is compared with K-Means, Bag-of-Concepts (BoC) [16], TESC (BoW) [25], and Doc2Vec [10]. To compare, there is a need for criteria to measuring the efficiency of the mentioned methods, which are described in the following.

The Normalized Mean Squared Error (NMSE) criterion expresses the quality of the clustering performed. This criterion calculates the average squares of the errors, and the normalized numerical value gives an output between 0 and 1, and smaller values show a lower variance within the cluster. The NMSE metric is defined in Equations (2) and (3), in which μ is the set of cluster centers, X is the set of data points, and μ_{c_i} is the cluster centroid of the data point x_i .

$$MSE(X, \mu) = \frac{1}{N} \sum_i (x_i - \mu_{c_i})^2 \quad (2)$$

$$NMSE(X, \mu) = \frac{1}{N} \frac{\sum_i (x_i - \mu_{c_i})^2}{\sum_i (x_i)^2} \quad (3)$$

The Normal Mutual Information (NMI) is a cluster criterion that evaluates the quality of data clustering according to their pre-given labels. The NMI evaluates how the clustering algorithm can reconstruct the original data labels [32]. This criterion can be used when the data label is available. The output of this numerical criterion is in the range [0,1], which shows the statistical similarity between the labels of the generated clusters and the original labels of the data. A value of zero indicates a failed cluster assignment, while values close to one indicate that clustering can recreate real data classes. The NMI criterion shows better performance in presenting the quality of clusters than the entropy criterion. This is because the entropy criterion depends on the number of clusters, and the higher the number, the better the entropy criterion. But the NMI standard is not like this and does not necessarily increase as the number of clusters increases. Equation (4) shows the mathematical definition of this criterion.

$$NMI = \frac{I(C;K)}{(H(C)+H(K))/2} \quad (4)$$

$$I(X;Y) = H(X) - H(X|Y) \quad (5)$$

Equation (5) is the mutual information between the random variables X and Y , $H(X)$ is the Shannon entropy of X , $H(X|Y)$ is the conditional entropy of X given Y , C is the set of class labels and K is the set of cluster labels.

In this paper, not only the quality of the generated clusters is evaluated, but also the real application of this method in the classification of news documents is evaluated. For this purpose, the classification accuracy criterion is introduced, which is a criterion that expresses the performance of a classifier with a percentage value. This value shows that of all the test data, how many data are rightly classified. By dividing the number of rightly classified samples by the total number of samples, the amount of accuracy is obtained. Equation (6) shows the

measure of accuracy. In this regard, \hat{y}_l is the class prediction for example l .

$$Accuracy = \frac{\sum_i 1(\hat{y}_i = y_i)}{|X|} \quad (6)$$

5. 1. Results

5. 1. 1. Effect of the Number of Concepts

In document representation, the number of concepts determines the length of the document vector. Therefore, it would have a significant effect on the performance quality of the proposed model. The performance of the proposed model, in terms of clustering quality and classification accuracy, when the number of concepts varies, is shown in Table 1. According to the results of this table, the best performance occurs when the number of concepts is 300 and after that, there is no noticeable increase in both clustering and classification accomplishments. Compared to BoW method, which depends on the number of words in the text, a significant improvement in classification accuracy is observed. Also, compared to BoC method, which displays the text conceptually, it is observed that with the addition of labeled documents, the proposed model shows its superiority. In subsequent experiments, the length of the document vector is assumed to be 300.

5. 1. 2. Effect of Window Size

In the suggested model, to maintain nonlinear semantic relations between words, a word embedding method Word2Vec is used. Word2Vec neural network training depends on parameters that one of the most important parameters is the size of the window. At each stage of the neural network training, a slider window is moved on the text so that the words in this window can be used as input and output of the neural network. Experiments have shown that the larger the window size, the model would be trained better, and the generated word vectors would be more effective as a result of clustering.

Tables 2 and 3 examine the effect of window size changes on clustering quality and document classification accuracy. As shown in Tables 2 and 3, the performance of the proposed model improves as expected by increasing the window size. This performance improvement is obtained because the neural network encounters more words at each stage and can predict output more likely. Semantic relationships between words are more discovered and have a significant effect on the weight of the neural network. In this experiment, 80 percent of data is used for training with 200 labeled documents.

The values mentioned for NMI and NMSE indicate that as the window size increases in word embedding, the

quality of the clusters also improves. For example, in Table 2 (Reuters-21578), when the window size changes from 4 to 20, the NMI value increases from 0.274 to 0.33, which indicates better quality. The mean squared error also shows a decreasing trend. As the evaluation metrics are negligibly improved in larger window sizes, in order to avoid additional overhead and reduce the time complexity, a window size of 8 is considered to train the Word2Vec model in subsequent experiments.

TABLE 1. Performance of the proposed model when the number of concepts varies - (Reuters-21578)

| Number of Concepts | 100 | 200 | 300 | 400 | 500 | 600 |
|---|-------|-------|--------|-------|-------|-------|
| Proposed Model Classification Accuracy (%) | 69.33 | 74.20 | 76.32 | 76.12 | 77.02 | 77.13 |
| BoC Classification Accuracy(%) [16] | | | 66.31 | | | |
| TESC (BoW) Classification Accuracy (%) [25] | | | 62.65 | | | |
| Proposed Model Clustering NMSE | 0.124 | 0.114 | 0.106 | 0.107 | 0.105 | 0.103 |
| BoC Clustering NMSE [16] | | | 0.1340 | | | |
| TESC (BoW) Clustering NMSE [25] | | | 0.1803 | | | |

TABLE 2. Performance of the proposed model when the size of the window varies - (Reuters-21578)

| Window Size | 4 | 8 | 20 |
|-------------------------|--------|--------|--------|
| Classification Accuracy | 63.9 % | 67% | 72% |
| NMI | 0.274 | 0.33 | 0.38 |
| NMSE | 0.1191 | 0.1031 | 0.1007 |

TABLE 3. Performance of the proposed model when the size of the window varies - (BBC News)

| Window Size | 4 | 8 | 20 |
|-------------------------|--------|--------|--------|
| Classification Accuracy | 74.5 % | 76.7% | 76.8% |
| NMI | 0.421 | 0.449 | 0.511 |
| NMSE | 0.1038 | 0.0961 | 0.0904 |

TABLE 4. NMI scores of news document clustering for proposed model compared with K-Means, TESC (BoW), and Doc2Vec at the various percentage of labeled documents – (Reuters-21578)

| The percentage of labeled documents (# of labeled documents) | 4% (100) | 9% (200) | 14% (300) | 18% (400) | 22% (500) | 27% (600) |
|--|--------------|--------------|--------------|--------------|--------------|--------------|
| K-Means | 0.198 | 0.261 | 0.305 | 0.342 | 0.367 | 0.345 |
| TESC [25] | 0.165 | 0.189 | 0.306 | 0.397 | 0.413 | 0.388 |
| Doc2Vec [10] | 0.243 | 0.292 | 0.362 | 0.375 | 0.413 | 0.421 |
| Proposed model | 0.331 | 0.370 | 0.435 | 0.457 | 0.460 | 0.481 |

5.1.3. Effect of the Number of Labeled Documents

Another factor influencing the quality of semi-supervised text clustering is the number of labeled documents. To observe the effects of labeled data on the quality of clustering, an experiment is designed in which the number of labeled data changes though the number of unlabeled data is kept constant. In this analysis, 80% of the documents are used for training and the remaining 20% for testing. Tables 4 and 5 show the NMI values of proposed model clustering for various numbers of labeled documents compare to other methods when the number of unlabeled documents is fixed.

Clustering with the proposed model on Reuters-21578 is of better quality than other methods. It is also noteworthy that as the number of labeled documents increases, the NMI value and therefore the clustering quality increases significantly. For example, in a case, when 9% of all documents are labeled (200 documents), the value of The proposed method is 0.370, TESC (BoW) 0.189, Doc2Vec 0.292, and K-Means 0.261. In the worst case, when only 4% of all documents are labeled (100 documents), the NMI value of the proposed model does not fall below 0.331, while other methods produce far fewer NMIs and lower quality clusters. The same trend and performance for the BBC News dataset can be seen in Table 5.

As can be concluded from Tables 4, 5, and Figure 2, with the increase of labeled documents, the quality of the resulting clustering has an increasing trend. Comparing the values in Tables 4 and 5, it can be seen that the architecture presented in this paper for semi-supervised clustering of documents has significantly improved the quality of news document clustering. Because of the concepts and components of the text have been extracted, the proposed method can create cluster labels corresponding to documents classes, which is why the NMI in the proposed method is higher than other methods.

Tables 6 and 7 show the accuracy of the classification of news documents for the proposed method compared to other methods. As can be seen from these tables, the

TABLE 5. NMI scores of news document clustering for proposed model compared with K-Means, TESC(BoW), and Doc2Vec at the various percentage of labeled documents – (BBC News)

| The percentage of labeled documents (# of labeled documents) | 4% (100) | 9% (200) | 14% (300) | 18% (400) | 22% (500) | 27% (600) |
|--|--------------|--------------|--------------|--------------|--------------|--------------|
| K-Means | 0.236 | 0.301 | 0.338 | 0.361 | 0.389 | 0.390 |
| TESC [25] | 0.200 | 0.237 | 0.352 | 0.432 | 0.463 | 0.469 |
| Doc2Vec [10] | 0.339 | 0.365 | 0.393 | 0.420 | 0.437 | 0.494 |
| Proposed model | 0.421 | 0.453 | 0.471 | 0.478 | 0.529 | 0.555 |

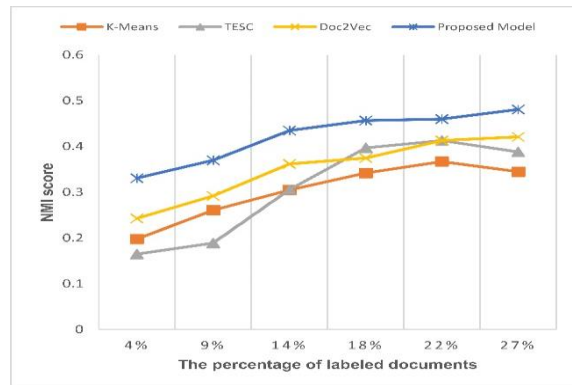


Figure 2. NMI scores of news document clustering for proposed model compared with K-Means, TESC(BoW), and Doc2Vec at the various percentage of labeled documents – (Reuters-21578)

TABLE 6. News document classification accuracy of the proposed model compared with TESC (BoW), and Doc2Vec at the various number of labeled documents – (Reuters-21578)

| Number of labeled documents | 200 | 250 | 300 | 350 | 400 | 450 |
|-----------------------------|--------------|--------------|--------------|--------------|--------------|--------------|
| TESC (BoW) (%) [25] | 63.32 | 64.02 | 64.23 | 65.36 | 66.32 | 66.90 |
| Doc2Vec (%) [10] | 64.00 | 67.23 | 70.64 | 72.23 | 71.62 | 73.17 |
| BoC [16] | 66.31 | | | | | |
| Proposed model (%) | 72.06 | 74.45 | 75.12 | 76.01 | 76.11 | 77.37 |

TABLE 7. News document classification accuracy of the proposed model compared with TESC (BoW), and Doc2Vec at the various number of labeled documents – (BBC News)

| Number of labeled documents | 200 | 250 | 300 | 350 | 400 | 450 |
|-----------------------------|--------------|--------------|--------------|--------------|--------------|--------------|
| TESC (BoW) (%) [25] | 64.68 | 68.19 | 69.46 | 71.37 | 72.11 | 72.45 |
| Doc2Vec (%) [10] | 67.81 | 69.60 | 73.42 | 76.35 | 76.57 | 77.92 |
| BoC [16] | 69.45 | | | | | |
| Proposed model (%) | 75.51 | 76.67 | 77.84 | 78.71 | 81.34 | 81.92 |

classification accuracy of the proposed method is at least 4% superior to other methods. It is clear that with the increase of labeled documents, the accuracy of classifying news texts has increased.

6. CONCLUSION

In this research, a concept-based method for semi-supervised clustering of news documents is presented. The main idea is that the way documents are represented affects the quality of clustering and classification of documents. For this purpose, a two-level semi-supervised clustering is proposed that extract concepts from corpus words, and represents documents based on the concepts. This method of document representation overcomes the weaknesses of previous methods and has high interpretability by describing documents in low dimensions. The method proposed for clustering document vectors is a semi-supervised method that uses a limited amount of labeled data. This method uses unlabeled data to capture the overall structure of clusters and labeled data to set cluster centers. It also identifies the structure and components of the text and creates clusters corresponding to the data classes. Experiments have shown that the method proposed in this paper has a significant advantage over other methods of semi-supervised clustering of the text. Also, the effect of various parameters such as window size, document length (number of concepts), and number of labeled documents have been studied and evaluated. The results are satisfactory but more studies can be done in the future. For example, the use of N-Grams in training the Word2Vec neural network model may produce better results.

7. REFERENCES

1. Forsati. R, Mahdavi. M, Kangavari. M, Safarkhani. B, "Web page

- clustering using harmony search optimization", In *2008 Canadian Conference on Electrical and Computer Engineering IEE* 1601-1604, <https://doi.org/10.1109/CCECE.2008.4564812>.
2. Bouras. C, Tsogkas. V, "A clustering technique for news articles using WordNet", *Knowledge-Based Systems*, Vol. 36, (2012) 115-128, <https://doi.org/10.1016/j.knsys.2012.06.015>.
 3. Karypis. M, Kumar. V, Steinbach. M, "A comparison of document clustering techniques", (2000). the University of Minnesota Digital Conservancy, <https://hdl.handle.net/11299/215421>.
 4. Bobadilla. J, Ortega. F, Hernando. A, Gutiérrez. A, "Recommender systems survey", *Knowledge-Based Syst.*, Vol. 46, (2013), 109-132, <https://doi.org/10.1016/j.knsys.2013.03.012>.
 5. Barzegar Nozari. R, Koochi. H, Mahmodi. E, "A Novel Trust Computation Method Based on User Ratings to Improve the Recommendation", *International Journal of Engineering, Transactions C: Aspects*, Vol. 33, (2020), 377-386, <https://doi.org/10.5829/IJE.2020.33.03C.02>.
 6. Djenouri. Y, Belhadi. A, Fournier-Viger. P, Lin. J, "Fast and effective cluster-based information retrieval using frequent closed itemsets", *Information Sciences*, Vol. 453, (2018), 154-167, <https://doi.org/10.1016/j.ins.2018.04.008>.
 7. Joty. S, Carenini. G, Ng. R, "Topic segmentation and labeling in asynchronous conversations", *The Journal of Artificial Intelligence Research*, Vol. 47, (2013), 521-573, <https://doi.org/10.1613/jair.3940>.
 8. Li. Y, Guo. H, Zhang. Q, Gu. M, Yang. J, "Imbalanced text sentiment classification using universal and domain-specific knowledge", *Knowledge-Based Systems*, Vol. 160, (2018), 1-15, <https://doi.org/10.1016/j.knsys.2018.06.019>.
 9. Jacovi. A, Shalom. O, Goldberg. Y, "Understanding Convolutional Neural Networks for Text Classification", *ArXiv*, (2018), arXiv preprint arXiv:1809.08037.
 10. Le. Q, Mikolov. T, "Distributed Representations of Sentences and Documents", *International Conference on Machine Learning*, PMLR, Vol. 32, (2014), 1188-1196.
 11. Zhang. W, Yoshida. T, Tang. X, Wang. Q, "Text clustering using frequent itemsets", *Knowledge-Based Systems*, Vol. 23, (2010), 379-388, <https://doi.org/10.1016/j.knsys.2010.01.011>.
 12. Cozman. F, Cesar Cirelo. M, "Semi-Supervised Learning of Mixture Models", *Proceedings of the Twentieth International Conference on Machine Learning (ICML-2003)*, Washington DC, Vol. 4, (2003), 4-24.
 13. Luo. X, Liu. F, Yang. S, Wang. X, Zhou. Z, "Joint sparse regularization based Sparse Semi-Supervised Extreme Learning Machine (S3ELM) for classification", *Knowledge-Based Systems*, Vol. 73, (2015), 149-160, <https://doi.org/10.1016/j.knsys.2014.09.014>.
 14. Dara. R, Kremer. S, Stacey. D, "Clustering unlabeled data with SOMs improves classification of labeled real-world data", *Proc. International Joint Conference on Neural Networks*, (2002), 2237-2242, <https://doi.org/10.1109/ijcnn.2002.1007489>.
 15. Zhang. W, Yang. Y, Wang. Q, "Using Bayesian regression and EM algorithm with missing handling for software effort prediction", *Information and Software Technology*, Vol. 58, (2015), 58-70, <https://doi.org/10.1016/j.infsof.2014.10.005>.
 16. Kim. HK, Kim. H, Cho. S, "Bag-of-concepts: Comprehending document representation through clustering words in distributed representation", *Neurocomputing.*, Vol. 266, (2017), 336-352, <https://doi.org/10.1016/j.neucom.2017.05.046>.
 17. Deerwester. S, Dumais. S.T, Furnas. G.W, Landauer. T.K, Harshman. R, "Indexing by latent semantic analysis", *Journal of the American Society for Information Science*, Vol. 41, (1990), 391-407, [https://doi.org/10.1002/\(SICI\)1097-4571\(199009\)41:6<391::AID-ASII>3.0.CO;2-9](https://doi.org/10.1002/(SICI)1097-4571(199009)41:6<391::AID-ASII>3.0.CO;2-9).
 18. Mikolov. T, Chen. K, Corrado. G, Dean. J, "Efficient estimation of word representations in vector space", *International Conference on Learning Representations, ICLR*, (2013).
 19. Edara. D.C, Vanukuri. L.P, Sistla. V, Kolli. V.K.K, "Sentiment analysis and text categorization of cancer medical records with LSTM", *Journal of Ambient Intelligence and Humanized Computing*, (2019), 1-17, <https://doi.org/10.1007/s12652-019-01399-8>.
 20. Dai. A.M, Olah. C, Le. Q, "Document Embedding with Paragraph Vectors", *Arxiv*, (2015), 1-8, arXiv preprint arXiv:1507.07998.
 21. Jia. C, Carson. M.B, Wang. X, Yu. J, "Concept decompositions for short text clustering by identifying word communities", *Pattern Recognition*, Vol. 76, (2018), 691-703, <https://doi.org/10.1016/j.patcog.2017.09.045>.
 22. Li. P, Mao. K, Xu. Y, Li. Q, Zhang. J, "Bag-of-Concepts representation for document classification based on automatic knowledge acquisition from probabilistic knowledge base", *Knowledge-Based Systems*, Vol. 193, (2020), <https://doi.org/10.1016/j.knsys.2019.105436>.
 23. Zhu. X.J, "Semi-Supervised Learning Literature Survey", (2005). <http://digital.library.wisc.edu/1793/60444>
 24. Basu. S, Bilenko. M, Mooney. R.J, "Comparing and Unifying Search-Based and Similarity-Based Approaches to Semi-Supervised Clustering", *Proceedings of the ICML-2003 workshop on the continuum from labeled to unlabeled data in machine learning and data mining*, (2003), 42-49.
 25. Zhang. W, Tang. X, Yoshida. T, "TESC: An approach to TEXT classification using Semi-supervised Clustering", *Knowledge-Based Systems*, Vol. 75, (2015), 152-160, <https://doi.org/10.1016/j.knsys.2014.11.028>.
 26. Li. P, Deng. Z, "Use of distributed semi-supervised clustering for text classification", *Journal of Circuits, Systems and Computers*, Vol. 28, No. 8, (2019), 1-13, <https://doi.org/10.1142/S0218126619501275>.
 27. Gan. H, Fan. Y, Luo. Z, Zhang. Q, "Local homogeneous consistent safe semi-supervised clustering", *Expert Systems with Applications*, Vol. 97, (2018), 384-393, <https://doi.org/10.1016/j.eswa.2017.12.046>.
 28. Diaz-Valenzuela. I, Loia. V, Martin-Bautista. M.J, Senatore. S, Vila. M.A, "Automatic constraints generation for semisupervised clustering: experiences with documents classification", *Soft Computing*, Vol. 20, No. 6 (2016), 2329-2339, <https://doi.org/10.1007/s00500-015-1643-3>.
 29. Lu. M, Zhao. X.J, Zhang. L, Li. F.Z, "Semi-supervised concept factorization for document clustering", *Information Sciences*, Vol. 331, (2016), 86-98, <https://doi.org/10.1016/j.ins.2015.10.038>.
 30. Mikolov. T, Sutskever. I, Chen. K, Corrado. G, Dean. J, "Distributed Representations of Words and Phrases and their Compositionality", In *Advances Neural Information Processing Systems*, (2013) 3111-3119.
 31. Robertson. S, "Understanding inverse document frequency: On theoretical arguments for IDF", *Journal of Documentation*, Vol. 60, No. 5 (2004), 503-520, <https://doi.org/10.1108/00220410410560582>.
 32. Strehl. A, Ghosh. J, Mooney. R, "Impact of Similarity Measures on Web-page Clustering", *Workshop on Artificial Intelligence for Web Search*, Vol. 58, (2000), 64.

Persian Abstract

چکیده

صفحات وب و رسانه‌های اجتماعی از نظر مقدار و تنوع مملو از اخبار هستند. خوشه‌بندی اسناد یک روش مفید است که به طور گسترده‌ای در سازماندهی و مدیریت داده‌ها به گروه‌های کوچکتر استفاده می‌شود. یکی از عوامل تأثیرگذار بر کیفیت خوشه‌بندی، نحوه بازنمایی اسناد است. برخی از روش‌های سنتی بازنمایی اسناد به تکرارهای کلمه در متن بستگی دارند و بردارهای سند پراکنده و بزرگی را ایجاد می‌کنند. این روش‌ها نمی‌توانند اطلاعات مجاورتی بین اسناد را حفظ کنند. علاوه بر این، روش‌های مبتنی بر شبکه عصبی که اطلاعات مجاورتی را حفظ می‌کنند، از تفسیرپذیری ضعیف رنج می‌برند. روش‌های بازنمایی متن مبتنی بر مفاهیم بر کاستی‌های روش‌های قبلی غلبه می‌کنند، اما روش‌های خوشه‌بندی نیمه‌نظارتی متن در حال حاضر از نمایش اسناد مبتنی بر مفهوم استفاده نمی‌کنند. در این مقاله یک روش خوشه‌بندی نیمه‌نظارتی متون خبری مبتنی بر مفهوم ارائه شده است که برای دستیابی به کیفیت خوشه‌بندی بالاتر از داده‌های دارای برچسب و بدون برچسب به طور همزمان استفاده می‌کند. در مرحله اول اسناد بر اساس مفاهیم استخراج شده از مجموعه اسناد نمایش داده می‌شوند. سپس، فرآیند خوشه‌بندی نیمه‌نظارتی داده‌های بدون برچسب را برای گرفتن ساختار کلی خوشه‌ها و مقدار کمی از داده‌های دارای برچسب را برای تنظیم مرکز خوشه‌ها به طور همزمان اعمال می‌کند. آزمایش‌های انجام شده بر روی مجموعه داده‌های Reuters-21578 و BBC News نشان می‌دهد که مدل پیشنهادی هم در طبقه‌بندی متن و هم در خوشه‌بندی متن از سایر روش‌های نیمه‌نظارتی بهتر عمل می‌کند.



Effects of Deceleration on Secondary Collisions between Adult Occupants and Vehicle in Frontal Crash Accidents

Z. Wei*

National Quality Supervision and Inspection Center for Engineering Machinery, China Academy of Machinery Science and Technology, Beijing, China

PAPER INFO

Paper history:

Received 20 June 2021

Received in revised form 28 September 2021

Accepted 29 September 2021

Keywords:

Deceleration

Secondary Collision

Adult Occupant

Frontal Crash

ABSTRACT

The paper seeks to highlight and analyze the relationship between the occupants' displacements of chest and pelvis and the deceleration of vehicle in frontal crash accidents. A testing scheme including 5 groups of dynamic tests was devised and conducted. Totally, 5 kinds of acceleration pulses were employed to simulate the real crash. The experimental finding indicates that the integral values and shapes of vehicle's deceleration pulses can influence the occupants' chest and pelvis displacements to some extent; thus, having effects on the risks of secondary collisions between occupants and the vehicle. How the deceleration pulses of vehicle influence the secondary collision is also clarified in the paper by a comprehensive comparison of testing results between different groups. Further research can be carried out on optimization of deceleration pulses of vehicle in the frontal collisions and on how to reduce the risks of secondary collisions based on the findings.

doi: 10.5829/ije.2021.34.12C.11

1. INTRODUCTION

Deaths and injuries from road traffic crashes continue to be major global public health problems and gradually draw more attention. In some countries, reduction in fatalities from road traffic crashes has been treated as one of public policy objectives. Many researches have been conducted and many measures have been taken to tackle the problems [1-3]. As a kind of protection device widely used in the field of passive safety of vehicles, seat belts are of great importance in securing safety and saving lives in frontal crash accidents by restraining the occupants and preventing secondary collisions between drivers or passengers and the vehicle [4]. Without the use of seat belts, frontal crash accidents could actually cause severe injuries and fatalities that should have been preventable or reduced to some extent if occupant restraint systems such as seat belts are employed and function normally [5]. Thoracic injury, lumbar spinal injury, pelvic injury, abdominal injury and many other

kinds of injuries are common in crash accidents, and to a great extent may occur in the secondary collisions without the proper restriction upon the adult occupants' chest and/or pelvic displacements [6, 7]. Displacements beyond limits have become an obvious phenomenon related with the secondary collision directly. Generally speaking, the fewer traffic-related injuries and deaths of occupants are reported in crashes in places with the higher usage rate of seat belts [8]. Therefore, it is necessary to improve seat belt usage rate and public awareness [9, 10]. In addition, measures could be taken to find the factors that affect the usage rate and to curb the misuse and neglect of seat belts crucial for occupants [11].

In many cases, occupants still suffer from injuries or fatalities even if they wear seat belts, for various factors including deceleration of the vehicle which influences occupant restraint systems' safety performance in frontal crash accidents that usually bring about abrupt deceleration [12, 13]. Especially in extreme cases, chances of restraint systems' failure increase and the occupants are exposed to the danger of secondary collisions. Therefore, it deserves deep research on the

*Corresponding Author Institutional Email: wzhk2008@yeah.net (Z. Wei)

failure mechanism of seat belts under specific testing conditions and how to avoid the risk of secondary collisions. To ascertain the effect of vehicle deceleration on the secondary collision between occupants and the vehicle is the essential prerequisite of further research, and also the emphasis of current research.

Compulsory seat belt legislation and corresponding technical standards play an important role in improving seat belt usage rate and promoting safety and standardization of products [14-16]. UN Regulation No. 16 being the uniform provisions concerning the approval of seat belts, specifies the requirements and test methods required for assessment of the safety performance. According to the test methods, dynamic tests can be conducted to obtain the information about the manikin's kinematic characteristics, thus simulating the real crash accidents. The process of real crash reconstruction involves choosing the proper equipment such as trolley and dummy, finishing the specified test procedure, collecting the essential information and analyzing the data obtained, and aims to provide test results as accurately as possible. Even though UN Regulation No. 16 provides a good reference for the current research, the test methods specified by the regulation are executed under the condition that the curve of trolley's acceleration or deceleration is within the zone defined by the low and high corridors. Meanwhile, in order to ensure the objectivity, accuracy and generality, a set of deceleration or acceleration curves should be taken into consideration, and could include but not be limited to the curve specified by the regulation, in view of various factors [17].

Until now there are fewer researches on the effect of vehicle deceleration on injury potentials of adult occupants caused by secondary collisions comparatively. Due to the rapid development of computation and inspection technologies, numerical simulations and experimental research have been conducted to optimize the restraint system, to evaluate the ability of seat belts to protect occupants, and even to investigate injury mechanisms in the crash, etc. [18-20]. As a complement to experimental study, numerical simulation can be used to predict the trends, and yet it needs to be validated by experimental methods [21, 22]. Besides, the accuracy is limited to the algorithm [23]. The research exclusively employs the experimental methods with the aim of getting the more exact results.

Actually, it is of benefit to ascertain the effect for improving the passive safety related with seat belts further. On the one hand, the vehicle deceleration influences the safety performance and poses risks for occupants when seat belts work normally [24]. Most of the time, seat belts can effectively restrain the adult occupants and protect them from the potential secondary collisions. But it doesn't mean that such restraint systems as seat belts can provide

comprehensive protection absolutely, instead it is still of great use in figuring out how to give full play to seat belts' functions. All possible aspects should be taken into consideration in the process, and the effect of vehicle deceleration undoubtedly belongs to the most obvious ones. On the other hand, the vehicle deceleration may be fatal under extreme conditions [25]. Once damages caused by the abrupt deceleration to seat belts make it unable for seat belts to function, or the failure of seat belts restraining occupants' displacements to a safety range occurs, secondary collisions become inevitable and subsequently result in injuries, and even fatalities [26]. Although all kinds of occupant restraint systems including seat belts reduce the risks of collisions between occupants and the vehicle, possibilities of secondary collisions still exist, for the fundamental reason is that the vehicle deceleration makes occupants subject to inertial forces that are closely related with thorax and pelvis displacements. There is a causal link between vehicle deceleration and secondary collisions to some extent. Values of displacements exceeding norms permitted constitutes part and parcel of secondary collisions, and therefore this research focuses on studying and exploring the relationship between vehicle deceleration and displacements of the chest and pelvis.

2. METHODOLOGY

2. 1. Dynamic Test Preparation In frontal crash accidents, the vehicle undergoes rapid or violent deceleration and in the process, the deceleration could be deemed as a function of time within stopping distance. Deceleration versus time profile could be obtained by an accelerometer mounted on the trolley that is employed to simulate real crashes and reproduce the required pulses. Trolleys can be classified into 2 kinds, one being the deceleration type, and the other being the acceleration type. The latter is convenient to use and has excellent properties of repeatability and reproducibility, with a lack of efficiency being the main disadvantage of the former. Therefore, acceleration trolley was chosen as the key equipment to conduct the research and acceleration pulses of the trolley were collected accordingly. Meanwhile, UTAC R16 dummy conforms to the technical regulations such as UN Regulation No. 16, and is suitable to measure the thorax and pelvis displacements. Cable extension position sensor shown in Figure 1 has the advantage of accuracy and reliability, and outweighs other devices used to measure displacements in dynamic tests. Two cable extension position sensors being the better means to measure the parameters required than high speed camera which induces deviations because of camera angles, could be adopted as the measurement devices for

collecting the data of displacements, as displayed in Figure 2.

Deceleration pulses that occur in real crashes could be easily reproduced and simulated by acceleration trolley, and reconstructing the frontal crash is mainly based on the reproduction of the pulses. Only under the conditions that pulses of acceleration are nearly identical to the ones in real crashes, specified by certain regulations or defined regularly can test results be comparable and analyzed. Hence, a testing scheme incorporating a set of dynamic tests using different acceleration pulses was devised in order to ensure objectivity and universality. The testing scheme contains 20 tests involving 5 different kinds of pulses, as is shown in Table 1, and tests generating pulses of the same kind are listed into the same group.

In order to reduce the interference of installation mode, 20 3-point seat belt samples of the same kind were used in the tests, and the coordinate values of anchorages were identical to each other. The recommendations about anchorages by UN Regulation No. 16 were given priority to, and the seat belts were all installed according to the requirements so as to ensure the consistency of test conditions.

2. 2. Test Procedure

The R16 fixture was employed to install seat belts and restrain UTAC R16 dummy to the seat. Before each test and in the process of installation, the retractor had been so installed that the retractor was able to operate correctly and stow the strap efficiently. A board 25 mm thick was placed between the back of the dummy and the seat back. The belt was firmly adjusted to the dummy. The board was



Figure 1. Cable extension position sensor

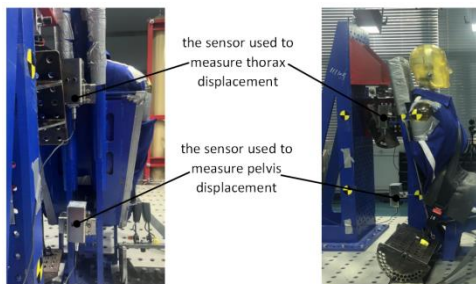


Figure 2. Two sensors installed respectively to measure thorax and pelvis displacements

then removed so that the entire length of its back was in contact with the seat back. A check was made to ensure that the mode of engagement of the two parts of the buckle would entail no risk of reducing the reliability of locking. The final state of the dummy restrained by a 3-point seat belt just before a dynamic test starts is illustrated in Figure 3. The mode was repeated in every installation process to ensure the same initial state before the acceleration trolley was propelled each time.

Besides, the accelerometer was mounted directly at the bottom of the trolley. As the device to monitor the acceleration of trolley, it collected the essential data and then the acceleration pulses were obtained in the tests. Cable extension position sensors were mounted behind the dummy and their heights were equal to those of the dummy's thorax and pelvis measuring positions respectively. Similarly the displacement pulses of dummy were captured and served as the information input for analysis of the risks of secondary collisions. The acceleration trolley was propelled to the acceleration strictly according to the target curves set previously.

2. 3. Safety Assessment

Only when the thorax and pelvis displacements of R16 dummy are controlled to a certain range, the possibilities of secondary collisions can be reduced. As specified in most regulations including UN Regulation No. 16, in the case of 3-point seat belts, the forward displacement shall be between 80 and 200 mm at pelvic level and between 100 and 300 mm at chest level. The evaluation criteria being oriented to injury prevention, are based upon comprehensive consideration of factors such as the inner space of a vehicle, injury mechanism of occupants, and emergency locking properties of seat belt assembly, etc. So values of displacements exceeding the limits could be perceived as non-conformance with regulations concerned, and then risks of collisions are generated.

Furthermore, safety assessment is made under certain conditions that test results are compared and analyzed within groups of tests generating the acceleration pulses that have certain relations with each



Figure 3. R16 dummy restrained by a 3-point seat belt on the trolley of acceleration type

other. On account of regularity of the test scheme especially in the physical specifications of acceleration pulses, the trends of displacements could be displayed by comparing the values acquired by sensors and pulses acquired by the accelerometer.

3. RESULT AND DISCUSSION

After all the dynamic tests, acceleration pulses of the trolley and dummy's displacements of chest and pelvis were collected, classified, and analyzed. As displayed in Figure 4, the first 3 groups of tests were carried out at 3 different settings of amplitudes of acceleration pulses, while the shapes of pulses showed no obvious differences except for the amplitudes, i.e., the lasting time and the trend of each pulse were almost identical to others, but the integral values of the pulses varied to some extent when different acceleration curves were adopted in tests. The integral value of acceleration pulse for the continuous time is equal to the velocity of the trolley, and the velocity has a positive effect on the trolley's kinetic energy, while the deceleration pulse which is related with many factors such as the vehicle structure, the weight, and collision angle etc., in real crashes, determines how the energy can be absorbed. A total amount of 12 pulses of 3 different kinds were generated in groups I, II and III of tests, as is illustrated in Figure 4. Among the 3 kinds of pulses, one kind is in compliance with requirements about the acceleration curve specified in UN Regulation No. 16, as Figure 5 shows. Figure 6 displays the differences of velocities of trolley. The differences between the 3 kinds of acceleration pulses mainly lie in the amplitudes that are related with the magnitude of kinetic energy under the condition that the lasting time or pulse width of deceleration in each test undergoes few changes. It can be seen from the test results that the condition has been satisfied. Therefore, further inferences can be made based on comparison between the displacement pulses of chest and pelvis, in view of the energy transfer from the trolley to the dummy. As is shown in Figures 7 and

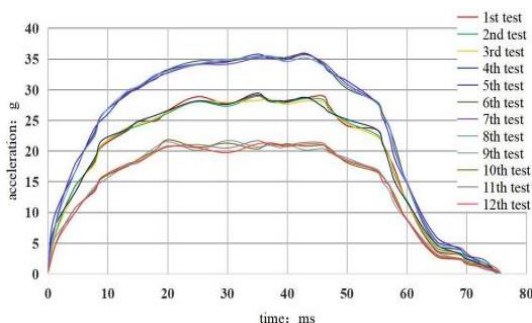


Figure 4. Comparison of acceleration pulses between groups I, II & III

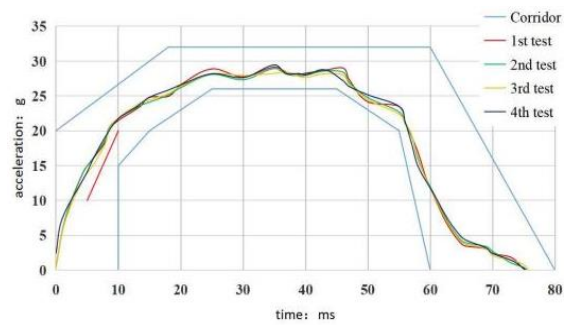


Figure 5. Acceleration pulses in the first 4 dynamic tests in accordance with UN Regulation No. 16

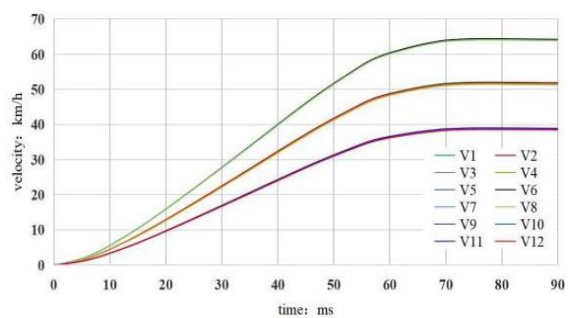


Figure 6. Comparison of velocities between groups I, II & III

8, the displacement pulses show obvious regularity accompanying the changes of acceleration.

In groups IV and V of tests, another 2 kinds of acceleration curves were used and repeated 4 times respectively and subsequently a total amount of 8 acceleration pulses were generated in dynamic tests, as is indicated in Figure 9. In order to facilitate comparison between the results, the 4 test pulses generated in line with the regulation were also displayed in Figures 9 and 10. Meanwhile, measurements of the dummy revealed different patterns of displacement pulses when tests were conducted with different setups, i.e., when different acceleration curves were selected as the objects to simulate in dynamic tests. Integral values of the 3 kinds of acceleration pulses were almost identical with each other, while the pulse widths and amplitudes were different. Although the kinetic energy of the trolley was almost the same in each test, the steep and narrow pulse had the reverse effect on the displacements of dummy with the flat and wide pulse. As displayed in Figures 11 and 12, comparison between displacements of chest and pelvis indicates that the shape of acceleration pulses can influence the possibility of secondary collision even when the velocities are the same.

The test results are summarized in Table 1. It shows that when velocity of the trolley is constant, displacement of the dummy and steepness of the pulse move in tandem, i.e., they have a positive correlation. If velocities of the trolley vary and the lasting time of

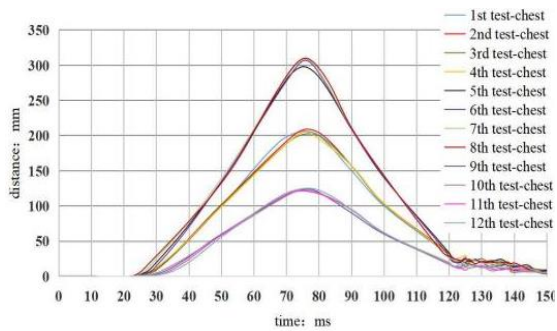


Figure 7. Comparison of distances of dummy’s chest movement between groups I, II & III

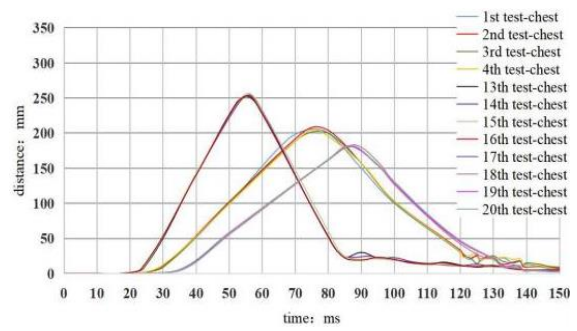


Figure 11. Comparison of distances of dummy’s chest movement between groups I, IV & V

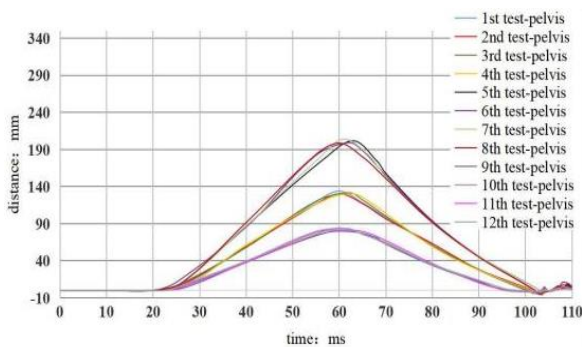


Figure 8. Comparison of distances of dummy’s pelvis movement between groups I, II & III

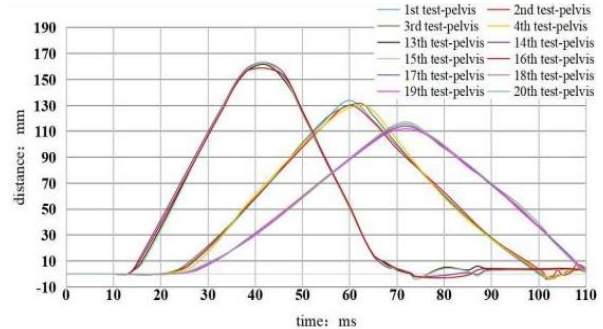


Figure 12. Comparison of distances of dummy’s pelvis movement between groups I, IV & V

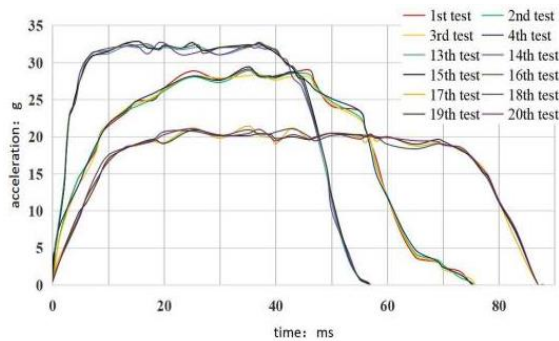


Figure 9. Comparison of acceleration pulses between groups I, IV & V

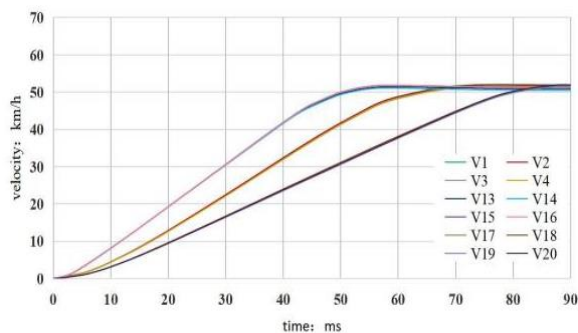


Figure 10. Comparison of velocities between groups I, IV & V

TABLE 1. Results of 20 dynamic tests

| Group No. | Test No. | Trolley velocity (Km/h) | Distance of dummy’s chest movement (mm) | Distance of dummy’s pelvis movement (mm) |
|-----------|----------|-------------------------|---|--|
| I | 1 | 52.1 | 206 | 134 |
| | 2 | 51.9 | 209 | 130 |
| | 3 | 51.6 | 202 | 132 |
| | 4 | 51.5 | 205 | 130 |
| | 5 | 64.2 | 298 | 202 |
| II | 6 | 64.4 | 307 | 199 |
| | 7 | 64.1 | 309 | 204 |
| | 8 | 64.1 | 310 | 198 |
| | 9 | 38.7 | 124 | 79 |
| III | 10 | 39.0 | 121 | 84 |
| | 11 | 39.0 | 122 | 82 |
| | 12 | 38.5 | 125 | 83 |
| IV | 13 | 51.4 | 253 | 162 |
| | 14 | 51.1 | 254 | 163 |
| | 15 | 51.8 | 257 | 163 |
| | 16 | 51.8 | 254 | 159 |
| | 17 | 51.5 | 181 | 114 |
| V | 18 | 51.9 | 183 | 115 |
| | 19 | 51.7 | 182 | 112 |
| | 20 | 52.0 | 183 | 117 |

acceleration pulses remains unchanged, with the shapes of pulses being similar to a great extent, the displacement of the dummy will also be influenced. Taken as 2 variables, displacement of the dummy will increase as velocity of the trolley increases, with other conditions being almost the same. Similarly, when velocity decreases, the displacement also shows the same trend.

4. CONCLUSION

The paper seeks to highlight and analyze the effect of deceleration on secondary collisions between adult occupants and the vehicle based on taking into consideration the relationship between the trolley's acceleration and R16 dummy's chest and pelvis displacements of movement in frontal crash accidents by means of experimental methods.

Findings of conducting the testing scheme reveal that the velocity of vehicle and the shape of vehicle deceleration pulses can both influence the displacements of occupants' chest and pelvis in a crash. Actually, the velocity equals the integral value of vehicle's deceleration. In other words, deceleration of the vehicle is the main factor that has obvious effects on occupants' displacements related directly with secondary collisions. In order to avoid the risk of secondary collisions, it's necessary to reduce the vehicle velocity which may lead to different amplitudes of deceleration pulses. Meanwhile, improving the structure of vehicle and safety performance of seat belts is also of importance, for it'll optimize the deceleration pulses and bring about lower possibilities of secondary collisions.

5. REFERENCES

1. Taheri, M., Arkat, J., Farughi, H., Pirayesh, M., "Modeling Traffic Signal Control System at an Isolated Intersection using Queuing Systems", *International Journal of Engineering, Transactions C: Aspects*, Vol. 34, No. 09, (2021) 2077-2086. DOI: 10.5829/ije.2021.34.09c.05
2. Habibi, M., Broumandnia, A., Harounabadi, A., "Improvement of Multi-agent Routing Guidance with an Intelligent Traffic Light Scheduling and the Ability to Select Intermediate Destinations", *International Journal of Engineering, Transactions A: Basics*, Vol. 34, No. 04, (2021) 854-862. DOI: 10.5829/ije.2021.34.04a.11
3. Muniraj, D., Sreehari, V. M., "Experimental Damage Evaluation of Honeycomb Sandwich with Composite Face Sheets under Impact Load", *International Journal of Engineering, Transactions A: Basics*, Vol. 34, No. 04, (2021) 999-1007. DOI: 10.5829/ije.2021.34.04a.26
4. Marco, C. A., Ekeh, A. P., Hardman, C., Lovell, M., Brent, A., Akamune, J., "Seat belt use among patients in motor vehicle collisions: Clinical and demographic factors", *The American Journal of Emergency Medicine*, Vol. 38, No.6, (2020), 1069-1071. DOI: 10.1016/j.ajem.2019.158367
5. Booker, N., Sung, J., "2088 - Protective Effects of Regular Seat Belt Use on Other Risky Motor Vehicle Behaviors Among Young Drivers", *Journal of Transport & Health*, Vol. 5, (2017), S103. DOI: 10.1016/j.jth.2017.05.262
6. Amiri, S., Naserkhaki, S., Parnianpour, M., "Assessment of lumbar spinal disc injury in frontal crashes", *Computers in Biology and Medicine*, Vol. 123, (2020), 103846. DOI: 10.1016/j.compbimed.2020.103846
7. Tomic, I., Dragas, M., Vasin, D., Loncar, Z., Fatic, N., Davidovic, L., "Seat-Belt Abdominal Aortic Injury—Treatment Modalities", *Annals of Vascular Surgery*, Vol. 53, (2018), 270.e13-270.e16. DOI: 10.1016/j.avsg.2018.05.047
8. Li, A., Shen, S., Nwosu, A., Ratnapradipa, K. L., Cooper, J., Zhu, M., "Investigating traffic fatality trends and restraint use among rear-seat passengers in the United States, 2000–2016", *Journal of Safety Research*, Vol. 73, (2020), 9-16. DOI: 10.1016/j.jsr.2020.02.005
9. Beck, L. F., Kresnow, M., Bergen, G., "Belief about seat belt use and seat belt wearing behavior among front and rear seat passengers in the United States", *Journal of Safety Research*, Vol. 68, (2019), 81-88. DOI: 10.1016/j.jsr.2018.12.007
10. Ojo, T. K., "Seat belt and child restraint use in a developing country metropolitan city", *Accident Analysis & Prevention*, Vol. 113, (2018), 325-329. DOI: 10.1016/j.aap.2018.02.008
11. Hezaveh, A. M., Cherry, C. R., "Neighborhood-level factors affecting seat belt use", *Accident Analysis & Prevention*, Vol. 122, (2019), 153-161. DOI: 10.1016/j.aap.2018.10.005
12. Schellenberg, M., Ruiz, N. S., Cheng, V., Heindel, P., Roedel, E. Q., Clark, D. H., Inaba, K., Demetriades, D., "The Impact of Seat Belt Use in Pregnancy on Injuries and Outcomes After Motor Vehicle Collisions", *Journal of Surgical Research*, Vol. 254, (2020), 96-101. DOI: 10.1016/j.jss.2020.04.012
13. Timonov, P., Goshev, M., Brainova-Michich, I., Alexandrov, A., Nikolov, D., Fasova, A., "Safety belt abdominal trauma associated with anthropometric characteristics of an injured person—a case report", *Egyptian Journal of Forensic Sciences*, Vol. 8, No. 1, (2018). DOI: 10.1186/s41935-018-0085-3
14. Boakye, K. F., Nambisan, S. S., "Seatbelt laws and seatbelt use among front- and rear-seat vehicle occupants in fatal crashes in the United States", *Case Studies on Transport Policy*, Vol. 8, No.3, (2020), 1030-1037. DOI: 10.1016/j.cstp.2020.04.003
15. Allsop, R., Carsten, O., Evans, A., Gifford, R., "Seat belt laws: why we should keep them", *Significance*, Vol.5, No.2, (2008), 84-86. DOI: 10.1111/j.1740-9713.2008.00295.x
16. Harper, S., Strumpf, E. C., Burris, S., Smith, G. D., Lynch, J., "The Effect of Mandatory Seat Belt Laws on Seat Belt Use by Socioeconomic Position", *Journal of Policy Analysis and Management*, Vol. 33, No. 1, (2014), 141-161. DOI: 10.1002/pam.21735
17. Nagasaka, K., Mizuno, K., Thomson, R., "Application of energy derivative method to determine the structural components' contribution to deceleration in crashes", *Traffic Injury Prevention*, Vol. 19, No. 6, (2018). DOI: 10.1080/15389588.2018.1456657
18. Saleh Mousavi-Bafrouyi, S. M., Reza Kashyzadeh, K., Khorsandijou, S. M., "Effects of Road Roughness, Aerodynamics, and Weather Conditions on Automotive Wheel Force", *International Journal of Engineering, B: Applications*, Vol. 34, No. 02, (2021) 536-546. DOI: 10.5829/ije.2021.34.02b.27
19. Bigdeli, M., Monfared, V., "The Prediction of Stress and Strain Behaviors in Composite Gears using FEM", *International Journal of Engineering, B: Applications*, Vol. 34, No. 02, (2021) 556-563. DOI: 10.5829/ije.2021.34.02b.29

20. Yang, K., Sha, Y., Yu, T., "Axial Compression Performance of Square Tube Filled with Foam Aluminum", *International Journal of Engineering, Transactions B: Applications*, Vol. 34, No. 05, (2021) 1336-1344. DOI: 10.5829/ije.2021.34.05b.29
21. Pan, J., Fang, H., Xu, M. C., Xue, X. Z., "Dynamic performance of a sandwich structure with honeycomb composite core for bridge pier protection from vehicle impact", *Thin-Walled Structures*, Vol. 157, (2020). DOI: 10.1016/j.tws.2020.107010
22. H. Hosseinnajad, M. A. Lotfollahi -Yaghin, Y. Hosseinzadeh, A. Maleki, "Evaluating Performance of the Post-tensioned Tapered Steel Beams with Shape Memory Alloy Tendons", *International Journal of Engineering, Transactions A: Basics*, Vol. 34, No. 04, (2021), 782-792.
23. Semenova, E. K., Berkov, D. V, Gorn, N. L., "Evaluation of the switching rate for magnetic nanoparticles: Analysis, optimization, and comparison of various numerical simulation algorithms", *Physical Review B*, Vol. 102, No. 14, (2020). DOI: 10.1103/PhysRevB.102.144419
24. Durrani, U., Lee, C., Shah, D., "Predicting driver reaction time and deceleration: Comparison of perception-reaction thresholds and evidence accumulation framework", *Accident Analysis and Prevention*, Vol. 149, (2021), 105889. DOI: 10.1016/j.aap.2020.105889
25. Gualniera, P., Scurria, S., Sapienza, D., Asmundo, A., "Thoracic aorta rupture due to deceleration injury in a motor vehicle accident", *Gazzetta Medica Italiana Archivio per Le Scienze Mediche*, Vol. 177, No. 5, (2018). DOI: 10.23736/S0393-3660.17.03549-5
26. Xie, K., Ozbay, K., Yang, H., "Secondary collisions and injury severity: A joint analysis using structural equation models", *Traffic Injury Prevention*, Vol. 19, No. 2, (2018), 189-194. DOI: 10.1080/15389588.2017.1369530

Persian Abstract

چکیده

این مقاله به دنبال برجسته سازی و تجزیه و تحلیل رابطه بین جابجایی سرنشینان در قفسه سینه و لگن و کاهش سرعت خودرو در تصادفات از جلو است. یک طرح آزمایشی شامل ۵ گروه آزمایش پویا طراحی و اجرا شد. در مجموع، ۵ نوع پالس شتاب برای شبیه سازی تصادف واقعی استفاده شد. یافته های تجربی نشان می دهد که ارزش ها و شکل های یکپارچه ضربان های کاهش سرعت وسیله نقلیه می تواند تا حدی بر جابجایی قفسه سینه و لگن سرنشینان تأثیر بگذارد. بنابراین، بر خطرات برخورد ثانویه بین سرنشینان و وسیله نقلیه تأثیر می گذارد. چگونگی تأثیر پالس های کاهش سرعت خودرو بر برخورد ثانویه نیز در مقاله با مقایسه جامع نتایج آزمایش بین گروه های مختلف روشن شده است. تحقیقات بیشتری را می توان بر روی بهینه سازی پالس های کاهش سرعت خودرو در برخوردهای جلویی و چگونگی کاهش خطرات تصادفات ثانویه بر اساس یافته ها انجام داد.



Engineering Properties of Soil Stabilized with Cement and Fly Ash for Sustainable Road Construction

D. T. Nguyen^a, V. T. A. Phan^{*b}

^a Campus in Ho Chi Minh City, University of Transport and Communications, No 450-451 Le Van Viet St., Tang Nhon Phu A Ward, Thu Duc City, Ho Chi Minh City, Vietnam

^b Faculty of Civil Engineering, Ton Duc Thang University, Ho Chi Minh City, Vietnam

PAPER INFO

Paper history:

Received 18 August 2021

Received in revised form 05 October 2021

Accepted 11 October 2021

Keywords:

Base Layer

Fly Ash

Splitting Tensile Strength

Stiffness of Modulus

Unconfined Compressive Strength

ABSTRACT

This study presents an experimental study of engineering properties of soil stabilized with cement and fly ash for layers in roadway construction. The fly ash was used in this study satisfies the requirement according to ASTM C618. Five proportion mixes were used in this work with varying quantities of ordinary Portland cement amounts of 8, 10% cement and combination of 8% cement with fly ash content of 2%, 4%, and 6%. Specified curing periods of 7, 14, 28 days were applied for all types of specimens. Some engineering tests were carried out, such as unconfined compressive strength (UCS), splitting tensile strength, stiffness of stabilized soil, SEM, and XRD techniques. SEM images, magnified 3000 times, showed that compacted soil structure was found as small and odd particles arranged without gel bound, while cement-fly ash stabilized soil was covered foam formation due to cement-fly ash crystal, and small particles cannot be observed. The peak intensity of silicon oxide was seen in the region 26-28° with an angle of 2θ. In addition, cement and fly ash significantly improved the mechanical properties of stabilized soils. Finally, the specimen containing 8% cement and 2% fly ash at 14-day curing had a splitting tensile strength greater than 0.45 MPa, satisfying the base layer of road construction requirement according to current Vietnamese standards. The obtained results provided a shred of evidence for capable of using fly ash for road construction in the context of an increase in the fly ash generated in thermal power plants.

doi: 10.5829/ije.2021.34.12C.12

1. INTRODUCTION

Vietnam significantly developed and constructed infrastructures such as roads, dams, and industrial zones in recent years. Among them, road construction was more paid attention because of the soft soil layers underneath that caused unexpected collapses and failure. For three past decades, the employments of ordinary cement and blended cement have been developing significantly. Ordinary Portland Cement (OPC) and Portland concrete are prevalent materials in civil engineering due to their strong, durable, and cheap characteristics; however, they have significantly affected environmental drawbacks. Cement manufacture releases significantly CO₂ emissions during the limestone combustion and calcination processes [1].

The properties of clayey soils are usually characterized by compression, low shear strength, low shear capacity, and highly swelling potential [2], resulted in not be capable of using in subbase and subgrade of road construction. Significantly, volume changes due to shrinkage and swelling cause road surface deformation and bearing capacity reduction [3].

Several methods have been considered and employed regarding the soil improvement techniques, including mechanical stabilization, stabilization using soft aggregates, bituminous stabilization, lime stabilization, cement stabilization, thermal stabilization, chemical and electric stabilizations. Various admixtures, such as cement, fly ash, lime, blast-furnace slag cement, enzyme, and calcium chloride, were used in different areas in the world [4-10].

* Corresponding Author Institutional Email: phantoanhvu@tdtu.edu.vn
(V. T. A. Phan)

Recently, pozzolans from waste materials, such as fly ash, rice husk ash, and slag, are considered eco-friendly cementitious materials to replace traditional materials. Literature reviews indicated that using fly ash and cement on soil stabilization materials from local materials can remarkably reduce the cost of construction, especially for road construction [11-18]. For instance, Phan [8] indicated that the unconfined compressive strength, shear strength parameters on consolidated-undrained and unconsolidated-undrained triaxial tests improved with various cement contents of 4-8% OPC; furthermore, results also indicated that Portland cement of 4% was the economical ratio for treated mudstone. Mahedi et al. [19] treated expansive soil with cement, lime, and fly ash and revealed that the Atterberg limits, pH, unconfined compressive strength, and volumetric swell were best with 10% -10% calcium oxide in stabilizers for expansive soils. Simatupang et al. [20] conducted fly-ash-stabilized sands and concluded that UCS and direct shear strength values increased by increasing fly ash content and curing time in the specimen. In Vietnam, although available studies have been conducted to understand the behavior and engineering properties of soil stabilization using cement and lime; there were no apparent reports on engineering properties of using fly ash-cement soil stabilization in the laboratory and practice.

This study investigates the engineering properties of soil stabilized with various concentrations of cement and fly ash contents. Specific engineering properties, such as unconfined compressive strength, splitting tensile strength, elastic modulus, SEM, and XRD methods, were determined with the curing periods of 7, 14, 28 days. The obtained results were expected to consume a high quantity of waste fly ash every year and create a sustainable material for layers in road construction.

2. EXPERIMENTAL PROGRAM

The materials used in this study composed of excavated soil, ordinary Portland cement (OPC), and fly ash (FA).

2. 1. Materials Used

Excavated soil The soil sample for the laboratory test was taken from Cu Chi province, Southern Vietnam. The disturbed soil sample was excavated with a depth of 1m from the surface. The basic physical properties of undisturbed samples are listed in Table 1. The grain size distribution is plotted in Figure 1.

FA Fly ash used in this study was collected from Formosa power station, Dong Nai Province, Vietnam. The engineering properties of fly ash are satisfied with the requirement in ASTM C618 [21]. The distribution of grain size smaller than 45 μ m is 71.9 %, the loss on ignition with the temperature is 3.2%, calcium oxide content is 3.3%.

OPC OPC, grade 40, used in this work was purchased from a local company. The compressive strength, setting time, fineness, specific gravity, and standard consistency gravity of OPC were determined. The test results of fundamental properties are listed in Table 2.

2. 2. Mix Proportions, Sample Preparation, and Testing Methods

Mix proportions Based on TCVN 10379-2014, soils stabilized with inorganic adhesive substances, chemical agent or reinforced composite for road construction, construction and quality control, the additive used is in range of 5-12% by dry soil weight. Thus, to reduce the cement consumption and make use of the fly ash; this

TABLE 1. Basic physical properties of undisturbed soil

| Basic properties | Test value |
|--|------------|
| Specific gravity, Gs | 2.65 |
| Liquid limit, (%) | 27.66 |
| Plastic limit, (%) | 15.48 |
| Plastic index, (%) | 12.18 |
| Maximum dry unit weight (g/cm ³) | 2.057 |
| Optimum water content (%) | 9.90 |

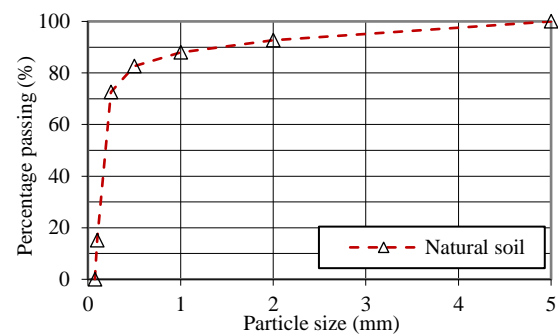


Figure 1. Grain size distribution curve of natural soil

TABLE 2. Properties of OPC 40

| Properties | Tested result |
|------------------------------|---------------|
| Compressive strength | |
| 28 days | 43.5 |
| Setting time, min. | |
| Initial | 133 |
| Final | 172 |
| Fineness, cm ² /g | 3850 |
| Specific gravity | 3.09 |
| Standard consistency, C/W, % | 31.5 |

study used 8, 10% cement, and a combination of 8% cement with 2% FA, 4% FA, and 6% FA which is expected to have enough strength of stabilized soil for subbase and base layers in road construction. A total of 5 sets of mixed proportions was carried out for this experimental program. Natural soil was mixed with five cement and fly ash ratios, including 8%C, 10%C, 8%C+2%FA, 8%C+4%FA, 8%C+6%FA, by dry weight. The specimens were conducted on five mix groups, namely M.8.0, M.10.0, M.8.2, M.8.4, M.8.6, respectively, as presented in Table 3.

Sample preparation This paper concentrates on investigating the optimum amount of fly ash and cement for evaluating the engineering properties of cement-fly ash stabilized soil (CFSS). The specimens were prepared by proctor method, conditioned at room temperature and above 80% relative humidity, then tested with soaked conditions at 7, 14, 28 days. Unconfined compressive strength, splitting tensile strength, the elastic modulus of CFSS specimens were obtained in this study. Furthermore, SEM and XRD techniques were also investigated on the compacted soil and CFSS specimens. This work presents one case as a component of a broader research effort on the properties of locally available soils for construction in Cu Chi province, located in southern Vietnam. The experimental data provide a quantitative basis for further road construction in this area.

Compaction test Standard Proctor compaction tests were performed by AASHTO T99-95, using method A. The specimens were of 101.6 mm diameter and 116 mm height. To conduct tests, the soil, cement, and FA were manually prepared in dry material and different moisture contents. A metal rammer was used with a mass of 2.50 kg and having a flat circular face of 50.8 mm. The rammer was dropped freely from the height of 305 mm. The specimen was prepared in three layers, and 25 blows compacted each layer. Finally, maximum dry unit weight and optimum moisture content were obtained through this test.

Unconfined compressive strength UCS tests of stabilized soil with different cement and FA contents for various curing ages were conducted under AASHTO T208. A metal mold prepared cylindrical specimens with 5 cm in diameter and 10 cm in height at the maximum

dry unit weight and optimum moisture content obtained in the standard Proctor compaction test. After that, the specimens were immediately packed in a plastic bag and stored in a chamber at room temperature, as shown in Figure 2. In addition, all specimens were conditioned by moisture curing and tested after soaking 2 days for a 7-day test and 7 days for 14- and 28-day test.

Splitting tensile strength (STS) ASTM C496-96 was used to test the splitting tensile strength of stabilized soil. The diameter and height of the specimen were 101.6 mm and 116 mm, respectively. Three specimens have been tested for each stabilized soil sample, and the average value of the result has been used for evaluation. The splitting tensile strength is calculated by Eq. [1], as follows:

$$T = 2P/(\pi HD) \quad (1)$$

where T is splitting tensile strength; P is maximum applied load; H and D are the length and diameter of the specimen, respectively.

Stiffness of soil Elastic modulus of stabilized materials is an important parameter required in layered elastic analysis of pavement structure. To determine the elastic modulus, the specimen with the diameter and height is 101.6 mm and 116 mm, respectively, as shown in Figure 3. The elastic modulus test conformed to TCVN 9843-2013 [22] was used in this study.

3. TEST RESULTS AND DISCUSSIONS

A series of tests have investigated the mechanical engineering properties of CFSS specimens. The UCS, STS, and the elastic modulus results are presented, respectively, as below.



Figure 2. Prepared samples



Figure 3. Elastic modulus test

TABLE 3. Proportion mixes

| No. | Mix | Mix proportion (%) | | |
|-----|--------|--------------------|----|----|
| | | Soil | C | FA |
| 1 | M.8.0 | 100 | 8 | 0 |
| 2 | M.10.0 | 100 | 10 | 0 |
| 3 | M.8.2 | 100 | 8 | 2 |
| 4 | M.8.4 | 100 | 8 | 4 |
| 5 | M.8.6 | 100 | 8 | 6 |

3. 1. Unconfined Compressive Strength

Unconfined compressive strength is a common property to evaluate the strength of CFSS specimens. Figure 4 plots the variation of UCS at 7-, 14-, and 28-day curing ages of stabilized soil with various percentages of cement and fly ash %. It can be seen in Figure 4 that the UCS of 7-, 14- day, and 28-day give the value of 4.12-4.99 MPa, 5.26-6.11 MPa, and 7.31-8.03 MPa, respectively. The UCS increased as the curing period increased due to the time-dependent pozzolanic reactions. As shown in Figure 4, the compressive strength of cement stabilized soil increases with a percentage of cement increases in the range of 8-10%. Adding 2% FA yields the greatest compressive strength compared to two other contents at the same cement content. The phenomenon can be attributed to the combination of 2% FA and 8% cement causing the best continuation of the cementitious-hydrated process in the mixture.

3. 2. Splitting Tensile Strength

The STS values of CFSS specimens with various percentages of cement and FA contents are presented in Figure 5. Regarding the effects of cement content on STS, it is depicted from this figure that the STS increased with an increase in cement content up to 10%. On the other hand, an increase in FA content up to 6% caused a decrease in STS, irrespective of curing day. The specimen with 8% C and 2% FA at 14-day curing has an STS greater than 0.45 MPa that satisfies the strength requirement of the base layer for road construction according to TCVN 8858-2011.

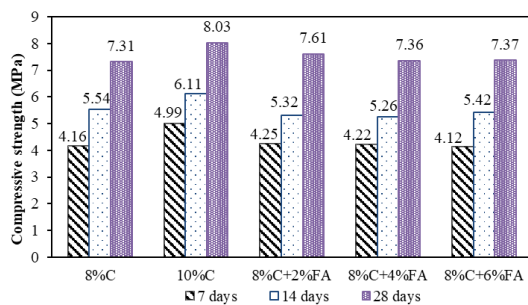


Figure 4. The UCS of cement/cement-FA stabilized soils

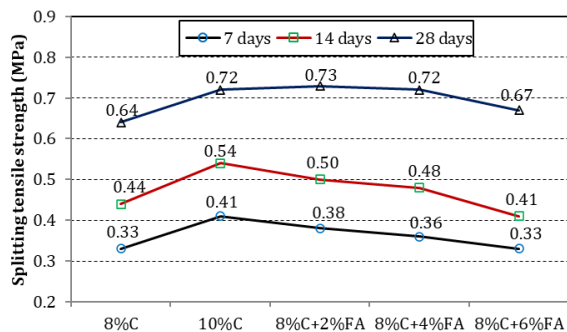


Figure 5. The STS of cement/ cement-FA stabilized soil

Furthermore, it is depicted in Figure 5 that the specimens with the FA contents of 4% and 6% FA are not applicable in a base layer for road construction.

3. 3. Elastic Modulus (E)

The elastic modulus of soil treated with different FA and cement percentages is plotted in Figure 6. The elastic modulus results were in a range of 976-111 MPa, 1033-1305 MPa, 1033-1305 MPa, and 1195-1329 MPa for 7, 14, and 28 days, respectively. Without using FA, a general tendency to increase elastic modulus was found to increase in cement content of 8-10%. More remarkably, using cement and FA improved the elastic modulus with the cement content of 8% and FA content of 2%; after that, the elastic modulus decreased value with a further increase in FA content. The obtained data provided some specific values of elastic modulus, which are very helpful and valuable for designers and site practice for future design and construction, especially for low-cost road construction.

3. 4. SEM and XRD Results

The Scanning Electron Microscope (SEM) technique was employed to investigate the surface of compacted soil and CFSS specimen, magnified by 3000 times, as shown in Figure 7. Figure 7a shows that compacted soil structure was found as small and odd particles arranged without gel bound. On the other hand, Figure 7b shows the foam formation due to the surrounding adhesive, and small particles cannot be observed. The phenomenon was likely attributed to cement, FA, and soil chemical reactions that established cementitious and pozzolanic gels consisting of calcium silicate hydrate (CSH) gel and calcium aluminate hydrate (CAH) gel. Based on the obtained images and the chemical reaction, it can be concluded that the CFSS significantly improved the strength compared to that of compacted soil.

X-ray Diffraction (XRD) is a technique to determine the crystallographic structure of a material. Figure 8 presents the comparison of XRD patterns between compacted soil and cement-FA treated soil specimens. In

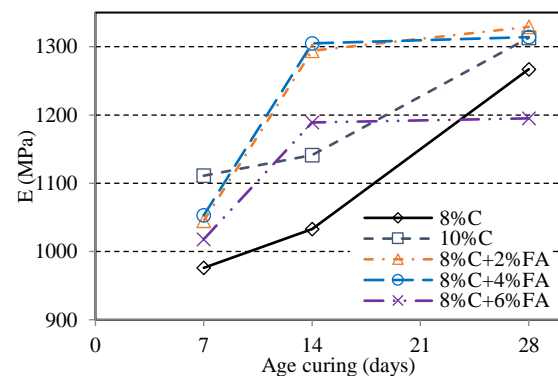
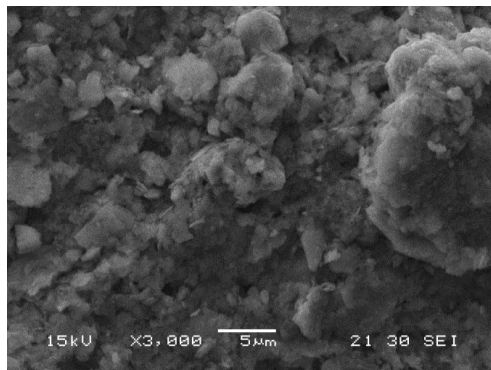
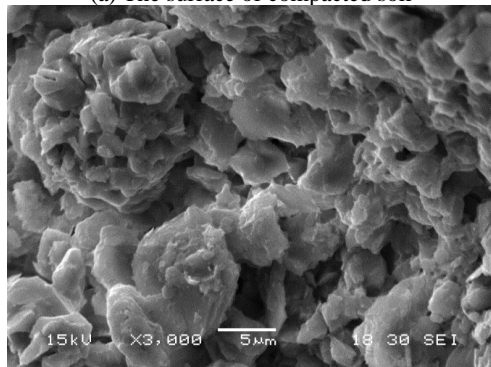


Figure 6. Elastic modulus of cement/ cement-FA stabilized soil

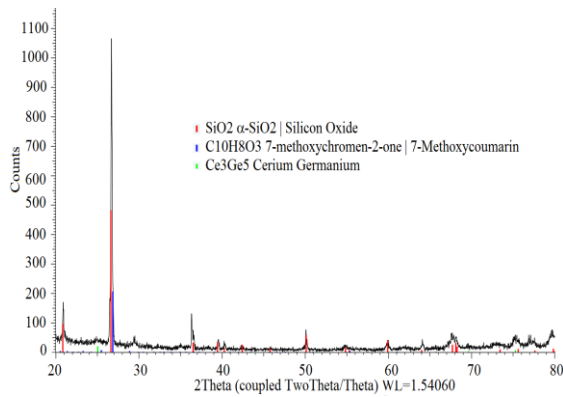


(a) The surface of compacted soil

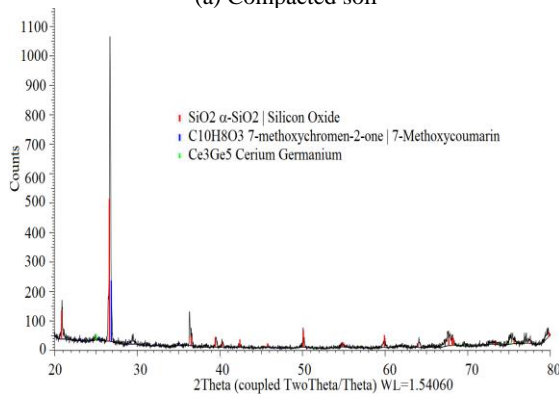


(b) The surface of CFSS specimens

Figure 7. SEM images, magnified by 3000 times



(a) Compacted soil



(b) CFSS specimen at 14 days

Figure 8. XRD patterns of specimens

this study, the cement-FA treated soil was made with 8%C and 2%FA and cured at room temperature until 28 days. In general, the peak intensity of Silicon Oxide is seen in the region 26-28° 2θ. In addition, Methoxycoumarin and Cerium Germanium were also obtained in two specimens.

3. 5. Effect of Different Size Samples on Compressive and Splitting Tensile Strength

As determined in the previous section, the optimum content containing 6% cement and 2% FA can be used for the base layer in road construction. In addition, to understand the effects of size specimen on the compressive strength and tensile strength of CFSS specimens, this study used two sizes of specimens such as D × H = 15.24 × 11.7 cm and D × H = 10.16 × 11.7 cm to test the compressive and tensile strengths.

Tables 4 and 5 indicated that a smaller specimen has a smaller compressive and greater splitting tensile strength with a conversion ratio of 0.74 and 1.09, respectively. This result may be used as a suitable ratio in practical and laboratory situations when using a standard proctor to prepare the specimen.

TABLE 4. UCS of CFSS specimens

| No. | Sample | Size (cm) | | Curing age (days) | Tested values (MPa) | Average Tested values (MPa) |
|-----|-----------|-----------|------|-------------------|---------------------|-----------------------------|
| | | D | H | | | |
| 1 | 8%C+ 2%FA | 15.24 | 11.7 | 28 | 8.0 | 8.02 |
| 2 | | 15.24 | 11.7 | 28 | 7.5 | |
| 3 | | 15.24 | 11.7 | 28 | 8.1 | |
| 4 | | 15.24 | 11.7 | 28 | 8.3 | |
| 5 | | 15.24 | 11.7 | 28 | 8.2 | |
| 6 | 8%C+ 2%FA | 10.16 | 11.7 | 28 | 5.8 | 5.95 |
| 7 | | 10.16 | 11.7 | 28 | 5.4 | |
| 8 | | 10.16 | 11.7 | 28 | 6.4 | |
| 9 | | 10.16 | 11.7 | 28 | 6.2 | |
| 10 | | 10.16 | 11.7 | 28 | 5.9 | |

TABLE 5. STS of CFSS specimens

| No. | Sample | Size (cm) | | Curing age (days) | Tested values (MPa) | Average Tested values (MPa) |
|-----|------------|-----------|------|-------------------|---------------------|-----------------------------|
| | | D | H | | | |
| 1 | 8%C +2%F A | 15.24 | 11.7 | 28 | 0.78 | 0.76 |
| 2 | | 15.24 | 11.7 | 28 | 0.82 | |
| 3 | | 15.24 | 11.7 | 28 | 0.72 | |
| 4 | | 15.24 | 11.7 | 28 | 0.78 | |
| 5 | | 15.24 | 11.7 | 28 | 0.69 | |

| | | | | | | | |
|----|-----------|-------|---|------|----|------|-------------|
| 6 | | 10.16 | × | 11.7 | 28 | 0.83 | |
| 7 | 8%C | 10.16 | × | 11.7 | 28 | 0.87 | |
| 8 | +2%F A | 10.16 | × | 11.7 | 28 | 0.80 | 0.83 |
| 9 | | 10.16 | × | 11.7 | 28 | 0.80 | |
| 10 | | 10.16 | × | 11.7 | 28 | 0.82 | |

4. CONCLUSIONS

An experimental study was performed to investigate the engineering properties of soil stabilized with cement and FA. Some specific conclusions can be made:

- Without using FA, the compressive strength, splitting tensile strength, and elastic modulus of stabilized soils significantly increased with the cement content in a range of 8-10 percent.

- An economical mixture was found of 8% cement and 2% FA, which simultaneously yielded the best performance in UCS, STS, and elastic modulus; furthermore, this also satisfied the requirement for the base layer in road construction according to the current Vietnamese standard.

- SEM images indicated that the compacted soil structure was found as small and odd particles arranged without gel bound, while the CFSS specimen showed foam formation due to the surrounding adhesive, and small particles cannot be observed. The XRD pattern showed that the peak intensity of Silicon Oxide was seen in the region 26-28° 2θ. Methoxycoumarin and Cerium Germanium crystals were also obtained in two specimens.

- Two sizes of specimens such as D×H= 15.24× 11.7 cm, and D×H= 10.16× 11.7 cm used to test the compressive and splitting tensile strengths with a conversion coefficient of 0.74 and 1.09, respectively.

5. REFERENCES

1. Toniolo, N. and Boccaccini, A.R., "Fly ash-based geopolymers containing added silicate waste. A review", *Ceramics International*, Vol. 43, No. 17, (2017), 14545-14551. <https://doi.org/10.1016/j.ceramint.2017.07.221>
2. Rao, S.M. and Thyagaraj, T., "Swell-compression behaviour of compacted clays under chemical gradients", *Canadian Geotechnical Journal*, Vol. 44, No. 5, (2007), 520-532. <https://doi.org/10.1139/t07-002>
3. Karatai Thomas, R., Kaluli James, W., Kabubo, C. and Thiong'o, G., "Soil stabilization using rice husk ash and natural lime as an alternative to cutting and filling in road construction", *Journal of Construction Engineering and Management*, Vol. 143, No. 5, (2017), 04016127. [https://doi.org/10.1061/\(ASCE\)CO.1943-7862.0001235](https://doi.org/10.1061/(ASCE)CO.1943-7862.0001235)
4. Al-Rawas, A.A., "Microfabric and mineralogical studies on the stabilization of an expansive soil using cement by-pass dust and some types of slags", *Canadian Geotechnical Journal*, Vol. 39, No. 5, (2002), 1150-1167. <https://doi.org/10.1139/t02-046>
5. Mymrin, V.A. and Ponte, H.A., "Oil-shale fly ash utilization as independent binder of natural clayey soils for road and airfield base construction", *Particulate Science and Technology*, Vol. 23, No. 1, (2005), 99-107. <https://doi.org/10.1080/02726350590902505>
6. Yilmaz, Y. and Ozaydin, V., "Compaction and shear strength characteristics of colemanite ore waste modified active belite cement stabilized high plasticity soils", *Engineering Geology*, Vol. 155, (2013), 45-53. <https://doi.org/10.1016/j.enggeo.2013.01.003>
7. Marto, A., Hassan, M.A., Makhtar, A.M. and Othman, B.A., "Shear strength improvement of soft clay mixed with tanjung bin coal ash", *APCBEE Procedia*, Vol. 5, (2013), 116-122. <https://doi.org/10.1016/j.apcb.2013.05.021>
8. Phan, V.T.-A., "Improvement in engineering properties of mudstone in southwestern taiwan through compaction and a cement additive", *Geotechnical and Geological Engineering*, Vol. 36, No. 3, (2018), 1833-1843. <https://doi.org/10.1007/s10706-017-0435-1>
9. Tran, B.H., Le, B.V., Phan, V.T.A. and Nguyen, H.M., "In-situ fine basalt soil reinforced by cement combined with additive dz33 to construct rural roads in gia lai province, vietnam", *International Journal of Engineering, Transactions B: Applications*, Vol. 33, No. 11, (2020), 2137-2145. DOI: 10.5829/ije.2020.33.11b.03
10. Suresh, R. and Murugaiyan, V., "Influence of chemical admixtures on geotechnical properties of expansive soil", *International Journal of Engineering, Transactions A: Basics*, Vol. 34, No. 1, (2021), 19-25. DOI: 10.5829/ije.2021.34.01a.03
11. Sharpe, G.W., Deen, R.C., Southgate, H.F. and Anderson, M., *Pavement thickness designs utilizing low - strength (pozzolanic) base and subbase materials*. 1984, Kentucky Transportation Center Research Report. 693.122-130, https://uknowledge.uky.edu/ktc_researchreports/693.
12. Mfinanga, D.A. and Kamuhabwa, M.L., "Use of natural pozzolan in stabilising lightweight volcanic aggregates for roadbase construction", *International Journal of Pavement Engineering*, Vol. 9, No. 3, (2008), 189-201, <https://doi.org/10.1080/10298430701303173>.
13. Malisa, A.S., Park, E. and Lee, J., "Effect of lime on physical properties of natural pozzolana from same, tanzania", *International Journal of Engineering Research & Technology* Vol. 3, No. 11, (2014), 1357-1361.
14. Javdanian, H., "The effect of geopolymerization on the unconfined compressive strength of stabilized fine-grained soils", *International Journal of Engineering, Transactions B: Applications*, Vol. 30, No. 11, (2017), 1673-1680, DOI: 1610.5829/ije.2017.1630.1611b.1607.
15. Tolleson, R.A., Mahdavian, E., Shatnawi, F.M. and Harman, E.N., *An evaluation of strength change on subgrade soils stabilized with an enzyme catalyst solution using cbr and ssg comparisons*. 2003: Project No. R-03-Utc-Alterpave-Geo-01. <http://www.scsu.edu/utc/old/research/Reports/2002/alterpave.htm>.
16. Phan, V.T.-A., "Ground improvement using soil-cement method: A case study with laboratory testing and in-situ verification for a highway project in southern vietnam", *Geotechnical Engineering Journal of the SEAGS & AGSSEA*, Vol. 47, No. 1, (2016), 45-49.
17. Tasthan, E., Edil, T., Benson, C. and Aydilek, A., "Stabilization of organic soils with fly ash", *Journal of Geotechnical and Geoenvironmental Engineering*, Vol. 137, No. 9, (2011), 819-833. [https://doi.org/10.1061/\(ASCE\)GT.1943-5606.0000502](https://doi.org/10.1061/(ASCE)GT.1943-5606.0000502)
18. Xing, H., Yang, X., Xu, C. and Ye, G., "Strength characteristics and mechanisms of salt-rich soil-cement", *Engineering Geology*, Vol. 103, No. 1-2, (2009), 33-38.

19. Mahedi, M., Cetin, B. and White David, J., "Cement, lime, and fly ashes in stabilizing expansive soils: Performance evaluation and comparison", *Journal of Materials in Civil Engineering*, Vol. 32, No. 7, (2020), 04020177. [https://doi.org/10.1061/\(ASCE\)MT.1943-5533.0003260](https://doi.org/10.1061/(ASCE)MT.1943-5533.0003260)
20. Simatupang, M., Mangalla, L.K., Edwin, R.S., Putra, A.A., Azikin, M.T., Aswad, N.H. and Mustika, W., "The mechanical properties of fly-ash-stabilized sands", *Geosciences*, Vol. 10, No. 4, (2020), 132. <https://doi.org/10.3390/geosciences10040132>
21. *ASTM C618: Standard Specification for Coal Fly Ash and Raw or Calcined Natural Pozzolan for Use in Concrete*. 2003: 100 Barr Harbor Drive, PO Box C700, West Conshohocken, PA 19428-2959, United States.
22. *TCVN 9843: Standard test method in the laboratory for resilient modulus of nonorganic adhesive substance stabilized aggregate material*. 2013: Hanoi, Vietnam.

Persian Abstract

چکیده

این مطالعه یک مطالعه تجربی از ویژگی های مهندسی خاک تثبیت شده با سیمان و خاکستر کوره برای لایه ها در ساخت جاده ارائه می دهد. خاکستر کوره در این مطالعه مورد استفاده قرار گرفته است و مطابق ASTM C618 نیاز را برآورده می کند. پنج مخلوط نسبت در این کار با مقادیر مختلف مقادیر مختلف سیمان پرتلند ۸، ۱۰ و ۸ درصد سیمان همراه با محتوای خاکستر کوره ۲ درصد، ۴ درصد و ۶ درصد استفاده شد. دوره های سخت شدن نمونه مشخص ۷، ۱۴، ۲۸ روز برای همه نوع نمونه اعمال شد. برخی از آزمایشات مهندسی مانند مقاومت فشاری نامحدود (UCS)، مقاومت کششی تقسیم، سفتی خاک تثبیت شده، تکنیک های SEM و XRD انجام شد. تصاویر SEM، که ۳۰۰۰ بار بزرگ شده اند، نشان داد که ساختار خاک فشرده به عنوان ذرات کوچک و عجیب بدون چسباندن زل یافت شده است، در حالی که خاک تثبیت شده با خاکستر سیمان به دلیل کریستال خاکستر سیمان کوره پوشانده شده است و ذرات کوچک قابل مشاهده نیستند. اوج شدت اکسید سیلیکون در منطقه ۲۶-۲۸ درجه با زاویه ۲ درجه مشاهده شد. علاوه بر این، سیمان و خاکستر کوره به طور قابل توجهی خواص مکانیکی خاکهای تثبیت شده را بهبود بخشید. سرانجام، نمونه حاوی ۸٪ سیمان و ۲٪ خاکستر بادی در زمان سخت شدن ۱۴ روزه دارای مقاومت کششی بیشتر از ۰.۴۵ مگاپاسکال بود، که طبق استانداردهای ویتنامی فعلی، نیاز اساسی راهسازی را برآورده می کرد. نتایج بدست آمده شواهدی را برای استفاده از خاکستر بکوره برای ساخت جاده در زمینه افزایش خاکستر کوره تولید شده در نیروگاه های حرارتی ارائه می دهد.



Design of Area Efficient Single Bit Comparator Circuit using Quantum dot Cellular Automata and its Digital Logic Gates Realization

R. Chakrabarty*, S. Roy, T. Pathak, N. Kumar Mandal

Department of Electronics and Communication Engineering, Institute of Engineering & Management, Kolkata, India

PAPER INFO

Paper history:

Received 31 August 2021
Received in revised form 05 October 2021
Accepted 09 October 2021

Keywords:

Quantum-Dot Cellular Automata
Comparator
Majority Voter
Kink Energy

ABSTRACT

Quantum dot cellular automata (QCA) is a promising transistor less nano-technology that is growing in popularity and it has the capability to replace the ubiquitous complementary metal oxide Semiconductor (CMOS) technology in the VLSI domain. The paper discussed the simple design of single bit comparator circuit using QCA. A single-bit comparator circuit compares its two inputs and indicates which one is larger or are they both equal. This paper has focused on creating an area efficient QCA comparator circuit and a comparative study of area consumption with the previously made designs. The designed comparator circuit is the most area-efficient design as it is made up of minimum possible number of cells. A comparator is used in equality testers and many other digital communications. The circuit proposed in this paper is a three layered circuit which can alternatively be used to realize the basic logic gates. The circuit can also be used as an alternative to the majority and universal gates in QCA.

doi: 10.5829/ije.2021.34.12c.13

1. INTRODUCTION

Though CMOS technology is currently the most preferred technology in VLSI circuit design, it has few drawbacks in terms of high leakage current. On the other hand, in QCA technology the power consumption, area required are very low. It also supports very high-speed operation (in the range of THz) because it uses the polarization as the mode of operation. These features give QCA the upper hand and research are going on in this domain. Figure 1 shows a QCA cell. The orientation of the electrons will give us the indication whether it's a Logic 0 or Logic 1.

The basic gate in this technology is a majority voter gate [1] which can be programmed to act as an AND gate or an OR gate depending on the control value given. When control value +1 is given, it acts like an OR gate and when the control input is -1, it acts like an AND gate. Many circuits have been implemented using this majority gate like adders and subtractors [2-3], multiplexers [4-5] and decoders [6] which are the basic building blocks of

any digital circuit. Figure 2 shows the QCA design of a majority voter gate. In this paper, we have discussed another building block, i.e., comparators (1-bit). A novel design of a 1-bit comparator has been proposed and then compared against the previously available comparators [7-18].

The paper is organized in this way: current section i.e. section 1 discussed about the introduction of QCA and role of kink energy in QCA based circuit, section 2 describes the detail design of the comparator circuit. Section 3 discussed implementation of various logic gates using the designed comparator circuit and section 4 is for the observation and conclusion of the work.

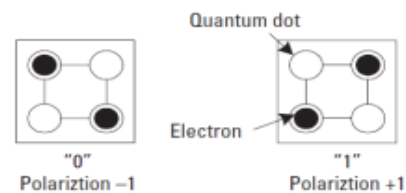


Figure 1. QCA cell with the polarizations

*Corresponding Author Institutional Email:
ratna.chakrabarty@iemcal.com (R. Chakrabarty)

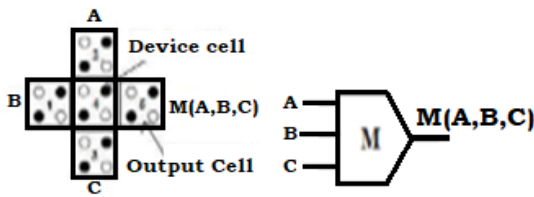


Figure 2. Majority Voter Gate

Kink energy plays an important role in QCA based designs as it should be minimum for the stable output of the circuit.

The kink energy (in Joule) between two electron charges is calculated using the formula: -

$$U = (k \cdot Q_1 \cdot Q_2) / r$$

Where $k = 1 / (4\pi\epsilon_0\epsilon_r) = 9 \times 10^9$,

$Q_1 = Q_2 = \text{charge of an electron} = 1.6 \times 10^{-19} \text{C}$.

$$U = 23.04 \times 10^{-29} / r$$

$r = \text{distance between the two charges}$.

$$U_T = \sum_i U_i$$

$U_T = \text{summation of all the individual kink energies (in Joule)}$.

For this calculation, the below postulates are considered. (This has been shown diagrammatically in Figure 3)

- 1) All cells are alike and the distance from end to end of each cell is 18nm.
- 2) The space between two neighbouring cells (interspacing distance) is 2nm.
- 3) The diameter of each quantum dot is 5nm.
- 4) The distance between the two layers used for the design is 11.5nm.

Another important aspect in every QCA design is the clock. In QCA, clock is used to define the direction of state transition. The clocks are what that gives power to the QCA cells to operate. Clocking plays an important role in synchronizing all parts of a complex digital circuit. There are four clocking zones namely, Switch, Hold, Release, Relax as shown in Figure 4. During switch phase, inter dot barriers are raised and the cells become polarized according to the driver polarization state. In the hold phase as the name suggests, the inter dot barriers continue to be high so that the cells preserve their current states. In release phase, the inter dot barriers become low and the cells go to an unpolarized state. The relax phase keep the barriers low so that the cells can remain in that unpolarized state.

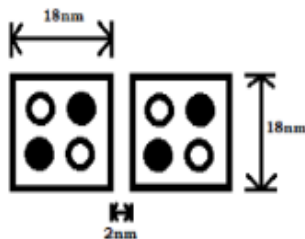


Figure 3. Dimensions of the QCA cells

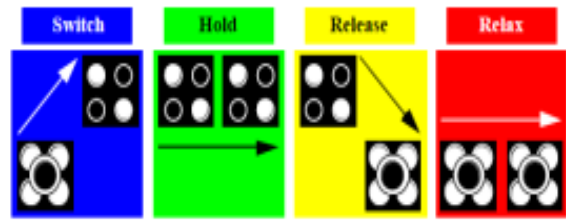


Figure 4. Four phases of a clock signal

2. SINGLE BIT COMPARATOR USING 14 CELLS

A single bit comparator is a combinational circuit that compares two bits. It has two inputs for two single bit numbers each and three outputs are for less than, equal to, and greater than comparison between two binary numbers.

Figure 5(a) shows the design of a more area efficient 1 bit comparator consisting of 14 cells. This design consists of only 14 cells which is the least number of cells used to design a QCA comparator circuit till date. Figure 6 shows the different layers of the circuit. The simulated output of the designed circuit is shown in Figure 7.

Figures 8a and 8b show the polarization and energy dissipation graph with respect to temperature respectively. Figure 8c shows the mapping of the power dissipation across the QCA cells. On mapping this result with the corresponding circuit diagram, we can see that the $A > B$ and $A < B$ output cells dissipates almost equal amount of power which is more than the power dissipated by the $A = B$ output cell. Table 1 shows the different energy calculations for the comparator circuit.

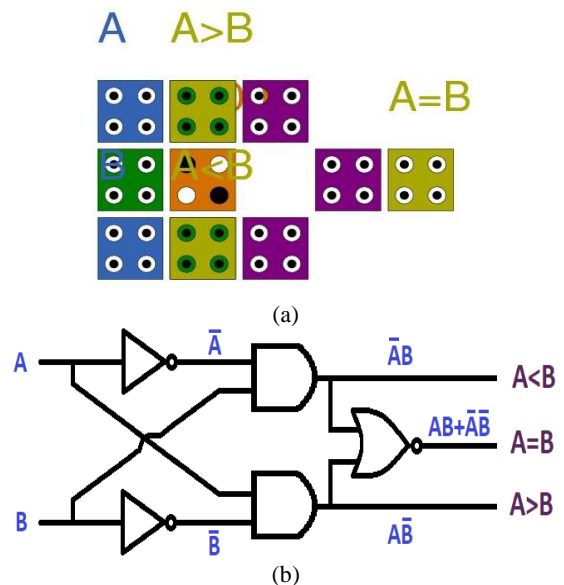


Figure 5. (a) QCA design of proposed comparator with 14 cells (b) Digital circuit diagram of a single-bit comparator

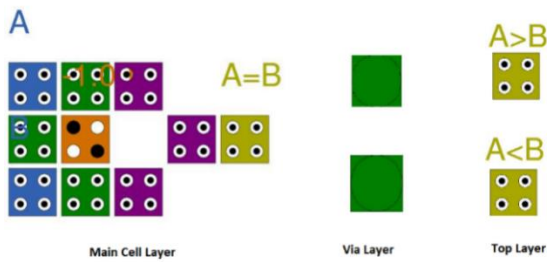


Figure 6. Breakup of the 3 layers in the circuit

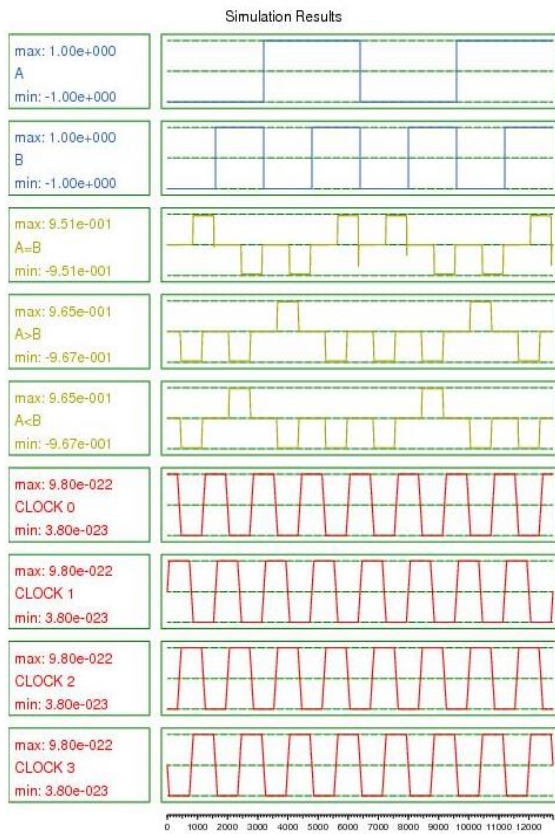
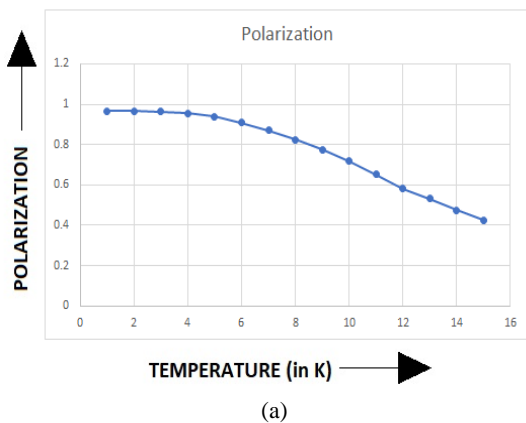
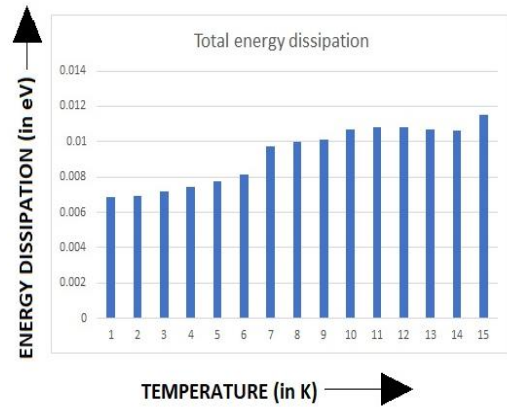


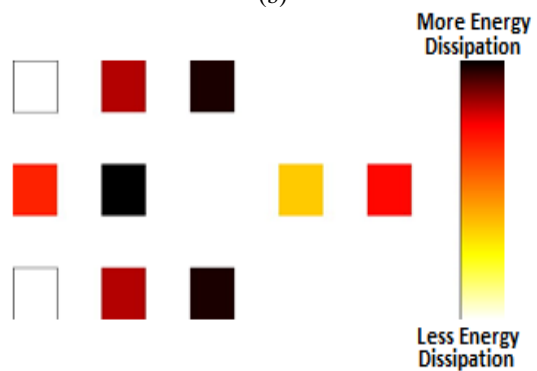
Figure 7. Output of proposed Comparator Circuit



(a)



(b)



(c)

Figure 8. (a) Polarization vs Temperature (b) Energy Dissipation vs Temperature (c) Power Dissipation Mapping using QCAPro[19-20]

TABLE 1. Power Parameters of the Comparator Circuit

| Power Parameters | Values |
|---|-------------------------|
| Total Energy Dissipation (in Joule) | 10.96×10^{-22} |
| Average Energy Dissipation per Cycle (in Joule) | 9.952×10^{-23} |
| Average Power Dissipation (in pico Watts) | 181 |

Now, we calculate the kink energy. Kink energy is basically defined as the energy difference between two neighbouring or adjacent cells. Kink energy between two cells depends on the dimension of the QCA cell as well as the spacing between adjacent cells. It is independent on temperature. It is one of the most significant parameters for the stability of the design. The state having minimum kink Energy is most stable state.

Below, two sets of input values are taken and the kink energy of all the corresponding output cells with respect to each input are calculated. The inputs taken are

a> A=1, B=0: Naturally as A is greater than B, the A>B output cell will give output as '1' and the rest outputs will be '0';

b> A=1, B=1: Similarly, the A=B output cell will give output '1' and the others will give output '0'.

The yellow cells indicate the output cells, green cells indicate the cells are in 1st clock (Clock 0) and pink cells indicate the cells are in 2nd clock (Clock 1). All the electrons (black dots) are arranged such that minimal possible energy configuration is achieved. Then the kink energies are calculated.

In a QCA cell, there are four quantum dots but maximum two electrons are present inside a cell which occupies the opposite cornered position as it is the most stable configuration i.e. the least energy state.

In Figure 9, x_1 and x_2 represents the two opposite cornered electrons of the output cells. Similarly, e_1 and e_2 represents the two electrons of the cell nearest to the output cell. For $A > B$ and $A < B$, the cells are present in two different layers, output cell (in the top layer) lies just above the neighboring cell (in the via layer) but for $A = B$, the cells are on the same the same layer adjacent to each other.

Other cells present in the circuit are further away from the output cell. That is why, the distance between the electrons of the output cell and other cells are so high that the corresponding individual kink energies are too negligible to be considered for the calculation. Tables 2 and 3 shows the kink energy calculations for different inputs of A and B.

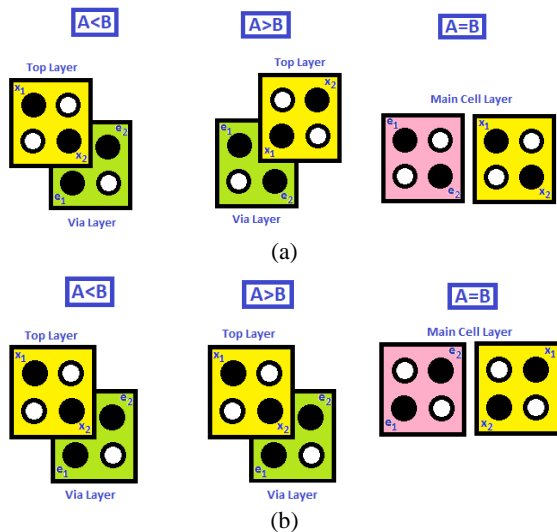


Figure 9. Reference Diagram for Kink Energy calculation for (a) $A=1$ and $B=0$ (b) $A=1$ and $B=1$

TABLE 2. Kink Energies for $A=1$ and $B=0$ ($\times 10^{-21}$)

| Kink Energy (Ue) | INPUT: $A=1, B=0$ | | | | | |
|---------------------------------|-------------------|-------------|-------------|-------------|-------------|-------------|
| | A>B | | A=B | | A<B | |
| | x1 | x2 | x1 | x2 | x1 | x2 |
| U_{e1} | 15.8 | 15.8 | 11.5 | 7.6 | 15.8 | 15.8 |
| U_{e2} | 15.8 | 15.8 | 16.2 | 11.5 | 15.8 | 15.8 |
| Total (U_T) | 31.6 | 31.6 | 27.7 | 19.1 | 31.6 | 31.6 |

TABLE 3. Kink Energies for $A=1$ and $B=1$ ($\times 10^{-21}$)

| Kink Energy (Ue) | INPUT: $A=1, B=1$ | | | | | |
|---------------------------------|-------------------|-------------|-------------|-------------|-------------|-------------|
| | A>B | | A=B | | A<B | |
| | x1 | x2 | x1 | x2 | x1 | x2 |
| U_{e1} | 15.8 | 15.8 | 11.5 | 16.2 | 15.8 | 15.8 |
| U_{e2} | 15.8 | 15.8 | 7.6 | 11.5 | 15.8 | 15.8 |
| Total (U_T) | 31.6 | 31.6 | 19.1 | 27.7 | 31.6 | 31.6 |

3. REALIZATION OF BASIC LOGIC GATES USING THE PROPOSED SINGLE BIT COMPARATOR

This section deals with the designing of basic logic gates using the structure of the single bit comparator. The same design can be used as an AND, OR, NAND, NOR, XOR, XNOR, BUFFER and INVERTER GATE.

As it can be seen from Figure 10(a), when the polarization at the centre is given to be -1, then the corresponding outputs from different cells are given. Figure 10(b) gives the outputs of the same cells when a polarization of +1 is given. We are taking the outputs $A'B$ as ($A < B$) output cell and AB' as ($A > B$) output cell. The $AB + A'B'$ gives the ($A = B$) output cell. Along with these we get some other outputs as well as illustrated in Figures 10(a) and 10(b). We get the AND and OR gates as well from the comparator circuit. It is not unknown that if we invert the output of AND and OR gates we get NAND and NOR respectively. In QCA this is done by adding a cell on top of the output cell in a different layer taking the inverted output from there. In this way we can get the AND, NAND, OR and NOR gates from our proposed comparator design.

As it can be seen in Figure 11, the same comparator structure is used to implement the basic logic gates along with a buffer.

Realization of the fundamental logic gates using the proposed comparator circuit design can be seen as below.

I) AND Gate: To make an AND gate, we just need to take the cell present between the two input cells as the output cell (refer to Figure 10(a)).

II) OR Gate: To make an OR gate, we just need to take the cell present between the two input cells as the output cell (refer to Figure 10(b)).

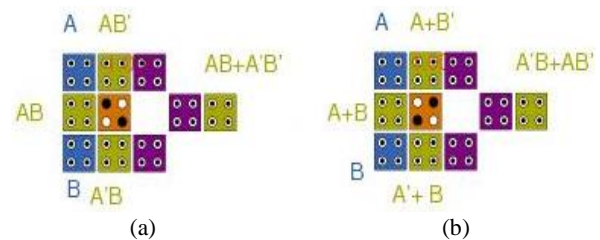


Figure 10. Outputs taken from the Comparator Circuit

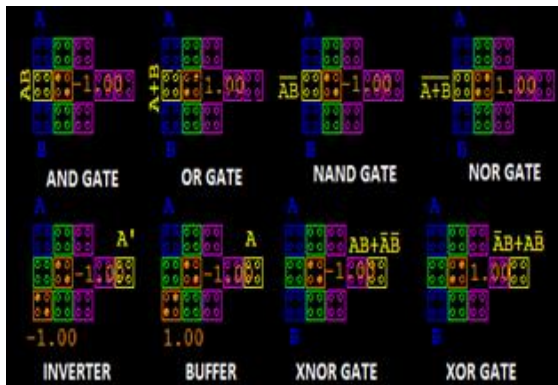


Figure 11. QCA layout of AND, OR, NAND, NOR, INVERTER, BUFFER XNOR and XOR

III) NAND Gate: $NAND = AND + NOT$. Hence, the cell just above the AND output cell in the new layer is taken as the NAND output cell (refer to Figure 11(top row, second from right)).

IV) NOR Gate: $NOR = OR + NOT$. Hence, the cell above the OR output cell in a different layer is taken as the NOR output cell (refer to Figure 11(top row, rightmost)).

V) INVERTER: In the XNOR gate, if we replace the input cell B with polarization -1, we shall get an INVERTER.

$XNOR \Rightarrow Y = AB + A'B'$. If $B=0$, then $Y = A' \Rightarrow$ an INVERTER.

VI) BUFFER: In the XNOR gate, if we replace the input cell B with polarization +1, we shall get a BUFFER.

$XNOR \Rightarrow Y = AB + A'B'$. If $B=1$, then $Y = A \Rightarrow$ a BUFFER.

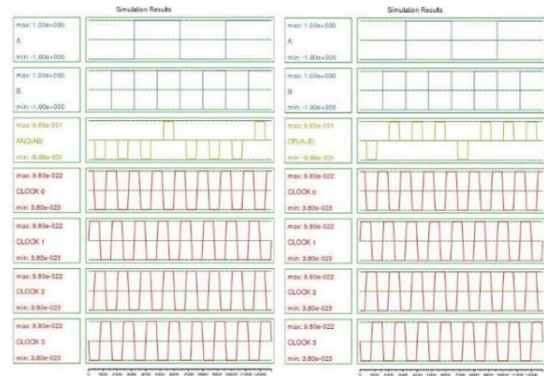
VII) XNOR Gate: In a comparator circuit, $A=B$ is calculated using the XNOR gate. Hence, no extra design is required for the XNOR gate because it can be obtained from the comparator circuit itself.

VIII) XOR Gate: To make a XOR gate, we just need to change the polarization of the polarized cell of the comparator from -1.00 to +1.00. The position of the output cell remains same as that of the $A=B$ comparator output (refer to Figure 11 (bottom row, rightmost)).

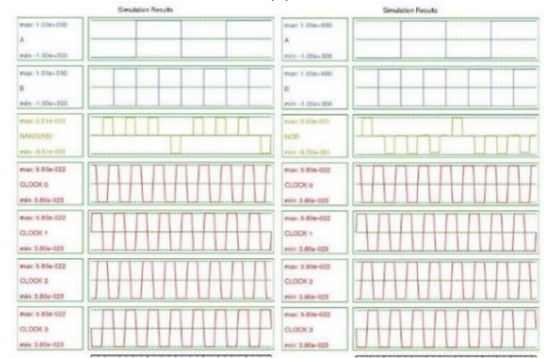
In Figure 12, output graphs of the fundamental logic gates using the proposed comparator circuit design are shown.

4. OBSERVATION AND RESULTS

Table 4 draws the comparisons among previously proposed single bit comparators to our proposed design with respect to cell count and area consumption. Proposed design consists of 14 cells and consumption of area is $0.0089 \mu m^2$. This design can be alternatively used as the basic logic gates which has been discussed in section 3.



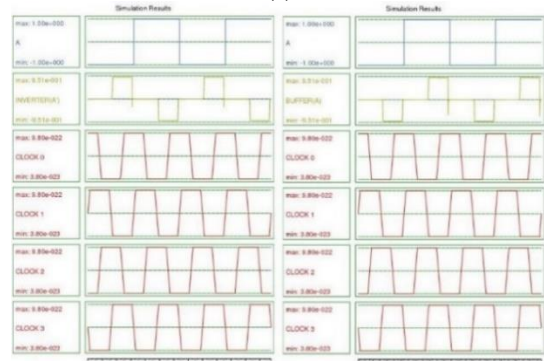
(a)



(b)



(c)



(d)

Figure 12. Output of the basic logic gates implemented using the proposed design. (a) AND & OR Gate, (b) NAND & NOR Gate, (c) INVERTER & BUFFER, (d) XNOR & XOR Gate

TABLE 4. Observations for 1-bit comparators

| Comparator Design | No. of Cells | Area (μm^2) | Delay (clock cycle) |
|-------------------|--------------|--------------------------|---------------------|
| [7] | 81 | 0.06 | 0.75 |
| [8] | 42 | 0.05 | 0.75 |
| [9] | 37 | 0.028 | 1 |
| [10] | 58 | 0.055 | 0.75 |
| [11] | 100 | 0.11 | 0.75 |
| [12] | 38 | 0.03 | 0.5 |
| [13] | 31 | 0.04 | 0.75 |
| [14] | 40 | 0.05 | 0.75 |
| [15] | 79 | 0.07 | 1 |
| [16] | 73 | 0.06 | 1 |
| [17] | 26 | 0.023 | 0.5 |
| [18] | 31 | 0.03 | 0.75 |
| Proposed Design | 14 | 0.0089 | 0.5 |

5. CONCLUSION

In this paper we have discussed about the design of 14 cell single bit comparator circuit and used it to design of the basic logic gates. During the comparison of the circuit with other previously proposed designs the number of cells used to formulate this is 14 which is the lowest till date. Thus we are able to propose a novel comparator design which is area efficient and also can be used in basic digital designs. The advantage of our design is that we are getting all the gates along with the comparator output. This comparator circuit can be used as a universal structure for forming the basic gates instead of the majority voter as this design is more compact and is less prone to errors.

6. REFERENCES

- Naqvi, S.R., Akram, T., Iqbal, S., Haider, S., Kamran, M., Muhammad, N., "A dynamically reconfigurable logic cell: from artificial neural networks to quantum-dot cellular automata", *Applied Nanoscience*, Vol. 8, (2018), 89-103, doi: 10.1007/s13204-018-0653-8
- Zoka, S., Gholami, M., "A novel efficient full adder-subtractor in QCA nanotechnology", *International Nano Letters*, Vol. 9, (2019), 51-54, doi:10.1007/s40089-018-0256-0
- Sen, B., Rajoria, A., Sikdar, B. K., "Design of Efficient Full Adder in Quantum Dot Cellular Automata", *The Scientific World Journal*, (2013), doi: 10.1155/2013/250802
- Tambe, A., Bhakre, S., Kassa, S., "Design and Analysis of (2x1) and (4x1) Multiplexer Circuit in Quantum dot Cellular Automata Approach", *International Journal of Innovative Technology and Exploring Engineering*, Vol. 8, (2019), 277-281
- Ahmad, F., "An Optimal Design of QCA Based 2n:1/1:2n Multiplexer/Demultiplexer and Its Efficient Digital Logic Realization", *Microprocessors and Microsystems*, Vol. 56, (2018), 64-75, doi: 10.1016/j.micpro.2017.10.010
- Abbasizadeh, A., Mosleh, M., "Ultra dense 2 to 4 decoder in quantum dot cellular automata technology based on MV32 gate", *ETRI Journal*, Vol. 42, (2020), 912-921, doi:10.4218/etrij.2019-0068
- D. Ajitha, K. V. Ramanaiyah and V. Sumalatha, "A novel design of cascading serial bit-stream magnitude comparator using QCA", *International Conference on Advances in Electronics Computers and Communications*, (2014), 1-6, doi:10.1109/ICAIECC.2014.7002449
- Deng, F., Xie, G., Zhang, Y., Peng, F., Lv, H., "A novel design and analysis of comparator with XNOR gate for QCA", *Microprocessors and Microsystems*, Vol. 55, (2017), 131-135, doi: 10.1016/j.micpro.2017.10.009
- S. S. Roy, C. Mukherjee, S. Panda, A. K. Mukhopadhyay and B. Maji, "Layered T comparator design using quantum-dot cellular automata", *Devices for Integrated Circuit (DevIC)*, 90-94, (2017), doi: 10.1109/DEVIC.2017.8073913
- S. Umira, R. Qadri, Z. A. Bangi and M. T. Banday, "A Novel Comparator-A Cryptographic Design in Quantum Dot Cellular Automata", 2018 International Conference on Sustainable Energy, Electronics, and Computing Systems (SEEMS), 1-10, doi: 10.1109/SEEMS.2018.8687363
- Jun-wen, L. and Yin-shui, X., "A Novel Design of Quantum-Dots Cellular Automata Comparator Using Five-Input Majority Gate", 14th IEEE International Conference on Solid-State and Integrated Circuit Technology (ICSICT), (2018), 1-3
- Shiri, A., Rezai, A., Mahmoodian, H. "Design of efficient coplanar 1-bit comparator circuit in QCA technology", *Facta Universitatis-Series: Electronics and Energetics*, Vol. 32, (2019), 119-128, doi: 10.2298/FUEE1901119S
- Gao, M., Wang, J., Fang, S., Nan, J., "A New Nano Design for Implementation of a Digital Comparator Based on Quantum-Dot Cellular Automata", *International Journal of Theoretical Physics*, (2020), doi: 10.1007/s10773-020-04499-w
- Majeed, A. H., Zainal, M. S., Alkaldy, E., MD Nor, D., "Single-Bit Comparator in Quantum-Dot Cellular Automata (QCA) Technology Using Novel QCA-XNOR Gates", *Journal of Electronic Science and Technology*, (2020), doi: 10.1016/j.jnlest.2020.100078
- Hayati, M., Rezaei, A., "Design and Optimization of Full Comparator Based on Quantum-Dot Cellular Automata" *ETRI Journal*, Vol. 34, (2012), 284-287, doi: 10.4218/etrij.12.0211.0258
- B. Ghosh, S. Gupta and S. Kumari, "Quantum dot cellular automata magnitude comparators", *IEEE International Conference on Electron Devices and Solid State Circuit*, (2012), 1-2, doi: 10.1109/EDSSC.2012.6482766
- Sharma, V. K., "Optimal design for digital comparator using QCA nanotechnology with energy estimation." *International Journal of Numerical Modelling: Electronic Networks, Devices and Fields*, Vol. 34, No. 7, (2020), doi: /10.1002/jnm.2822
- V. Satyanarayana, M. Balaji, K. Neelima, "Optimal of 1-bit Comparator design and Energy Estimation using Quantum Dot Cellular Automata", *Internal Journal of Engineering and Applied Physics*, Vol. 1, No. 2, (2021), 103-110, Source: <https://ijeap.org/ijeap/article/view/22>
- S.Kassa and S. Nema, "Energy Efficient Novel Design of Static Random Access Memory Memory Cell in Quantum-dot Cellular Automata Approach", *International Journal of Engineering, Transactions B: Applications* Vol. 32, No. 5, (2019), 720-725, doi: 10.5829/ije.2019.32.05b.14.
- H. Alamdara, G. Ardeskira and M. Gholami, "Using Universal Nand-nor-inverter Gate to Design D-latch and D Flip-flop in Quantum-dot Cellular Automata Nanotechnology", *International Journal of Engineering, Transactions A: Basics* Vol. 34, No. 7, (2021), 1710-1717, doi: 10.5829/ije.2021.34.07a.15

Persian Abstract

چکیده

آنتن کوانتوم دات سلولار (QCA) یک ترانزیستور نویدبخش با فناوری نانو کمتر است که محبوبیت روزافزون خود را افزایش می دهد و این قابلیت را دارد که در همه جا از فناوری نیمه هادی اکسید فلزی مکمل (CMOS) در حوزه VLSI استفاده کرد. این مقاله به طراحی ساده مدار مقایسه کننده تک بیتی با استفاده از QCA پرداخته است. یک مدار مقایسه ای تک بیتی دو ورودی خود را مقایسه می کند و نشان می دهد که کدام یک بزرگتر است یا هر دو برابر هستند. این مقاله بر ایجاد یک مدار مقایسه ای QCA کارآمد در منطقه و مطالعه مقایسه ای مصرف سطح با طراحی های قبلی تمرکز کرده است. مدار مقایسه شده طراحی شده از نظر مساحت کارآمدترین طرح است زیرا از حداقل تعداد ممکن سلول تشکیل شده است. یک مقایسه کننده در آزمایش کننده های برابری و بسیاری دیگر از ارتباطات دیجیتال استفاده می شود. مدار ارائه شده در این مقاله یک مدار سه لایه است که به طور متناوب می تواند برای تحقق دروازه های منطقی اساسی مورد استفاده قرار گیرد. این مدار همچنین می تواند به عنوان جایگزینی برای دروازه های اکثریت و جهانی در QCA استفاده شود.



Prolong Stability Period in Node Pairing Protocol for Wireless Sensor Networks

A. Yadav^{*a}, N. Kohli^b, A. Yadav^c

^a Research Scholar, A.P.J. Abdul Kalam Technical University, Lucknow

^b Harcourt Butler Technical University, Kanpur

^c Computer Application Department, UIET, CSJM University, Kanpur

PAPER INFO

Paper history:

Received 7 April 2021

Received in revised form 8 July 2021

Accepted 07 August 2021

Keywords:

Wireless Sensor Networks

Stability Period

Network Lifetime

Throughput

ABSTRACT

Wireless sensor networks are efficient way to monitor important parameters in various fields of science and engineering. These sensors are battery operated and in each round of transmission some energy is used. Therefore, over the period of time battery drains, and thus effect the stability period of the networks. To conserve battery nodes are divided as normal and advance nodes. The energy of the advanced nodes is higher than normal nodes. Further clustering mechanism is used to reduce energy dissipation. This paper proposes a mechanism by which stability period, network lifetime and throughput can be increased significantly. The proposed mechanism considers S-SEP protocol and nodes are coupled to form pairs, then number of clusters and radius of the clusters are optimized such that isolated nodes are zero. It is found that using proposed mechanism stability period can be improved by 17% in comparison to recently proposed work.

doi: 10.5829/ije.2021.34.12c.14

1. INTRODUCTION

Recently, we have witnessed a lot of advancement in the field of Wireless sensor networks (WSNs) [1]. The transmission using sensor nodes is reliable and secures [2]. The data collected by these nodes is further transmitted to the BS either directly or with the help of cluster heads (CHs) [3]. The source of energy of these nodes is batteries, which are not replaceable. Hence, it is quite important to have a long lifetime of these nodes for the efficient transmission system. As soon as the first node dies out, the network becomes unstable [4]. Thus, the major issue with the WSNs is to enhance the lifetime and reduce the energy consumption of the nodes [5]. A number of techniques are proposed to reduce the consumption of energy of the SNs [6-8] like energy-aware medium access control and power-aware storage protocols [8]. To some extent, these protocols have upgraded the lifetime and battery replacement time of WSNs, but failed to provide sufficient energy for the proper functioning of the system. The positioning of the nodes also plays an important role in reducing energy

consumption. The nodes must be deployed in such a way that they must cover the main area which is to be focused concentrated to have proper and precise collection of data [5]. In this work we are analyzing the effect of number of clusters, radius of the clusters and distance of the nodes in the optimization of stability period. We would like to increase the radius of the clusters such that no isolated node remain, but under the condition that the pairing of node will only be done for the nodes which follows free space model. The free space model demands smaller radius of the cluster circle while to avoid isolate node radius of the clusters should be large enough to accommodate distant nodes. Two requirements are inverse to each other. Therefore, optimization of radius of the clusters is necessary to maximize stability period.

2. RELATED WORKS

A new protocol, stable election protocol (SEP) is proposed for improving the lifetime of the nodes. In this protocol, we have two kinds of nodes: advanced and

*Corresponding Author Institutional Email: amityadaktu@gmail.com
(A. Yadav)

normal nodes. The selection of cluster head is based on the residual energy in each node. Many researchers have proposed various heterogeneous protocols similar to SEP using some improvement mechanism. In the other clustering protocol named as zonal-stable election protocol [9], the basic concept of working is based on the zonal division. Further modification is done where considered area is divided into sectors (S-SEP) [10].

Each node in a WSN network collects and transmits data, which causes some consumption of energy. In the case of uneven distribution of nodes in a WSN, some nodes left as isolated as shown in Figure 1. The consumption of energy by isolated nodes is a major problem in a WSN network. This problem can be solved by deciding whether the isolated nodes will send the data to a CH node or to sink on the basis of the distance between the isolated nodes and the sink. Recently, we proposed modified Sectorial SEP protocol; here field is divided into sectors, and as shown in Figure 2 [11], nodes away from sink node are advanced nodes and have more energy as compared to normal nodes and they follow clustering mechanism and a group of nodes lie within a

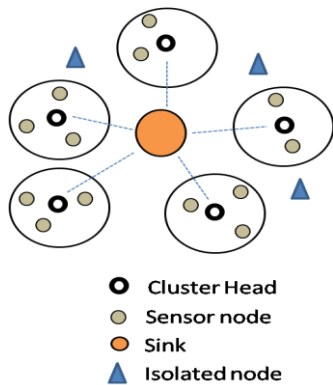


Figure 1. Schematic of isolated nodes

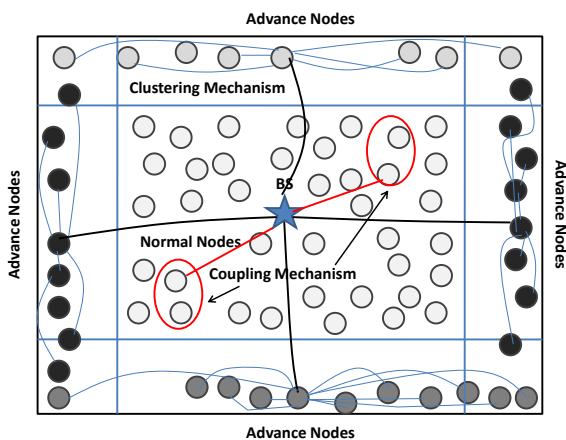


Figure 2. Node deployment in $(2X+Y) \times (2X+Y) m^2$ square field

cluster elect cluster head among themselves. However, the normal nodes also follows clustering mechanism and within a cluster each node do not transmit to cluster head but two nearby nodes combine using node coupling mechanism and in each round one node awake and transmit to cluster head and other node goes to sleep mode after transferring its data to its coupled partner. Initially all the nodes are active and they broadcast their positions, node_ids and type of applications they run. On the basis of message received from other nodes each node maintain a table and select pairing node which is closet to neighbouring nodes and run same application. Let initial energy of each node is $2E_0$ but due to neighbour formation some of the energy is lost therefore we assume that initial energy of each node is $E_0(1+U)$ where U is uniform random number between 0 and 1. It is also noticeable that in n number of nodes forms clusters, without node pairing because node pairing will not be beneficial as distance between the nodes is larger. We define this region as 1. Let ' p_1 ' is the probability of a node to become cluster head, then the average number of clusters would be np_1 . Similarly, m nodes forms pairing of nodes, and further let that isolated nodes are denoted by I , therefore number of pairing active nodes in a particular round would be $A = [m/2 - I]$, and we define this area as region 2. Let ' p_2 ' is the probability of a node to become cluster head, then the average number of clusters would be $C = Ap_2$. In regions 1 and 2, the average number of nodes in each cluster except cluster head are $(1/p_1 - 1)$ and $(1/p_2 - 1)$, respectively.

In region 2, the cluster head selection is done using Equation (1), in the equation R denotes the round.

$$Th(n) = \begin{cases} \left(1 - p_2 \left(R \times \text{mod} \frac{1}{p_2} \right) \right) \times \frac{E_r(i)}{E_0(1+U)} & \text{if } n \in (A_L) \\ 0 & \text{otherwise} \end{cases} \quad (1)$$

3. ENERGY CALCULATION

For the description and simulation of proposed protocol first order, radio model is used and list of symbols used and their descriptions are detailed in Table 1. For the packet size of ' S ' bits and distance between transmitter and receiver as ' d ' the transmission energy will be given by:

$$E_{TX} = \begin{cases} SE_{et} + SE_{fs}d^2 & d \leq d_0 \\ SE_{et} + SE_{mp}d^4 & d > d_0 \end{cases} \quad (2)$$

$$\text{where, } d_0 = \sqrt{\frac{E_{fs}}{E_{mp}}}$$

And the receiver energy is:

$$E_{RX} = SE_{el} \quad (3)$$

Region 1:

In a single round, energy dissipated at node cluster head (CH) is:

$$E_{CH} = SE_{el} \left(\frac{1}{p_1} - 1 \right) + SE_{DA} \frac{1}{p_1} + SE_{el} + SE_{fs} d_{CH-BS}^2 \quad (4)$$

Or

$$E_{CH} = SE_{el} \left(\frac{1}{p_1} - 1 \right) + SE_{DA} \frac{1}{p_1} + SE_{el} + SE_{mp} d_{CH-BS}^4 \quad (5)$$

where, $d_{CH-BS}^{2,4}$ is the distance of cluster head to base station. Energy dissipation in non-cluster head (N-CH) is:

$$E_{N-CH} = SE_{el} + SE_{fs} d_{CN-CH}^2 \quad (6)$$

where, d_{CN-CH}^2 is the distance of cluster nodes to cluster heads. Total energy dissipated in a cluster in a round is:

$$E_{CH}^T = E_{CH} + \frac{1}{p_1} E_{N-CH} \quad (7)$$

Region 2:

In a single round, energy dissipated at non-cluster head node is:

$$E_{CH} = \left(\frac{1}{p_2} - 1 \right) (E_{el} \times S + E_{amp} \times S \times d_{CN-CH}^2) \quad (8)$$

Energy dissipation in data receiving is:

$$E_{Rc} = SE_{RX} \left(\frac{1}{p_2} - 1 \right) \quad (9)$$

Data aggregation energy is:

$$E_{AG} = SE_{AD} \frac{1}{p_2} \quad (10)$$

Energy dissipated by cluster to transmit aggregated data to BS is (by following Equation (2))

$$E_T = S \times E_{el} + E_{amp} \times S \times d_{CH-BS}^2 \quad (11)$$

Or

$$E_T = S \times E_{el} + E_{amp} \times S \times d_{CH-BS}^4 \quad (12)$$

Total energy dissipated in a cluster in a round is

$$E_{CH}^T = E_{Rc} + E_{AG} + E_T \quad (13)$$

Therefore, in both the regions dissipated energy is different; distance among the nodes is more in region 1 as compared to region 2. Therefore different packet transfer schemes are adopted.

In the proposed method, we aim to minimize isolated nodes. For mathematical point of view, we consider, the area of the field is $L \times L$, and let 'n' numbers of nodes are uniformly distributed over the given area, the clusters are circular in shape and each cluster has same size and area (Figure 3). Let initially there are m numbers of nodes, the numbers of coupled nodes are c , and numbers of isolated nodes are I .

$$m = c + I \quad (14)$$

Therefore, numbers of alive nodes in a round are

$$A_L = \frac{c}{2} + I \quad (15)$$

Therefore, numbers of clusters are:

$$C = \left(\frac{c}{2} + I \right) p_2 \gamma \quad (16)$$

As in each round the isolate will transfer packets to sink node directly; therefore energy depletion will be fast and further if distance of isolated node from sink is larger then energy depletion problem becomes two folds. We aim to increase the radius of the clusters to bring isolated nodes to zero, i.e., and the maximum number of clusters will be

$$C_{\max} = \left(\frac{m}{2} \right) p_2 \gamma \quad (17)$$

The covered area can be represented as:

$$\left(\frac{m}{2} \right) p_2 \gamma \times \pi r^2 = L^2 \quad (18)$$

or

$$r = \sqrt{\frac{2L^2}{\pi m p_2 \gamma}} \quad (19)$$

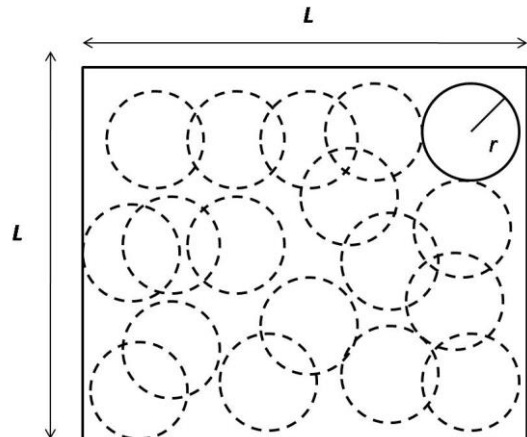


Figure 3. Schematic of cluster area coverage

The maximum radius can be evaluated as:

$$r_{\max} = \sqrt{\frac{2L^2}{\pi m p_2^{\min} \gamma}} \quad (20)$$

Referring Figure 3, it can be seen that if overlapping clusters are chosen such that each node is covered by four adjacent clusters than isolated nodes can be set to zero. But the number of clusters cannot be chosen arbitrarily; therefore we should increase the radius of the clusters to get k node coverage. But radius cannot be increased beyond a limit which is set as:

$$r_{\max} = \frac{d}{2} = \frac{\sqrt{E_{fs} / E_{mp}}}{2} = 43.85m \quad (21)$$

Node Coupling Mechanism

```

ID=0;
for i=1:1:n
for j=1:1:n
if (j~i)
 $d_{i,j} = \sqrt{(x_i - x_j)^2 + (y_i - y_j)^2}$  (distance between the
nodes)
if ( $d_{i,j} \leq d_o$  (coupling distance))
if ( $d_{i,j} < d_{i,j}(n)$  (neighbour distance ))
 $d_{i,j}(n) = d_{i,j}$ ;
ID=j;
end
end
end
end
end
if (ID>0)
pair nodes
 $x=x+1$ ;
else
isolated nodes
 $y=y+1$ ;
 $d_{i,j}^{CH} = \sqrt{(x_i - x_j^{CH})^2 + (y_i - y_j^{CH})^2}$  (distance between
cluster head and isolated nodes)
 $\min[d_{i,j}^{CH}]$ , (select cluster head  $j$  for data forwarding)
end

```

Referring to Figure 4, and coupled nodes are marked as 1 and 2, respectively. We know that using wireless channel model if distance between nodes is less than thresholds ($d \leq d_0$) then the power loss is proportional to d^2 and known as free space and when thresholds ($d \geq d_0$) then the power loss is proportional to d^4 and known as multi-path propagation. Let us first consider that node 2 transmit to sink node. Therefore, we have:

$$L^2 = D^2 - d^2 + 2Dd \cos \phi \quad (22)$$

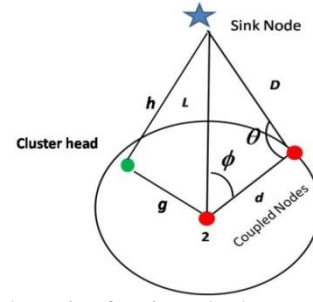


Figure 4. Schematic of cosine rules between nodes, cluster head and sink

We have four cases

Case 1: If distance between the coupling nodes is small i.e., ($d \leq d_0$) the energy loss will be proportional to d^2 and distance between node 2 and sink node is small then energy loss will also be proportional to L^2 . Therefore, total energy loss will be proportional to $L^2 + d^2$.

Case 2: If distance between the coupling nodes is large and distance between node 2 and sink node is small then the total energy loss will be proportional to $L^2 + d^4$.

Case 3: If distance between the coupling nodes is small and distance between node 2 and sink node is large then the total energy loss will be proportional to $L^4 + d^2$

Case 4: Again if distance between the coupling nodes is large and distance between node 2 and sink node is large then the total energy loss will be proportional to $L^4 + d^4$

Case 1 is applicable for the nodes which are close to sink node. Case 2 will lead to unfeasible solution, case 3, is applicable for the nodes which are moderate distance from sink, and finally case 4, is applicable for nodes which are away from the sink nodes. In our proposed method optimum numbers of clusters with radius which satisfies Equation (21) are chosen such that, d , g and h are less than d_0 . Referring Figure 4, Equations (5) and (12) are modified as:

$$E_{CH} = \left(\frac{1}{P_2} - 1 \right) (E_{ei} \times S + E_{amp} \times S \times g^2) \quad (23)$$

$$E_T = S \times E_{ei} + E_{amp} \times S \times h^2 \quad (24)$$

Problem Constraints

The objective is to maximize the stability period and can be written as

$$\max \sum_r S_p \quad \forall r \in R \quad (25)$$

Subjected to

$$A_{is} = \begin{cases} 1 & \text{if } i \text{ establishes a link with } s \\ 0 & \text{otherwise} \end{cases}$$

$$A_{fs} = \begin{cases} 1 & \text{if } f \text{ establishes a link with } s \\ 0 & \text{otherwise} \end{cases}$$

A_{is} represents the connectivity between i and s . similarly A_{fs} is the connectivity between f and s . therefore all the links establish connection is given by:

$$A_{is} = A_{fs} = 1 \quad \forall i, f \in N \quad (26)$$

No packet drops at the cluster head is given by

$$P_{ic} - P_{cs} = 0 \quad \forall (i \in N, c \in C_H) \quad (27)$$

Node having energy less than minimum energy will stop transmission:

$$E_i \leq E_{\min} \quad \forall i \in N \quad (28)$$

$$\sum_i \lambda_i t \geq cb_i \quad \forall i \in N \quad (29)$$

says that the data generation rate of a given node i during a time period t should not exceed its buffer capacity cb_i . To achieve above objective we should have:

$$\min \sum_r I \quad \forall r_n \in R_n \quad (30)$$

$$\max \sum_{r_n} r \leq r_{\max} \quad \forall r_n \in R_n \quad (31)$$

where I are isolated nodes.

5. SIMULATION RESULTS

In this section simulation results are presented. In simulation various results are detailed using graphs. The parametric values are detailed in Table 1 which is also used in Monte Carlo simulation. 100 nodes are considered with a radius of 10m and 25m in Figures 5 and 6, respectively. Referring Figure 5 in case of smaller radius it is not possible to cover entire field, and some of the nodes remain as isolated nodes (marked in dotted red colour); however in case of larger radius it is possible to cover entire field, and isolated nodes can be bring down zero. Referring case 1 above and Equation (19), radius cannot be increased beyond set limit. A very large radius

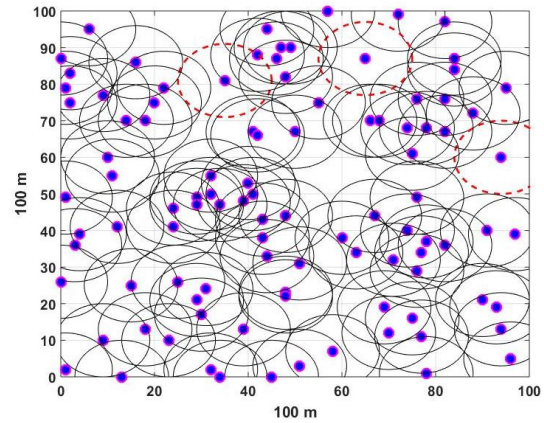


Figure 5. Cluster coverage 10 m

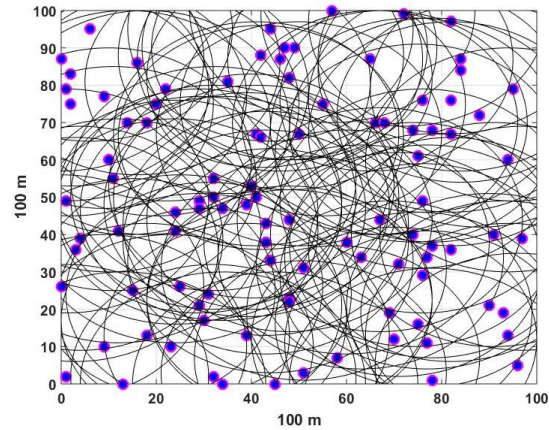


Figure 6. Cluster coverage 25 m

will not bring any further improvement as a node will be covered by a large number of clusters which will not affect node coverage.

In Figure 7, $\gamma = \frac{E_r(i)}{E_0(1+U)}$ normalized residual energy

is plotted for round number 10 when all the nodes are alive and 6000 rounds when nearly 40% nodes are dead. Initially all 80 nodes are alive and energies values lie between 0.5 and 1, and as the round progresses the value of γ falls and after 6000 round its value is around 0.1 only. As the value of $A_L p_2 \gamma$ goes less than 1, the cluster formation stops and the leftover nodes, directly transmit data to base station.

In Figure 8, radius vs. $p_2 \gamma$ for 10%, 50% and 100% alive nodes are presented. When all the nodes are alive for $p_2 \gamma = 0.05$ radius is 40m for $p_2 \gamma = 0.5$ the radius is 12.62m, similarly, when 50% nodes are alive for $p_2 \gamma = 0.05$ radius is 56.42 m for $p_2 \gamma = 0.5$ the radius is 17.84. Finally, when 10% nodes are alive for $p_2 \gamma = 0.2$ radius is 63.08 m for $p_2 \gamma = 0.4$ the radius is 44.6. In Figure 9, radius vs. alive nodes is presented for $p_2 \gamma$ for 0.2, 0.3, 0.4 and 0.5. for $p_2 \gamma = 0.2$ the clustering mechanism will break

TABLE 1. Simulation Parameters [10]

| Parameters | Value |
|--|-----------------------------|
| Initial Energy E_0 | 0.5 J |
| Energy for data aggregation E_{DA} | 5 nj/bit |
| Transmission and Receiving energy | 5 nj/bit |
| Amplification energy for short distance E_{fs} | 10 pj/bit/m ² |
| Amplification energy for long distance E_{amp} | 0.013 pj/bit/m ⁴ |
| Probability P_1 | 0.3 |
| Probability P_2 | 0.4 |

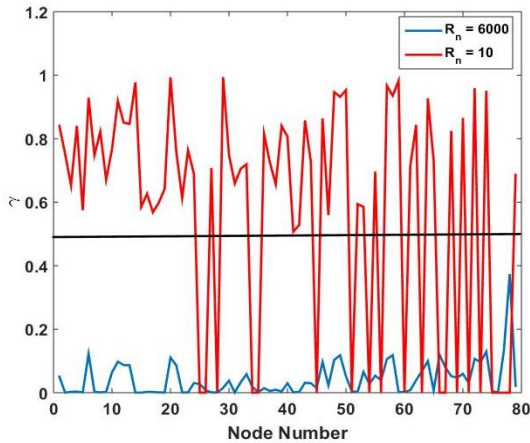


Figure 7. The value of γ for all 80 nodes

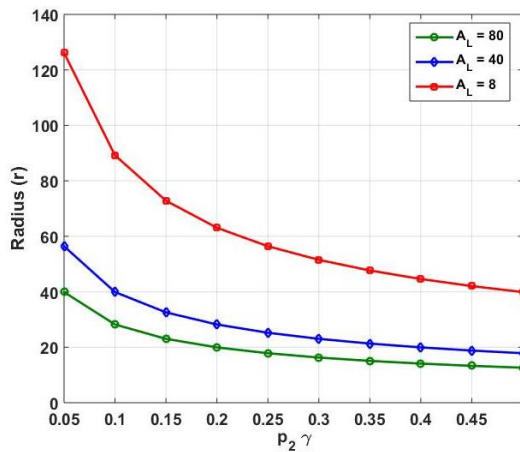


Figure 8. Radius vs. $p_2\gamma$ for 10%, 50% and 100% alive nodes

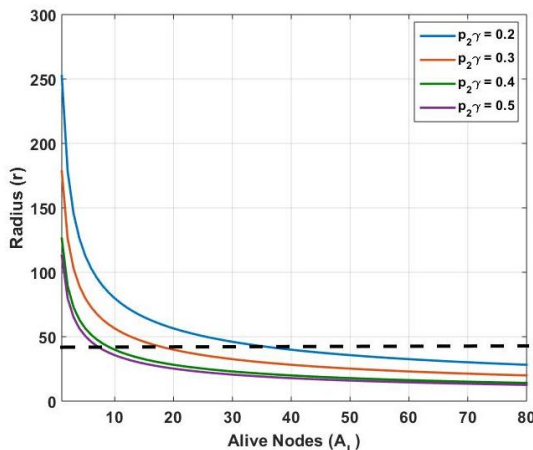


Figure 9. Radius vs. alive nodes for various values of $p_2\gamma$

when alive nodes are nearly 35, and lower value of $p_2\gamma$ also means less number of clusters. Similarly if we choose $p_2\gamma = 0.5$, clustering mechanism will break when alive nodes are nearly 6, but initially the value of $mp_2\gamma$ is

40, therefore all the alive nodes will transfer data to base station and there will not any advantage of clustering mechanism. If we consider, $p_2\gamma = 0.4$, clustering mechanism will break when alive nodes are nearly 10, and clustering will become effective from round 1 of the simulation. Therefore in our simulation we have considered $p_2\gamma = 0.4$.

Next we have simulated effect of coupling distance on the number of coupled nodes and detailed are shown in Figure 10. The cluster diameter is considered to be twice of coupling distance. For small diameter 2m the numbers of coupled nodes are 4 and isolated nodes are 76. While increasing diameter from 2m to 15 m the numbers of coupled nodes becomes 70 and isolated nodes are 10. For diameter range from 25 m to 55m the numbers of coupled nodes are 78 and isolated nodes are 2, and from diameter of 60 m onwards the numbers of coupled nodes are 80 and isolated nodes are none. Considering Equation (14) and Equation (15), we conclude that the optimal coupling distance is around 30-35 m and cluster diameter is around 60-70 m. The optimal distances are also depends on the distribution of the nodes therefore while evaluating parameters like stability period, network life time and throughput optimal distance may differ slightly.

In Figure 11, stability period vs. cluster diameter is shown, for lower value of cluster diameter stability period is very less due to the reason as stated above (more number of isolated nodes). For cluster diameter of 10 m stability period is 2437, which increases to 2729 for cluster diameter of 20 m. If we compare results with recently proposed work [11] the stability period is 2185, 2471 for cluster diameter of 10 m and 20 m respectively. For cluster diameter of 60 m the stability period for yadav et. al. [11], work is 2862, and for proposed work stability period is 2854. For the proposed work, the stability period reaches its maximum value 2888 for cluster diameter of 65 m. It is important to note that for diameter more than 60m the number of isolate nodes are zero.

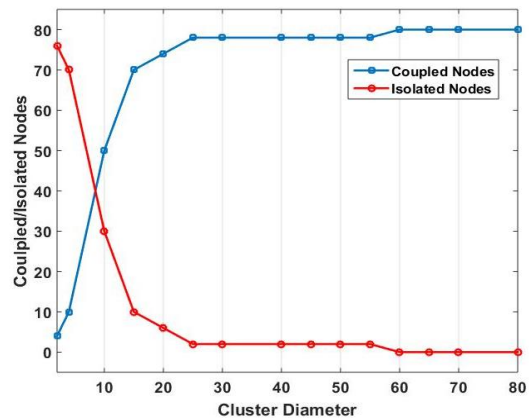


Figure 10. Numbers of coupled/Isolated nodes vs. Cluster Diameter

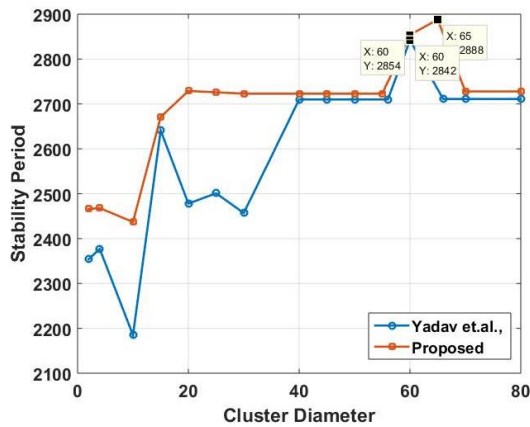


Figure 11. Stability Period vs. Cluster Diameter

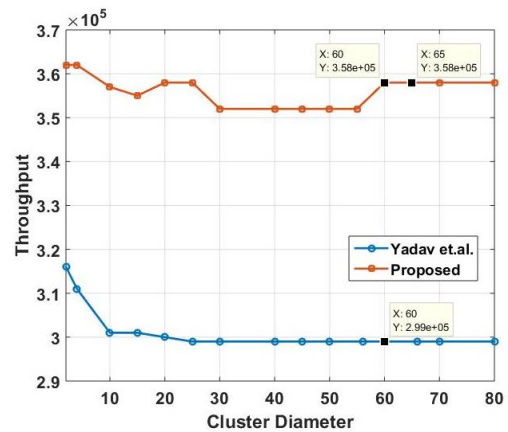


Figure 13. Throughput vs. Cluster Diameter

However, as diameter increases as nodes are covered by more than one cluster and a few nodes change their cluster heads and lead to the better stability period.

In Figure 12, network lifetime vs. cluster diameter is shown. For cluster diameter of 10 m network lifetime is 7582 and remains nearly same for any cluster diameter. If we compare Yadav et. al. [11], works with proposed work network lifetime at the cluster diameter of 60 m is 7248 and 7616 rounds respectively. It is further to note that network life time does not change with rise in cluster diameter as energy dissipation remain proportional to d^2 but as diameter increases a few nodes change their cluster heads therefore distance from cluster heads also alters, and it has been found that this reorganization of nodes does not bring any significant change in energy dissipation in fact it increases slightly for diameter of above 60m. The network life time is maximum for diameter of 60 m.

In Figure 13, Throughput vs. cluster diameter is shown. For cluster diameter of 10 m throughput is 3.62×10^5 and remains nearly same for any cluster diameter. If we compare Yadav et. al., [11] works with

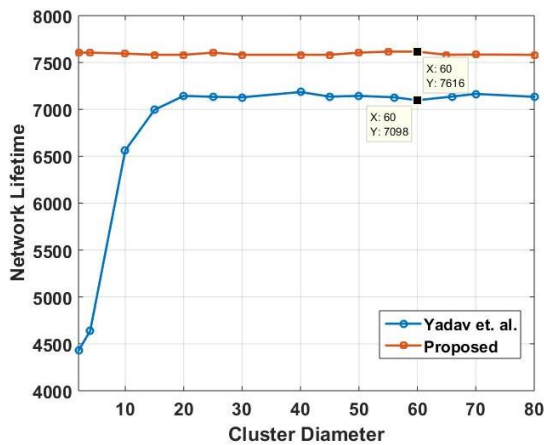


Figure 12. Network Lifetime vs. Cluster Diameter

proposed work network lifetime at the cluster diameter of 60 m is 2.99×10^5 and 3.58×10^5 rounds, respectively. Again it is noticeable that that network throughput does not change with rise in cluster diameter as energy dissipation does not change and it remains proportional to d^2 , but as diameter increases as discussed above a few nodes change their cluster heads therefore distance from cluster heads also alters, and it has been found that this reorganization of nodes does not bring any significant change in energy dissipation, thus throughput remains nearly same. The throughput is maximum for diameter of 60 m.

6. COMPARISON WITH RECENT NOTABLE SCHEMES

In Table 2, results of the recently proposed protocol are detailed. It can be seen that for LEACH, SEP, Z-SEP, EECF-EI, DDEEC, DEEC and MAHEE stability period

TABLE 2. Comparison with notable schemes

| Protocol | Stability Period (Rounds) | Network Lifetime (Rounds) | Throughput (Packets) |
|-------------------|---------------------------|---------------------------|----------------------------|
| LEACH [12] | 1018 | 4685 | 1.99×10^4 |
| SEP [13] | 2471 | 3005 | 3.43×10^4 |
| Z-SEP [9] | 1089 | 3791 | 2.16×10^5 |
| S-SEP [10] | 1422 | 3824 | 2.32×10^5 |
| EECF-EI [14] | 1763 | 5143 | 1.51×10^5 |
| DDEEC [15] | 1433 | 3399 | 6.89×10^4 |
| DEEC [16] | 1233 | 3166 | 4.61×10^4 |
| MAHEE [17] | 1333 | 3690 | 1.84×10^5 |
| Yadav et al. [11] | 1455 | 7248 | 2.99×10^5 |
| PROPOSED | 2888 (d=65 m) | 7616 (d=60 m) | 3.58×10^5 (d=60m) |

is less than 1500 rounds. For SEP stability period is 1763 rounds, and in Yadav et al. [11] work stability period is 2471 rounds. However in the proposed work stability period is around 2888 rounds which is 16.87% better than Yadav et al. [11] work. Similarly improvements are also observed in network lifetime and throughput. In comparison to S-SEP improvement is around 100%, therefore it can be concluded that in S-SEP using node coupling mechanism and optimization of parameters such that isolated nodes are zero a significant improvement is possible. It is further to note that stability period is maximum for diameter of 65 m, while network lifetime and throughput is maximum for diameter of 60 m.

7. CONCLUSIONS

This paper presents a wireless sensor network based protocol. The main objective considered in the work is the improvement in the stability period. We have optimized the relevant parameters in such a way that the numbers of isolated nodes can bring down to zero. A detailed mathematical as well simulation results are discussed for the optimization done. It is found that cluster diameter of 65 m produces best stability period results. It is also found that both network lifetime and throughput also improves significantly. Results are also compared with recently proposed protocol and it is found that all three parameters stability period, network lifetime and throughput improves significantly.

8. REFERENCES

- Jiang Q, Ma J, Lu X, Tian Y. "An efficient two-factor user authentication scheme with unlinkability for wireless sensor networks." *Peer-to-Peer Networking and Applications*, Vol. 8, No. 6, (2015), 1070-1081. <https://doi.org/10.1007/s12083-014-0285-z>
- Wang F, Liu J. "Networked wireless sensor data collection: issues, challenges, and approaches." *Communications Surveys & Tutorials*, *IEEE*. Vol. 13, No. 4, (2011), 673-687. [10.1109/SURV.2011.060710.00066](https://doi.org/10.1109/SURV.2011.060710.00066).
- Tiwari A, Ballal P, Lewis FL. "Energy-efficient wireless sensor network design and implementation for condition-based maintenance". *ACM Transactions on Sensor Networks (TOSN)*, Vol. 3, No. 1, (2007), <https://doi.org/10.1145/1210669.1210670>.
- Akyildiz IF, Lee W-Y, Vuran MC, Mohanty S. "NeXt generation/dynamic spectrum access/cognitive radio wireless networks: a survey" *Computer Networks*, Vol. 50, No. 13, (2006), 2127-2159. <https://doi.org/10.1016/j.comnet.2006.05.001>
- Akyildiz IF, Su W, Sankarasubramaniam Y, Cayirci E. "A survey on sensor networks." *Communications Magazine, IEEE.*; Vol. 40, No.8, (2002), 102-110. [10.1109/MCOM.2002.1024422](https://doi.org/10.1109/MCOM.2002.1024422)
- Hosseini-rad, S. M., "A Hierarchy Topology Design Using a Hybrid Evolutionary Algorithm in Wireless Sensor Networks", *International Journal of Engineering, Transactions A: Basics*, Vol. 31, No. 10, (2018), 1651-1658. [10.5829/ije.2018.31.10a.06](https://doi.org/10.5829/ije.2018.31.10a.06)
- Ahmadi, M., Jameii, S. M., "A Secure Routing Algorithm for Underwater Wireless Sensor Networks", *International Journal of Engineering, Transactions A: Basics*, Vol. 31, No. 10, (2018), 1659-1665. [10.5829/ije.2018.31.10a.07](https://doi.org/10.5829/ije.2018.31.10a.07)
- Kia, G., and A. Hassanzadeh. "HYREP: A hybrid low-power protocol for wireless sensor networks." *International Journal of Engineering, Transactions A: Basics*, Vol. 32, No. 4 (2019): 519-527. [10.5829/ije.2019.32.04a.09](https://doi.org/10.5829/ije.2019.32.04a.09)
- Faisal, S., Javaid, N., Javaid, A., Khan, M.A., Bouk, S.H. and Khan, Z.A., "Z-SEP: Zonal-stable election protocol for wireless sensor networks" arXiv preprint arXiv:1303.5364.
- Sharma, N., Singh, K. and Singh, B.M., "Sectorial Stable Election Protocol for Wireless Sensor Network," *Journal of Engineering Science and Technology*, Vol. 13, No. 5, (2018) 1222-1236.
- Amit Yadav, Narendra Kohli, Anil Kumar Yadav, "An Advanced Node Pairing Protocol for Wireless Sensor Networks" *International Journal of Integrated Engineering*, Vol. 13, No. 1, (2021), 75-87. [10.30880/ije.2021.13.01.008](https://doi.org/10.30880/ije.2021.13.01.008)
- Heinzelman, W., Chandrakasan, A., and Balakrishnan, H., "Energy-Efficient Communication Protocols for Wireless Microsensor Networks", Proceedings of the 33rd Hawaii International Conference on Systems Science (HICSS), January 2000. [10.1109/HICSS.2000.926982](https://doi.org/10.1109/HICSS.2000.926982)
- Smaragdakis G, Matta I, Bestavros A, editors. "SEP: A stable election protocol for clustered heterogeneous wireless sensor networks." Second international workshop on sensor and actor network protocols and applications (SANPA 2004); 2004.
- Khan, M.A., Qureshi, M.A., Raza, I. and Hussain, S.A., "EECP-EI: energy-efficient clustering protocol based on energy intervals for wireless sensor networks." In Proceedings of the International Conference on Information and Communication Technology (113-119). ACM. (2019). [10.1145/3321289.3321316](https://doi.org/10.1145/3321289.3321316)
- B. Elbhiri, R. Saadane, S.Fldhi and D. Aboutajdine. "Developed distributed energy-efficient clustering (DDEEC) for heterogeneous wireless sensor network," in: 5th International Symposium on I/V Communications and Mobile Networks (ISVC), (2010), 10.1109/ISVC.2010.5656252
- L. Qing, Q. Zhu, and M. Wang. "Design of a distributed energy-efficient clustering algorithm for heterogeneous wireless sensor networks," *Computer Communications*, Vol. 29, (2002), No. 12, 2230-2237. <https://doi.org/10.1016/j.comcom.2006.02.017>
- Ayoub, N., Asad, M., Aslam, M., Gao, Z., Munir, E. U., Tobji, R. "MAHEE: Multi-hop advance heterogeneity-aware energy efficient path planning algorithm for wireless sensor networks." In 2017 IEEE Pacific Rim Conference on Communications, Computers and Signal Processing (PACRIM) (1-6), IEEE. [10.1109/PACRIM.2017.8121915](https://doi.org/10.1109/PACRIM.2017.8121915)

Persian Abstract

چکیده

شبکه های حسگر بی سیم راهی کارآمد برای نظارت بر پارامترهای مهم در زمینه های مختلف علوم و مهندسی هستند. این سنسورها با باتری کار می کنند و در هر دور انتقال مقداری انرژی استفاده می شود. بنابراین ، با گذشت زمان ، باتری تخلیه می شود و بنابراین دوره پایداری شبکه ها را تحت تأثیر قرار می دهد. برای حفظ گره های باتری به گره های معمولی و پیشرفته تقسیم می شوند. انرژی گره های پیشرفته بیشتر از گره های معمولی است. مکانیسم خوشه بندی بیشتر برای کاهش اتلاف انرژی استفاده می شود. این مقاله مکانیزمی را پیشنهاد می کند که به موجب آن می توان دوره ثبات ، طول عمر و توان شبکه را به میزان قابل توجهی افزایش داد. مکانیسم پیشنهادی پروتکل S-SEP را در نظر می گیرد و گره ها به هم متصل می شوند تا جفت شوند ، سپس تعداد خوشه ها و شعاع خوشه ها به گونه ای بهینه می شود که گره های جدا شده صفر باشند. مشخص شده است که با استفاده از مکانیسم پیشنهادی دوره پایداری می تواند در مقایسه با کارهای اخیراً ۱۷ درصد بهبود یابد.

AIMS AND SCOPE

The objective of the International Journal of Engineering is to provide a forum for communication of information among the world's scientific and technological community and Iranian scientists and engineers. This journal intends to be of interest and utility to researchers and practitioners in the academic, industrial and governmental sectors. All original research contributions of significant value focused on basics, applications and aspects areas of engineering discipline are welcome.

This journal is published in three quarterly transactions: Transactions A (Basics) deal with the engineering fundamentals, Transactions B (Applications) are concerned with the application of the engineering knowledge in the daily life of the human being and Transactions C (Aspects) - starting from January 2012 - emphasize on the main engineering aspects whose elaboration can yield knowledge and expertise that can equally serve all branches of engineering discipline.

This journal will publish authoritative papers on theoretical and experimental researches and advanced applications embodying the results of extensive field, plant, laboratory or theoretical investigation or new interpretations of existing problems. It may also feature - when appropriate - research notes, technical notes, state-of-the-art survey type papers, short communications, letters to the editor, meeting schedules and conference announcements. The language of publication is English. Each paper should contain an abstract both in English and in Persian. However, for the authors who are not familiar with Persian, the publisher will prepare the latter. The abstracts should not exceed 250 words.

All manuscripts will be peer-reviewed by qualified reviewers. The material should be presented clearly and concisely:

- *Full papers* must be based on completed original works of significant novelty. The papers are not strictly limited in length. However, lengthy contributions may be delayed due to limited space. It is advised to keep papers limited to 7500 words.
- *Research notes* are considered as short items that include theoretical or experimental results of immediate current interest.
- *Technical notes* are also considered as short items of enough technical acceptability with more rapid publication appeal. The length of a research or technical note is recommended not to exceed 2500 words or 4 journal pages (including figures and tables).

Review papers are only considered from highly qualified well-known authors generally assigned by the editorial board or editor in chief. Short communications and letters to the editor should contain a text of about 1000 words and whatever figures and tables that may be required to support the text. They include discussion of full papers and short items and should contribute to the original article by providing confirmation or additional interpretation. Discussion of papers will be referred to author(s) for reply and will concurrently be published with reply of author(s).

INSTRUCTIONS FOR AUTHORS

Submission of a manuscript represents that it has neither been published nor submitted for publication elsewhere and is result of research carried out by author(s). Presentation in a conference and appearance in a symposium proceeding is not considered prior publication.

Authors are required to include a list describing all the symbols and abbreviations in the paper. Use of the international system of measurement units is mandatory.

- On-line submission of manuscripts results in faster publication process and is recommended. Instructions are given in the IJE web sites: www.ije.ir-www.ijeir.info
- Hardcopy submissions must include MS Word and jpg files.
- Manuscripts should be typewritten on one side of A4 paper, double-spaced, with adequate margins.
- References should be numbered in brackets and appear in sequence through the text. List of references should be given at the end of the paper.
- Figure captions are to be indicated under the illustrations. They should sufficiently explain the figures.
- Illustrations should appear in their appropriate places in the text.
- Tables and diagrams should be submitted in a form suitable for reproduction.
- Photographs should be of high quality saved as jpg files.
- Tables, Illustrations, Figures and Diagrams will be normally printed in single column width (8cm). Exceptionally large ones may be printed across two columns (17cm).

PAGE CHARGES AND REPRINTS

The papers are strictly limited in length, maximum 6 journal pages (including figures and tables). For the additional to 6 journal pages, there will be page charges. It is advised to keep papers limited to 3500 words.

Page Charges for Papers More Than 6 Pages (Including Abstract)

| | |
|------------------------------|--------------------------|
| For International Author *** | \$55 / per page |
| For Local Author | 100,000 Toman / per page |

AUTHOR CHECKLIST

- Author(s), bio-data including affiliation(s) and mail and e-mail addresses).
- Manuscript including abstracts, key words, illustrations, tables, figures with figure captions and list of references.
- MS Word files of the paper.



THOMSON REUTERS

WEB OF SCIENCE



Scopus®



CAS®
A DIVISION OF THE
AMERICAN CHEMICAL SOCIETY



 Crossref



Scientific Indexing Services

Google
Scholar